# DNA Transformation and Type IV Pili in Neisseria gonorrhoeae

Vui Yin Seow

Sorbonne Université

Ecole doctorale Physique en Île-de-France (ED564)

*Laboratoire Jean Perrin (UMR8237)*

# DNA Transformation and Type IV Pili in *Neisseria gonorrhoeae*

## *Transformation de l'ADN et pili de type IV chez Neisseria gonorrhoeae*

Par Vui Yin SEOW

Thèse de doctorat de Physique

Dirigée par Nicolas BIAIS

Présentée et soutenue publiquement le 26 Janvier 2024

Devant un jury composé de :

| | |
|---|---|
| M. BIAIS Nicolas | Directeur de Thèse |
| M. COUREUIL, Mathieu | Rapporteur |
| Mme FOREST Katrina | Examinatrice |
| Mme ROBERT Lydia | Examinatrice |
| Mme SCLAVI, Bianca | Examinatrice |
| M. VEYRIER Frédéric | Rapporteur |

*Dedication*

*Papa, my first Physics teacher*

*Mummy, my first Experimentalist*

*My brother, my first friend*

*And*

*Nature, my playground*

*La Science remplace du visible compliqué par de l'invisible simple. – Jean Perrin*

# Acknowledgement

*The way I see it, every life is a pile of good things and bad things. The good things don't always soften the bad things, but vice versa, the bad things don't always spoil the good things and make them unimportant.- Doctor Who*

Reflecting on this PhD journey, I have come to see it as a tapestry woven with joyous and challenging threads. I navigated the disruptive waves of the COVID-19 pandemic. I traversed continents from the cosy confines of the Mechano-Micro-Biology lab (MMBL) at 307 Ingersoll Hall in Brooklyn College to the Laboratoire Jean Perrin (LJP) at Sorbonne Université.

$$\rho \frac{D\vec{V}}{Dt} = -\nabla p + \mu \nabla^2 \vec{V} + \boldsymbol{\rho \vec{F}}$$

Life mirrors a flowing stream comprising diverse elements in the continuum of existence. This segment highlights **external forces** akin to the principles delineated by the Navier-Stokes equation.

*Tell me and I forget, teach me and I may remember, involve me and I learn. - Benjamin Franklin*

First and foremost, my deepest gratitude extends to my thesis advisor, Nicolas Biais, a mentor par excellence. His unwavering support and encouragement empowered me to explore my passions freely. His infectious enthusiasm for science, which initially drew me to the MMBL, continues to resonate as a guiding principle. Under his tutelage, I've expanded my scientific horizons and imbibed invaluable life lessons.

To the members of MMBL (especially Jingbo) and the GC CUNY MCD Cohort: your camaraderie accompanied me through the peaks and valleys of this journey. Group hugs—a testament to our collective strength! To the members of Laboratoire Jean Perrin (LJP), your accompaniment has enriched this life's melody. Your presence has contributed immensely to the symphony of experiences that shaped this journey.

I've been fortunate to cross paths with exceptional mentors, such as Prof Too, Prof Gan, Prof Kini, Prof Clement, Ruiyang, Simon, Xixian, and Bhaskar. Their guidance has moulded me into a better individual, shaping my philosophy on life. A heartfelt appreciation goes to the Graduate Center, CUNY, Sorbonne Université (particularly the team at Laboratoire Jean Perrin), and collaboratores, for granting me the opportunity to pursue doctoral research.

My gratitude extends to my circle of friends, the steady anchors in the turbulence of life. Their presence has been a constant source of joy, solace, and tolerance for my whimsical humor.

Finally, my deepest thanks to my family. To my father, wherever he may be, I hope this gratitude reaches him, carrying with it the echoes of our scientific debates. To my mother, your unwavering support always assures me of a place to call home. To my brother, you helped me laugh in the face of difficulties.

# Contents

# Chapter 1 : Introduction

## 1.1 Antibiotic Resistance

This thesis braved the COVID-19 pandemic. It is also a time in which the world is united, for once (in a long time), to ensure the survival of humanity through these difficult times. This instance also reminds us that global health is of high importance. Scientists, healthcare workers, and hopefully, the rest of the population are now more aware of potential global health threats. One of them is antibiotic resistance. The World Health Organization has listed antibiotic resistance as one of humankind's top global health threats. As of 2013, antibiotic-resistant infections record more than 2.6 million cases and nearly 44000 deaths[1]. While common perceptions towards antibiotic resistance have medical implications, antibiotic resistance impacts our lives in many ways, like food safety and environmental sustainability.

### 1.1.1 What are Antibiotics? How do they work?

Antibiotics are molecular weapons against bacteria. They are low molecular weight molecules, usually less than one kiloDalton[2]. In nature, antibiotics can be produced by microorganisms like fungi or bacteria. While most of the earlier laboratory work in microbiology relied heavily on culturing microorganisms in test tubes, researchers have slowly expanded the scope of understanding microorganisms through complex settings such as co-culture, biofilm, bacterial communities, and microbiome[3–7]. This is primarily due to our realization that microorganisms exist in different forms in nature, and the context of their environment is equally important.

In many cases, microorganisms co-habit an environment and are involved in several interactions (some will be discussed further in Chapter 6). It is also due to these interactions, that microorganisms evolved to equip themselves with means for survival, either through metabolic or survival fitness, colonization strategy or hijacking competitors[8]. Some of the tools microorganisms evolved to equip include toxin-antitoxin system in bacteria and antibiotics.

There are in general two classes of antibiotics based on their working mechanism: bactericidal and bacteriostatic [2]. Bactericidal antibiotics work by killing target microorganisms[2]. Whereas bacteriostatic antibiotics can inhibit the proliferation of bacteria, rendering the slowdown of its viability and population growth[2]. In the context of medical treatment, while bactericidal antibiotics will be more efficient in eliminating infections, bacteriostatic antibiotics can be administered to stall infectious bacterial growth, giving time for the host immune system to ramp up and clear the infection out of the system. Generally, antibiotics, target on five key mechanisms in bacteria to achieve either bactericidal or bacteriostatic effect[2]: (a) inhibition of cell wall synthesis, (b) inhibition of protein synthesis, (c) inhibition of DNA or RNA synthesis, (d) inhibition of folate synthesis, and (e) membrane disruption (Figure 1.1).

Susceptibility of antibiotics, especially those targeting cell wall and membrane disruption, are also highly dependent on the bacteria cell surface structure[2,9,10]. Gram-negative bacteria are less susceptible to antibiotics. The extra outer membrane in Gram-negative bacteria make it difficult

for antibiotics to easily penetrate through the cell membrane compared to Gram-positive bacteria.

Here, we understand that antibiotics can be produced naturally by microorganisms, but then, how did antibiotics go from being microorganisms' own little tools to our so-called ‘miracle drugs’? We will have to travel a bit back in time for that.

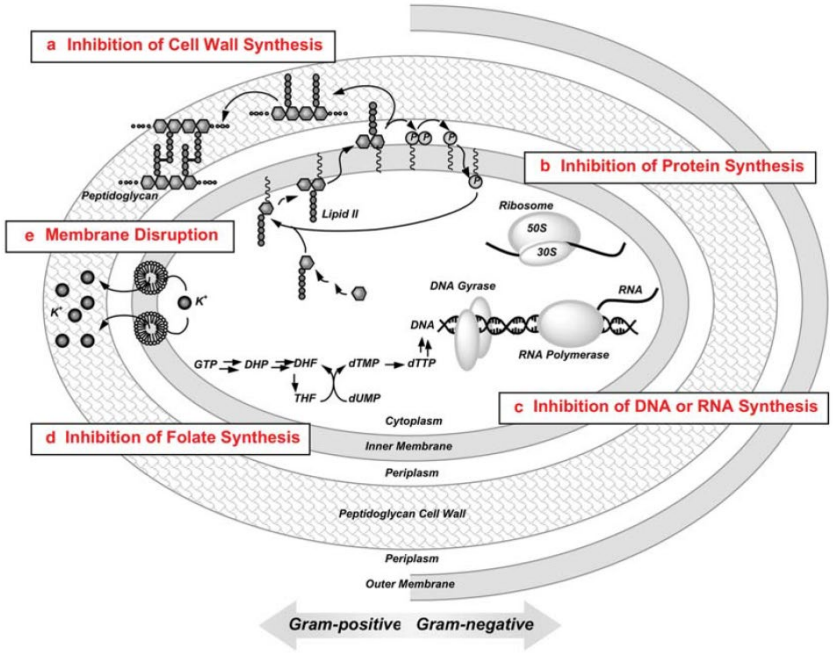


*Figure 1.1 Antibiotics Mechanism of Action* [2]

### 1.1.2 Discovery of antibiotics

The power of antibiotics was not known by humankind until the 1900s. While many might remember Alexander Fleming for his discovery of penicillin, the first known discovery of natural antibiotics, antibiotics discovery work actually commenced way before that (Figure 1.4). The first antimicrobial agent commercialized was an organoarsenic compound discovered and synthesized by Paul Ehrlich [Bonus: he met Albert Neisser, who coined *Neisseria* later, while studying in the same secondary school in Breslau[11]] and his chemist Alfred Bertheim in 1907, arsphenamine[12,13]. Sahachiro Hata, a collaborator of Paul Ehrlich, helped screen for drug against syphilis in search of the ‘magic bullet’, discovered that ‘Compound 606’, which was in fact arsphenamine, was effective against syphilis without affecting normal host cells[12,14,15]. This compound was later commercialized as Salvarsan, both targeting syphilis and trypanosomiasis[16]. Unfortunately in the 1920s, resistance against Salvarsan emerged[8]. The trend of antibiotics was led towards synthetic drugs sulfonamidochrysoidine (KL730) discovered by Gerhard Domagk in 1935, which won him the Nobel Prize in Physiology or Medicine in 1939[8,16–18]. This drug is commercialized as Prontosil and is the first sulphonamide group antibiotics. However, due to the chemical nature of both arsphenamine and sulfonamidochrysoidine, they are mostly considered the pioneer of chemotherapy rather than

of its antibiotic nature[13,14]. These treatments did not live long since resistance against sulfonamide started to surface in the 1930s (Figure 1.2).

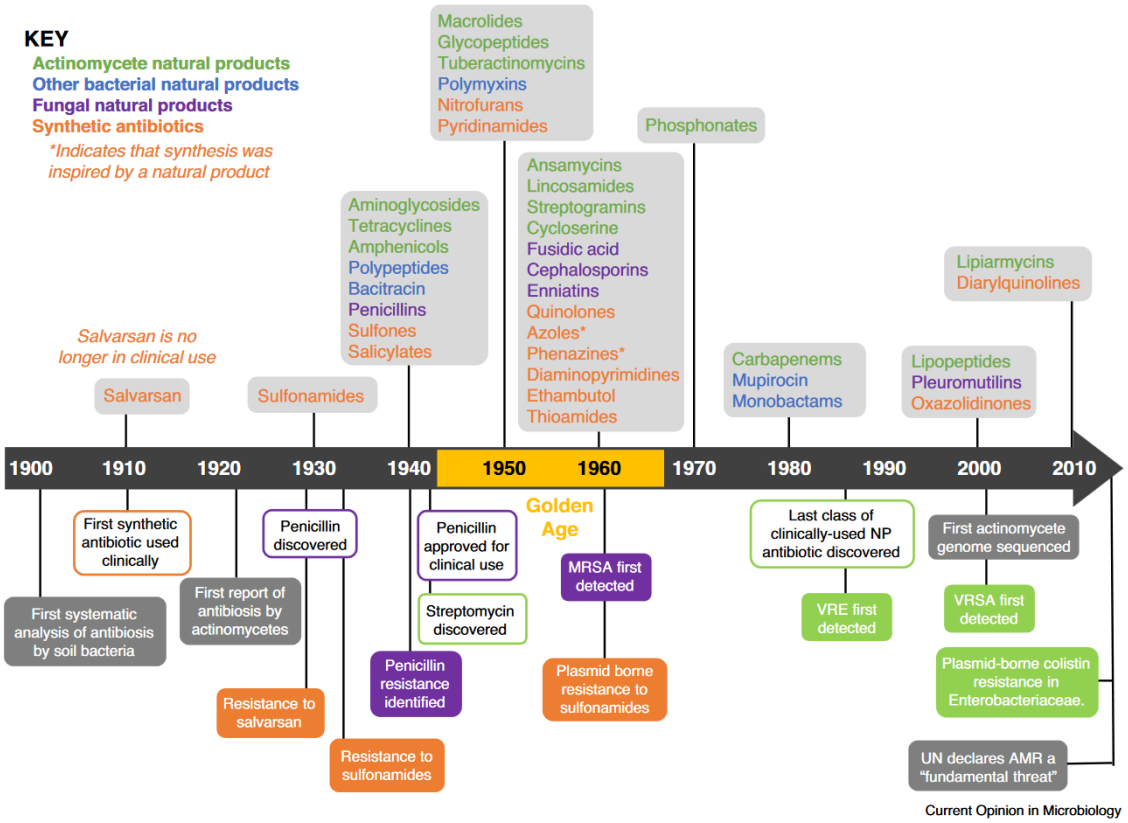


*Figure 1.2 Timeline of antibiotics discovery and resistance* [8]

Around the same time, in 1928, Alexander Fleming left his lab for a two-week vacation without cleaning his workspace, only to return to discover the *Penicillium* mould that allowed him to chance upon the well-known Penicillin[18,19]. The road from discovery to application first was aided by Howard Florey and Ernst Chain in isolating pure penicillin for investigation purposes[18,20,21]. The efforts done from then on, was realized by Norman Heatley, who pioneered the back-extraction technique (known mostly by organic chemists now as liquid-liquid extraction) of penicillin to enable extraction of large quantity of penicillin for clinical use[20,22–24]. It is obvious given the time penicillin was discovered, it became a crucial player in military medicine during the World War II. The power of antibiotics became apparent especially to the United States that they poured in resources in manufacturing penicillin for war use. Just for the preparation of the D-Day invasion of Normandy, a total of 21 U.S. companies produced a total of 2.3 million doses of penicillin in total[25]. The discovery of penicillin undoubtedly led to a Nobel Prize in Physiology or Medicine in 1945, awarded to Fleming, Florey and Chain, not including Heatley because it cannot be awarded to more than three recipient[26].

The discovery and wide use of penicillin marks the opening of the Golden Age of antibiotics discovery. In the 1950s to the 1960s, there was a surge in antibiotics being discovered and synthesized. The advancement in Science and Technology also allowed the development of synthetic derivatives of antibiotics discovered in nature[8,17]. Without understanding the

consequences of the misuse of antibiotics, the prescription and consumption of antibiotics increased during this period. Together with this, antibiotic resistance slowly creeped into the scene.

### 1.1.3 What is antibiotic resistance?

We mentioned the word 'antibiotic resistance' quite a few times, and how they popped up shortly after each antibiotic was discovered can be alarming if one knows what it implicates. In short, antibiotic resistance can be described as when the antibiotic administered is no longer effective in eliminating the infection it is intended for. Most of the time, there was a misconception that antibiotic resistance was observed like an 'on-off' switch, one day it works, and another it does not anymore. In fact, gauging antibiotic resistance requires the understanding of minimum inhibitory concentration (MIC), a technique developed by Alexander Fleming himself, together with the 'ditch-plate' method (Figure 1.3), he used to determine the MIC [19]. More methods have been developed to determine MIC more accurately since then, including liquid culture method, disc-diffusion test and E-test. Any student who took a Toxicology or Pharmacology class will be introduced first to this sentence '*dosis sola facit venenum*' ('The dose alone makes the poison')[27]. This is a great reminder that anything, given enough dosage, can become a poison. The same principle applies to antibiotics. When a compound is deemed successful as an antibiotic, that usually means that this compound, within a given range of concentration, has an antimicrobial effect and yet does not harm the host. With resistance, that means the concentration required to have an effect on bacteria has increased and may soon reach a point where it will not be usable for treatment without causing harm to the host. There are a few ways bacteria can achieve antibiotic resistance.

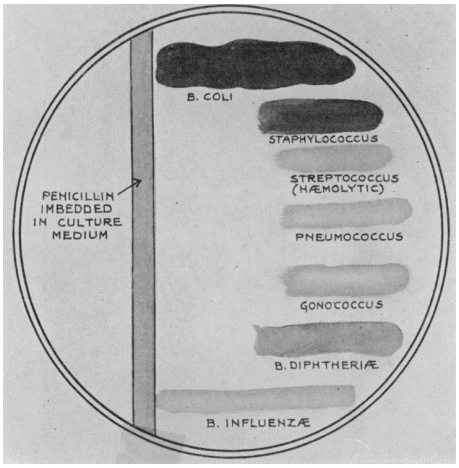

*Figure 1.3 Illustration of 'ditch plate' experiment by Fleming to determine MIC[19]*

### 1.1.4 Mechanism of action of antibiotic resistance

Molecularly, antibiotic resistance can occur through mechanisms in which they alter the pathway in which antibiotics work on bacteria[2,10,28–30] (Figure 1.4). Typical mechanisms include the modification of porin that allows the passing of antibiotics into the cell. Modification in its structure can block the entrance of some antibiotics. Another common target is the efflux pumps. Efflux pumps work as the route for molecules to exit the cell body. With modification on the efflux pump, the pump could be more efficient or less selective in the compound they allow out of the cell, hence keeping antibiotics in the cell at low or sublethal concentration. Resistance can also occur through modifying the target. For example, some antibiotics can bind to ribosomes and affect its protein synthesis pathway, by modifying their own ribosome to have less binding affinity to the antibiotics can confer resistance in bacteria. Bacteria can also acquire the ability to deactivate antibiotics by producing enzymes that can counter the

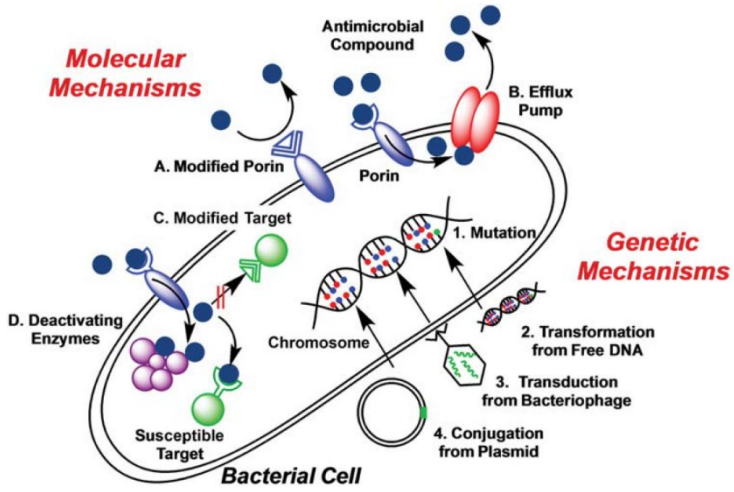


*Figure 1.4 Mechanisms of antibiotic resistance* [2]

antibiotics. One of the most known examples is β-lactamase. All these molecular mechanisms employed by bacteria in antibiotic resistance are closely linked to the acquisition of these abilities through genetic mechanisms. These will be explained in detail in Section 1.2. To add on to the resistance mechanism, more recent studies are also by focusing not just on single cell biology but population studies. It has been reported that collective behaviour of bacteria can also help bacterial population in resisting antibiotics, either through persistence cell or biofilm formation[31–36]. All these are interesting fields to investigate, and a proof of how little we know about the microbe world.

### 1.1.5 Epidemic of antibiotic resistance

Clinically, antibiotic resistance carries a much grimmer outlook. Emergence of resistant bacteria strains that should be kept at bay in humans means that the available treatment for infections are getting constraints. The concentration of antibiotics administered has to be increased, leading to the narrowing of the range of antibiotics concentration medical workers can work around before causing adverse effects in patients. The following excerpt reflects this situation aptly.

> *In 1941, 10,000 units of penicillin administered four times a day for 4 days cured patients of pneumococcal pneumonia. Today, a patient could receive 24 million units of penicillin a day and die of pneumococcal meningitis.*[10]

Moreover, emergence of resistant strains also means we are getting fewer options in patient management. In 2020s, as a human population, we have passed the Golden Age of antibiotics discovery[8]. In fact, while researchers are dabbling around derivatives of existing drugs, there was less new class of antibiotics being discovered. When we take the example of antibiotic resistance in *N. gonorrhoeae* (Figure 1.5), we can observe why this can be a problem. With the rise of antibiotic resistance, gonorrhea infection nowadays are no longer treated through monotherapy (using only one antibiotic). Instead since the 1980s, gonorrhea has to be treated with combination therapy for effective treatment. Up till now, healthcare workers have to resort to the combination of azithromycin (CRO) and amoxicillin (AZM) or doxycycline (DOX)[37]. This is given that the patient only have gonorrhea infection. With the nature of gonorrhea infection as a sexually-transmitted disease (STD), it is likely the patient comes with complications of other STDs, like Human Immunodeficiency Virus (HIV) and chlamydia. Given such situations, the spectre of a world with untreatable gonorrhea looms large[38–40].

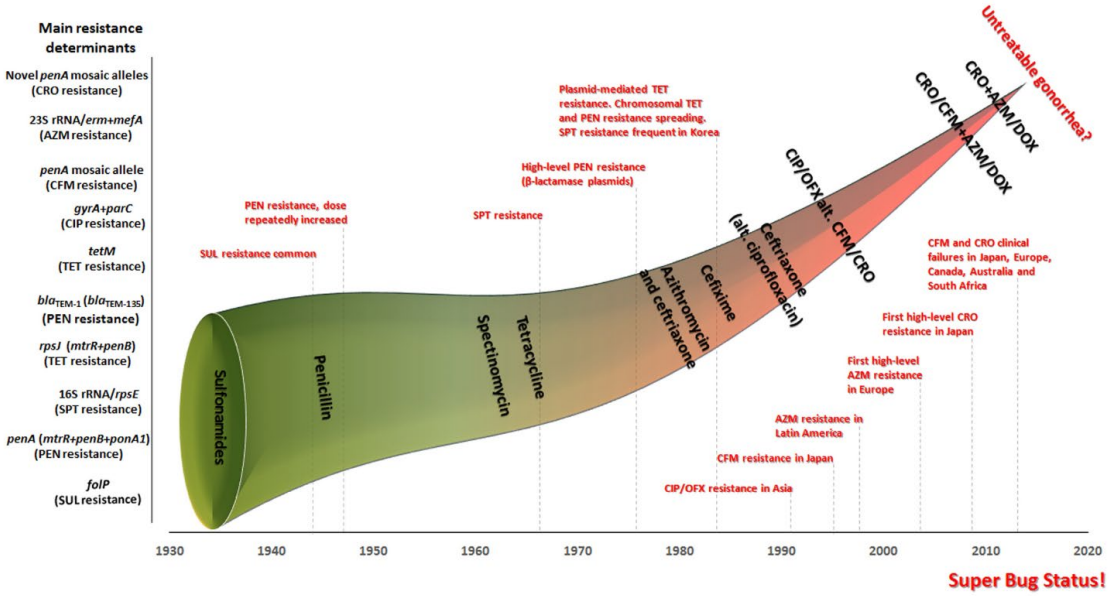


*Figure 1.5 Antibiotics resistance and treatment trend of gonorrhea infections over the year* [37]

With advancement of scientific research, we have learned a lot more about antibiotics resistance and its effect. Efforts have been put to reduce the amount of antibiotics administered unnecessarily. The public are also made more aware of the importance of consuming antibiotics responsibly and appropriately. The industry is more aware in producing consumer's products without the abuse of antibiotics[28]. Scientific research in infection management now expands across different fields, other than mining the nature for more antibiotics, we are now equipped with technological firepower to synthesize molecules against novel targets in bacteria[2,8]. Not only that, but other means of tackling infections are now being proposed, for example phage therapy[41–43], bacteriocins[44,45], probiotics[46,47], antimicrobial peptides[47–49], and microbiome-engineering[50,51], to name a few. Researchers are also working intensively to provide insights into antibiotics resistance to find ways to reverse or combat antibiotic resistance. This thesis, for example, is trying its best to do that.

## 1.2 Horizontal Gene Transfer

Similar to all other living organisms, bacteria have several means of sharing and maintaining their population genetic pool. One method to do that is through the inheritance of genetic material from parent to daughter cells, called vertical gene transfer[52]. The other method is by a process called horizontal gene transfer (HGT). In HGT, bacteria can share and transfer genetic information with the generations of bacteria that co-exist in the same population or community[53]. HGT is an essential process in prokaryotic evolution, working hand-in-hand with other processes like genetic drift, selection, and spontaneous mutation[53]. HGT can incite prokaryotic evolution through several different aspects, including driving catabolic dependencies in prokaryotes[54], tuning the conflict or cooperation dynamics between prokaryotes[55,56], eventually steering the evolution of microbiota[57], and having an impact on diseases-progression by the dissemination of antibiotic resistance traits among the population[58].

In nature, HGT is actually far more common that we first thought, even occurring rampantly in eukaryotes[58]. Yet, we still have very little understanding of the true mechanistic nature of HGT in prokaryote[59]. Hence, HGT has also caught the interest of many researchers, intending to crack the mechanisms of HGT in prokaryotes.

Conventionally, there are three main pathways of horizontal gene transfer in prokaryotes: (i) conjugation, (ii) transduction, and (iii) transformation. **Conjugation** is a process shared by bacteria and some archaea species[60]. In bacteria, it is usually described as bacterial sexual reproduction or mating due to the requirement of direct contact between bacteria and genetic information exchange. In fact, when conjugation was first discovered by Joshua Lederberg and Edward Tatum in 1946, it was simply observed as the ability of gene recombination in *Escherichia coli*[61]. In 1950, Bernard Davis, who was working with *E. coli* for the same purpose, expected to find a competence factor based on Avery's work in 1944[62,63]. However, he soon found out that unlike in *Streptococcus pneumoniae*, the 'genetic recombination factor' was not filterable and was later coined by Esther Lederberg as the fertility factor, F[62–64]. Nonetheless, science has moved forward since then, and the conjugation process has been illustrated further. The conjugation process requires the bacteria's ability to encode conjugation systems or mobile elements, including plasmids, conjugative transposons and integrative conjugative elements[65]. One of the more well-known examples of conjugation is the F-pilus in *Escherichia coli*. During conjugation, the donor cell expresses F-pilus and attaches to the recipient cell[66,67]. This act brings the two cells close together. The mobile plasmid from the donor cell will then be nicked and separated into single-stranded DNA (ssDNA). One of the ssDNA will then be transported through the pilus into the recipient cell. Because this process happens entirely within the hollow F-pilus, conjugation is described as DNase resistant, similar to that of transduction, which will be discussed later in this section. After successful transport of the ssDNA, both cells will synthesize the complementary strand for the ssDNAs now existing in both cells, resulting in a complete plasmid. The pilus may break at this point, and the two cells will separate. With the newly-acquired plasmid, both cells can now act as F-factor donors. In summary, conjugation is the exchange of genetic material, usually a conjugation plasmid, and requires contact between two bacteria through conjugation pili. Unlike conjugation, the requirement for physical contact between two bacteria is absent in transduction.

**Transduction** was first discovered and characterized in *Salmonella* by Norton Zinder and Joshua Lederberg in 1952[68]. Not requiring contact between donor and recipient bacteria cells, transduction requires the aid of a virus or viral vector instead. Generally, there are two types of transduction: generalized and specialized transduction(Figure 1.6)[69]. The type of transduction performed depends on the type of virus, for example, bacteriophages P1 and P22 can perform generalized transduction, while λ bacteriophage can perform specialized transduction[69]. In the case of bacteriophage Mu, on the other hand, can perform both types of transduction[69]. These processes occur through the different life cycles of the virus, the lytic cycle and the lysogenic cycle[69]. In generalized transduction, the bacteria host DNA is broken down, and part of the DNA is packed in the new viral particle before their following transfection. In specialized transduction, however, the virus goes through a lysogenic cycle by integrating its genetic

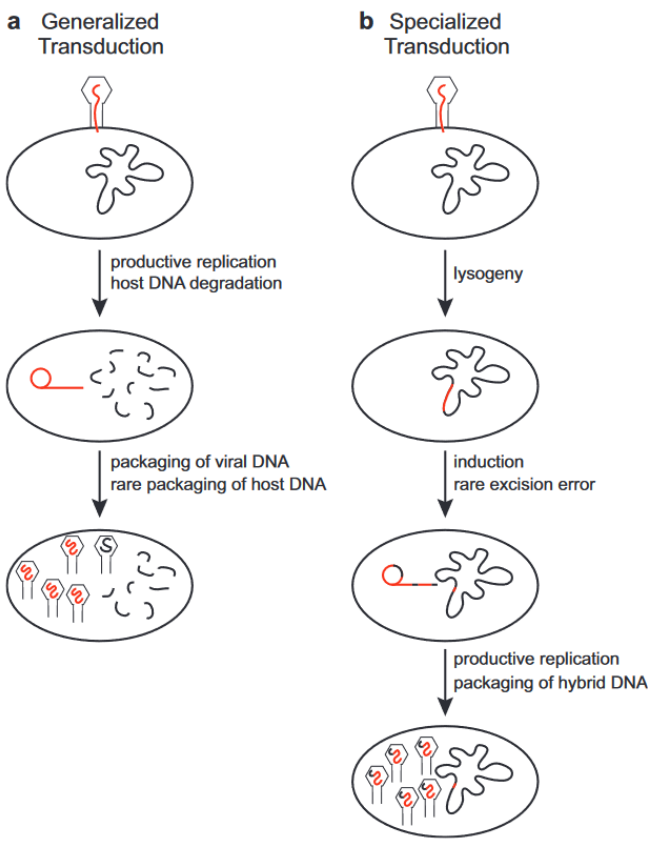


*Figure 1.6 Different types of transduction*[68]

material into the bacterial genome. So, in the later part, when the viral genome is reconstituted into the new viral package, part of the bacterial genome will be restricted and packed together with the viral genetic material. Studies on transduction have also flourished along the years, contributing not only towards the understanding of HGT, but also used as tools for genetic manipulation in bacteria. The work on conjugation and transduction resulted in Joshua Lederberg winning The Nobel Prize in Physiology or Medicine 1958. Together with George Beadle and Edward Tatum, they were awarded the prize for showing DNA as the genetic material that can be expressed as an enzyme, and these genetic materials can be transferred to other bacteria through conjugation and transduction[70]. Transformation, however, was the earliest to be discovered and also the only one that was never awarded a Nobel Prize.

Way before the discovery of conjugation in 1946 and transduction in 1952, in 1928, Frederick Griffith described how the non-virulent *Streptococcus pneumoniae* could up a specific **"Transforming Principle"** from heat-killed *S. pneumoniae*, leading to virulence[71]. His colleagues later confirmed this work in vivo and in vitro[72,73,73]. However, it took years and combinations of discovery from other HGT pathways for Oswald Avery, Colin MacLeod, and Maclyn McCarty to later confirm this "Transforming Principle" as DNA[62]. What we know as natural transformation today is the process of bacteria acquiring genetic material from their environment sans contact with other bacteria. Usually, bacteria that can perform natural transformation are described as naturally competent. This ability stems from the expression of DNA uptake machinery. Interestingly, DNA uptake machinery is also one of the most-conserved system in Gram-positive and Gram-negative bacteria[74,75]. In Gram-negative bacteria, there are two systems for DNA uptake: Type II Secretion System (T2SS) and Type IV Pili (T4P)[75]. These two systems are highly conserved and are of close homologs[76]. Since these nanomachines are essentially extracellular appendages binding to extracellular molecules before uptake, meaning the DNA molecule is exposed to the extracellular environment before being transported into the cell body. Therefore, natural transformation is also the only one out of the three HGT pathways that is not protected from DNAse. Other than possessing the machinery necessary for DNA uptake, natural transformation also relies on the bacteria's

competence status. Not all bacteria are constitutively competent. Some bacteria only induce competence under specific nutrient or growth conditions[77]. There are also gaps in knowledge in terms of the fate of the DNA after transformation as there is hypothesis of them being used as nutrient[78]. These are knowledge that will push the frontiers of biotechnology, medical applications and scientific research. Therefore, it is still an excellent venue for research and to find the correct requirements for competence in different bacteria.

In recent years, a few studies emerged suggesting new pathways towards HGT other than the three conventionally described pathways[53]. These new suggestions revolve around the assistance of vesicles, nanotubes and phage-like gene transfer agents to disperse genetic materials among the populations(Figure 1.7)[79–82]. However, there is much to study to provide a concrete review of these processes. Even for the three conventionally recognized HGT pathways, while these pathways had been illustrated quite some time ago, many of their mechanisms are still not known. However, the incomplete knowledge of these pathways did not stop scientists and inventors worldwide from using this information. The ability to transform DNA into bacteria in various ways has since been exploited in fields like synthetic biology, drug production and molecular biology research. For example, instead of natural competence, many of the molecular biology techniques used in the laboratory are artificially inducing competence in bacteria. These include heat shock and electroporation, which chemically and physically transform the bacteria. Yet, with the scope of HGT's application on biological advancements, it is remarkable that we are still very far from fully understanding the process.

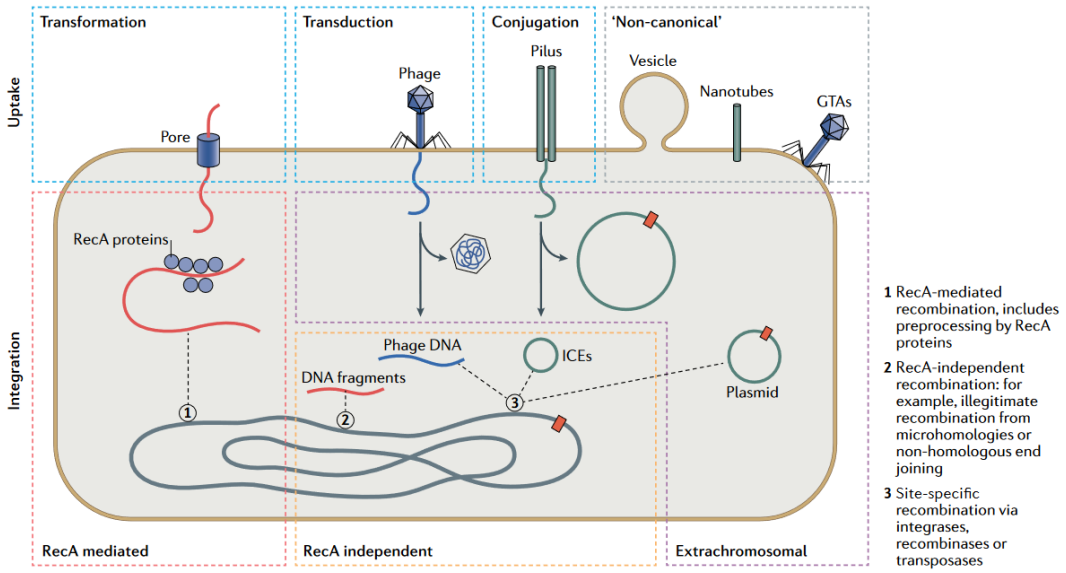


*Figure 1.7 Illustration of the DNA uptake and integrate pathways in bacteria.* [53]

In this thesis, we intend to contribute a small brick to this house of knowledge. We focus on natural transformation in *Neisseria gonorrhoeae*. In the following sections, we will illustrate more on natural transformation in the context of this bacteria.

## 1.3 *Neisseria gonorrhoeae*

### 1.3.1 Discovery

Gonorrhea is one of the oldest sexually-transmitted diseases (STD) dating from the ancient Greek and Chinese eras[83]. However, the records on gonorrhea then were ambiguous and may have been misreported with other STDs[83]. It was in 1879 when its causative agent, *Neisseria gonorrhoeae,* was discovered as a bacteria and coined by Albert Neisser, whose lab also developed the first vaccine against *N. gonorrhoeae*[83,84]. Following that, Leistikow and Bumm succeeded in growing *N. gonorrhoeae* in culture media in 1882 and 1885, respectively[83]. In 1906, Muller and Oppenheim, using gonococcus as an antigen, successfully diagnosed gonorrheal arthritis using a complement-fixation test, the first recorded[85]. Due to its clinical relevance, techniques to culture *N. gonorrhoeae* continue to improve, usually as a variety of salt veal agar[86–89]. It was soon recognized that since diagnosis at that time relied solely on culturing, the major drawback in this protocol was that the diagnosis could only be done within the proximity of a well-equipped laboratory. To overcome this drawback, the transportation system for *N. gonorrhoeae* has been devised[90]. One of the earliest transport media, Stuart's medium, was formulated at that time[90]. This medium has also been improved[91]. With advancements in scientific methods, diagnosis for the presence of *N. gonorrhoeae* is no longer limited to culturing. Methods like nucleic acid detection and serological typing are also commonly used[92].

### 1.3.2 Pathogenesis

*N. gonorrhoeae* is the bacteria that causes gonorrhea infection, the second most common human STD, with worldwide yearly new cases of around 100 million[93]. The infection mainly occurs in the urogenital tracts, as an infection specific only in human species. Gonorrhea infection can be symptomatic and asymptomatic. For symptomatic infections, gonorrhea can lead to severe effects, including pelvic inflammatory disease and infertility[94]. Although gonorrhoea infections are usually treatable, if left untreated, gonorrhoea infections can lead to serious problems. For example, untreated gonorrhea infection can lead to its spread into the blood circulatory system, causing disseminated gonococcal infection, which can be life-threatening[94–96]. If a child was born through a birth canal infected with gonorrhea, the newborn could have ophthalmia neonatorum. This disease was noticed as early as 1914 in England and Wales[83]. When a patient has an asymptomatic gonorrhea infection, the infection usually resolves naturally, but they can also unconsciously become a carrier of *N. gonorrhoeae*.

Due to the dual nature of gonorrhea infections and its status as an STD, the pathogenesis of N. gonorrheae is frequently studied. The inoculation and colonization of *N. gonorrhoeae* is commonly found in the mucosal layer of urogenital areas in humans. There were a few cases in which *N. gonorrhoeae* was isolated from nasopharyngeal, anal and ocular mucosa[97]. Colonization of *N. gonorrhoeae* is usually linked with the presence of Type IV Pili (T4P), opacity protein (Opa), the major porin (PorB) and lipooligosaccharide (LOS)[94–96,98,99]. The initial colonization process involved the adherence of bacteria to the epithelial layer with the

help of T4P and Opa (Figure 1.8). T4P is known to equip adhesins that can interact with receptors on epithelial cells. Meanwhile, Opa can interact with carcinoembryonic antigen-related cell adhesion molecules (CEACAMs) and heparan sulfate proteoglycans[100,101]. This attachment not only brings closer the distance between host and pathogen, it also protects the bacteria from shear stresses.

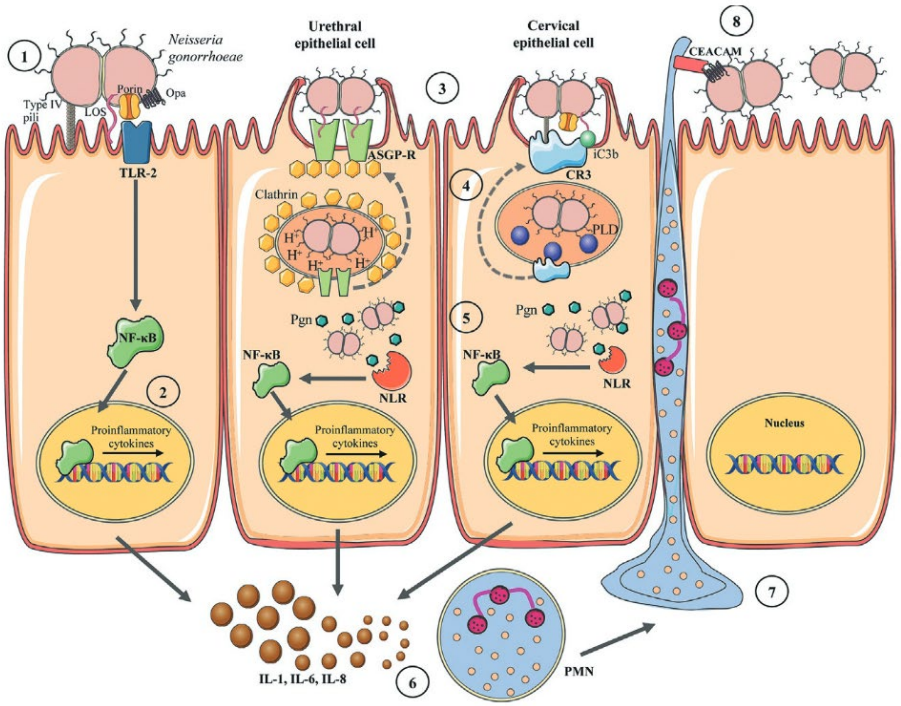


*Figure 1.8 Epithelial cell adherence and invasion by Neisseria gonorrhoeae.*[94]

From an immunology point of view, gonorrhea colonization kickstarts a series of immune responses. *N. gonorrhoeae* can bind to polymorphonucleocytes (PMSs) through opsonic and non-opsonic mechanisms. However, due to mechanism from *N. gonorrhoeae* itself, for example, pilin antigenic variation (a recombination process that can result in different types if pili subunit) and the sialylation of LOS, phagocytosis mainly occurs through the non-opsonic pathway. From the *N. gonorrhoeae* side, *N. gonorrhoeae* can sometimes evade macrophages and the complement system. To evade macrophages, *N. gonorrhoeae* possesses a few strategies. Since *N. gonorrhoeae* is often an intracellular pathogen, one of the major intracellular PMN-killing mechanisms is generating reactive oxygen species (ROS) against *N. gonorrhoeae*[94,96,102–105]. However, *N. gonorrhoeae* has developed some mechanisms to resist oxidative extracellular killing and anti-oxidant defence mechanisms. To prolong its intracellular survival, *N. gonorrhoeae* can also delay the fusion of primary granules leading to delayed phagolysosomal maturation and avoid non-oxidative killing by neutrophils. To survive the complement system, *N. gonorrhoeae* can bind to the Complement component(C4b) through PorB protein and evade killing through this pathway[94–96,106]. Its ability to sialylate LOS can also inhibit complement cascade and evade host response. In the adaptive immune response, *N. gonorrhoeae* can suppress adaptive immune response through the induction of IL-10 and Transforming growth factor beta (TGF-β) production. The induction of TGF-β suppresses the Type I T helper cells (Th1) and Type II T helper cells (Th2)[107].

Taken together, GC infection can lead to an immune response through different pathways. However, the evolutionary dependence between the host and pathogens has also resulted in its ability to hijack the host's adaptive immune response and prevent the formation of immunological memory. Therefore, it is always important to consider the co-evolutionary and co-dependency relationship between *N. gonorrhoeae* and the hosts when studying on this bacteria.

### 1.3.4 Natural Transformation in *Neisseria gonorrhoeae*

Natural transformation is one of the main pathways *N. gonorrhoeae* achieve horizontal gene transfer. With that, *N. gonorrhoeae* is described as being naturally competent[77,108–111]. Being naturally competent may mean that the bacteria can take up DNA molecules from the extracellular environment. Still, some naturally competent bacteria require specific cues or conditions to kickstart their competence status. This, however, is not the case in *N. gonorrhoeae*, which maintains its competence throughout its life cycle. *N. gonorrhoeae* can pick up extracellular DNA and transport it across the cell body. The binding of a DNA molecule to the pilus and its subsequent retraction is supposed to be the first step of a series of coordinated molecular events culminating in the DNA molecule getting within the bacterial cytoplasm and ultimately integrated into the genome if enough homology exists[112–114]. Pili and pseudopili are distinguished based on the extent of the extension of the appendage outside of the bacterial cell[115]. Yet all these structures have a very close evolutionary relationship (now generally under the umbrella term type IV filaments[114,116]) and are a common feature of natural transformation.

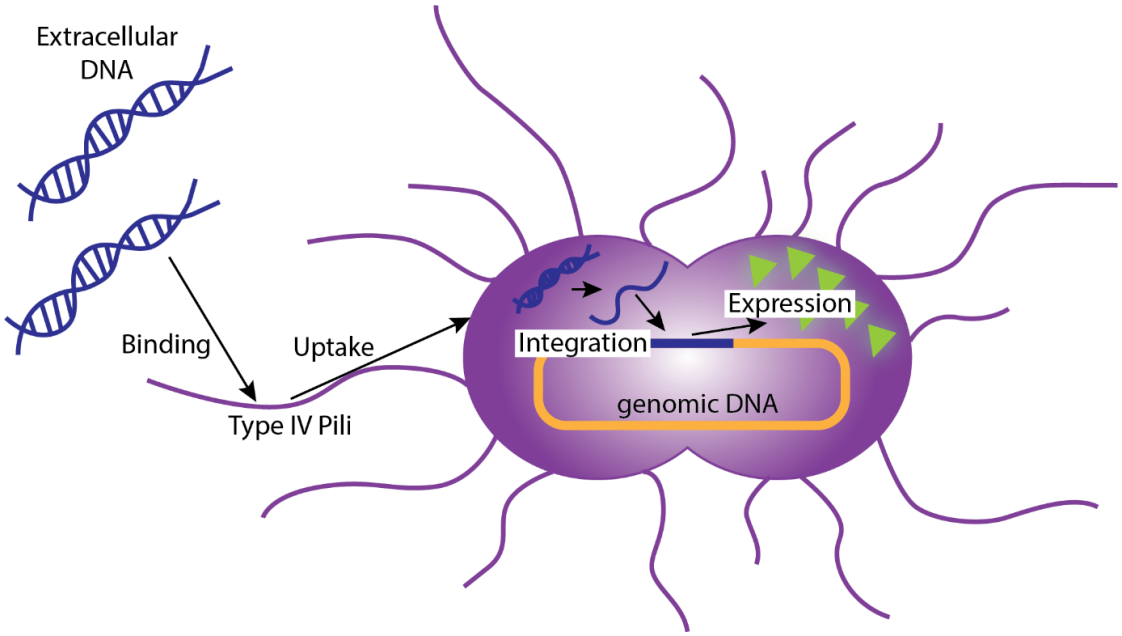


*Figure 1.9 A simplified illustration of DNA transformation in Neisseria gonorrhoeae*

In *N. gonorrhoeae*, natural transformation is done largely through Type IV Pili[117]. It is an extracellular appendage of *N. gonorrhoeae* that is constitutively expressed in the bacteria throughout their life cycle. The transformation process occurs by binding DNA molecules to Type IV pili. As the dynamical Type IV Pili retracts, it pulls the DNA molecule past the outer

membrane through PilQ into the periplasmic space. Though, study on the dynamics of intake of DNA molecules still argues for pili retraction not being the sole structure to mediate DNA uptake in the periplasm[118]. Studies point to the process of separating the DNA double helix in periplasmic space into single-stranded DNA (ssDNA)[119–121]. These ssDNA are then bound with DprA protein and transported across the inner cell membrane with the help of ComE protein[122–125]. The ssDNA is then free to recombine with the genomic DNA(gDNA) if there is enough homologous region. This process occurs similarly to the DNA repair and recombination pathway, involving proteins like RecA, RecB, RecC, RecQ, and RecO. Successful recombination sometimes results in a mutation, whether point mutation, insertion or deletion. These genomic alterations sometimes will result in meaningful consequences, for example, the acquisition of antibiotic-resistance genes. These mutations will also be maintained as the cell divides into daughter cells.

## 1.4 Type IV Pili

The outer surfaces of bacteria are the first contact bacteria have with their extracellular environment. One can find extracellular appendages on these outer surfaces in prokaryotes and even in Archaea. These extracellular appendages are polymeric organelles consisting of monomeric subunits. Depending on their structural differences, they are categorized into flagella, injectisomes, or pili[126,127]. This thesis will focus on pili, specifically the Type IV Pili.

Other types of pili besides Type IV Pili are mostly put in the same category because of their hair-like structure protruding from the cell surface. In Section 1.2, we discussed briefly about conjugative pili. Other pili include fimbrae and curli. In *Neisseria gonorrhoeae*, the main extracellular appendages one can find is the Type IV Pilus.

Type IV Pili are ubiquitous among prokaryotes and most archaea[126–130]. The pervasiveness of this system across the phylogeny tree hints towards its functional importance. In bacteria, Type IV Pili can play several roles in twitching motility, pathogenesis, mechanosensing[131–135], and DNA uptake[116,129,136–138]. From an evolutionary point of view, Type IV Pili come from the Type IV Filament (T4F) family that also houses Type II Secretion Systems (T2SS), likely evolved from a single common ancestral structure[136]. Being in the same family, they share the component homology of their nanomachines (Figure 1.10). However, Type II Secretion Systems are only found exclusively in Gram-negative bacteria, while Type IV Pili can be found in both Gram-negative and Gram-positive bacteria[139].

Type IV Pili systems have similar core proteins: the major pilin subunit that makes up the majority of the pili, prepilin peptidase that processes prepilins into mature pilins before incorporation into the pili, the ATPases involved in assembly and disassembly of the pili, the inner membrane protein complexes involved in pili assembly and an outer membrane protein that serves as a secretin channel for pili to go through into the extracellular space. There are three main classes of Type IV Pili: Type IVa (T4aP), Type IVb (T4bP), and Type IVc (T4cP, Tad) (Figure 1.11). Each type of Type IV Pili in different species may differ slightly in their sequences, but they do share structural homology. There is still some debate on the

classification of Type IV Pili. In general, there is T4aP, and either T4bP and T4cP are separated, or they are grouped under the same umbrella. T4aP are relatively homogenous and commonly found, whereas the others are diverse and less well characterized. Compared to other pili classes, T4aP genes tend to spread throughout the genome in several operons, too. The other distinction between T4aP and T4bP is the length and sequence of the leader peptides[126]. T4aP typically has around six residues for the leader sequence, whereas T4bP has around 15-30 residues. The resulting mature sequence of T4bP is also larger than T4aP. We will discuss more on pilin processing in Chapter 5.

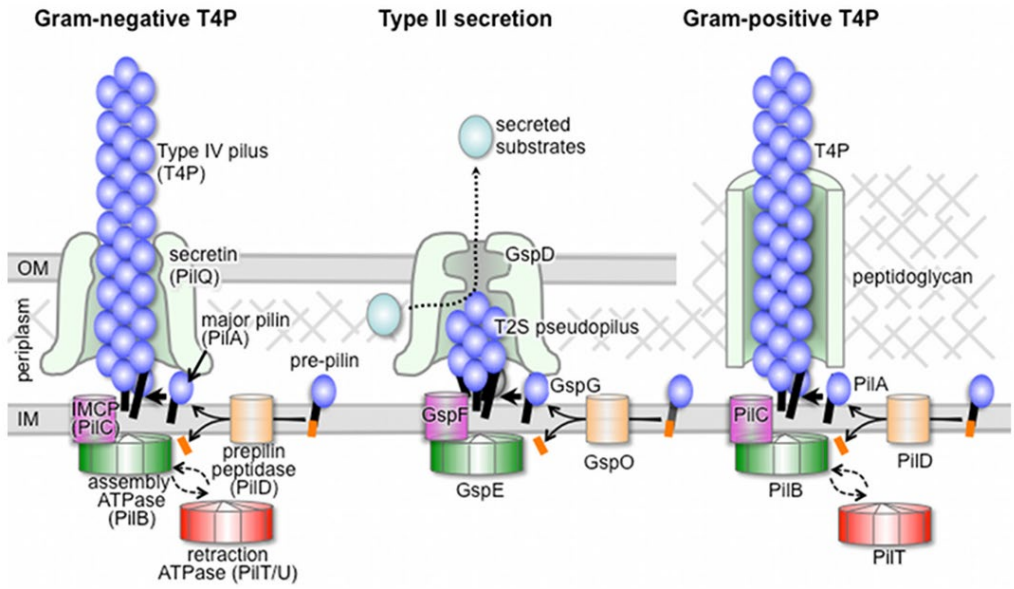


*Figure 1.10 Illustration of key components in the Gram-negative T4P and T2S systems and the Gram-positive T4P system and their localization in the bacterial envelope.* [130]

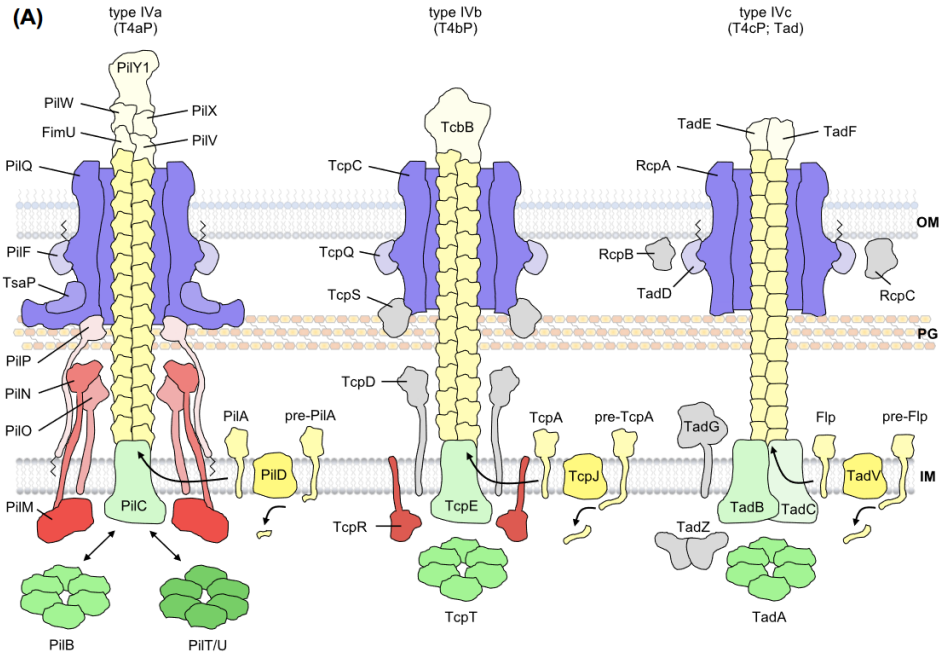


*Figure 1.11 Protein composition and architecture of the three subgroups of type IV pili (T4P): type IVa (T4aP), type IVb (T4bP), and type IVc (T4cP), also known as Tad.* [129]

This thesis works focuses on Type IV Pili in *N. gonorrhoeae*. Coincidentally, as of today, there is only one type of known Type IV Pili in *N. gonorrhoeae*, T4aP. Therefore, from here onwards, unless mentioned otherwise, all Type IV Pili discussed refer to T4aP-class Pili. It is also important to note that the nomenclature of Type IV Pili-associated protein can differ between bacteria species, as shown in Figure 1.12. In the remainder of this thesis, we will use the nomenclature specific to *Neisseria* species.

| T4a minor pilins | | | T2SS minor pseudopilins | | |
|---|---|---|---|---|---|
| *Pseudomonas* | *Escherichia* | *Neisseria* | *Pseudomonas* | *Escherichia* | *Vibrio* |
| FimU | ppdA | PilH | GspH | XcpH | EspH |
| PilV | ppdC | PilI | GspI | XcpI | EspI |
| PilW | ppdB | PilJ | GspJ | XcpJ | EspJ |
| PilX | ygdB | PilK | GspK | XcpK | EspK |
| PilE | N/A | PilX/L PilV | N/A | N/A | N/A |
| PilY1 | N/A | PilC2 | N/A | N/A | N/A |

*Figure 1.12 The different nomenclature of the same homolog across different bacteria species. Note: There are PilC1 and PilC2 in Neisseria* [140]

### 1.4.1 Type IV Pili in *N. gonorrhoeae*

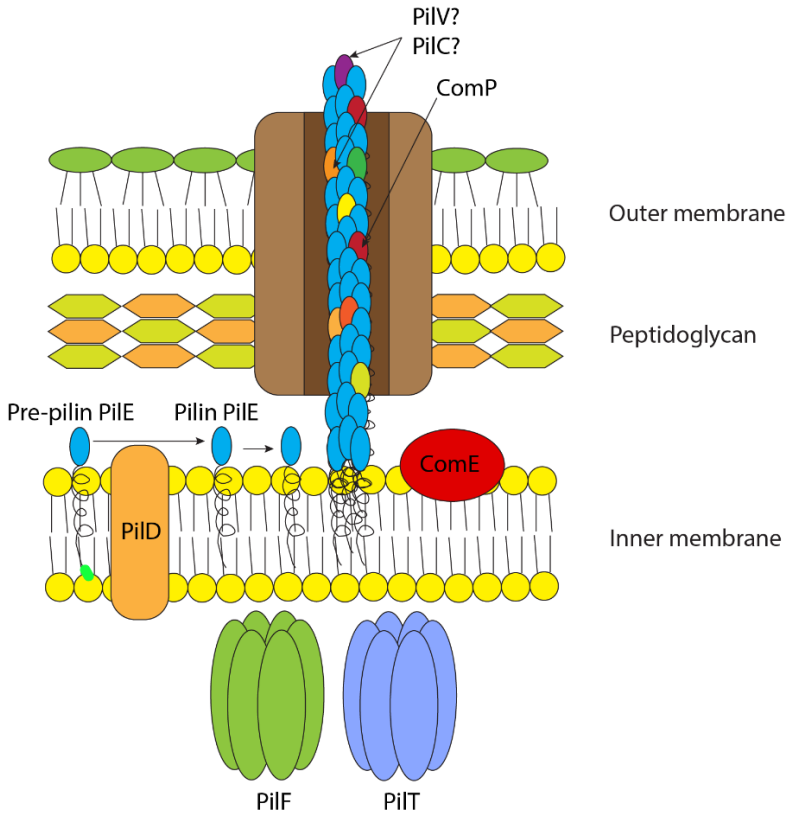


*Figure 1.13 A simplified illustration of Type IV Pili machinery in N. gonorrhoeae*

In *N. gonorrhoeae*, there is currently one known type of Type IV Pili**, Type IVa Pili.** Yet, this sole type of Type IV Pili is responsible for many functions, beyond transformation: adhesion, motility and pathogenesis[141–144]. Type IV Pili machinery include the pili and an assembly of protein in the system. These proteins are encoded by gene in several different locus in the genome. There are some components of the Type IV Pili come as a gene cluster, for example, the core protein PilM, PilN, PilO, PilO, and PilQ are clustered together. Each of the component locations can be found in the Genomic locations (see link).

Prior to pili biogenesis, the major pilins, PilE and other minor pilins, are expressed as prepilins. They are then processed before being incorporated into the pilus at the base of the core protein. The pili that is assembled with the help of core proteins and ATPases, PilF, will elongate and protrude to the extracellular space through the secretin channel PilQ, that span across outer membrane and peptidoglycan through its N0, N1 and N2 domains[145,146]. In *N. gonorrhoeae*, Type IV Pili are expressed throughout their life cycles and can represent as much as 100 µm of pili per cell[147]. The retraction of pili can be achieved with the help of ATPases, PilT[148], situated at the base of the machinery, near the inner membrane. As that happens, pili retracts and disassembled with the subunits of pili dissociates from the main pili[149,150]. There is still much to investigate on what happened to these dissociated pilins after pili retraction and on the parameters controlling the pili dynamics as a whole. We will introduce briefly a few components of Type IV Pili that will be studied throughout this thesis: **PilE, PilV, PilC, and PilD**.

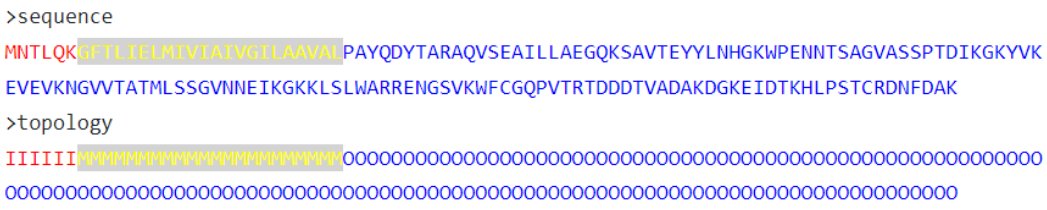


*Figure 1.14 Prediction of PilE protein using transmembrane protein prediction server, CCTOP.*

As described, the major pilin, **PilE**, are expressed first as prepilins. With the recognition of their leader peptide towards the Sec machinery, these prepilins are translocated to embed at the inner membrane. The N-terminal leader peptide is then cleaved by prepilin peptidase, PilD, which recognizes the GFTLIE motif and cleaves after the glycine. The cleaved pilin is then methylated at the N-terminus into what we know as mature pilin. In fact, there are also studies recognizing these are not the only modification PilE has to undergo at the cell surface, glycosylation or phospho-form modification has been reported. From structural studies, we know that the pilin PilE has a 'lollipop'-shaped tertiary structure. The N-terminal of the PilE is alpha-helix in structure, divided into the α1-N region and the α1-C region. As predicted through the transmembrane protein prediction server, CCTOP, the first 20 amino acids in α1-N are hydrophobic and hence are predicted to be the transmembrane domain (Figure 1.14). The Proline at the 22nd amino acid (P22) residue right after the predicted transmembrane domain can be the location for a kink allowing the whole alpha helix domain to bend. The P22 residue could be an interesting aspect of Type IV Pili to study its evolutionary impact since it is highly conserved throughout phylogenetic tree, reported well not just in *N. gonorrhoeae*[151], but also *Neisseria meningitidis*[152], *Pseudomonas aeruginosa*[153,154] and *Geobacter sulfurreducens*[155]. At the C-terminal segment forms the signature 'lollipop' head, consists of the α-β roll structure. This region is also known as the 'hypervariable region' that enables *N. gonorrhoeae* to evade host immune response[156,157].

Other than the major pilin, Type IV Pili are composed of minor pilins, that incorporated into the pili in small amount. Some of them include ComP, PilC, and PilV.

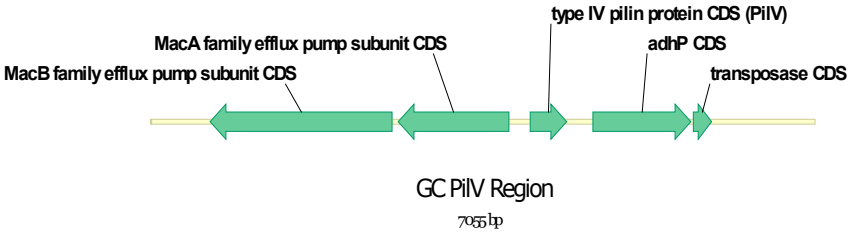


*Figure 1.15 Region around pilV ORF in MS11*

During the course of this thesis, **PilV** is one of the least studied minor pilin in Type IV Pili. The genomic location of the *pilV* gene, which transcribes into minor pilin PilV, was identified in earlier studies through screening open reading frame (ORF) in the FA1090 genome for a sequence sharing identical N-terminal sequence as PilE[158]. This method has been used similarly before to identify another minor pilin, ComP[159]. The basis of this method stems from the fact that many major and minor pilins in *N. gonorrhoeae* shared the same 'Type III' signal sequence that could be recognised by prepilin peptidases[126]. With the help of sequencing and annotations from other studies, we could identify the location of ORF in the *N. gonorrhoeae* MS11 genome. MS11's *pilV* coding sequence (CDS) is located at 1479624-1480013 (Figure 1.15). Additionally, the *pilV* gene is not located near any other Type IV Pili-related locus.

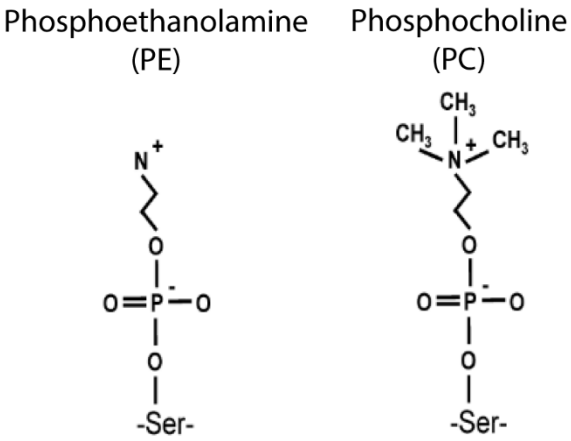


*Figure 1.16 Phosphoethanolamine (PE) and phosphocholine (PC)*

Function-wise, earlier studies identified PilV as a Type IV Pili-associated protein playing an essential role in epithelial cell adherence. Subsequently, PilV mutants are also shown to affect the macro- and micro-heterogeneity of Type IV Pili by affecting the phospho-form modification of the major pilin PilE. The study showed that ΔPilV mutant have a heterogeneous PilE modification with a mixture of phosphoethanolamine (PE) and phosphocholine (PC) (Figure 1.16)[160–162]. This is in contrast to wild type strain where PilE will undergo multisite, covalent modification of PE[162]. These alterations in PilE modification can affect the colonisation ability and are hypothesised to affect the sub-localisation of pilin in *N. gonorrhoeae.*

Other than its role in adhering to epithelial cells[158,163], removing PilV in *N. gonorrhoeae* leads to **enhanced competence**[164]. PilV's role relating to competence and DNA binding was briefly described as a DNA binding inhibitor by acting as an antagonist to ComP[164]. This phenotype encourages researchers to utilise ΔPilV as a powerful tool to study DNA uptake due to it producing heightened signals compared to the Wild Type[118,120,165]. Beyond that, the role of PilV is largely understudied. Studies on PilV in other bacteria are also quite limited and mostly limited to its adhesion properties, especially in *N. meningitidis* [163,166]. In this thesis, other than

using ΔPilV as a tool to study DNA uptake, we performed a series of investigations to understand its role.

Another minor pilin that we will also study in this thesis is **PilC**. The hypothesis of PilC's involvement in T4P biogenesis, cell adherence to epithelial cells, and transformation competence came into light when it was first studied for its adhesion activity, one of the important properties in bacterial pathogenesis[167–171]. At first, cell adhesion study observed strains expressing pili with different binding properties, for example, the 'α-pili', that bind human erythrocytes and buccal epithelial cells[172], and 'β-pili', that bind to Chang conjunctiva epithelial cell line[173]. It is postulated that these observations result from pili variants, which is what we know today as the variation of PilC protein[169,172].

Initially identified as a 110kDa outer membrane protein, Jonsson et al. identified two complete copies of pilC in the *N. gonorrhoeae* genome: pilC1 and pilC2[174–176]. A chromosome mapping experiment speculated a locus showing partial homology to a region in pilC2, tentatively termed pilC3[169]. However, Rudel and Meyer deemed this region insignificant[169]. PilC adhesion with epithelial cells interact in a CD46-independent manner[171]. It is hypothesised that the host cell receptor for PilC is a surface protein and is endocytosed together with the PilC protein via receptor-mediated endocytosis, and recycled later on[171].

In this thesis, we focus more on the role of PilC in **pili biogenesis** and **competence**. PilC was at first stipulated to be necessary for adherence but not pili assembly[169]. Later on, when PilC was shown to be located at the membrane and tip of Type IV Pili, its role in pili biogenesis was first suggested[169,170,174]. Studies show that knocking out either *pilC1* or *pilC2* does not affect pilin expression in *N. gonorrhoeae*, but double mutant *pilC1 pilC2* does express low levels of pilin[174]. However, the investigation of PilC in *N. gonorrhoeae* was limited to these.

Studies of PilCs is also common in *N. meningitidis* and *Pseudomonas aeruginosa*. In *N. menigitidis*, their two copies of PilCs affect piliation and adhesion[177,178]. The understanding of PilC is *N. meningitidis* also include finding out that there is a contact-dependent regulation of PilC1[179,180]. There is also study suggesting the possibility of conformational specificities in the N-terminal region of PilC1 contributing to its adhesive properties[176], a property that is similarly found in the PilC of *Pseudomonas aeruginosa*, PilY1.

In *P. aeruginosa*, PilY1 is proposed and proved as an adhesin through atomic force microscopy (AFM)[181]. Structurally, there was a mechanosensitive Von Willebrand (vWA) Factor-like domain in the PilY1 N-terminal region [181]. Mutation in the vWA domain in PilY1 results in lower surface adhesion force, c-di-GMP signalling, and biofilm formation[135,182]. In particular, a cysteine mutation (C152S) was identified to separate its role in twitching motility and surface-sensing signalling[135,182]. This prompted the hypothesis that cysteine in vWA plays a role in the domain's mechanosensitive property, which also suggested how the diversity of cysteine amino acids in PilY1 vWA of different strains explained their different adhesion strategy[135,182]. This interesting evolutionary aspect of PilY1 within its own species can also be seen across bacteria species.

One of the interesting similarities between bacteria expressing PilC or its homolog is the C-terminal domain. The crystal structure of the C-terminal domain of PilY1 in *Pseudomonas aeruginosa* revealed a beta-propeller fold and a novel calcium-binding motif[183]. In *Kingella kingae*, while the calcium-binding was dispensable for piliation, it was necessary for twitching motility. Another interesting example of the evolutionary aspect of PilC was that there are surprising similarities between PilC homologs across species. For example, *N. elongata* and *K. kingae*, being members of *Neisseriaceae*, share more PilC1 and PilC2 similarities with *Pseudomonas aeruginosa* compared to *N. gonorrhoeae* and *N. meningitidis*[184]. Nonetheless, as a preliminary study on PilC in *N. gonorrhoeae*, our thesis focuses on PilC focuses on its role in pili biogenesis and competence.

Other than the two minor pilin being studied, our thesis also perform some investigation on **PilD**, the prepilin peptidase. As briefly introduced, Type IV Pili pilins are expressed as precursors with six or seven amino acids N-terminal leader peptides[185]. The presence of N-terminal leader peptides in pilins is the same across many species with Type IV pili, including *Pseudomonas aeruginosa*, *Neisseria gonorrhoeae*, *Bacteroides nodosus*, and *Moraxella bovis*[185]. The maturation of prepilin to pilin involves two processes: the proteolysis that removes the leader sequence and subsequent methylation of the N-terminal of the cleaved protein[186]. The cleavage of the leader sequence is crucial for the translocation of mature pilin but not the methylation[187,188]. This protein involved in this maturation process of pilin was identified as PilD[189]. An earlier structural study on *Pseudomonas aeruginosa* PilD predicts it to be very hydrophobic with at least five membrane-spanning segments based on its most likely sequence [189]. It was later confirmed that the location of PilD is in the cytoplasmic membrane[185].

The prime focus of the PilD function was initially on its **peptidase activity**. In *P. aeruginosa*, the pilin subunit precursor has six residue leader peptide sequences, which are signal peptides[185,187]. This leader sequence and the next 30 amino acids share the same homology with prepilins in Gram-negative pathogens. In an in vitro experiment, *P. aeruginosa* and *N. gonorrhoeae* prepilins were cleaved when incubated with the total membrane of mutant overexpressing PilD with dependence on cardiolipin in-vitro[185]. When heterologously expressed in *Escherichia coli*, other than cleaving prepilin from its own species, *Neisseria gonorrhoeae* PilD can also cleave prePulG, a Type IV-pili like protein in *Klebsiella oxytoca*[190]. In the same study, PilD could also partially complement a mutant PilO strain, in which PilO was a prepilin peptidase-like protein involved in PulG-PulO-dependent extracellular secretion of pullanase[190]. When tested on other substrates, PilD from *N. gonorrhoeae* can also cleave PddD, a component of protein export machinery from *P. aeruginosa*[186]. Besides PilD's ability to cleave prepilin-like protein from other species, PilD can mediate cleavage of both major and minor pilins within its species[187,191]. This broad function of PilD across species may point towards its essential role in either the pili biogenesis or secretion pathway, rendering its function conserved through evolution. The fact that PilD can process both major and minor pilins also suggests its potential role in regulating the processing and assembly of Type IV Pili.

It is interesting to note that the insensitivity of prepilin cleavage to high concentrations of salt and its inhibition by sulfhydryl reagents suggest that prepilin peptidase is quite different from

leader peptidases that had been described[185]. Other than cleaving prepilin, studies have shown that functional PilD is also required for the excretion of protein that contributes to virulence, including exotoxin A, phospholipase C, and elastase in *P. aeruginosa*[192,193]. These findings suggest peptidase activity is not PilD's sole function and its molecular mechanism may be different from what we understand that of a leader peptidase.

Next to peptidase activity, the second most studied function of PilD is its **methyltransferase activity**. What is interesting about this function is that methylation is a common post-translational modification in both prokaryotes and eukaryotes, but unlike 'the side-chain carboxyl methylation/demethylation of L-glutamic residue', methylation of α-amino groups is quite rare in prokaryotes[186]. In an in vitro study, incubation of prepilin, purified homogenous PilD and [$^3$H]AdoMet (S-Adenosyl-L-[methyl-$^3$H]methionine) shows PilD is responsible for the methylation of pilin[186]. The study suggests that PilD first cleave the prepilin and then adds a methyl group to the N-terminal phenylalanine, the first amino acid of the mature pilin[186]. The study also suggested that the two reaction does not necessarily depend on each other and that cleaved pilin can dissociate from PilD prior to methylation[186]. The similarity rates of prepilin and mature pilin substrate methylation suggest the two reactions could be uncoupled. To further prove that, methylation inhibitor, sinefungin, was used and showed cleavage of prepilin was unaffected[186]. Therefore, it is concluded that the sites for binding and cleaving of prepilin do not overlap with the methylation site[186]. In the same study, PilD could not methylate pilin isolated from pili[186]. Given the findings, it is currently proposed that PilD is a bifunctional enzyme and that there are no second methylation sites after N-methylphenylalanine[186].

### 1.4.3 Pilin Antigenic Variation

One of the interesting traits of Type IV Pili in *Neisseria gonorrhoeae* is its ability to perform pilin antigenic variation. Another pathogenic species that share this trait in the *Neisseria* genus is *Neisseria meningitidis*. In summary, pilin antigenic variation is the process by which *N. gonorrhoeae* switches the genetic sequence of its main pilin through recombination with those of pseudopilin, *pilS*[194,195,195–201]. On the genetic level, *N. gonorrhoeae* contains *pilE* locus and five *pilS* loci, in which 19 silent gene copies, *pilS,* are located[202]. Most Type IV pili were assembled with the major subunit pilin, expressed by *pilE* gene. During pilin antigenic variation, *N. gonorrhoeae* can exchange the genetic sequence of *pilE* with any of the 19 *pilS* gene copies (reported in FA1090 strain), that share several homologous regions with *pilE* gene[194,200,202–205]. In this thesis, we used the strain *Neisseria gonorrhoeae* MS11. In this strain, the locus and *pilS* gene copies are slightly different from those in FA1090. In FA1090, the 19 copies of *pilS* are arranged in five loci other than the *pilE* locus. In MS11, there are only 15 other *pilS* gene copies, also arranged in five loci other than the *pilE* locus. However, the arrangement of these gene copies are not exactly the same as in FA1090 (Figure 1.17).

When pili antigenic variation occurs, the expressed pilin are translated as different amino acid sequences. These changes can affect T4P functions, including colony morphology, aggregation ability, aggregation and competence. Interestingly, as of today, *N. gonorrhoeae* and *N. meningitidis* are the only two species in *Neisseria* genus that can undergo pilin antigenic

variation. Coincidentally, these are also the only two recognized pathogenic species in the genus[206]. This interesting correlation may hint at the advantage of this ability to alter pilin sequences among a population. Since Type IV Pili is one of the main contacts between the bacteria and the host, pilin antigenic variation can be a very successful strategy for pathogens to evade the immune system by displaying a different pili.

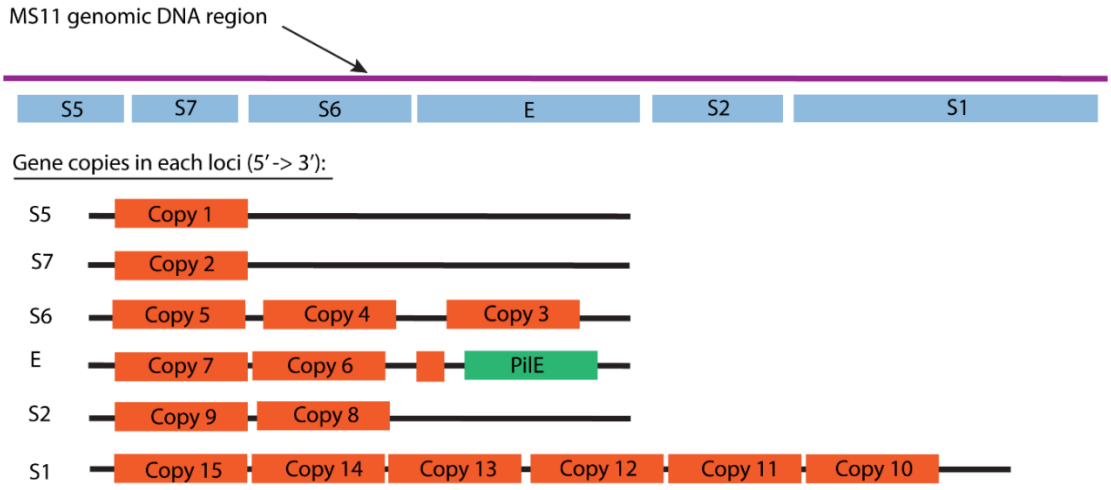


*Figure 1.17 Location of PilS locus and copies in MS11 genome*

In the lab, this phenomenon can be a concern for researchers intending to study the function of Type IV Pili. Researchers attempted to bypass this possibility for a long time by using recombination-deficient strains, *ΔrecA* or consistently selecting colonies that looked piliated for studies. More recently, there were newer reports on the guanine quadruplex structure (G4) upstream of *pilE* gene in *N. gonorrhoeae*[207–210]. It is found that altering the G4 structure can significantly reduce the pilin antigenic variation frequency[207,211–216]. Therefore, subsequently, these two have been used as strategies to lock the *pilE* gene sequence as it is.

### 1.4.4 DNA Uptake Sequence (DUS)

Many factors affect competence in *N. gonorrhoeae*, for example, pili retraction, DNA molecule size, DNA homology region, cell number, and the presence of magnesium. Two components seem to co-evolve in the *Neisseria* species: the DNA Uptake Sequence (**DUS**)[217,218] and the **ComP** minor pilin. Outside of *Neisseria*, the closest DUS-like system that was discovered in other bacteria is the uptake signal sequence (USS) in the *Pasteurellaceae* family that houses *Haemophilus influenzae*[113,219,220].

**DUS** are 10-12bp sequences found in high abundance in their genomes[219–221]. DUS enhance the transformation and can be used for the transformation of desired DNA in the context of genetic engineering[222,223]. In the genomic study, evolutionary footprints of horizontal gene transfer and the maintenance of genomic stability lead to a biased DUS distribution[224,225]. The inverted repeats of DUSes in *N. gonorrhoeae* can also work as bi-directional terminators for both DNA strands, which enable researchers to differentiate genomic regions of foreign origin[226].

The exact nature of the interaction between the DNA molecule and the Type IV Pili machinery is still the subject of active debate. The fact that a very small number of Type IV Pili seems to

maximize competence[227] or the fact that pilins not assembled into polymers can still mediate transformation[228] has, similarly to the case of pseudopilus, put into question the necessity for direct interaction between the DNA and the pilus. Whether direct or through the interaction of the minor pilin **ComP**[229–231], the specific interaction between DNA and Type IV Pili is established[232]. The binding of DNA molecules does not only stop at the chemical nature of DNA molecules. These 10-12bp sequences seem to co-evolve within their own species, working like a dialect between *Neisseria* species[113,221]. The phylogenetic closeness of DUS also correlates with those of their ComP.

Some interesting questions between DUS and ComP are that the density of DUS in the *Neisseria* genome is around 1 in every thousand basepairs, which is hypothesized as the average size for a gene during HGT. Other than that, it is also interesting to ponder if incorporating ComP in the Type IV Pili corresponds to the spacing of DUS in genomic DNA for efficient DNA uptake.

## 1.5 Thesis objectives

With the rising concern of *N. gonorrhoeae's* multi-drug resistance, this study aims to contribute to the body of knowledge and the understanding of the most common pathway leading to multi-drug resistance, natural transformation. Natural transformation is usually described as the whole process from extracellular DNA uptake, transport across the outer and inner membrane, integration into genomic DNA, and the expression or maintenance of the new integration.

This study aims:

- To understand natural transformation at single cell level
- To visualize the process of natural transformation at a single-cell level
- To elucidate quantitatively the process of natural transformation

During the thesis, we achieved some of these aims. At the same time, we will provide some related studies to strengthen our understanding of Type IV pili during DNA transformation in *N. gonorrhoeae* further. A summary of the thesis can be found (Figure 1.18).

To build my thesis around *N. gonorrhoeae*, we faced certain limitations in genetically engineering the bacteria. In **Chapter 2**, we illustrated a fundamental study on genetic modification in *N. gonorrhoeae*. In this chapter, we developed a substantial array of tools sufficient to generate mutants and strains used in this thesis.

**Chapter 3** outlines the step-by-step rationale for developing tools and protocols to study DNA transformation, with a focus on visualization and quantification. The chapter begins by describing the optimization of solid medium in *N. gonorrhoeae* for microscopy purposes. Additionally, a link between starch and fatty acid towards gonococcal growth was discovered. To investigate the dynamics of Type IV pili during DNA uptake, we developed tools and a workflow to visualize and quantify both the pili and DNA molecules. Additionally, we automated the analysis of hydrogel micropillars to examine the mechanical properties of pili

retractions. We also modified the coating of these micropillars to study pili retractions that interact with DNA.

During the development of our tools, we identified several promising candidates for the study of Type IV Pili dynamics and regulations. Among these candidates is PilV, which will be discussed in **Chapter 4**. In this chapter, we provide a detailed characterization of PilV mutants. We employed the tools developed in Chapter 3 to investigate DNA uptake and Type IV Pili dynamics in the context of PilV. Our observations will yield insights into this protein and a model for DNA uptake and Type IV Pili regulation in *N. gonorrhoeae*.

In **Chapter 5**, we included another two studies linking Type IV Pili and DNA uptake in the context of the role of other proteins, PilC and PilD. In the study of PilC, we hypothesized the co-evolution of Type IV Pili and DNA uptake. Through our study in PilD, we provided some insight into the effect on pilin modification in Type IV Pili and how these modifications play a part in DNA uptake.

**Chapter 6** encompasses a case study regarding the role of DNA transformation in the interactions between pathogenic and commensal *Neisseria*. It was a follow-up and response to a reported observation in which *Neisseria elongata* kills *Neisseria gonorrhoeae* in a DNA-dependent manner. We provide a further study on it using the tools we built through this thesis and would like to suggest an alternative hypothesis.

Finally, in our **Conclusion**, we combined all the findings we collected from each experiments to provide the audience an overview of our understanding of Type IV Pili in DNA transformation. As last words, we will propose our hypotheses and prospectives in the research regarding Type IV Pili and DNA transformation in *Neisseria gonorrhoeae*.

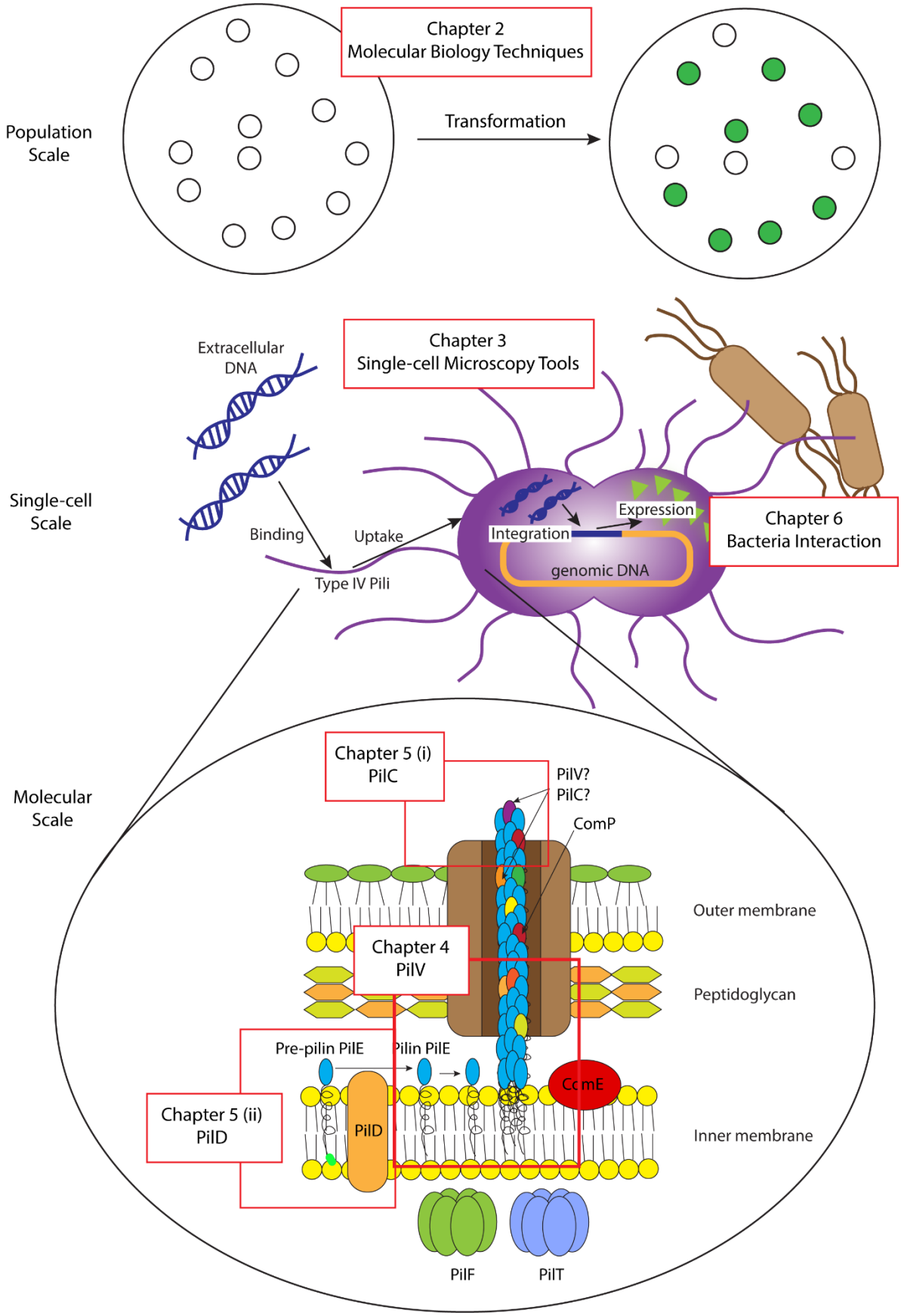


*Figure 1.18 Summary of thesis*

# Chapter 2 : DNA Transformation and Molecular Biology Tools Development

Natural transformation, or the uptake of naked DNA from the external milieu by bacteria, holds a unique place in the history of biology. This is both the beginning of the realization of the correct chemical nature of genes and the first technical step to the molecular biology revolution that sees us today able to modify genomes almost at will. Yet the mechanistic understanding of bacterial transformation still presents many blind spots and many bacterial systems lag behind powerhouse model systems like *Escherichia coli* in terms of ease of genetic modification. In this chapter, we present both some aspects of the mechanistic nature of bacterial transformation and new molecular biology technique in *Neisseria gonorrhoeae.* With some of these understanding, we also provide a suite of new techniques to quickly obtain modifications of genes and genomes in the Neisserial naturally competent bacteria.

*A majority of this chapter has been accepted/published at Front. Microbiology: Antimicrobials, Resistance and Chemotherapy at doi: 10.3389/fmicb.2023.1178128*[233]

## 2.1 Background and Motivation

Many bacteria like *Haemophilus influenzae*, *Vibrio cholerae* or *Streptococcus pneumoniae*, are naturally competent[113]. Yet the exact molecular mechanisms behind their ability to take up naked DNA from their environment are still murky despite close to a century of scientific inquiry. Frederick Griffith's seminal work on transformation *of Streptococcus pneumoniae* was published in 1928[71]. With *N. gonorrhoeae*'s looming antibiotic resistance epidemic, there is an urgent need to understand its natural competence. Other than the contribution of natural competence to antibiotic resistance, the pace of studying *N. gonorrhoeae* has increased. However, compared commonly used model microbe, like *E. coli*, *N. gonorrhoeae* has a relatively scarcer repertoire of molecular biological tools.

Being naturally competent, that means that the simple fact of putting into contact DNA molecules bearing homology with the genomes of *N. gonorrhoeae* with *N. gonorrhoeae* cells can allow the obtention of genetically modified bacteria. Yet, many factors can drastically affect the yield: the degree of homology, the specific strain used, the presence or absence of DNA Uptake Sequences (DUS), the presence or absence of magnesium, the quantity of DNA and the concentration of cells used, to name a few parameters. But the exact methodology used to put into contact the DNA molecules and the bacterial cells also have an impact on the success of the transformation. Therefore, any new knowledge on the molecular mechanisms behind bacterial transformation will help optimize the transformation protocols and thus the efficiency of genetic manipulations in *N. gonorrhoeae*.

One of the poorly characterized features of natural transformation is the amount of DNA that can be transferred within bacteria at the same time. Quantitation of fluorescently labelled DNA in *N. gonorrhoeae* showed that one cell can harbour up to 40 kbp of DNA in its periplasm at once[165]. But the number of DNA molecules that can enter a given cell over the course of a

transformation protocol is unknown. Can a cell acquire a second piece of DNA after acquiring a first one? With the prospect of easing genetic manipulation of both the *Vibrio* and *Streptococcus* genus, multiplex transformations have been performed with DNA molecules with homology with different loci across the genome[234–236]. Here, we aim to present new means of performing genetic modifications in this important human pathogen that should be easily applicable to naturally competent members of the *Neisseria* genus. In the same spirit, we have decided to look at multi-molecule transformation in *N. gonorrhoeae*.

In this chapter, we first established different transformation protocols aimed at controlling the condition of contact between bacteria and the DNA molecules. In particular, we have designed a hybrid protocol stemming from existing techniques[222] with attention to the concentration of DNA used and the conditions (liquid or agar plate) of the transformation. We have then quantified the co-transformation between DNA in two different genetic loci and show that co-transformation can occur at rates above 70%. We go on to present the logic behind an interchangeable cassette system where only two antibiotic selection markers are sufficient to make any number of successive genetic integrations throughout the *N. gonorrhoeae* genome. Combining co-transformation and the interchangeable cassette system, we present a case of proof-of-concept by obtain different mutants in *N. gonorrhoeae* through sequential cloning. Beyond this system, we also proposed a novel possibility in introducing up to 3 bp mutation through one-directional mutagenesis, either through sole or co-transformation. We conclude the chapter hoping to convince the reader that natural transformation can be a powerful tool with the potential for applications through attempts at removing antibiotic resistance by leveraging on *N. gonorrhoeae* natural transformation ability.

It is our hope that these techniques will help speed up the much-needed unravelling of *N. gonorrhoeae* general physiology in order to curb the prevalence of this important sexually transmitted disease while also presenting a framework for genetic manipulation in the *Neisseria* genus as a whole.

## 2.2 Materials and Methods

### 2.2.1 Strains and growth conditions

#### 2.2.1.1 Growth conditions

The strains used in this study are all derivative of *N. gonorrhoeae* strain MS11 (a gift from Magdalene So). All strains were grown on GCB agar plates supplemented with Kellogg's Supplements I and II at 37°C and 5% $CO_2$. Antibiotics were supplemented to GCB agar plates when needed for selection with appropriate concentration (Culture Media).

#### 2.2.1.2 Construction of GyrB1 MS11 mutant strain

The strain carrying the gyrB1 mutation D429N[223] was obtained by PCR amplifying the MS11 gyrB1 gene with the primers gyrB1_ampli_F et gyrB1_ampli_R (Oligos List) and cloned into a II-TOPO vector (Invitrogen). Site-directed mutagenesis (Quikchange, Stratagene) was performed on the plasmid to obtain the point mutation G to A leading to the D429N mutation with the primers gyrB1_MS11_F and gyrB1_MS11_R (Oligos List). This plasmid was

transformed into the MS11 strain and selected to lead to the GyrB1 MS11 mutant strain ($MS11_{GyrB1}$).

#### 2.2.1.3 Construction of MS1 AR::Kan

The strain carrying the kanamycin resistance cassette was obtained by PCR amplifying a plasmid found in Bacteria Strains with primers ResistanceF and ResistanceR (Oligos List). Roughly 400 bps on either side of the AR (Antibiotic Resistance) insertion point were PCR amplified with primer pairs UpGCF and UpGCR_resistance on one hand and DownGCF_resistance and DownGCR on the other hand. Fragments were joined by using Gibson Assembly Mix. The assembled product was further amplified by the external primers, transformed into MS11 and selected to obtain the AR::Kan MS11 strain (MS11AR::Kan).

#### 2.2.1.4 Construction of MS1 AR::E (MS11 with Erythromycin-resistant cassette)

To obtain MS11AR::Erm strain, Erythromycin cassette consists of Erythromycin resistance gene was amplified from MS11 Strain 306[237] using AR_Erm_F and AR_Erm_R. Flanking regions around the AR insertion region was amplified as follows: the upstream region was amplified with UpGCF and UpGCR, the downstream region was amplified with DownGCF and DownGCR. These amplified fragments were then assembled using Gibson Assembly Mix. The assembled product was amplified through PCR using primers UpGCF and Down GCR. The product of this PCR was then transformed into MS11 and selected with erythromycin to yield the MS11AR::Erm strain.

### 2.2.2 Transformation assay

#### 2.2.2.1 Liquid transformation

Overnight cultures of *N. gonorrhoeae* were obtained from streaking on GCB agar plates incubated at 37°C and 5% $CO_2$. These cultures were resuspended in Transformation Medium (GCB + 5 mM $MgSO_4$, Refer to Culture Media for details). The cell suspension was used directly or diluted to 5 × $10^8$ CFU/mL. In this paper, extracellular DNA added for transformation will be called transformation DNA (tDNA). DUS tDNA was added to 200 µL of Transformation Medium in a separate tube and kept at 37°C. A volume of 30 µL of the cell suspension was then added to the DUS tDNA mixture. The combined product was incubated at 37°C for 15 min, in a 5% $CO_2$ incubator. After incubation, the mixture was pipetted into a 60 mm × 15mm petri dish containing 1 mL of pre-warmed GCB+ liquid medium (see Culture Media). The Petri dishes were incubated at 37°C for 3 h, in a 5% $CO_2$ incubator. After incubation, cells were scraped from the petri dish and resuspended in 1 mL of GCB liquid. The mixture was disrupted and prepared into serial dilutions. 5 µL spots of different dilutions were left to air dry on GCB and selection plates (refer to Culture Media for details). The plates were then incubated at 37°C for 16–20 h, in a 5% $CO_2$ incubator. Colonies were counted to measure transformation efficiency.

#### 2.2.2.2 Spot transformation

A known amount of DNA was prepared in a total volume of 10 µL and let to air dry on a GCB agar plate. A *N. gonorrhoeae* colony was selected from an overnight culture and picked up with a swab. The swab was used to lawn bacteria uniformly across the marked spot where the DUS

tDNA was air dried. The transformation plate was incubated at 37°C for 16–20 h, in a 5% $CO_2$ incubator. All growth from the spot previously with dried DUS tDNA was swabbed and resuspended in 1 mL of GCB medium. The mixture was disrupted and prepared into serial dilutions. Dilutions were then spotted on GCB+ agar and selection plates and left to air dry. The plate was then incubated at 37°C overnight, in a 5% $CO_2$ incubator. Colonies were counted to measure transformation efficiency.

#### 2.2.2.3 New spot transformation

An overnight culture of *N. gonorrhoeae* on an agar plate was resuspended in GCB liquid medium adjusted to cell density with optical density at 600 nm wavelength ($OD_{600}$) = 0.7 (approximately $5 \times 10^8$ cells/ml). 10 µL of the culture was mixed with DUS tDNA. The mixture was then spotted on a GCB+ agar plate and left to air dry. Once the spot was air-dried, the agar plate was incubated at 37°C for 16 h, in a 5% $CO_2$ incubator. After incubation, all growth from the spot was swabbed and resuspended in 1 mL of GCB medium. The mixture was disrupted and prepared into serial dilutions. Dilutions were then spotted on GCB and selection plates and left to air dry. The plate was then incubated at 37°C overnight, in a 5% $CO_2$ incubator. Colonies were counted to measure transformation efficiency.

### 2.2.3 Optimization of $OD_{600}$ for Transformation

*N. gonorrhoeae* bacteria grown overnight on GCB agar plate were swabbed and resuspended in 1 mL of GCB medium and disrupted to a single cell suspension using a disruptor for 2 min (Genie Cell Disruptor). A cell suspension with an $OD_{600}$ of 0.7 was prepared from the stock. 10-fold serial dilutions were prepared from $OD_{600}$ = 0.7 cell stock. 10µL of each dilution was mixed with 500 ng of gyrB mutant DUS tDNA and transformed following the Spot and Dry transformation as illustrated in "New Spot Transformation".

### 2.2.4 Co-transformation

*Table 2.1 Amount of mutant gyrB tDNA based on different tDNA sizes*

| gyrB DNA size | gyrB DNA (ng) used |
|---|---|
| 2 kbp | 100 |
| 4 kbp | 200 |
| 6 kbp | 300 |

This experiment used two types of tDNA: mutant gyrB1 (gyrB12kbp, gyrB1-4kbp, and gyrB1-6kbp tDNA) and a Kanamycin-resistant cassette (AR::Kan tDNA). Mutant gyrB DNA were amplified from a Nalidixic acid resistance strain containing a point mutation within the gyrB gene[223], the MS11GyrB1 strain. Different sizes of gyrB1 mutant tDNA were amplified to be 2kbp, 4kbp, and 6kbp using primers in Oligos List. The Kanamycin-resistant cassette was amplified from the strain MS11AR::Kan with primers Insert1kbGCF and Insert1kbGCR. To compensate for the DNA copy number due to different molecule sizes, different amounts of tDNA were added depending on their sizes. In this set of experiments, all conditions used 0.1 ng of Kanamycin -resistant cassette. The amount of mutant gyrB tDNA used based on different sizes were listed in Table 2.1.

### 2.2.5 Interchangeable Cassette System (ICS)

A specific region in the *N. gonorrhoeae* genome has been selected for gene insertion based on previous studies[222], between the lactate permease (*lctP*) gene and the aspartate aminotransferase (*aspC*) gene. This region was historically used as a complementation site and referred to later as the *neisseria intergenic complementation site* (nics)[238,239]. This region will be called the AR insertion region in this paper. Gene insertion in this region has shown no phenotypic changes in the bacteria[240]. Cassettes containing selection markers are designed to have similar sized flanking regions on both sides of the AR insertion region. For transformation, the AR insertion region was amplified to ensure cassettes containing different selection markers have the same homologous recombination region. The cassettes (AR::Kan or AR::Erm tDNA) used for study were amplified from strains containing respective selection markers (either strain $MS11_{AR::Kan}$ or $MS11_{AR::Erm}$) using primers listed in Oligos List. The transformation procedure used was the new spot transformation presented earlier.

### 2.2.6 Proof of concept for cloning using co-transformation

For examples intended to show deletion, we chose the *cidA* and *cidB* genes. We amplified the upstream DNA sequence around 3.2kbp and the downstream DNA sequence around 2kbp of cidA/lrgA and lrgB genes using the primers stated in CidAB--153-F and CidAB-p73-R. After checking the PCR reaction on gel electrophoresis and clean-up, we stitched the two fragments together using Gibson Assembly mix. The assembled product was used as the template for PCR to get enough copies of the big fragments. The final PCR product was used directly with 1 ng of kanamycin AR cassette for co-transformation in the MS11 strain. Next, to introduce a point mutation in the pilD gene, we did two sets of tests. For the first set, we amplified an upstream fragment and downstream fragment of the intended mutation (from CCTGCTGTCCCAAA**T**GCCGTGTGCCG to CCTGCTGTCCC AAA**A**GCCGTGTGCCG representing a non-synonymous mutation pilDC72S). The fragments were then assembled using NEB HiFi DNA Assembly Master Mix. The assembled product was amplified again through PCR and the product was checked through gel electrophoresis. For the second set, we amplified a DNA fragment from mutant MS11 pilDC72S genomic DNA, which already carries the intended mutation, using Q5 High-Fidelity 2x Master Mix and primers stated in Oligos List. After ensuring good PCR results on gel electrophoresis, we co-transformed the fragment from both sets with 1 ng of erythromycin AR cassette into the MS11ΔcidAΔcidB AR::kan strain. Following that, we intended to obtain a N-terminally tagged YFP-ComM protein. Similar to what we did for the point mutation, we introduced two sets of tests. The first set consisted of assembled DNA fragments, while the second set consisted of DNA fragments amplified directly from an existing mutant. For the first set, we located the *comM* gene in the MS11 strain. We amplified the *yfp* gene (gift from Lucy Shapiro [241]) with the FluoComM-fluo-F and YFPComM-yfp-R including a linker. Two DNA fragment including the Upstream region of *comM* gene and the *comM* gene and part of its Downstream region were amplified, respectively, with the primer pairs ComM-Up-F and ComM-Up-R and ComM-Down-F and ComM-Down-R. The three fragments were assembled using NEB Hi-Fi DNA Assembly Kit. The product was further amplified by the primers ComM-Up-F and ComM-Down-R. For the

second set, DNA fragments were amplified from MS11$_{yfp\text{-}ComM\ AR::Erm}$. After checking for good amplified PCR product by gel electrophoresis, fragments from both sets were mixed with 1 ng of AR::Kan cassette and co-transformed into MS11$_{\Delta cidAcidB\ pilDC72S\ AR::Erm}$ using conventional spot transformation. The transformed cells were lawned on an erythromycin selection agar plate. Colonies were selected the day after, resuspended in water, and used as the template for PCR using DreamTaq and colony PCR primers, ComM--525-F and ComM-787-R. The PCR product result was loaded onto 1% agarose gel to check for colonies with successful insertion.

### 2.2.7 One-directional mutagenesis

#### 2.2.7.1 On *gyrB* gene mutations

In this test, three types of *gyrB* tDNA was prepared: gyrB1-4kbp, 5', and 3', and AR::Kan cassette for co-transformation. The preparation of each fragment can be found in tDNA List. Single transformation protocol was performed as described in New Spot Transformation. Co-transformation was performed according to described procedure. The tDNA amount used for *gyrB* tDNA was 500ng each while the amount used for AR::Kan cassette was 1ng. Following the same New Spot Transformation protocol, the transformation efficiencies were determined based on growth on plates with no selection, Nalidixic acid, Kanamycin, and both Nalidixic acid and Kanamycin.

#### 2.2.7.2 On *pilE* gene mutations

To test One-directional mutagenesis in *pilE* gene, two types of tDNA was prepared to introduce two different point mutations in *pilE* gene, T132C and T138C. Fragments were amplified as mentioned in tDNA List. Using Spot Transformation, the tDNA fragments were transformed into MS11. During selection, transformants were selected on GCB agar plate containing 120ug/ml Kanamycin. Colonies grown on these plates were selected and amplified using colony PCR and verified through sequencing for successful mutation.

### 2.2.8 Switching out of cassette and point mutation

#### 2.2.8.1 Switching out ICS cassette

Overnight grown culture plate of MS11$_{AR::Erm}$ was resuspended in GCB and prepared into $OD_{600}$ of 0.0007 solution. In 10ul of this solution, 3ug of AR::Nil tDNA was added and spot on GCB agar plate and left to air dry. The next day, the growth on plate was resuspended in GCB liquid media and prepared into 10x serial dilution. Then, 100ul of $10^{-3}$ dilution stock was plated on GCB agar plate and incubated at 37°C and 5% $CO_2$ overnight. The next day, plates with clear individual colonies were used for replica plating on Erm-containing plates. Both plates were incubated at 37°C and 5% $CO_2$ overnight. The next day, both plates were taken for comparison and identify colonies that only grow in GCB agar plate.

#### 2.2.8.2 Switching out gyrB1 mutations

Overnight grown culture plate of MS11$_{gyrB1}$ mutant was resuspended in GCB and prepared into $OD_{600}$ of 0.0007 solution. In 10ul of this solution, 500ng of wt*gyrB1* tDNA was added and spot on GCB agar plate and left to air dry. On the next day, the spot in which bacteria grew was resuspended in GCB liquid medium and prepared into 10x serial dilutions. These dilutions were

then spot on both GCB agar plate and plates containing NA for selection. The plates are then incubated at 37°C and 5% $CO_2$ overnight. Growth on each plates were observed the next day for quantification.

## 2.3 Results

### 2.3.1 Modification of transformation assay for quantification

Historically, there are two commonly used lab techniques for transformation in *N. gonorrhoeae*: Spot Transformation and Liquid Transformation[222]. Both methods are illustrated in Figure 2.1. In the **Spot Transformation**, a known quantity of the DNA to be transformed (tDNA) is dried on an agar plate. Bacteria are overlaid on top of the dried tDNA spot using a swab. While this technique is versatile and requires minimal intervention from the experimenter, it has shortcomings when it comes to quantification of transformation efficiency. It is difficult to ensure that all the bacteria that will be tested for transformation have been in contact with the same amount of DNA or even in contact at all with DNA. In the **Liquid Transformation** technique, a known quantity of tDNA is added to bacteria in liquid supplemented with magnesium. After a brief incubation, the DNA bacteria suspension is added to another volume of liquid and left in the incubator for a few hours. This technique ensures a uniform access between DNA and bacteria cells, but it requires many steps not easily scalable when many samples need to be handled at the same time.

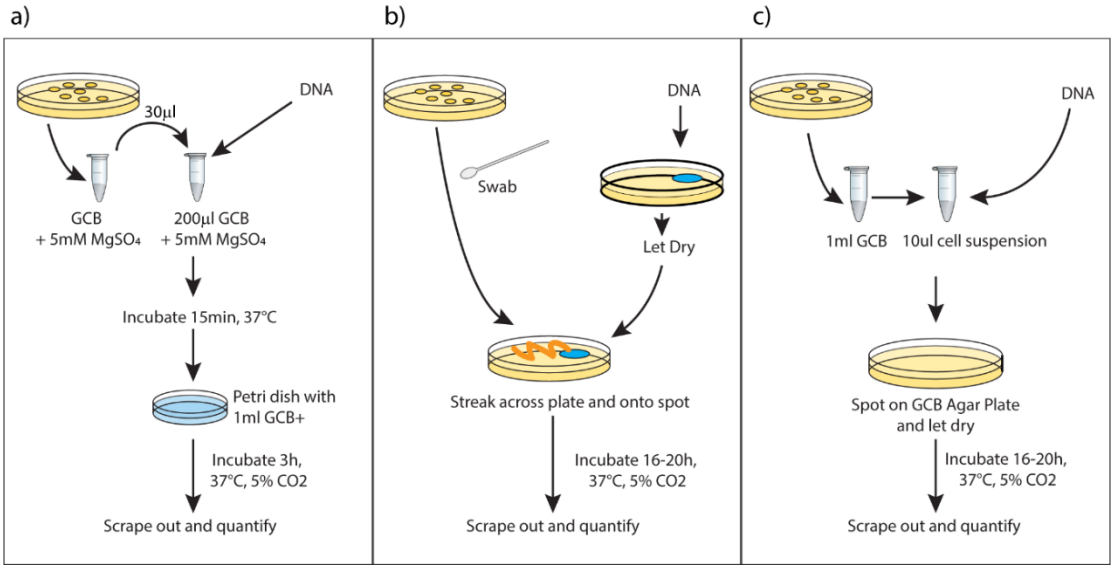


*Figure 2.1 Different protocols for transformation: a) Liquid Transformation b) Spot Transformation c) New Spot Transformation*

We have decided to combine these two techniques to allow an easy and accurate quantification of transformation. In a nutshell, we add tDNA to a suspension of bacteria cells of known density that is dried on an agar plate. In this case, all bacteria are thus put into contact with the tDNA. After some incubation time, the entirety of the DNA-bacteria spot is resuspended and transformation efficiency is assessed. This new methodology will be referred to as the **New Spot Transformation**.

In order to directly compare these different techniques, we have chosen one type of tDNA. The tDNA is a DNA carrying a point mutation in the *N. gonorrhoeae* gyrB gene (gyrase B) known to confer resistance to the fluoroquinolone Nalidixic Acid (DUS tDNA). Throughout this series of experiments, 500 ng of mutant gyraseB (gyrB) DNA was used as transfer DNA (DUS tDNA). Since it is observed that more tDNA amount led to higher transformation, we standardized the amount due to its good yield, practicality of experiments and easy comparison across experiments.

We can see in Figure 2.2 that the Liquid Transformation and the new technique, New Spot Transformation, can both achieve high transformation yield. The main advantage of the Spot Transformation technique is its technical ease, the limited steps involved and the possibility to process many samples in parallel. We see here that it does present a lower transformation yield. Evidently, there are other factors that can affect these outcomes, for example, the amount of cells collected through each method can differ and the growth stage of the cells used differs due to the nature of protocol too.

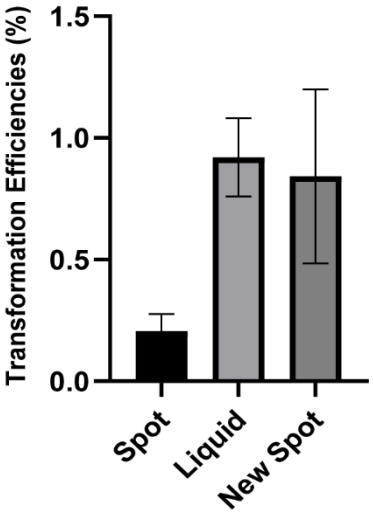


Nonetheless, our new techniques still represent a good middle ground between the two previously described techniques that maximizes the efficiency of transformation, minimizes the efforts of the experimenters and allows accurate quantification of transformation. In this experiment, we intend to broaden the choice of available protocols for future experimenters.

*Figure 2.2 Comparison between three transformation protocols*

### 2.3.2 Optimal DNA to cell ration for transformation

There are several factors that can affect transformation efficiency in *N. gonorrhoeae*. Their sheer number makes it difficult to tackle all of them at the same time. This includes the presence of competence pili, tDNA sizes, amount of DNA, and incubation time[242]. Following the development of the new spot transformation aiming at quantification, we applied this newly established methodology to study the optimal cell number input for natural transformation fixing a few of those parameters. We have maintained the amount of tDNA (500 ng). The result shows that transformation using an input suspension of cells with an $OD_{600}$ of 0.0007, together with 500 ng of tDNA yields a higher

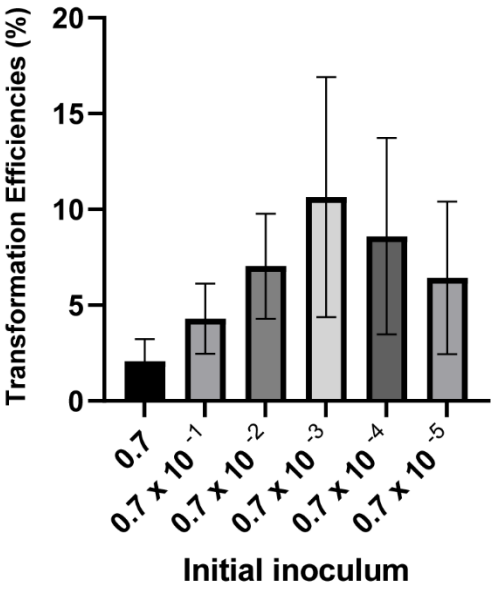


*Figure 2.3 Transformation with different amounts of inoculant. Figure shows the fold change of transformation efficiencies of 10x dilutions of $OD_{600}$ 0.7 against $OD_{600}$ 0.7*

transformation efficiency as demonstrated in Figure 2.3. This suggests that there is an optimal cell to tDNA ratio in each transformation condition.

To dissect this results, for 500 ng of the DUS DNA tDNA (1300 bp), it means there are $3.56 \times 10^{11}$ copies of tDNA incubated in each reaction. Given the optimal inoculum condition is from the stock of $OD_{600}$ 0.0007, 10 µl of the stock gives $5 \times 10^3$ cells. That means, the stochastic optimal control for efficient transformation seems to be $7 \times 10^7$ copies of DNA per cell. This result itself opens up more questions since to be successfully transformed, one single bacterium will only require one copy of tDNA successfully integrated in their genome. Therefore, it is worth pondering the dynamics of these tDNA molecules when interacting with the cell and inside the cell body. Nonetheless, with this optimal condition nailed, this optimal input cell density is used in subsequent experiments in this thesis unless mentioned otherwise.

### 2.3.3 Co-transformation

Compared to other genetically tractable bacterial organisms like *E. coli*, *Bacillus subtilis* or *Pseudomonas aeruginosa*, *N. gonorrhoeae*, can be seen as possessing a limited array of genetic tools. While the natural competency status of *N. gonorrhoeae* might have thwarted the efforts from the community to further optimize genetic modification techniques, this dearth of techniques might also be linked to mechanistic specificities of *N. gonorrhoeae*. For instance, *N. gonorrhoeae* does not have the plethora of cloning vectors designed and engineered for E. coli. To date, *N. gonorrhoeae* can harbour three categories of plasmids, conjugative plasmids, β-lactamase plasmids and cryptic plasmids[243,244]. These plasmids are mainly known for their role in spreading antibiotic resistance among gonococci[243]. In a laboratory setting, however, available vectors used for cloning in *N. gonorrhoeae* research are largely limited to shuttle vectors for replication in *E. coli* [240]. These vectors will eventually be cleaved upon uptake and reintegrated into its genome. They will have limited stability within *N. gonorrhoeae* cells. Some of the early genetic manipulation of *N. gonorrhoeae* rely largely on transforming the bacteria with genomic DNA, for example, acquiring streptomycin resistance after transforming with genomic DNA isolated from resistant strains[245]. As knowledge on DNA repair and recombination expands and with it an ever easier ability to create synthetic DNA molecules, studies moved toward transforming *N. gonorrhoeae* with synthesized double-stranded DNA molecules containing the genomic manipulation of interest (insertion, deletion or point mutation), usually together with a selection marker with sometimes another step to remove it [246,247]. Yet, the selection schemes and the necessity for multiple antibiotic markers in the case of their use or the many steps when performing markerless modifications still impose many technical constraints on the genomic modification of *N. gonorrhoeae* cells. We have decided to see if some of these constraints could be relaxed.

We have explored the possibility of multiplex genome editing in *Neisseria*, building on existing genetic manipulation protocols in other naturally competent organisms. Researchers succeeded in performing multiple-site genome editing at once in *Vibrio cholerae, V. natriegens*[235,236]. In a nutshell, multiple DNA molecules with homology with different parts of the genome of the targeted organisms are transformed simultaneously. Only one of the pieces will bear an

antibiotic marker that will be selected for. Yet multiple mutations can be seen in the selected clones. *V. cholerae* and *N. gonorrhoeae* both perform natural transformation via Type IV Pili. We thus surmised that a similar experimental design will also work with *N. gonorrhoeae* and has the potential to ease the design and execution of genomic modifications in this organism.

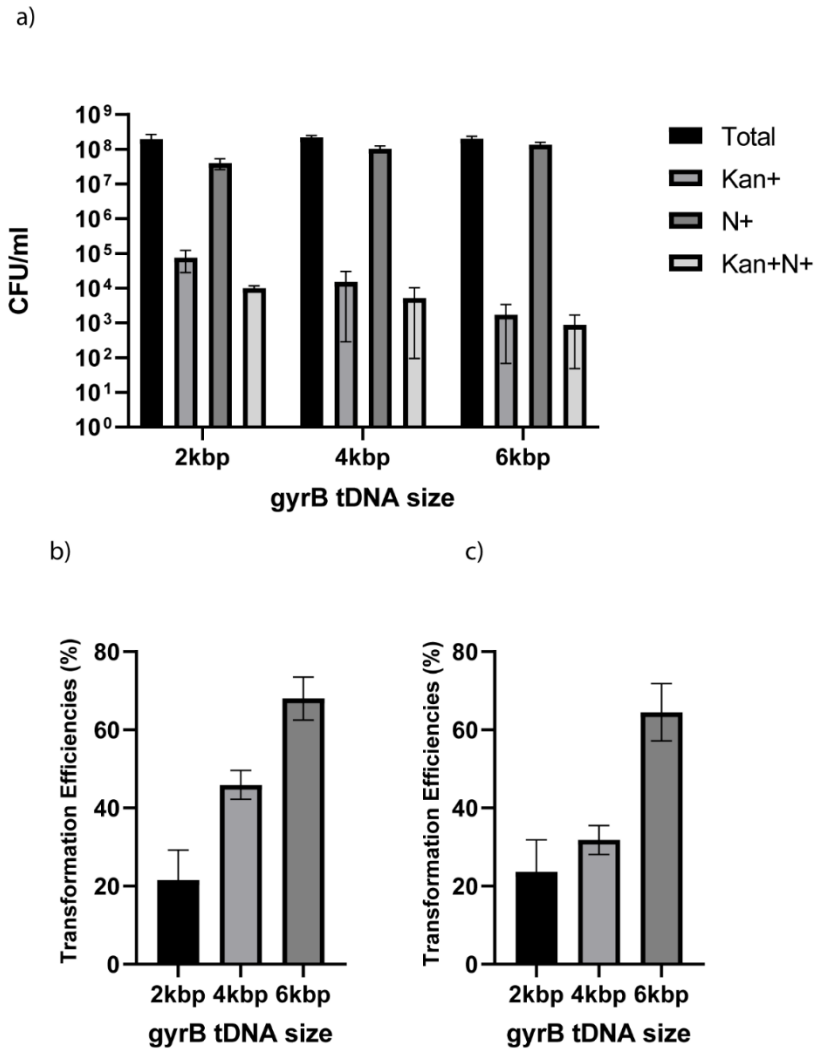


*Figure 2.4 Transformation efficiencies using co-transformation (a) CFU/ml of cells transformed with tDNA of 2kbp, 4kbp and 6kbp length on different agar plate: GCB+ (Total), Kanamycin (Kan+), Nalidixic acid (N+) and Kanamycin and Nalidixic acid (Kan+ N+) (b) Transformation efficiencies of nalidixic acid resistant cells over the total amount of cells for different tDNA length. (c) Percentage of Kanamycin and nalidixic acid resistant cells over Kanamycin resistant population in each co-transformation condition. All experiments were performed in a minimum of three biological replicates with technical triplicates for each. The detection level of the transformation assays is below 5.10-5 %. DNA free controls were below the detection limit.*

In order to test our hypothesis, we have chosen a site historically used to insert antibiotic markers in *N. gonorrhoeae*, the region between the *lctP* and *aspC* genes[240], hereafter dubbed the AR (antibiotic resistance) region. We have paired this site with the *gyrB* point mutation presented in the previous section. We will combine these two types of tDNA in these co-transformation experiments mixing them together to perform a New Spot transformation with optimized concentration of *N. gonorrhoeae* cells. On the one hand, DNA molecules with various degrees of homology with the *lctP-aspC* gene region will allow the insertion of an

antibiotic selection marker, the intended selection during co-transformation (AR::Kan tDNA). On the other hand, DNA molecules of various lengths carrying the point mutation conferring resistance to nalidixic acid (gyrB1-2kbp, gyrB1-4kbp, and gyrB1-6kbp) will allow us to measure how many cells selected with the AR gene also incorporated the *gyrB* point mutation. In this study, we used selection cassettes which include an antibiotic resistance (AR) gene, flanked with around 1,000 bp homologous regions on each side of the insertion site. Therefore, during successful insertion, the two homologous flanking regions will recombine with the genomic DNA and insert the antibiotic resistance gene at the desired location while conferring resistance to the chosen antibiotics, here kanamycin (Figure 2.7). Selection of co-transformed colonies on kanamycin plates enables to measure the numbers of successful AR incorporation. Similarly, successful insertion at the *gyrB* region is measured by CFU on nalidixic acid selection plates and successful double mutants are measured by CFU on selection plates containing both the AR antibiotics (here kanamycin) and nalidixic acid. The ratio between these two different types of tDNA will be the main parameter in these experiments. The transformation efficiency of mutant *gyrB* tDNA increases as molecular size, and thus the degree of homology, increases (Figure 2.4). This observation is similar to what is reported in *V. natriegens*[236]. The increased pattern of transformation efficiency is most likely due to longer flanking regions available for recombination. It could also further enhance by a specificity of the *Neisseria* genus, the existence of DNA Uptake Sequences already mentioned. These 10–12 base pair sequences facilitate uptake and transformation of DNA molecules in the *Neisseria* genus [217,218]. DUS sequences occur on average every thousand base pairs in *N. gonorrhoeae* and the number of their occurrences in a given tDNA molecule might also contribute to the increased transformation rate [221,223].

With an experimental mindset, what is worth noting is the proportion of double mutants among the kanamycin resistant population.

Even though we have only selected for kanamycin, as high as 60–70% of the cells are also resistant to nalidixic acid (Figure 2.4). Thus, if we were to perform co-transformation with an AR tDNA and another tDNA bearing a desired genomic modification that is not selectable, we can still obtain the incorporation of that not selectable genomic mutation by solely selecting with the AR antibiotic. This scheme opens up fully the design of genetic modifications, as we will see later, while providing a method requiring only one transformation step. This observation is of extreme practical use since it provides an opportunity for new flexibility when manipulating the *N. gonorrhoeae* genome. During random bacterial genetic manipulation, it is quite rare that the genetic change thought after will lead to any selectable or recognizable phenotype. The goal is more often to remove a gene and look for the potential phenotype associated with the removal in order to ascribe a function to the gene. Thanks to the high rate of co-transformation seen above, we see that it is technically possible to always use the same genetic locus to receive a selectable marker and get a high rate of modification in a totally independent locus on the genus that you are not selecting for. This opens the door for a quick and easy methodology for obtaining genome-wide modifications in *N. gonorrhoeae*.

### 2.3.4 Interchangeable Cassette System (ICS)

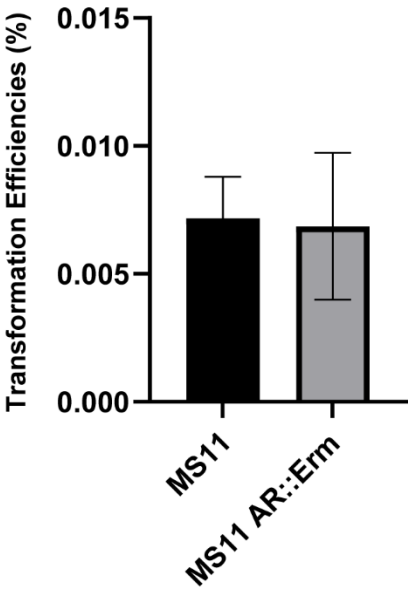


*Figure 2.5 Consistency of AR region recombination Figure shows the transformation efficiency of transforming MS11 and MS11AR::Erm with 1ng of AR cassette containing Kanamycin selection.*

Following the results on co-transformation from the previous section, the possibility of performing multiplex genome editing opens up. One of the advantages stemming from a co-transformation technique is the use of only one selection marker to obtain multiple-site manipulation. Given the limited number of selection markers that are available in *Neisseria*, we wondered whether we could use co-transformation to limit the number of selection markers used without limiting the number of mutations we could obtain. One appealing method would be to keep using the same historical locus to sequentially integrate different selection markers. We thus investigated the versatility of the AR region by switching in cassettes with different selection markers. We compared the transformation of kanamycin selection cassette (AR::Kan tDNA) into wild type (MS11) and a strain that possessed an erythromycin resistance cassette at the AR locus ($MS11_{AR::Erm}$). Our results showed that the transformation efficiency between the two are similar (Figure 2.5). This result shows that an AR region inserted with a selection cassette is equally likely to recombine with a new selection cassette when given the opportunity. This finding implies the possibility to indeed apply co-transformation for multiple sequential genetic manipulations. Besides, it is possible to perform limitless sequential co-transformations with as little as two types of selection cassettes by using them alternately. For instance, we can limit ourselves to just the kanamycin cassette and erythromycin cassettes presented here and use the one not present at the AR locus to select for the next co-transformation, leading to the desired genetic modification(s) at any other site in the genome. We hope that the use of this Interchangeable Cassette System (ICS) will prove useful in the *N. gonorrhoeae* research arena as a means to reduce the use of antibiotic resistance makers and provide an efficient technique to obtain multisite modifications with limited steps and maximized efficiency.

### 2.3.6 Proof-of-concept examples

In order to show the versatility of these techniques, we will illustrate it in common experimental situations. Here, we present three common types of genetic editing: **(1) deletion, (2) point mutation**, and **(3) insertion**. Besides the type of modifications, the examples are also coupled with tDNA prepared from different sources, namely amplified DNA fragments from DNA assembly or genomic DNA to further exemplify the flexibility of the methods to respond to the reality of a wide range of molecular biology applications. On top of that, this proof of concept illustrated the versatility of this gene modification workflow by performing all three types of gene editing consecutively through co-transformation. For the first example, we demonstrated gene **deletion** by co-transformation. We amplified two PCR fragments, one

3.2kbp upstream of the *cidA* gene and another 2 kbp downstream of the *cidB* gene, that are assembled and amplified again. With that, we obtained a PCR product with the desired deletion of both *cidA* and *cidB*. After co-transformation with AR::Kan cassette into MS11 strain. The expected band will be 1,263 bp (smaller band near the bottom) without the deletion and 226 bp when the deletion occurs. We observed 3 out of 16 colonies selected through the co-transformed selection (kanamycin) also carry the deletion of *cidA* and *cidB* (Figure 2.6a). By doing this first genomic manipulation, we obtained MS11ΔcidAcidB AR::Kan.

We followed up the procedure by introducing a **point mutation** in a gene named *pilD*. The mutation intended was from CCTGCTGTCCCAAA**T**GCCGTGTGCCG to CCTGCTGTCCCAAA**A**GCCGTGTGCCG leading to the non-synonymous pilDC72S mutation. We tested two forms of co-transformation: amplified products from DNA assembly and genomic DNA carrying the mutation. These arrangements will reflect well the two most common sources of implementing genetic modifications: introducing mutations by assembling DNA fragments or amplifying DNA fragments from another strain that already carry the intended mutation. After obtaining the intended tDNA with the point mutation of T-> A, we co-transformed these fragments with AR::Erm cassette into $MS11_{\Delta cidAcidB\ AR::Kan}$. To check the success rate of co-transformation, the amplified products of colony PCR were cleaned up and sent for sequencing. The success rate for the assembled DNA set was 1 out of 16 (Figure 2.6b), and 3 out of 16 for the direct amplification set (Figure 2.6c). From this experiment, we obtained $MS11_{\Delta cidAcidB\ pilDC72S\ AR::Erm}$. At the same time, we also proved the possibility of switching the selection cassette, a great application of the rationale in designing the Interchangeable Cassette System (ICS).

For the last common genomic modification, we introduced a gene **insertion**. In this example, we also tested two forms of co-transformation as previously. We prepared tDNA amplified either from assembled DNA or genomic DNA carrying the intended modification. From that, the PCR product was co-transformed with AR::Kan cassette into $MS11_{\Delta cidAcidB\ pilDC72S\ AR::Erm.}$ The expected band for unsuccessful insertion and successful insertion are 1312 bp and 2032 bp, respectively. We obtained 1 successful mutant out of 16 colonies for those from assembled product (Figure 2.6d) and 6 successful mutants out of 16 colonies for those from direct amplification (Figure 2.6e). Therefore, the successful mutants are now $MS11_{\Delta cidAcidB\ pilDC72S\ yfp\text{-}ComM\ AR::Kan}$.

Through these few examples, we showed the flexibility of co-transformation using DNA molecules from different sources, different homology lengths, for different purposes. While the success rate varies greatly with the specifics of the genetic manipulation at hand, the success rate is compatible with a rapid obtention of the desired mutation. A more systematic study of co-transformation, beyond the scope of the present work, might help to further unravel the reasons for these discrepancies. It could be that the recombination rates across the genome are not uniform, the stability of the DNA molecules getting inside the cell might depend on their sequence, the uptake of all the DNA molecules might not be equal to their relative concentration outside the cell, as a few possible contributors to the differences. But a few key guiding principles have ensured successful co-transformation: maximize the ratio of the non-

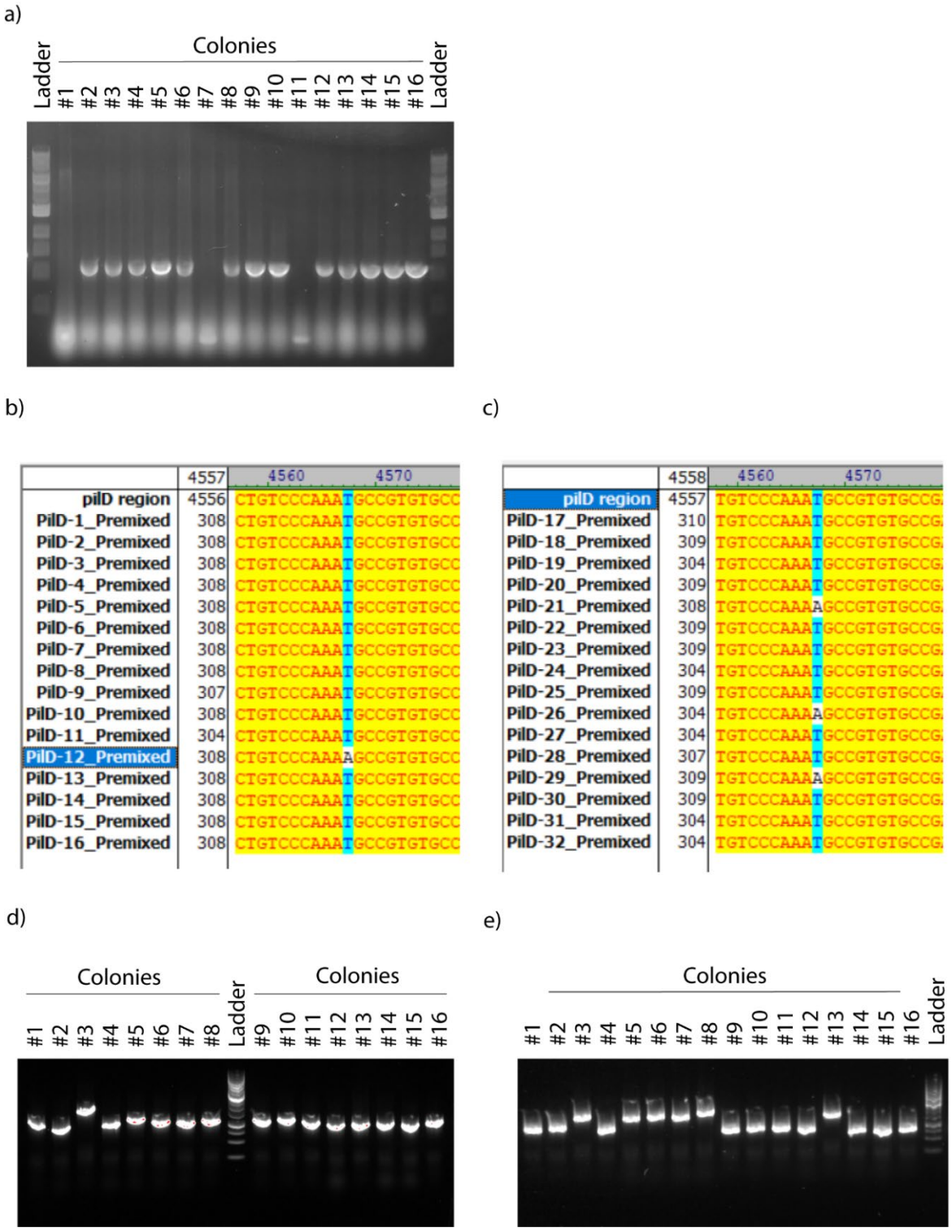


*Figure 2.6 Application of co-transformation in creating mutants by different means (a) Deletion. The genes cidA and cidB were selected to be deleted. Transform DNA flanking upstream of cidA and downstream of cidB was assembled and transformed into MS11 strain. Agarose gel shows the product of colony PCR. Successful mutants could be observed with smaller molecular size. (b) Point mutation: co-transformation of amplified assembled DNA fragments. The figure shows the sequencing results compared to the original PilD sequence. A successful mutation was marked by the change from AAATGCCGTG to AAAAGCCGTG. (c) Point mutation: co-transformation of direct amplification product from genomic DNA. The figure shows the sequencing results compared to the original PilD*

*sequence. A successful mutation was marked by the change from AAATGCCGTG to AAAAGCCGTG. (d) Insertion: co-transformation of amplified assembled DNA fragments. Each lane shows colony PCR of one single colony of transformants. A successful insertion was marked by the bigger DNA size on agarose gel. (e) Insertion: co-transformation of direct amplification product from genomic DNA. Each lane shows colony PCR of one single colony of transformants. A successful insertion was marked by the bigger DNA size on agarose gel.*

selected tDNA to the selected one, have more homology in the non-selected piece than the selected one and minimize the amount of selected tDNA aiming for a few hundred selected clones per co-transformation. Moreover, the utilization of ICS in this proof of concept also proves the possibility of performing consecutive genetic modification with as little as two types of selection cassette. Plus, this system is compatible with co-transformation throughout three different genetic modifications. With these rules of thumb in mind, co-transformation is a highly flexible and rapid tool for genetic engineering in *N. gonorrhoeae*, minimizing the design and steps required by other techniques (Figure 2.7).

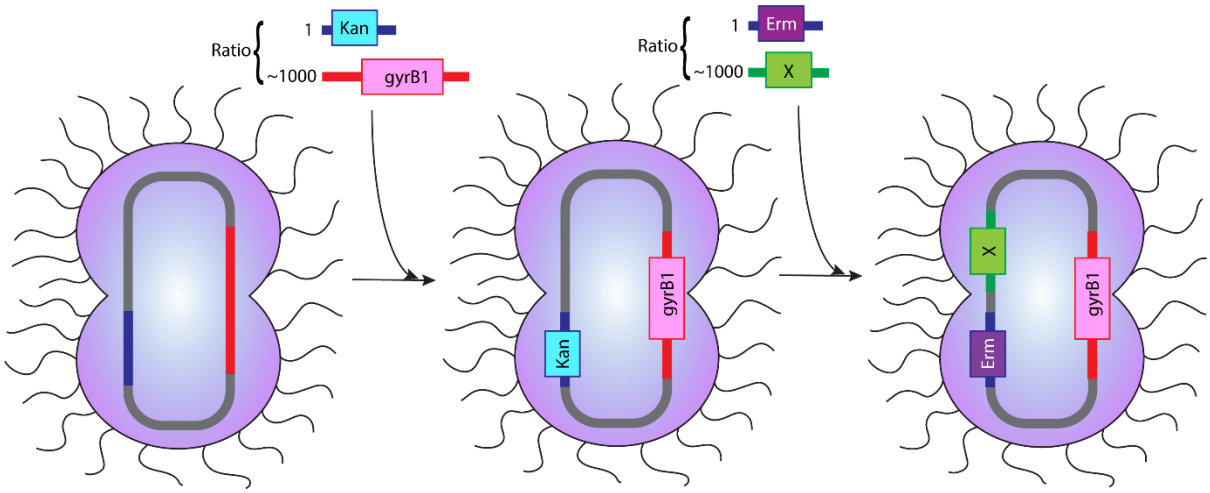


*Figure 2.7 Depiction of the procedure of co-transformation. The procedure of co-transformation described in the 'Co-transformation' section. A tDNA with the Kan cassette:gyrB1 tDNA ratio of 1:1000 was used to assess the effect of gyrB1 tDNA flanking region length in co-transformation. The procedure of co-transformation when applied to cloning strategies. The image illustrated the application of Erm cassette:modification(labelled as X) with the ratio 1:1000 into bacteria that has been co-transformed successfully prior. These two images depict a summary of co-transformation procedure and the possibility of subsequent co-transformation with a different selection cassette.*

### 2.3.7 1-directional mutagenesis

The ability to engineer the genetics of bacteria requires robust molecular cloning techniques. Molecular cloning is a set of techniques used to manipulate DNA molecules, either by introducing mutations or creating recombinant DNA (DNA molecules assembled together to be replicated in host organisms). There are a plethora of cloning techniques each with their own strengths and weaknesses. Some of them are restriction enzyme cloning, TOPO cloning (also known as TA cloning), Gibson Assembly, Golden Gate and Modular Cloning that take advantage Type IIS restriction endonucleases properties, and Ligation Independent Cloning (LIC)[248]. With the boom of synthetic biology, these conventional cloning methods have been

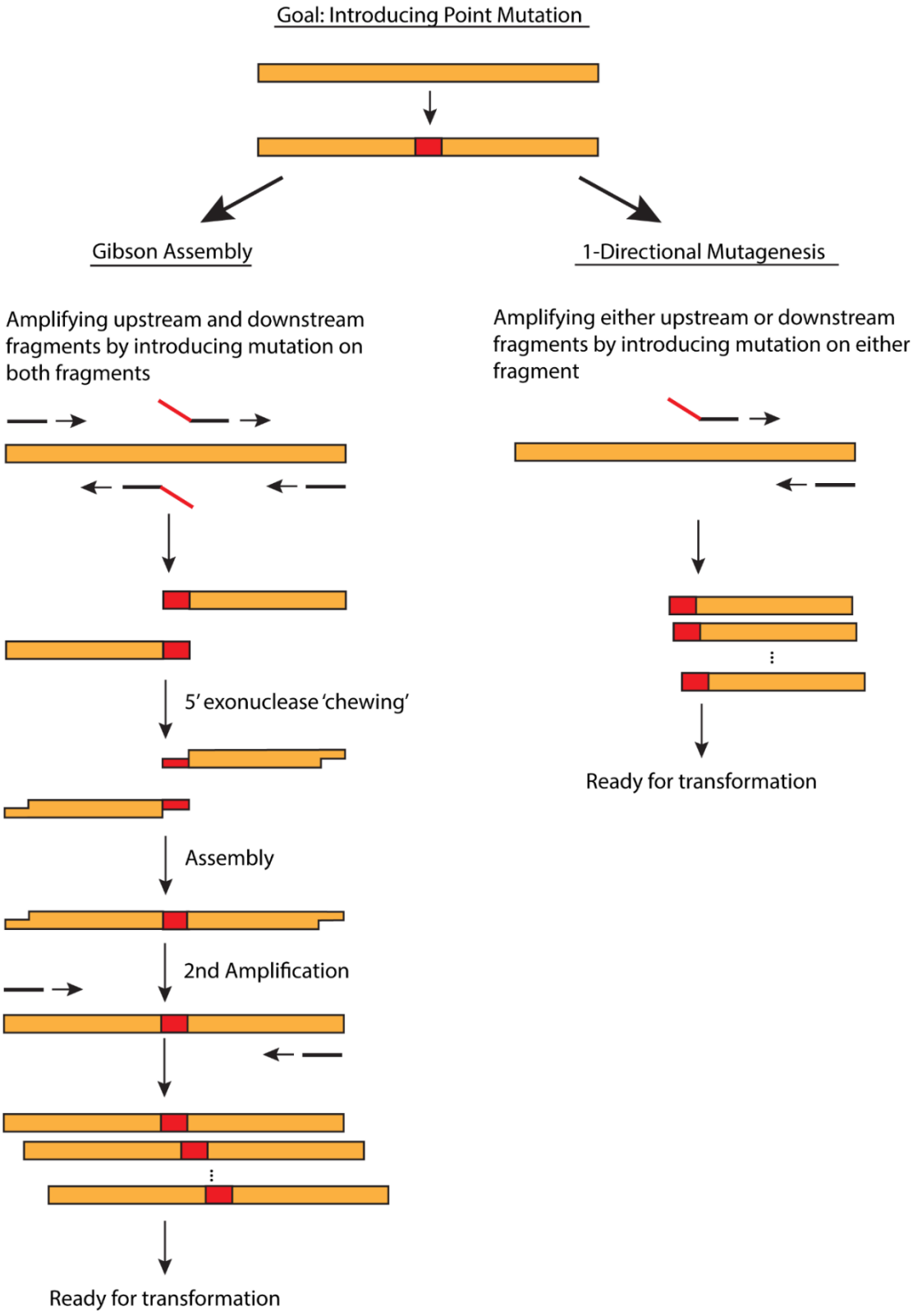


*Figure 2.8 Comparison between the cloning workflow of Gibson Assembly and 1-Directional Mutagenesis*

repeatedly challenged to meet current technological needs. Undoubtedly, there are improvements made based on our understanding of the biology, physical and chemistry of DNA molecules, for example, Cross-Lapping In Vitro Assembly (CLIVA) method that does not rely

on the biology of T4 polymerase exonuclease properties but on phosphorothioate chemistry[249]. All these does not suggest one method is better than the other. On the contrary, tools invention and development have always been a communal benefit. There are two approaches to innovation, to search in the junkyard and create something useful; or go back to the field and collect new material for the junkyard. Both approaches are important. Having more choices and tools will provide flexibility to future research in their quest to ask more questions. In this section, we would like to propose a possible method to introduce point mutations in DNA sequences.

More often, during Gibson Cloning, to introduce a mutation, one will amplify an upstream fragment and a downstream fragment with intended mutation introduced on the overlapped region through oligos. In 1-directional mutagenesis, all these steps are not required. The steps comparison between the two methods can be seen in Figure 2.8.

The rationale of this test was inspired by one of the failed cloning experiments in Chapter 5. During an attempt to introduce point mutation, we used a Taq polymerase amplified fragments for Gibson Assembly method and transformed the whole reaction into MS11. We obtained several clones not only with the intended mutation, but also with an extra A/T mutation at position which we realized were at the end of the primer binding site, most probably introduced when amplified with Taq polymerase. With this observation, we suspect that *N. gonorrhoeae* may have the ability to take up and recombine DNA sequences that are quite short on one end. Studies thus far has always focused on improving the efficiency of recombination in cloning, hence most of the time a longer flanking regions are studied. In our case, we intend to explore the lower end of the spectrum by questioning how flexible is the recombination process in incorporating minimal homologous region on one end of the transform DNA.

To do that, we leverage on the gyrB-4kbp tDNA. We have three different gyrB tDNA format: a full length 4kbp fragment amplified with the **point mutation** in the middle of the fragment, and 2kbp fragments that are amplified on either side of the point mutation with the point mutation side amplified with oligos that have 13bp homologous region after the point mutation (Figure 2.9). We also tested two conditions: single transformation and co-transformation.

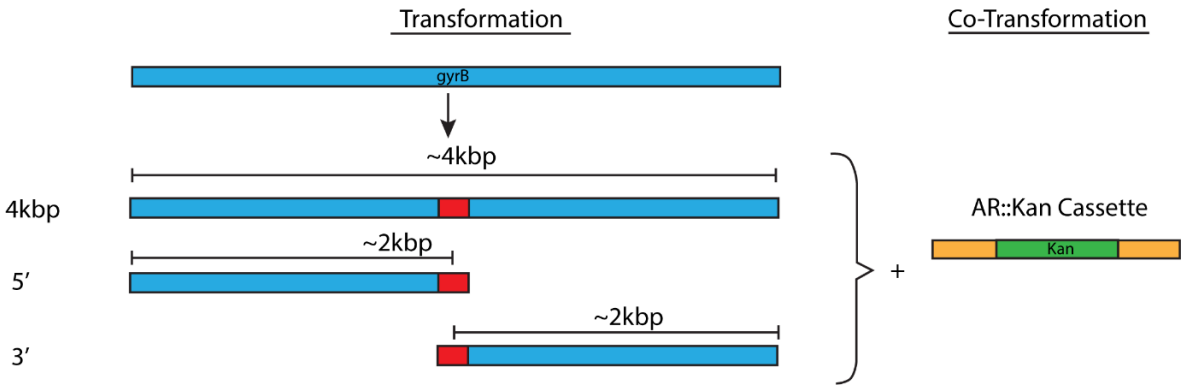


*Figure 2.9 Experimental setup to examine transformation efficiencies of 1-directional mutagenesis in sole and co-transformation*

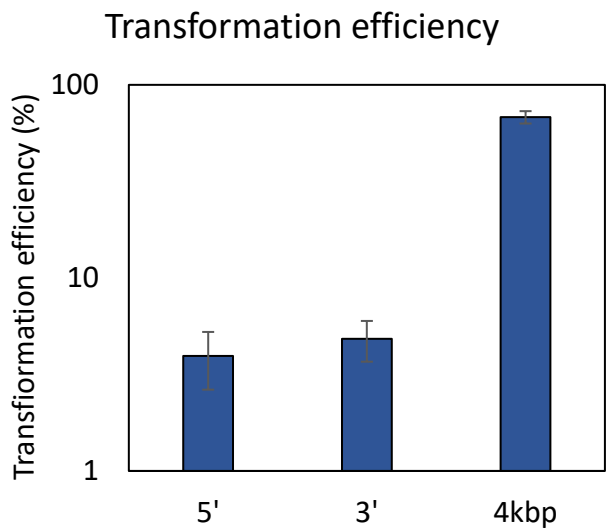


*Figure 2.10 Transformation efficiency of 1-directional mutagenesis in sole transformation*

In our results, we proved that 1D-directional mutagenesis can indeed occur, at least in the condition we tested (2kbp homologous region on one side and 13bp on the other side). This can be observed from the transformed population that grow on plates with Nalidixic acid in both 5' and 3' setting (Figure 2.10). Though, it is also expected that the transformation efficiencies of 5' and 3' are not as high as the 4kbp tDNA. This is most likely due to the reduced homologous region of the tDNA. Since we learned from our co-transformation study that the size of co-transformed tDNA fragments can affect the co-transformation efficiencies, we expect to see better transformation in the 5' or 3' sets.

Our results show that indeed, in the case of co-transformation, with the shorter homologous region of *gyrB* tDNA, 5' and 3', it is still possible to select double mutants through kanamycin resistant population albeit with lower efficiencies than the 4kbp (Figure 2.11). Ideally, this exact setup will need to be verified with as many other examples as possible. Nonetheless, this study proved the possibility of using 1-Directional Mutagenesis, and we can even leverage on this possibility to optimize with co-transformation.

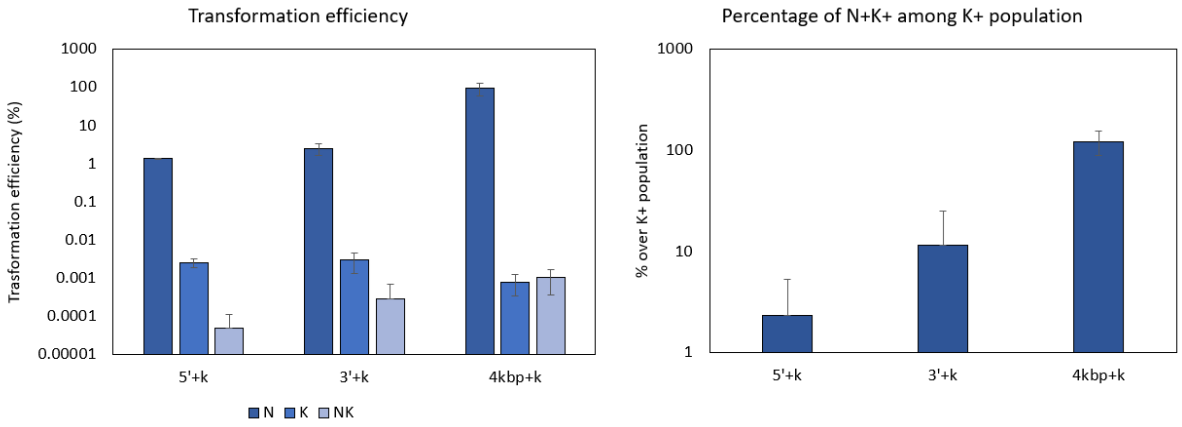


*Figure 2.11 Transformation efficiencies of 1-directional mutagenesis in co-transformation: (a) the efficiency of respective transformed tDNA against total population (b) the percentage of double mutants among kanamycin resistant population*

Previous experiment introduced only a point mutation. This can be a potential limitation of this methodology. While it is understandable that the effort to alter a large fragment between the 13bp and a 2kbp homologous region can be challenging, but this is still technically an unknown territory. To step up from the previous experiment, we utilized one of the cloning example we

know that will be discussed in detail in Chapter 3. In this setting, we intend to introduce a amino acid point mutation in the *pilE* gene of *N. gonorrhoeae*. In our previous study (Kan, unpublished), this mutation was introduced into a *ΔrecA* mutant, N400 *ΔrecA*. On top of that, to select for successful mutants, a Kanamycin cassette was attached to the 3' end of *pilE* gene. Although this mutant served as great tool for our study, this genetic construct pose a problem with lower pilin expression level. This observation is probably due to potential antisense promoter downstream of *pilE* gene that could serve as a regulator of pilin expression. To bypass those problem, we intend to tap on another strain which has reduced pilin antigenic variation frequency, ΔG4. In this strain, the guanine-quadruplex complex structure upstream of *pilE* promoter was replaced by a Kanamycin cassette. Even though there are regulatory regions within the *pilE* promoter, ΔG4 does not show any severe decrease in pilin expression.

With ΔG4 as parental strain, we performed a 1-Directional Mutagenesis by amplifying region from upstream of the the Kanamycin cassette till the region we used an oligo to introduce the amino acid point mutation. In this case, instead of one basepair change, we had to introduce **3 and 2 basepair changes** for T132C and T138C respectively (Figure 2.12). In this case, we introduced a 16bp overhang on the other side of mutation for homologous recombination. The amplified fragments were transformed directly into MS11 wild type strain and selected with Kanamycin. We did use a higher concentration of kanamycin in agar plate since we encountered polyploidy in ΔG4 strains prior to this. Among the successfully growing colonies, we selected four for each construct and sequenced to check if they indeed took up the mutation. We saw 2 out of 4 successful mutants in T132C and 1 out of 4 successful mutants in T138C (Figure 2.13).

This result is promising since it expands the options we could have in the future in genetic manipulation. For some DNA region in which amplification and Gibson Assembly can pose difficulties or take longer time to perform, researchers can weigh in their option to try using 1-Directional Mutagenesis.

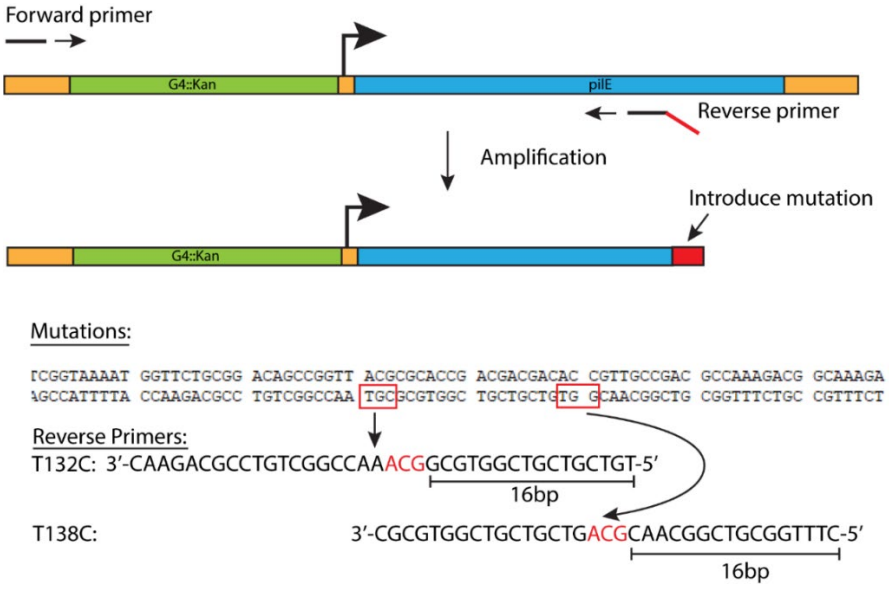


*Figure 2.12 Illustration on the introduction of mutation through 1-directional mutagenesis up to 3 bp in pilE gene*

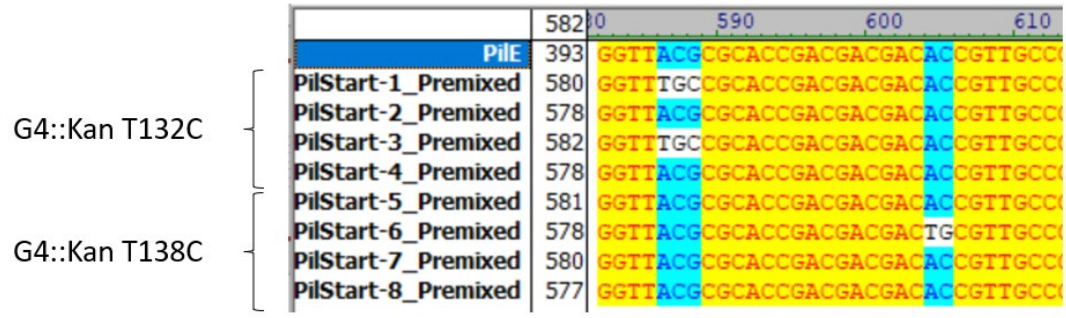


*Figure 2.13 Sequence alignment of sequencing result for ΔG4::Kan T132C and ΔG4::Kan T138C*

### 2.3.8 Potential application

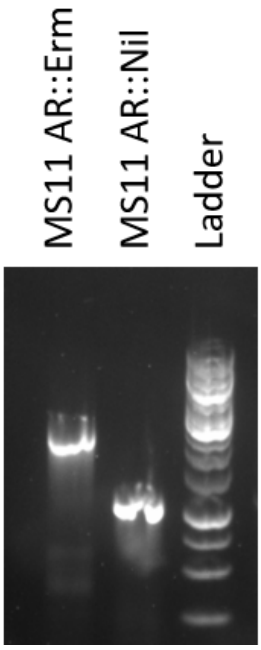


*Figure 2.14 Agarose gel showing the removal of AR cassette from MS11 AR::Erm*

Some of the potential applications of these developed tools had been considered. Although they're not tested in a large scale, we aim to show some proof-of-concept study to present them as possible future directions, either for genetic manipulation or potential research tools. With the introduction of Interchangeable Cassette System, we proved that we could interchange the selection marker in that selected region through sequential transformation. The other region in which such manipulation can potentially be performed on is the region between *trp* and *iga*. However, the versatility of the concept of ICS also include the possibility of removing the said selection marker in the event of a desire to remove antibiotic resistance in the strain. In our hands, we attempted exactly that. We amplified the AR region from a Wild Type strain, which does not contain any selection marker and transformed the fragments as tDNA into strains with Erythromycin marker MS11 AR::Erm. Before the step for selection, we did serial dilution to a concentration of cells in which we can obtain individual colonies on agar plate, the solution were plated on both non-selective agar plate. After a day of growth, the grown colonies were replicated on an Erythromycin selective plate, through replica plating technique. Both of the plates were left to grow and compared after 24h incubation. Out of 3 plates with around 300 colonies each, we found two possible candidates that grew on the non-selective plate but not the selective plate. We did a colony PCR and indeed these colonies had had their AR cassette removed Figure 2.14.

While this result seems positive in proving the possibility of switching out of an antibiotic resistant gene, the efficiency has proven to be very low compared to that of insertion. We tried transforming the same AR::Nil with a longer flanking region (4kb on each side of the cassette) and still did not observe any significant improvements. With that, we decided to explore the limitation of this switching out process.

In the next test, we targeted antibiotic resistance caused by point mutation, nalidixic acid resistance through *gyrB* mutation. We used a 6kbp gyrB mutant tDNA as used in previous study

and transformed them into a MS11 *gyrB* mutant (Figure 2.15). In our quantitative result, we can observe obvious revertant of the mutation. We observed more cells that could not grow on nalidixic Acid plate. There are only around 20% of the cell that retain the mutation, meaning close to 80% successful transformation of the wild type *gyrB* tDNA (Figure 2.16).

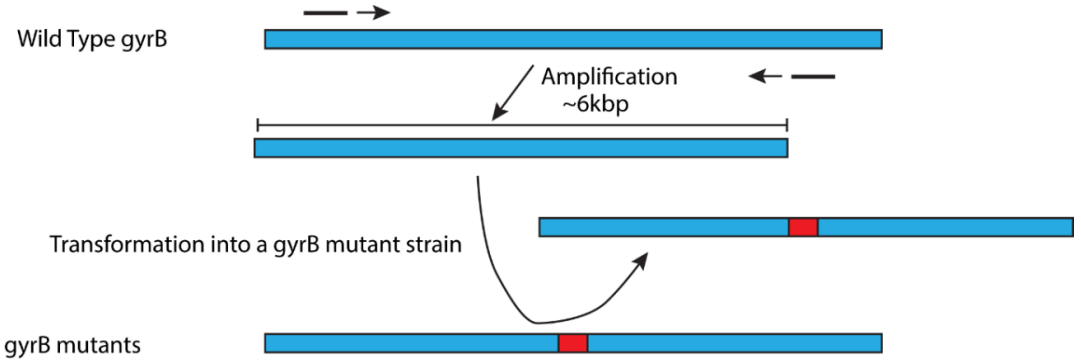


*Figure 2.15 Illustration of the concept for removing nalidixic acid resistance from MS11 gyrB mutants*

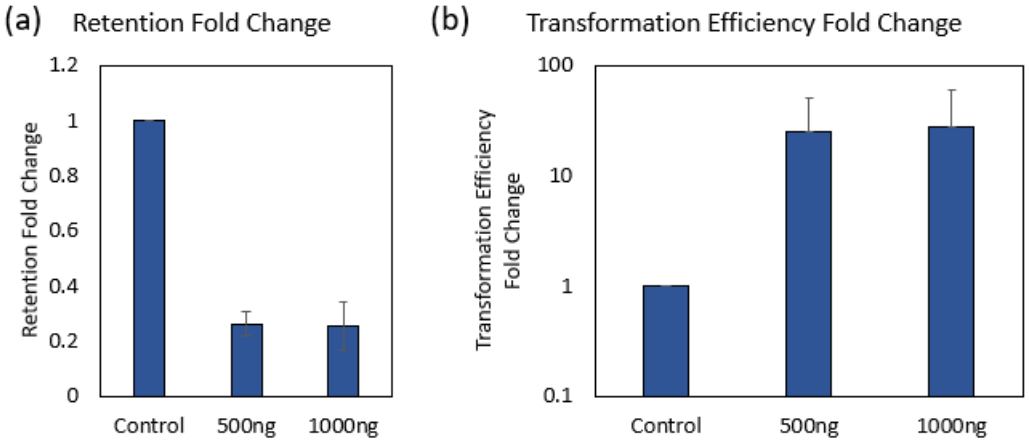


*Figure 2.16 (a) The retention percentage and (b) transformation efficiency of nalidixic acid resistance after transformation with wild type gyrB tDNA*

This result is a positive sign that **reverting mutation** may not be as difficult as it seems, even when it is the case of without a selection pressure. From both cases, we can hypothesize that the limitation of removing resistance probably come from optimizing transformation efficiencies or DNA uptake and the nature of mutation. We suspect that in the case **of removing selection marker in the AR cassette**, the DNA repair mechanism has to match the both side of homologous flanking region by bending the DNA in the middle (the selection marker). This process may be challenged by the physical property of DNA molecules in the cell. However, these findings will hopefully be a great stepping stone for others to accumulate more information on these and sharpen our transformation tools for applications.

## 2.4 Discussion

In this Chapter, we developed and showed the versatility of molecular biology techniques in engineering *N gonorrhoeae.* We introduced a modified transformation protocol for quantitation, **New Spot Transformation**, during the first part. This proposed modification provides a

protocol that minimizes quantitative error and good dynamic range for DNA transformation study. For example, we can identify the **optimized DNA-to-cell ratio** for transformation efficiency using this protocol.

With the help of a streamlined workflow for quantitation, we can explore the efficiencies and robustness of newly developed transformation techniques. With that, we showcased the versatility of **Co-transformation** and **Interchangeable Cassette System (ICS)**. With Co-transformation, we provide the flexibility in marker-less and scarless genetic engineering. Together with ICS, these techniques theoretically allow users to perform multi-site genetic engineering and infinite sequential cloning even with only two selection markers. We also provided a proof-of-concept example in this chapter.

Other than optimizing the transformation pipeline, we also worked on expanding possibilities on the cloning method. During this chapter, we proposed an alternative method, **1-directional mutagenesis**. With this method, we showed that Gibson Assembly may not be necessary for *N. gonorrhoeae* transformation for mutations up to 3bp changes. This proposal will provide researchers flexibility to optimise their resources' usage.

At the end of this chapter, we explored the possibilities of applying our findings in **removing resistance in a bacterial population**. Although we did not have great success in removing a selection marker cassette, we proved that we can remove resistance resulting from point mutations from a population successfully.

# Chapter 3 : Tools Development to Understand The Dynamics of Type IV Pili and DNA Uptake

In the previous Chapter, we introduced the development of tools intended to impose genomic modification in *Neisseria gonorrhoeae*. Those tools allow us to develop mutants of interest and standardized protocols to understand DNA transformation. This Chapter will show the development of tools intended to study DNA Uptake and Type IV Pili dynamics in *N. gonorrhoeae*. We will discuss our attempts in media optimization, visualization of Type IV Pili and DNA molecules, visualization and quantification of DNA uptake and the quantification of pili retraction events through polyacrylamide micropillars. These developed tools and protocol workflow will be the foundation for our studies in the following few chapters. This chapter is quite extensive and is meant as a reference for people trying to reproduce our results. The main results of these experiments are summarized at the end of this chapter. The summary might suffice for the cursory reader mainly interested in the biological results exposed in the subsequent chapters of this thesis.

## 3.1 Media Optimisation for Microscopy

### 3.1.1 Background and Motivation

#### 3.1.1.1 Motivation

One of the main goals of this study is to understand DNA transformation in *N. gonorrhoeae* through microscopy. Therefore, we vie to obtain an optimal experimental setup to visualize the process. Many factors contribute to good live imaging in *N. gonorrhoeae*. First, *N. gonorrhoeae* has twitching motility. Hence, having the means to set the bacteria in place is crucial for good visualization. Some studies attempted to immobilize bacteria on coated surfaces in liquid media[250]. Another simple method involves using an agar pad or gellan gum slab to sandwich the bacteria sample on a glass slide[251]. We have been using the agar pad method in our laboratory, as illustrated in Figure 3.1, so we decided to build on this system. However, this experimental setup has two major concerns for fluorescence microscopy in studying DNA uptake: i) imaging quality and ii) DNA molecule diffusion.

First, the agar pad used can affect the imaging quality. To work with *N. gonorrhoeae*, one of the major solid media used is GCB Agar. This medium is slightly opaque and tends to have a slight autofluorescence background when observed through a fluorescence channel. The autofluorescence background will also reduce the signal-to-noise ratio of our experiments. The content of the agar can contribute to this. A similar problem has been reported, identifying the presence of flavins and flavoproteins as reasons for background autofluorescence and cell autofluorescence[252,253]. At the same time, the slight opacity of the media may not be ideal for bacteria detection during analysis. While this problem has not been investigated in detail, it will be identified and described further in this section.

Secondly, our procedure uses naked extracellular DNA molecules since our study is interested in natural transformation. In the setup for long-term imaging under an agar pad, the diffusion

of DNA molecules can lead to biases, for example, the location of the DNA molecules or their interaction with the bacteria. While the diffusion of DNA molecules in water or cytoplasm[254,255] and the movement of DNA molecules in agarose during electrophoresis[255] has been reported, the characterization of DNA molecule diffusion in agar or agar-like medium is rare. One literature reports that the diffusion coefficient for DNA molecules around thousands of base pairs in 2% agarose gel can be as high as a micron square per second[256]. The normal agar concentration in GCB Agar is around 1.125%. Therefore, the feasibility of using GCB Agar for a long-term DNA transformation experiment is still questionable.

Taking into account these two concerns, we intend here to optimize a solid medium suitable for studying DNA uptake while maintaining bacteria at their normal physiological condition. We can usually circumvent the problems from the agar for the imaging quality issue by changing to a minimal medium. However, this can be tricky for fastidious bacteria like *N. gonorrhoeae*. Efforts to develop minimal or alternative media for *N. gonorrhoeae* are scarce. We also intend to explore slowing the DNA molecule diffusion by adjusting the medium density. Since we aim to optimize the solid medium for *N. gonorrhoeae* for imaging purposes, we must dive into the basics of *N. gonorrhoeae* culture medium.

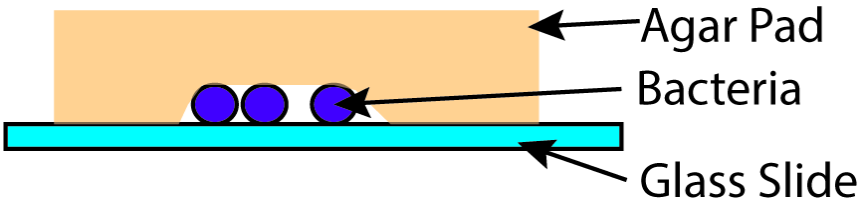


*Figure 3.1 Sample preparation setup for microscopy in Neisseria gonorrhoeae*

### 3.1.1.2 Culture Media for *Neisseria gonorrhoeae*

Salt-free veal agar was one of the earliest media used to cultivate *Neisseria gonorrhoeae*. The main application of cultivating gonococci at that time was to isolate bacteria from infection patients. However, it was well known that growing gonococci is a relatively difficult task and bacteria cells needed to be transferred frequently, even on available media, to keep them viable[257]. In 1915, Edward Vedder and his lab assistant, Sergeant Frederick Abner, discovered that adding starch into beef infusion agar increased the success of cultivating gonococci[89]. They optimized the starch concentration to one per cent, stating that commercial corn starch works as well as corn starch for medicinal use[89]. They also observed that potato and tapioca starch helps with growth, though not as much as corn starch[89].

Culture media for gonococci have been consistently modified over the years based on pre-existing recipes with starch added based on this observation, resulting in the birth of Mueller Hinton Media, which is still used to this day[88]. Mueller and Hinton also noted that hydrolyzed starch will lose its growth-promoting effect[88]. As studies were dedicated to the identification of growth factors required for gonococci growth, cysteine was discovered to stimulate gonococci growth[87]. Gould also observed that many growth requirements were largely strain-specific among gonococci[87]. At the same time, other bacteria, such as meningococci, have grown well on starch agar, too[87]. Several hypotheses were made. However, the quest to understand the

usage of starch was not conclusive until around 1946 when Herbert and Mueller identified the 'inhibitor' in agar for gonococci growth[258]. By methanol extraction, they postulated that fatty acids are the inhibitors present in agar and that the added starch adsorbs (adsorbs would work as well here) the fatty acid, therefore promoting the growth of the gonococci[258].

After the use of starch and its relationship with fatty acid has been addressed, starch continued to be the essential ingredient in various culture media modified for gonococcal cultivation[259,260]. Further studies on the inhibition of fatty acids were not conducted until 1974, when it was found that *N. gonorrhoeae* growth inhibition may not be a result of the presence of fatty acids in the agar alone. Some strains of *N. gonorrhoeae* can produce free fatty acids that can inhibit other strains or entire species, too[261]. This study hypothesized that the 'bacteriocin' effect resulted from the degradation of phosphotidylethanolamine to long-chain fatty acids and monoacyl phosphotidylethanolamine inhibiting bacteria growth[261]. Following this revelation, a few studies followed up on the toxicity effect of fatty acids and monoglycerides towards *N. gonorrhoeae*, even potentially identifying some of the exact chemical groups at play, for example, myristic acids and palmitoleic acids[261–263]. Similarly to what was observed before, the specificity of toxicity varies across strains[261–263]. What is worth noting is that there are other bacteria in which fatty acids are toxic, such as Group B streptococci and Chlamydia[262]. Group B streptococcus culture methods also include starch as an essential agar medium component[264]. Meanwhile, being an obligate intracellular pathogen, Chlamydia trachomatis relies on the host long-chain Acyl-CoA synthetases' (ACSLs) activity for growth and development[265]. Based on this, this toxicity effect observed on an agar medium could well be intricately linked with the cell metabolic pathways.

Although this identification was revealed in 1946, the knowledge seems to have been lost over time. Solid media modified to cultivate *N. gonorrhoeae* continued to be developed with added starch. There was no clear attempt to create a medium without starch. Meanwhile, the development of liquid media has significantly improved over time, with even defined media being produced. Some examples include Wong-Shockley-Johnston Medium (WSJM) and GW Medium[266,267]. These media improved in the limitation of the size of the initial inoculum and also maximum growth density. However, WSJM suggested using conventional agar and starch base to add to its recipe while GW wasn't intended for solid medium cultivation purposes.

### 3.1.2 Materials and Methods

Solid medium preparation

Conventional GCB agar medium was prepared based on the ingredients in Culture Media. For the modified GCB-based medium, GCB Liquid was used as the base and different amounts of agar or starch were added accordingly. The conventional agar concentration used was around 1.13%, but 2%, 3% and 5% were used for this study. The types of agar and agarose used were Bacto Agar (Becton Dickinson) and UltraPure Agarose (Invitrogen). Additionally, we used 0.1% or 1% of starch, according to the nature of the experiment, when added to the GCB Liquid base for modification. Details will be described in detail, together with the investigations.

Depending on each experiment, the types of starch used were corn starch, potato starch (Sigma Aldrich) and soluble starch (Sigma Aldrich).

Transform DNA (tDNA) preparation

All tDNA was prepared with the same protocol as Chapter 2. Information on any mentioned tDNA used in this study can be found in the tDNA List.

Microscopy test for solid medium

Bacteria strains of interest were resuspended in a GCB liquid medium, and a stock of $OD_{600}$ 0.7 was prepared. According to the experiment, 2ul of this stock was added to a glass slide and sandwiched with an agar pad. The agar pad was cut out from the plate to the size of around 1cm x 1cm (width x length). The set up was then left in the incubator for 3h, at 37°C and 5% $CO_2$. After 3 hours, the setup was taken out and observed under an inverted Nikon Ti microscope.

Disc Test

An appropriate concentration of fatty acid was prepared. 10ul of the solution was added to a 6mm diameter sterile filter paper disc. The disc was left to air-dry. On an agar plate (depending on the test), bacteria were lawned on the surface using a swab. The disc was then placed on top of the lawn. The plate was then incubated overnight at 37°C and 5% $CO_2$. The observation was made the next day, including the diameter of the zone of inhibition.

### 3.1.3 Results

#### 3.1.3.1 Development of Solid Media

The solid medium that is commonly used is GCB Agar Medium to work with *N. gonorrhoeae*. This solid medium is slightly opaque. On the other hand, the liquid medium, GCB Liquid medium, is transparent. Further comparison between the ingredients shows that GCB Liquid medium does not contain starch and Bacto agar. The importance of starch in growth did not occur to us at first. During the development of solid media for microscopy, we intend to replace ingredient in the solid medium that may contribute to the opaqueness, **starch** and **agar**. Amylose in starch can be a big contributor of the visibility in the medium. We assumed that the starch acts as a gelling agent and can be replaced by agar. Moreover, the bacto agar used in conventional GCB medium is not a purified agar. Therefore, we decided to change it to the chemically purer alternative agarose. Therefore, we establish a solid medium with **GCB Liquid medium mixed with purified agarose for DNA gel electrophoresis**. Later on, we discovered starch's potential importance and tested these modified media with **0.1% starch**.

On the side, we also looked into alternative media through literature. Unfortunately, most alternative or chemically-defined media for *N. gonorrhoeae* are liquid media. They are usually developed for diagnostic purposes. Ultimately, we selected one of the most suitable candidates, a chemically-defined medium, GW medium[266]. In this attempt, we prepared **GW medium** from scratch and added a similar amount of gel electrophoresis-grade agarose.

With these versions of modified media, we plated a similar bacteria cell number on them to check if they grow equally well. To test the robustness of these media, we experimented with both *N. gonorrhoeae* and *N. elongata*.

### 3.1.3.2 Bacterial growth on different media

From this experiment, we compared the viability of *Neisseria* bacteria on different media. Here, we note that when no starch is added to the GCB-based solid medium, the growth of *N. gonorrhoeae* on plates is affected (Figure 3.2). In contrast, the growth defect is immediately rescued when 0.1% corn starch is added to the medium. This pattern is the same regardless of the type of agar used (Bacto agar or agarose). The importance of starch in *N. gonorrhoeae* growth was roughly reported in 1915 by Vedder, who noted that 1% of starch is optimal for gonococci growth as he tried to develop a culture medium for gonococci [89]. However, the reason behind this particular requirement has been left ambiguous throughout the years. There was speculation that the starch would lock some impurities in the medium that would inhibit *N. gonorrhoeae* growth. Moreover, it is also important to note that there are a few conditions in which cell dilutions were not reflected across the serial dilution, as shown in the GCB-base medium without starch. This hinted that the inhibitory effect is only observable when the cell number is below a certain threshold. However, our observation in GW solid medium shows that starch may not be necessary in all growth conditions.

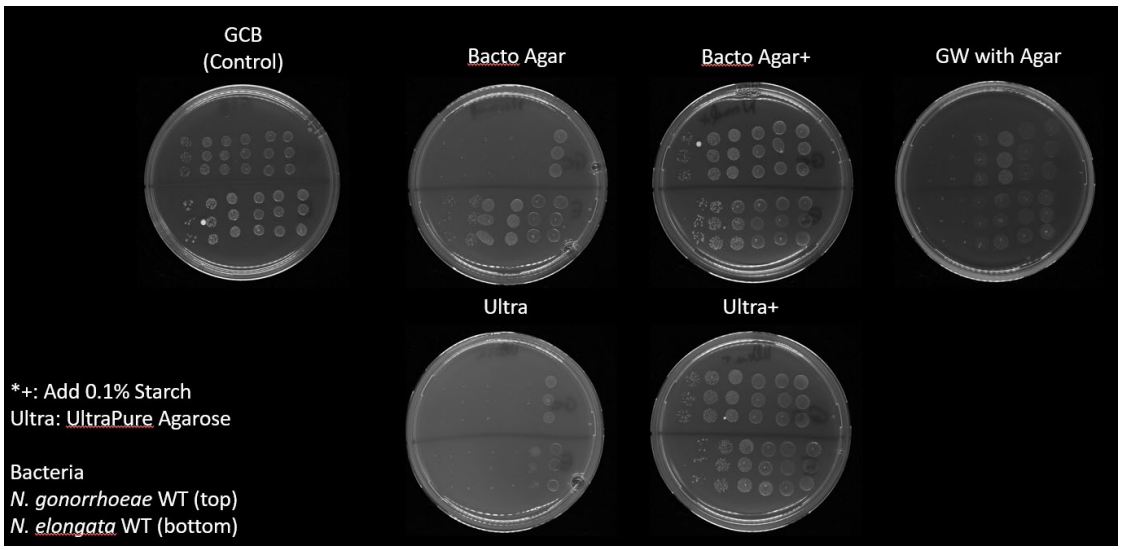


*Figure 3.2 The effect of starch in media on the growth of N. gonorrhoeae and N. elongata*

Meanwhile, we observed growth comparable to the GCB agar plate (control) on the GW solid medium, even though there was no starch in the GW solid medium. However, it is interesting to note that the colonies grown on the GW solid medium have a different colony morphology than those on the control plate. At this stage, while the GW solid medium can sustain viability similar to that of the control plate, we hypothesized that they are probably in a different metabolic or physiological state. On a side note, *the growth of N. elongata* is not affected as severely as *N. gonorrhoeae* in any of the different media. This shows that *N. elongata* is not as sensitive to the effect of starch on bacteria growth. To understand the significance of starch, we would need to probe further through *N. gonorrhoeae.*

### 3.1.3.3 Effect of Agar % on *Neisseria gonorrhoeae* growth

Our other plan was to devise a method to slow down DNA molecule diffusion. We planned to do this by increasing the density of the agarose in the solid medium. However, we have no good reference in the literature on whether such fluctuation in the mechanical properties of the culture medium can affect cell growth. To that, we did a simple test of cell viability on GCB-base agar plates added with different concentrations of agarose: 1.13% (control), 2%, 3% and 5%. Starch was added in all of them to ensure any observations would be due to the different agar percentages. In this test, we observed that the higher the concentration of agarose, the lesser the viability of *N. gonorrhoeae* (Figure 3.3). This effect can be observed similarly in *N. elongata* but to a lesser extent. We suspect that higher agarose concentration changes the culture medium's physical properties. This can be observed during the experiment in which the surface tension of each agar plate is different. Moreover, plates with a higher percentage of agarose tend to dry out faster after preparation.

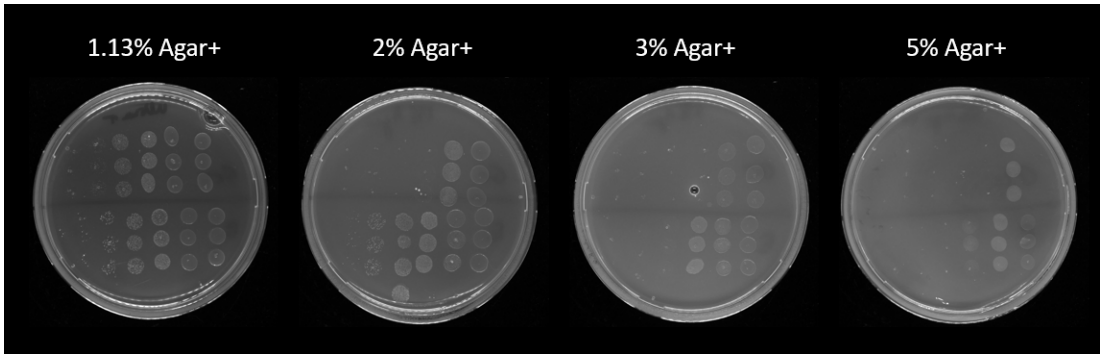


*Figure 3.3 The effect of agarose percentage on the growth of N. gonorrhoeae (upper half of plates) and N. elongata (lower la fog plates)*

### 3.1.3.4 Effect of different media conditions under microscopy setup

Although increasing the agarose percentage in the culture medium may not be the most feasible route, we tested the effect of different media conditions on cell growth with the microscopy setup. This experiment will best reflect its feasibility to perform DNA transformation imaging. We included GCB agar plate (control), GCB-base media (with or without starch and 1.13% or 5% agarose), and GW medium (1.13% or 5% agarose).

In the observation, the growth of *N. gonorrhoeae* under an agar pad of culture media with 1.13% agar reflects exactly what is observed in Section 3.1.3.2 (Figure 3.4). The lack of starch impedes *N. gonorrhoeae* growth, while the addition of 0.1% starch restores the growth. Similarly, the GW medium seems to grow like the control agar. For conditions using an agar pad with 5% agarose, however, growth appears to be slower in all other conditions than the control plate, regardless of the presence of starch. It is also worth noting that compared to 1.13% GCB agar without starch, 5% agar seems to compensate for the growth defect imposed by the lack of starch. From this observation, we can be sure that for the experimental setup of GCB Liquid with 1.13% agar and 0.1% starch, the growth of GC is not affected and, hence, is suitable for DNA uptake experiments. This study also hints at the possible effects of mechanical force on cell growth based on the 5% agar results.

However, with these findings, there seem to be more factors that we need to fully understand and investigate to be sure that increasing agar concentration will not affect the physiological state or DNA transformation in the cell. Therefore, we decided to take a step back and re-investigate the effect of diffusion in our DNA transformation studies.

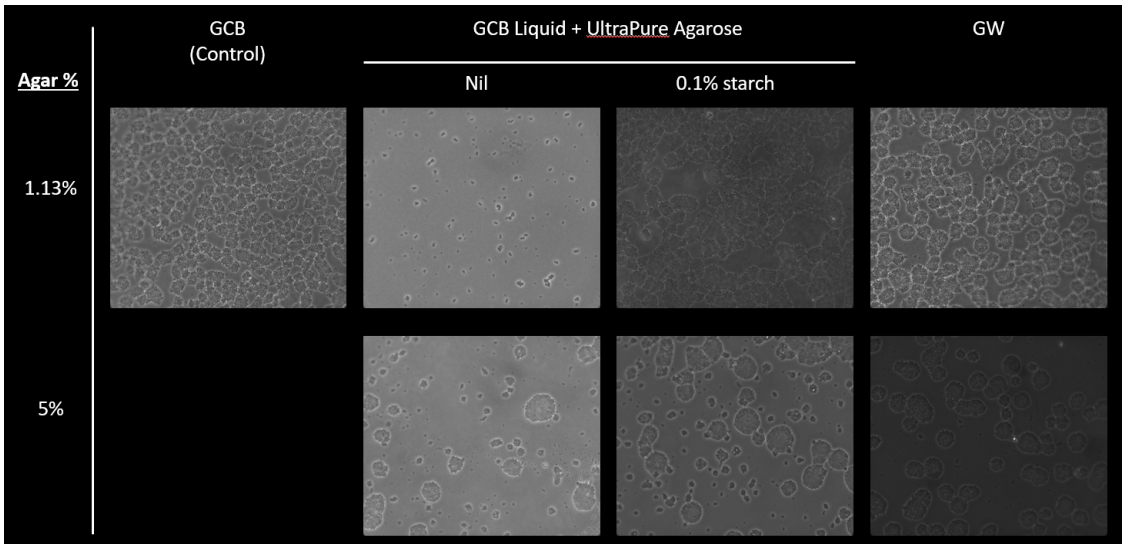


*Figure 3.4 The effect of different media ingredients on Neisserial growth under microscopy experimental setup*

### 3.1.3.5 Fatty Acid inhibits GC growth and could be rescued by starch in a dose-dependent manner

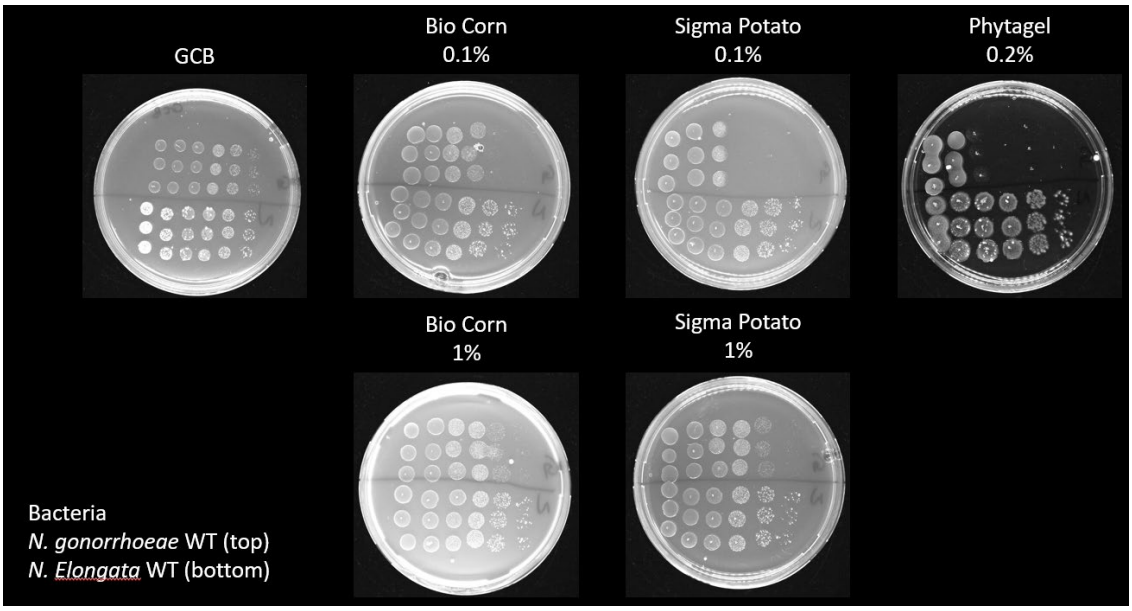


*Figure 3.5 Different types of starch can change the effect of protection. Phytagel is not suitable to replace agar.*

Our first suspicion led us to look into starch breakdown and amylase activity. This is due to several early reports on how *N. gonorrhoeae* growth can be inhibited by amylase activity, breaking down the starch in the medium [268]. Hydrolyzed starch is also reported to work less

effectively in protecting against the inhibitory effect on *N. gonorrhoeae* viability [268]. This further strengthens the statement that starch plays a role in locking certain agar substances that could harm *N. gonorrhoeae*. The fact that starch was only conventionally added for solid mediums but not liquid mediums also led us to believe that the culprit is indeed in the agar. However, two studies under our investigation do not support this hypothesis. We observed no change in viability when bacteria was grown in GW solid medium (Section 3.1.3.2). GW solid medium does contain agar. If the harmful ingredient is indeed originated from agar, then the only possibility was that there are other ingredient in this medium that can also lock the compound just like starch did in GCB agar. The other experiment we tested was to try using Phytagel, a gelling agent commonly used in plant culture. By replacing agar with phytagel, we observed a similar drop in viability as when no starch was added (Figure 3.5). There was no agar in Phytagel. Hence, the compound that inhibits growth in *N. gonorrhoeae* most likely does not come with agar but most probably from the GCB-base.

Together with our findings on the importance of starch and GCB-based liquid medium as potential culprits, we also noted that *N. gonorrhoeae* usually has a minimum requirement for initial inoculum in liquid media. However, the reason behind this requirement is not discussed extensively. We checked if the starch effect would change the required initial inoculum. This is partially due to our observation that the inhibition of growth on the plate is sometimes diminished in areas closer to more colony growth (a crescent/gradient of colonies), hinting that there might be a community-protection effect (Figure 3.5).

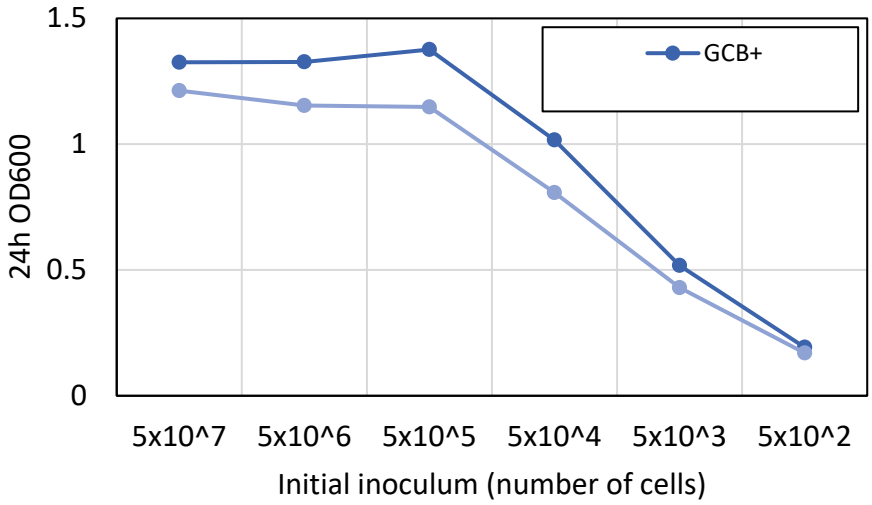


*Figure 3.6 Growth as measured in $OD_{600}$ of N. gonorrhoeae at 24h in different media, starting with different numbers of initial inoculum*

Our results show that the growth at 24 hours indeed tapered off when the initial inoculum lessened (Figure 3.6). When we observed the growth under the microscope, we noticed that the wells with lower initial inoculum tended to make bigger microcolonies that spread more sparsely than those with higher initial inoculum (Figure 3.7 and Figure 3.8). This stark difference is, however, absent in the GW liquid medium (Figure 3.9). This result suggests that the different growth patterns observed in the GW liquid medium are strong evidence that *N.*

*gonorrhoeae* grown in the medium is in a different growth phase and physiological state than those of the GCB-based medium. This mechanism probably protects *N. gonorrhoeae* from the inhibitory effect of the harmful compound.

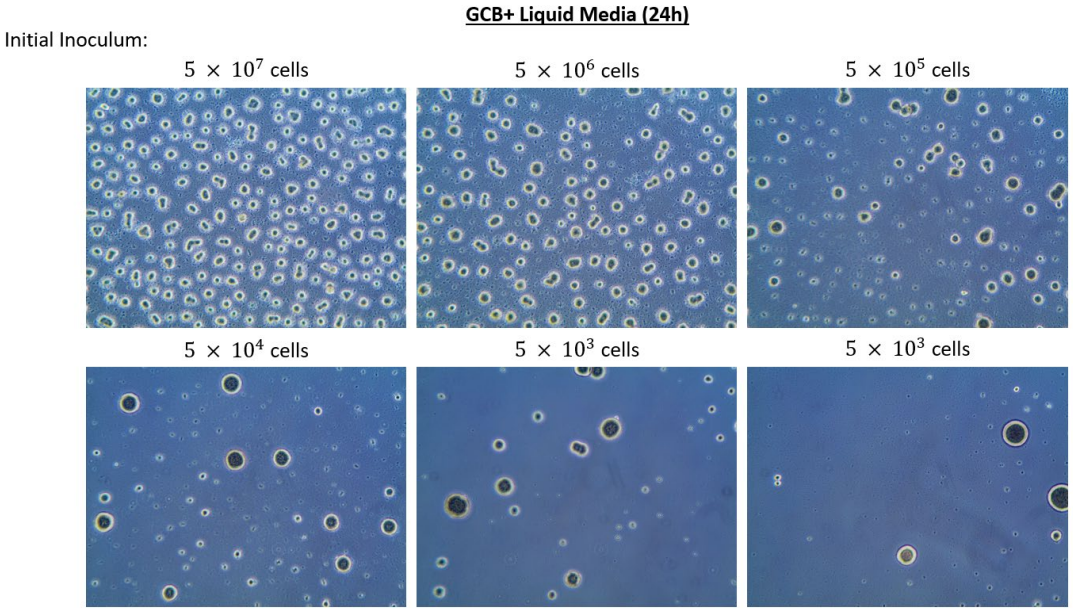


*Figure 3.7 Observation of N. gonorrhoeae growth at 24h in GCB+ Liquid media with different numbers of initial inoculum*

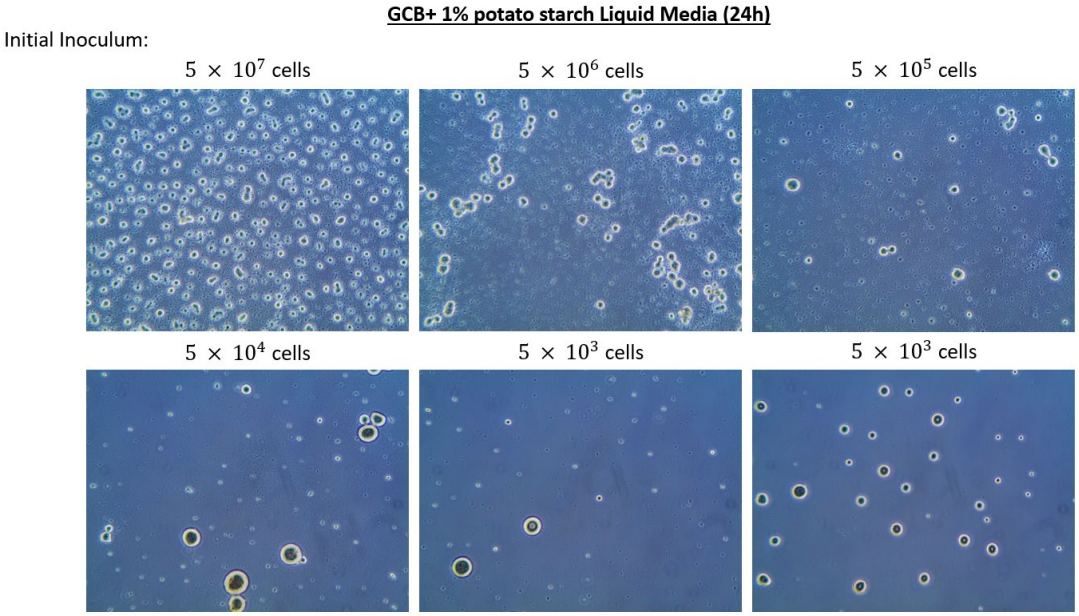


*Figure 3.8 Observation of N. gonorrhoeae growth at 24h in GCB+ 1% potato starch Liquid media with different numbers of initial inoculum*

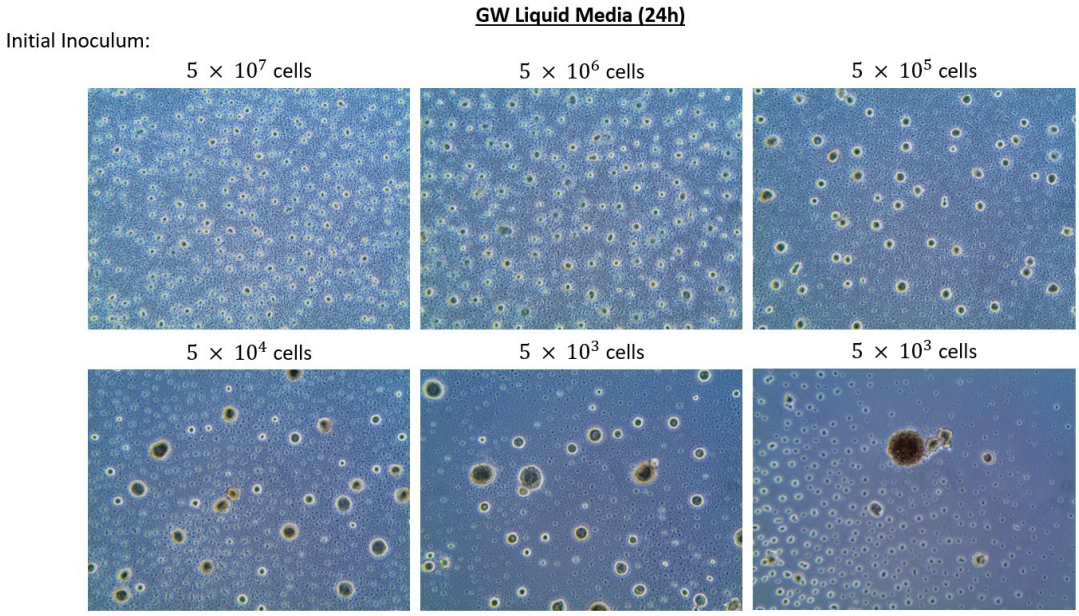


*Figure 3.9 Observation of N. gonorrhoeae growth at 24h in GW Liquid media with different numbers of initial inoculum*

At the same time, in the literature, we found another candidate of the possible compound inhibiting *N. gonorrhoeae* growth. Studies report different fatty acids affecting *N. gonorrhoeae* viability, highlighting their potential as antimicrobials[262,263,269]. Coincidentally, susceptibility to fatty acids and monoglycerides is not limited to *N. gonorrhoeae* but group B streptococcus and *Chlamydia trachomatis*[262]. With this information, we decided to dive into the culture conditions of these two bacteria to find any similarities. Surprisingly, group B *streptococci* are usually grown on a medium with 1.5% soluble starch[264]. *Chlamydia trachomatis* is generally cultured with host cells due to their considerably reduced genome, causing them to depend on host biosynthetic pathways, metabolites and enzymes for growth. One interesting finding includes their reliance on host Long-chain Acyl-CoA Synthetases (ACSLs) to convert fatty acids into acyl-CoA[265]. Schoch and Williams have also noted the adsorption of fatty acids by the linear component of corn starch[270], pointing towards the high possibility that the target we are looking for is, in fact, fatty acids.

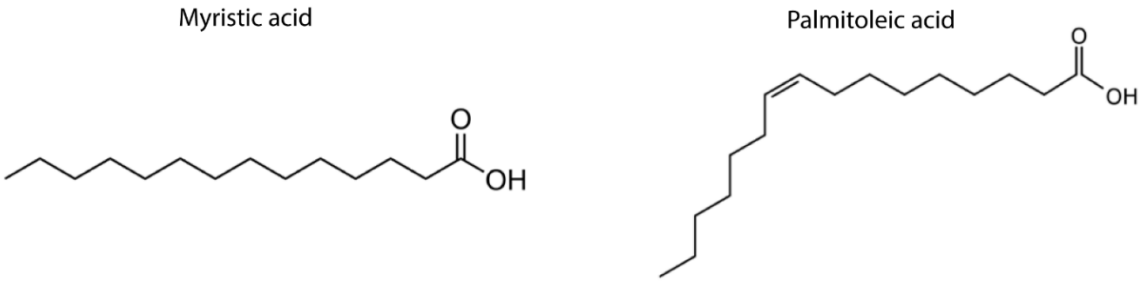


*Figure 3.10 Two identified fatty acid candidates: (a) myristic acid and (b) palmitoleic acid*

By combing through a few key literature papers, we identified a few fatty acid candidates to test on our strain, MS11. Since the inhibitory effect of different fatty acids can vary among different strains of *N. gonorrhoeae*[261], we look at candidates with an inhibitory effect on more

strains[261–263]. We landed on two candidates: myristic acid and palmitoleic acid (Figure 3.10). We did a simple disc diffusion test on a lawn of wild-type *N. gonorrhoeae* and *N. elongata* with these two candidates using the recommended concentration from the literature. Our result shows that our wild-type *N. gonorrhoeae*, MS11, is sensitive to palmitoleic acid (Figure 3.11). On the plate with myristic acid, we saw a smaller zone of inhibition (Figure 3.11). We tested the same myristic acid concentration prepared in ethanol and observed the same result. For *N. elongata*, neither myristic acid nor palmitoleic acid show any effect (xvii). This seems to match very well with our observation in Section 3.1.3.2. To further prove that the compound that inhibits the growth of *N. gonorrhoeae* and yet protected by starch is indeed fatty acid, we used the same disc diffusion assay with palmitoleic acid on different agar plates containing different starch concentrations. Through this experiment, we observed that starch protects against the inhibitory growth effect from palmitoleic acid in a dose-dependent manner (Figure 3.12).

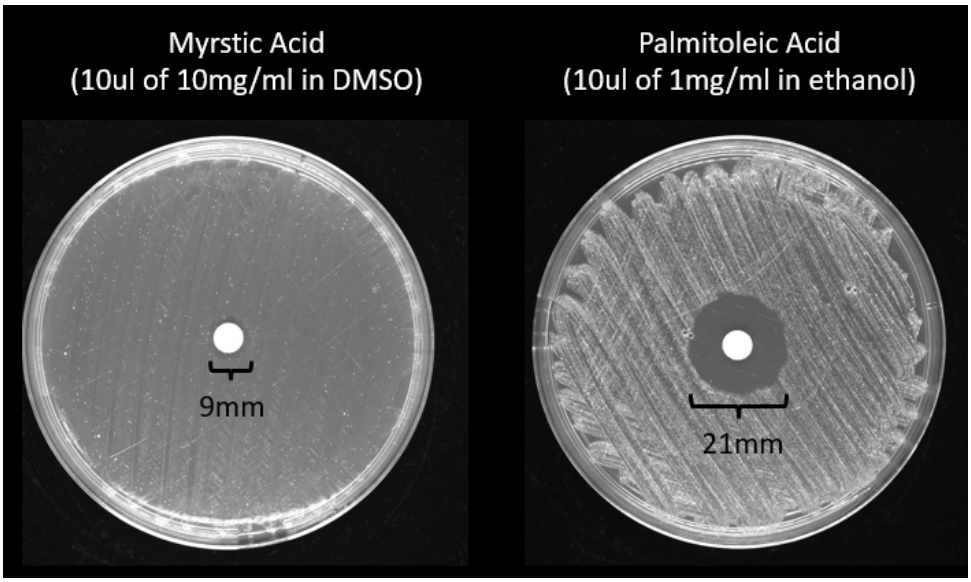


*Figure 3.11 Zone of inhibition comparison between myristic acid and palmitoleic acid on GCB plates lawned with N. gonorrhoeae*

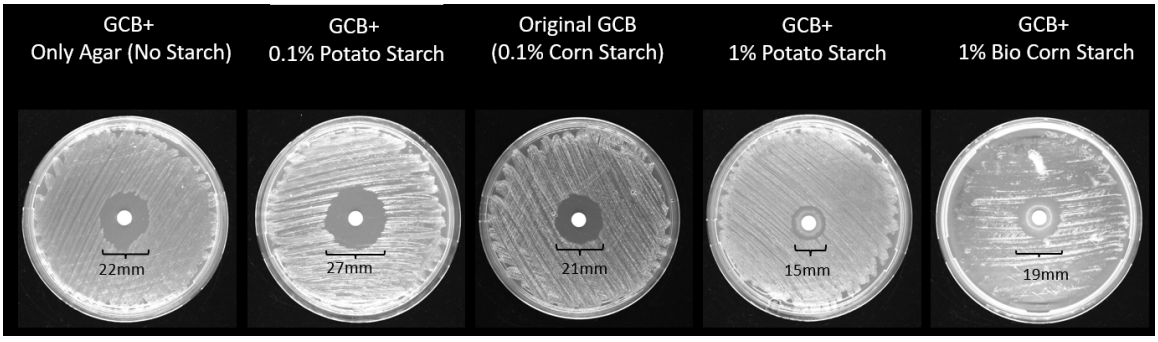


*Figure 3.12 The effect of fatty acid on the type and percentage of starch content in media*

With these findings, we recognized the importance of starch in GCB-base solid media for *N. gonorrhoeae* growth. This mechanism is probably due to fatty acid-like substances from the GCB base that can inhibit growth in *N. gonorrhoeae*. This phenomenon is absent in GW media. One of the top candidates for the source of this substance could be the Peptone protease No.3

that was used in the GCB-based medium. On top of that, the growth inhibitory effect can be cell-number or metabolically dependent, resulting in the requirement of a particular cell concentration threshold for growth under inhibitory conditions. Since this study might need further investigation that requires more effort, we focused mainly on setting up the most suitable media for our imaging process before doing other investigations.

### 3.1.3.6 Transformation efficiencies on different media

Since this Chapter aims to optimize the solid medium for microscopy in studying DNA transformation, we aim to ensure these modified media do not affect the transformation efficiency of *N. gonorrhoeae*. From our venture through previous Sections, we understood more about the medium used for *N. gonorrhoeae* and decided on a few suitable candidates to proceed with our study. At this stage, we focused on GCB agar, GW agar, GCB+ 1% potato starch, and GCB+ 0.1% soluble starch. Replacing different starch will provide us with agar pads with better visibility and will be helpful during image analysis.

To test if these media are suitable for DNA transformation study, we performed spot transformation as described in Chapter 2. Due to the slightly different growth patterns in GW medium and GCB-base medium with starch, we used 10ul of $OD_{600}$ 0.7 cells to test their competence. The results show that compared to the GCB control plates, all modified media do not change much regarding transformation efficiency (Figure 3.13). GW medium shows a slightly lower general growth, which is what we expected (Figure 3.13). This indicates that GW medium affects *N. gonorrhoeae* growth in ways we have yet to understand. We also tried the same experiment with cells with $OD_{600}$ of 0.0007, but the growth on GCB+ starch started to show slower growth. In conjunction with our observations with previous studies, even though adding starch to the GCB+ liquid medium does not generally affect growth, there is still a required minimum inoculum density to reflect the growth in the GCB control plate.

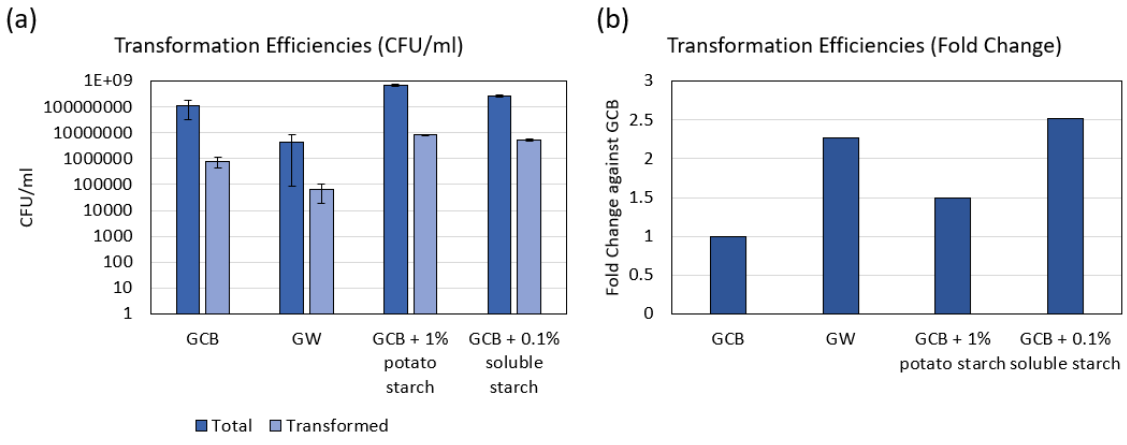


*Figure 3.13 (a) CFU/ml on control (Total) and selection (Transformed) plate and (b) Transformation efficiencies fold change for transformation assay with different selected solid media. Results are from triplicate experiments*

With the findings from this Section, we know that GCB+ 1% potato starch and GCB+ 0.1% soluble starch are suitable for DNA transformation experiments in *N. gonorrhoeae*. Given that the reduced growth we observed when bacteria were grown on the agar was not observed when

we sandwiched the bacteria with the glass slide (Section 3.1.3.4), we concluded that we could proceed with our study with these media that help provide a better imaging quality.

## 3.2 Visualization of Type IV Pili and DNA Molecules

### 3.2.1 Background and Motivation

#### 3.2.1.1 Type IV Pili Visualization

Due to the various important functions of Type IV Pili, it has been of great interest to study them. With the advancement of microscopy, there have been several attempts to visualize Type IV Pili. Visualization of Type IV Pili allows the researcher to understand this machinery's property structurally and observe their interactions with other components inside or outside of the bacteria cell. The structure of Type IV Pili has been greatly illustrated through data obtained through crystallography and cryo-electron microscopy[151,271,272]. Other works allow us to understand the components and locations of specific minor pilins through immunofluorescence microscopy or immunogold labelling transmission electron microscopy[166,170,273,274]. All these techniques have been reported on Type IV Pili in *Pseudomonas aeruginosa, Neisseria meningitidis* and *N. gonorrhoeae*. However, it is evident by now that these techniques failed to capture one of the main features of Type IV Pili, its dynamical nature. These techniques require bacteria cell fixation; hence, researchers' observations are limited to static structural information of Type IV Pili, not to mention the possible effects of sample processing towards Type IV Pili structures.

Realizing this crucial knowledge gap, researchers also try to obtain live imaging of Type IV Pili. Common techniques in labelling protein in biological systems include tagging a fluorescent protein to the protein of interest. Yet, given the structural basis of Type IV Pili as a polymer, tagging an extra protein to each pilin subunit may be difficult and alter the dynamic of the pili. Another technique that succeeds, on the other hand, is the use of label-free interferometric scattering microscopy (iSCAT) in *Pseudomonas aeruginosa* Type IV Pili and Archaeal type IV pili in *Haloferax volcanii*[60,275]. This method has been successful in imaging the activity of Type IV Pili. However, this microscopy technique relies on refraction; therefore, it may be tricky to have a satisfactory resolution when pili activities are abundant or crowded. This is probably the case in *Neisseria gonorrhoeae.* Here, we are applying another method of visualizing Type IV Pili used in *Vibrio cholerae* through maleimide dye-labelling [276,277]. We leverage the thiol group of cysteine amino acids that can bind to maleimide dye, which can be labelled with fluorescence. To do that, we target the major component of Type IV Pili in *Neisseria gonorrhoeae*, PilE. Even though cysteine residues exist in the wild-type PilE, the pili are not readily labelled and visible. Therefore, we intend to enhance the effect by introducing another point mutation in the PilE. A previous study identified two mutants that behave similarly to Wild Type strain and are labelled well, K9C and C7G. With these identified mutations, we also established another set of mutants, T132C and T138C, based on different genetic backgrounds and constructed for better pili expression. In all cases, we successfully labelled the Type IV Pili and observed their activities using fluorescent microscopy. Although T132C and T138C express a pilin level on par with the wild type, less is more concerning

microscopy. K9C (PilE T132C) and C7G (PilE T138C) provide a better visualization and are more amenable to analysis. Nonetheless, our study also provides us with insights on the nature of Type IV Pili in *Neisseria gonorrhoeae* in terms of its dynamics.

#### 3.2.1.2 DNA molecules visualization

The aim to visualize the DNA transformation process also necessitates the ability to image DNA molecules. Successful single-molecule microscopy can be achieved by using appropriate microscopy techniques like Structured Illumination Microscopy (SIM), Stimulated Emission Depletion (STED) microscopy and Single Molecule Localisation Microscopy[278]. In this case, our laboratory equipment at that time was limited to an epifluorescent microscopy. Thus, we focused on choosing the more suitable labelling techniques for single-molecule microscopy[279]. DNA visualization is not news. Researchers have been using DNA dyes and probes to detect DNA molecules for a long time. Some are Ethidium Bromide, 4',6-diamidino-2-phenylindole (DAPI), and Propidium Iodide (PI)[280]. These dyes are, unfortunately, more commonly used in fixed cells and not advisable for live cells. Dyes or probes used for live cells include dUTP-conjugated Probes, Hoechst, and YOYO-1. In some cases, DNA can also be radiolabelled. These probes can detect fluorescence-labelled, biotin or Digoxigenin (DIG)-labelled, or radiolabelled DNA molecules through in situ hybridization, microarrays, or live imaging. In this thesis, we utilized fluorescence-labelled DNA molecules for imaging with bacteria cells. We also used YOYO-1 iodide and end-labelled probe through PCR to detect DNA molecules on micropillars, which will be discussed in Section 3.4. We turned to Label IT Reagent from Mirus Bio LLC to prepare a DNA molecule sample for DNA uptake assay. The initial rationale for preferring this kit is its covalent reaction with nucleic acid, and it presumably does not alter the secondary structure of the DNA molecule. Other than that, the sample preparation technique is fool-proof, simple and quick. Moreover, there are DNA uptake studies[165,232,276,281] prior to this using the same reagent, hence reducing possible setbacks in the experimental setup.

This Section will discuss how we successfully label and visualise Type IV Pili and DNA molecules simultaneously. We also provide some information on our initial observations of this interaction.

### 3.2.2 Materials and Methods

#### 3.2.2.1 Transform DNA (tDNA) preparation

All tDNA was prepared with the same protocol as Chapter 2. Information on any mentioned tDNA used in this study can be found in the tDNA List

#### 3.2.2.2 Strain construction

All strains used in this study and their information can be found in Bacteria Strains. Strain construction is similar to the process described in Chapter 2 unless mentioned otherwise.

#### 3.2.2.3 Type IV Pili visualization

Bacteria were swabbed from overnight agar plates and resuspended in GCB. A stock of $OD_{600}$ 0.7 was prepared. 200ul of the stock was then taken and spun down. The supernatant was then removed, and the cell pellet was resuspended in 100ul of DMEM F-12. 25 µg/ml of AlexaFluor

488 maleimide dye (Thermo Fisher Scientific) was added to the solution and mixed gently. The reaction was incubated at 37°C, 5% $CO_2$ for 30 min. After that, the reaction was centrifuged at 15krpm for 1min. The supernatant was removed and replaced with 100ul of GCB to quench the dye. The solution was then centrifuged again. The supernatant was removed, and around 20 to 50ul of GCB was added to resuspend the cell pellet, depending on the pellet size.

#### 3.2.2.4 Anti-bleaching agar pad for microscopy

For some of the experiments intended for pili analysis, we improved the image quality with an 'anti-bleaching reaction mix'. Before imaging for pili analysis, we prepared molten GCB agar and mixed it with the 'anti-bleaching reaction mix'. The final concentration of the mix in the molten agar contains 3mM DTT, 150 µg/ml glucose oxidase, 20 mM D-glucose, 25 µg/ml catalase and 1mM Trolox[282]. The molten agar mix was pipetted onto a microscope glass slide, sandwiched with another thin glass slide to form a thin layer, and left to set. After the pad was set, we cut the flattened pad into suitable dimensions and used it to sandwich the bacteria sample for imaging (Nikon Ti Microscope).

#### 3.2.2.5 DNA labelling

Label IT Nucleic Acid Labeling Reagents from Mirus is the labelling kit used to label DNA. Types of fluorophore used in this study are Tm-Rhodamine, Cx-Rhodamine and MF488. The labelling procedure was done based on recommendations from the kit. 5 µg of tDNA was added to a 50 µl reaction and incubated at 37°C for one hour in the dark. After that, 5 ul of sodium acetate and 100 µl of 100% ethanol were added to the solution. The reaction was left at -20 °C for at least an hour before spinning down at 15k rpm for 20 minutes. The supernatant was removed, and the pellet was washed with 300 µl of 70% ethanol. The solution was then spun down again at 15krpm for 5 minutes. After that, the supernatant was removed, and the pellet was left to dry. The dried pellet was then resuspended with 20 µl of nuclease-free water. The amount of DNA was then measured.

### 3.2.3 Results

#### 3.2.3.1 Type IV Pili labelling and imaging

*This procedure was pioneered by a previous PhD student, Kan Jingbo, and is further expanded in this thesis.*

A previous study identified C7G and K9C strains as the two *N. gonorrhoeae* strains that produced the best-labelled pili result. C7G has a point mutation at the 132$^{nd}$ Threonine residue of PilE to Cysteine residue, while K9C has a point mutation at the 138$^{th}$ Threonine residue of PilE to Cysteine residue. Both strains were constructed on the N400 WT3 parental strain, N400 *ΔrecA*, to prevent pilin antigenic variation[198]. However, one of the findings in the previous study also includes that these strains have a lower pilin expression level even though these strains behave similarly to N400 WT3 in terms of survival and pili retraction mechanical properties. One of our suspicions is that a selection marker gene was directly linked at the downstream region after pilE while constructing this strain, removing a part of the sequence before the SmaI/ClaI region[119,200,201]. This region has been reported to have a nonsense strand R-loop that may affect the pilin expression[283]. To test if this is true, we can build the same

mutant on a different construct that retains this region. Coincidentally, we obtained the ΔG4 strain during this dissertation.

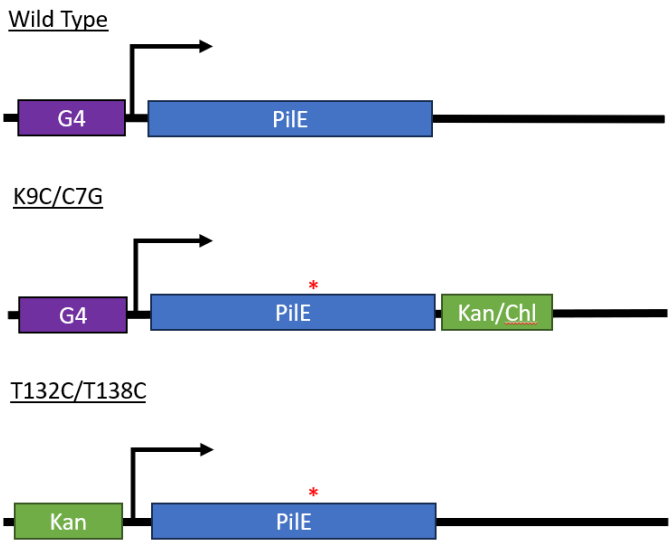


*Figure 3.14 Details about the different modifications done in different PilE mutants construct*

ΔG4 is constructed from wild-type MS11 parental strain by removing the G4 guanine quadruplex structure upstream of the *pilE* promoter and replacing it with a Kanamycin selection cassette (xviii). Removing the G4 region means we can significantly reduce pilin antigenic variation[211]. *N. gonorrhoeae* can carry more than one copy of genomic DNA, known as polyploidy[284]. So, it can be difficult to select an absolute knockout when cloning some genes. During ΔG4 strain construction, we have to select the strain using Kanamycin with a concentration as high as 120 μg/ml due to polyploidy tendency when cloning at near *pilE* gene. We passed this strain for at least six generations and sequenced to find no pilin antigenic variation. With ΔG4, we constructed T132C and T138C using 1-directional mutagenesis as described in Section 2.2.6 (Figure 3.14). During our study, we also have a detailed report on pilin expression in T138C in Chapter 5. T138C do express comparable pilin as wild-type parental strain. On top of that, we can also observe labelled Type IV Pili on these strains (Figure 3.15).

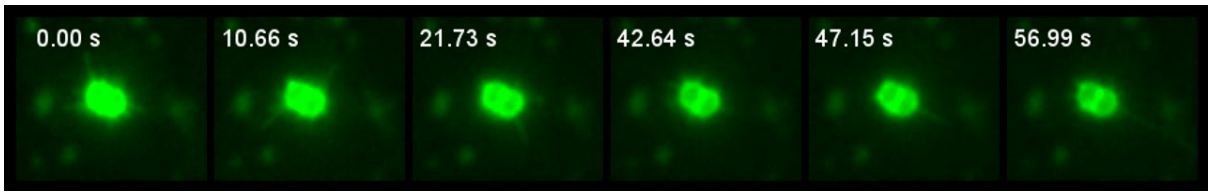


*Figure 3.15 An example of the dynamics of labelled Type IV Pili*

Unfortunately, the lower pilin expression in C7G and K9C probably worked towards our advantage in pili analysis. We noted that the resolution for C7G and K9C is better than that of T132C and T138C. This can be due to a higher pili amount in T132C and T138C, leading to more pili activities and, thus, difficulties in imaging isolated pili activities.

In our previous study, due to the quality of image and image analysis technique, pili activities were usually measurements taken from **long protruding pili** that extend away from the cell body. With our current resolution, we can recognize that other than the longer pili, *N. gonorrhoeae* also constitutively expressed frequent pili activities that are **shorter and closer to the cell**. They looked fuzzy, and the cell may look like a burning sun. We have thus greatly

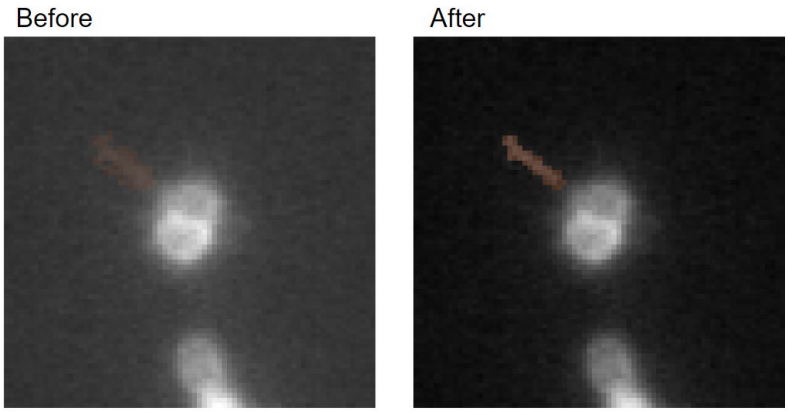


*Figure 3.16 Image cleanup that allows identification of most pili activities by reducing the noise surrounding the pili*

benefited from the help and advice of a local expert in image analysis at the LJP, Raphaël Candelier, to devise a workflow to clean up and process the images for analysis. Combining the improvement from the anti-bleaching reaction mix and the new image processing workflow, we obtained a more resolved image and information on pili activities.

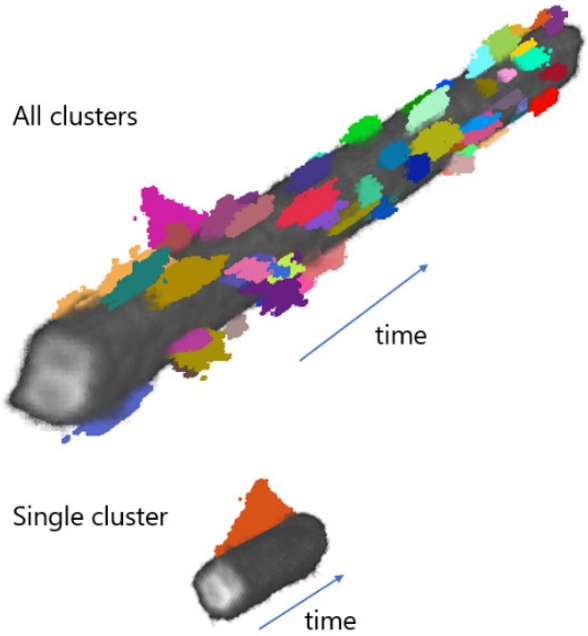


*Figure 3.17 An example of a collection of pili activities that can be detected corresponding to the cell body*

In this workflow, after applying image filters and removing background noise, we can identify at least most of the pili activities around the cells. The difference between the original video and the cleanup image can be compared in Figure 3.16. After identifying each pili activity, these activities can be mapped back to correspond to each cell body, and the profile of each activity across a certain timescale can be recorded (Figure 3.17). Due to the heterogeneity of labelled cells in our procedure, it is still challenging to automatize cell detection, and hence, the workflow is still largely semi-automatic. Nonetheless, this workflow greatly improves the information we can obtain from Type IV Pili labelling experiments. In Chapter 4, this workflow will provide fascinating details about Type IV Pili in different mutants, leading to exciting discoveries.

#### 3.2.3.2 DNA molecules labelling and imaging

DNA molecule labelling is one of the crucial parts of achieving this thesis goal. Initially, we have two candidates for DNA labelling: YOYO-1 iodide and Mirus Label IT Nucleic Acid Labelling Kit. When tested with Yoyo-1, due to its nature as a dynamic cyanine dye, the binding of the dye to DNA molecules is a reversible reaction and sometimes leads to inconsistent signals. At the same time, we also explored the option of Mirus Label IT Nucleic Acid Dye. This is a more strategic option because it has been used in literature for DNA uptake studies. On top of that, we obtained labelled λ-DNA molecules and did a quick test on our microscopy setup.

Another advantage of using this kit is that we can choose from a wide array of fluorophores within the same dye series. This allows us to select the suitable fluorophore based on our experiment and wavelength requirement from our microscope. In our case, we used three types of fluorophores across this thesis: CX-Rhodamine, TM-Rhodamine, and MF488. Our early decision includes determining the best fluorophore for our TxsRed channel (545nm/620nm). We noted different fluorescence or signal levels based on the fluorophore type when using the same amount of labelled DNA. TM-Rhodamine gives us a better fluorescence than CX-Rhodamine, given the same image acquisition setting. This enhancement allows our experiment a more extensive working range since the DNA uptake signal may not be very high. Henceforth, we selected TM-Rhodamine as the main fluorophore for most of our studies.

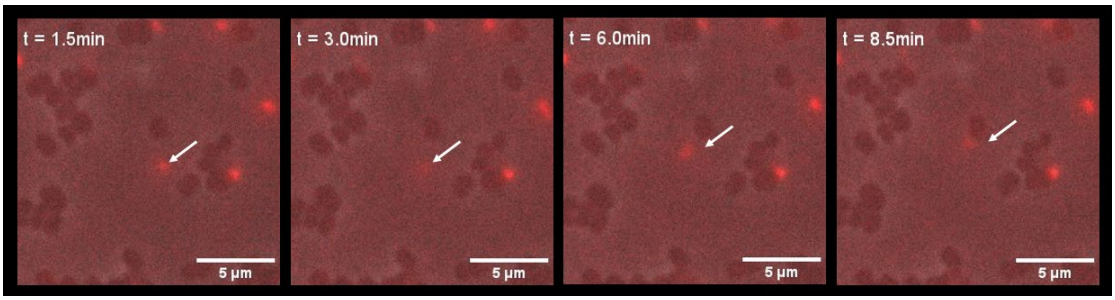


*Figure 3.18 Example of labelled DNA molecule (red) interacting with N. gonorrhoeae*

To study DNA uptake using labelled DNA, we incubated *N. gonorrhoeae* with labelled DNA molecules to observe the interaction between DNA molecules and the bacterial cells. This experiment aims to check if we can capture any potential interaction between bacteria and DNA molecules and ensure our experimental setup is feasible. We try to ensure the acquisition settings can capture DNA molecules yet do not result in autofluorescence or false signals from the cell body. We also tested the same acquisition settings for longer, up to hours, to ensure the optics do not affect cell growth. Hence, it probably does not affect cell activities, including pili activity. In our observations, we observed the usual Brownian motion of DNA molecules and more movement of DNA molecules around the cells. On top of that, we aimed to find DNA molecules that are pulled towards the cell body. Among our video samples, we did find some examples of such, but there are not enough (Figure 3.18). To further investigate this variety of DNA molecules' interaction with the cell, we combine both Type IV Pili labelling and DNA labelling experiments.

### 3.2.3.3 Simultaneous imaging of Type IV Pili and DNA molecules

Since we succeeded in imaging both labelled Type IV Pili and labelled DNA molecules, it would be advantageous to video both simultaneously. However, thus far, we have only tested the protocols separately. We had no prior experience in ensuring there was no crosstalk between our choice of the fluorophores or whether each labelling process affects the other's readout. Therefore, it is only logical to test out this protocol. To do this, we first labelled the Type IV Pili of the cells. Then, we quenched the cell solution with cyanine-rich buffers. After that, we incubate these labelled cells with labelled DNA molecules (Figure 3.19). Our experiment used Alexa Fluor 488 for Type IV Pili labelling and TM-Rhodamine for DNA labelling.

In this experiment, we got sufficient signals from both channels, observing both Type IV Pili and DNA molecules. However, there are a few limitations in this setup. Due to the nature of optics, we can see some bleed-through from the GFP channel (detecting Alexa Fluor 488) to the TxsRed channel (detecting TM-Rhodamine). Therefore, the signals in the red channel, especially those in the cell body, can't be fully distinguished between both channels. Fortunately, the background signals in the GFP channel outside the cell body are close to none. Hence, we can detect extracellular DNA molecules very well in the TxsRed channel. The only issue we might face is distinguishing between the Brownian movement of DNA molecules and the active pulling of DNA molecules. These two movements can be characterised based on their mean square distance if they are individually tracked.

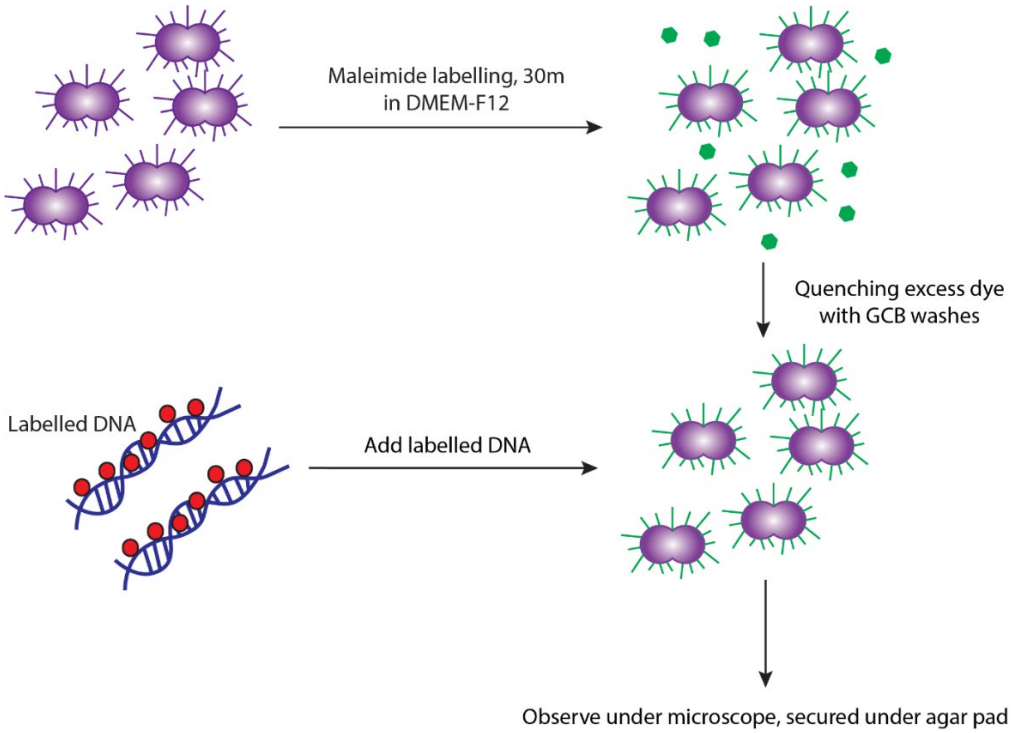


*Figure 3.19 Illustration of experiment workflow for imaging Type IV Pili and DNA molecules*

Interestingly, most of the DNA molecules' signals oscillated around the cell body (Figure 3.20). At this stage, we hypothesized that these movements coincide with pili closer to the cell body. We will investigate this further in Chapter 4 with other pili mutants. Occasionally, we observe DNA molecule signals that follow the path of pili retraction, but these events are rare (Figure 3.21). This might be due to the lower frequency of such events, or our microscope setup may not be fast enough to capture such a rapid process. All these doubts will be addressed in Chapter 4 during our investigation through other pili mutants. Nonetheless, in this section, we successfully showcase the visualization of both Type IV Pili and their interaction with DNA molecules. With these advances, we can use these techniques to elucidate the DNA uptake process through Type IV Pili in *N. gonorrhoeae*.

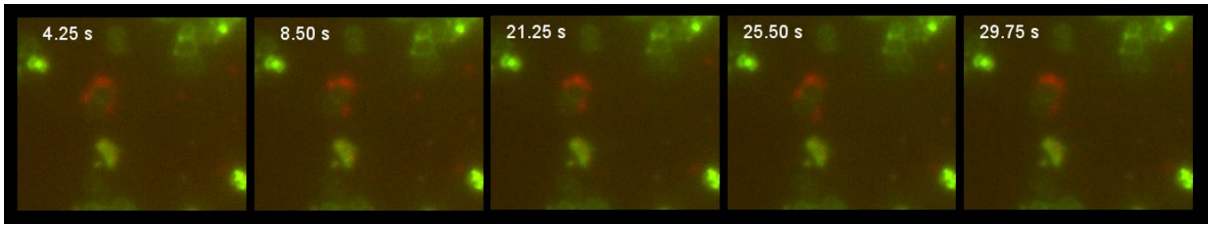


*Figure 3.20 Example of the oscillating labelled DNA molecules around the cell with labelled Type IV Pili*

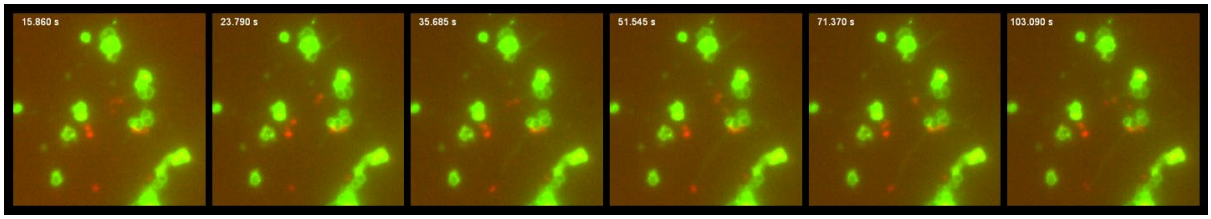


*Figure 3.21 Both labelled DNA molecules and Type IV Pili can be observed well*

## 3.3 Visualization and Quantification of DNA Uptake

### 3.3.1 Background and Motivation

DNA transformation was studied as a whole process when bacteria competence was first studied. Most of the time, competence was described as acquiring foreign DNA that led to a phenotypic alteration like antibiotic resistance. Now that more information about the DNA transformation process has been unravelled, we know that this process takes several steps, from DNA binding at the extracellular milieu to observing phenotype expression. On top of that, we recently also understood that these steps are most likely not temporarily coupled[111]. Taking that into account, it became clear that it is equally important to develop protocols to break down this pathway, for example, to examine DNA uptake, transport and recombination. Undoubtedly, these are all studies that had been reported before, each time focusing on the researcher's intended research interest.

This section aims to establish an experimental workflow to study DNA uptake. The rationale for starting with this step is that it is the first step of DNA transformation and its intricate relationship with Type IV Pili. Together with this workflow, we aim to uncouple DNA uptake and transformation pathways (Figure 3.22). Together with techniques developed in Chapter 2, we will be able to investigate both pathways and understand the route the DNA molecules take from being taken up until its expression as a phenotype. There are many ways one can study DNA uptake. We intend to visualize this process in our study and provide a quantitative illustration. With available microscopy techniques, DNA uptake microscopy has been showcased in several other bacteria like *Escherichia coli*[285], *Helicobacter pylori*[281], *Vibrio cholerae*[111], and *Bacillus subtilis*[286]. Protocol to visualize DNA uptake in *Neisseria gonorrhoeae* has also been reported[165,232,287]. While these studies provide some information regarding DNA uptake or DNA molecules in microcolonies, it is rare to see studies that put DNA uptake and DNA transformation side by side for comparison. Moreover, we would like

to set up such a system to further study the dynamics of DNA uptake and answer different questions. With that in mind, we used the successfully labelled DNA molecules in Section 3.2 and developed and optimized a workflow to investigate DNA uptake.

During optimization, we developed an experiment that best illustrates DNA uptake through a feasible workflow. On top of that, we include our strategy in understanding our observation with quantitative and qualitative analysis through DNA uptake analysis and DNA localization. The development of this assay allows us to illustrate the DNA uptake process both qualitatively and quantitatively.

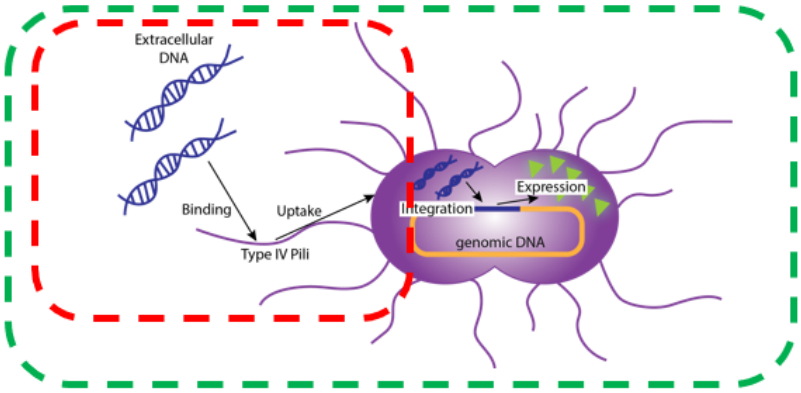


*Figure 3.22 Uncoupling DNA uptake (red bracket) and DNA transformation (green bracket)*

### 3.3.2 Materials and Methods

#### 3.3.2.1 Transform DNA (tDNA) preparation

All tDNA was prepared with the same protocol as Chapter 2. Information on any mentioned tDNA used in this study can be found in the tDNA List.

#### 3.3.2.2 DNA Uptake Assay

Due to the scarcity of labelled DNA, the DNA uptake assay intends to replicate the same condition in liquid transformation described in Chapter 2, but a scaled-down version. Bacteria were resuspended in a supplemented transform medium (GCB liquid added with Supplement I, Supplement II, and 5 mM $MgSO_4$). The tDNA used was scaled to 1ng/µl in the final reaction. The reaction was then left for incubation. The time of incubation depends on the time point decided in each experiment. When the time point arrived, the reaction was taken for processing before imaging. For the trial, the reaction could be used directly, washed once with a transform medium, or treated with 1ug/ml DNase I before being washed with the transform medium. For those that are washed, the final pellet was concentrated around 2x to account for lost cells due to the washing process.

### 3.3.3 Results

#### 3.3.3.1 Image acquisition and analysis workflow development

With previously optimized image acquisition (Section 3.2), we no longer have a problem imaging Type IV Pili or labelled DNA molecules. However, we aim to quantify this process

further to understand the DNA uptake mechanics. During a typical liquid transformation, a similar protocol used for our DNA uptake assay, extracellular DNA molecules are always in excess. When these molecules are fluorescently labelled, that will also mean potential artefacts during the imaging process if we aim to study the uptake of DNA molecules into the cells but not outside. Below is an example of how fluorescently labelled DNA molecules in excess can affect the image quality. While some of the cells that take up DNA molecules have a higher fluorescent signal as expected, the background signal is increased, and there are also aggregations of molecules that can affect the reading during quantification. We did a few tests to curb this issue to streamline our future workflow.

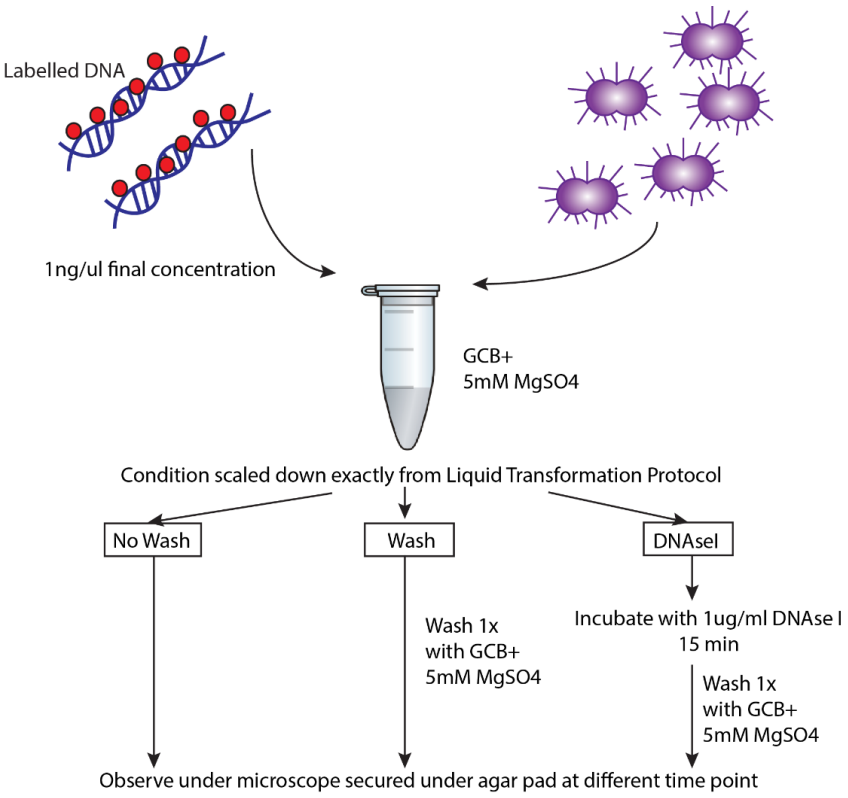


*Figure 3.23 Illustration of workflow for DNA uptake assay*

We designed two more methods to remove excess extracellular DNA molecules, the primary source of unwanted fluorescent signals: performing an extra wash step by pelleting the cell, removing the supernatant, and digesting excess DNA using DNAse I (Figure 3.23). Since we do not wish to perturb any cellular activity, the DNAse I digestion step was only done briefly for 15 minutes, and there was no enzyme-killing step. A similar protocol has been used in literature[165]. We also ensured DNAse I digestion can reduce excess fluorescence signal in vitro. With our tests, we compared the different methods and concluded that an extra wash itself is sufficient to remove most of the excess DNA molecules. This step has a limitation in which we might wash away some cells. An additional DNAse I digestion steps can also reduce some excess DNA molecules. With this conclusion, our following DNA uptake assay includes the washing and DNAse I digestion steps.

Using this protocol, we did some pilot experiments to observe the general DNA uptake signal in cells using wild-type MS11 and ΔPilV mutant. We can easily observe a difference between the experiment set incubated with and without DNA among both strains and an increased DNA uptake in ΔPilV that will be further discussed in Chapter 4 (Figure 3.24). We observed among the images the variety of fluorescent signals in the cells due to DNA uptake, including single cells with fluorescent signals spreading evenly around the cell body or as bright puncta and clusters of cells with fluorescent signals (Figure 3.25). This means that we might need to decide which type of cells to consider for quantitative readout in our experiment. Since clustered cells might have extracellular DNA molecules that are protected from DNAse I digestion and washes due to their physical structure, we decided to omit this category of cells in our quantification. To better understand and quantify DNA uptake, we will standardise our image analysis workflow.

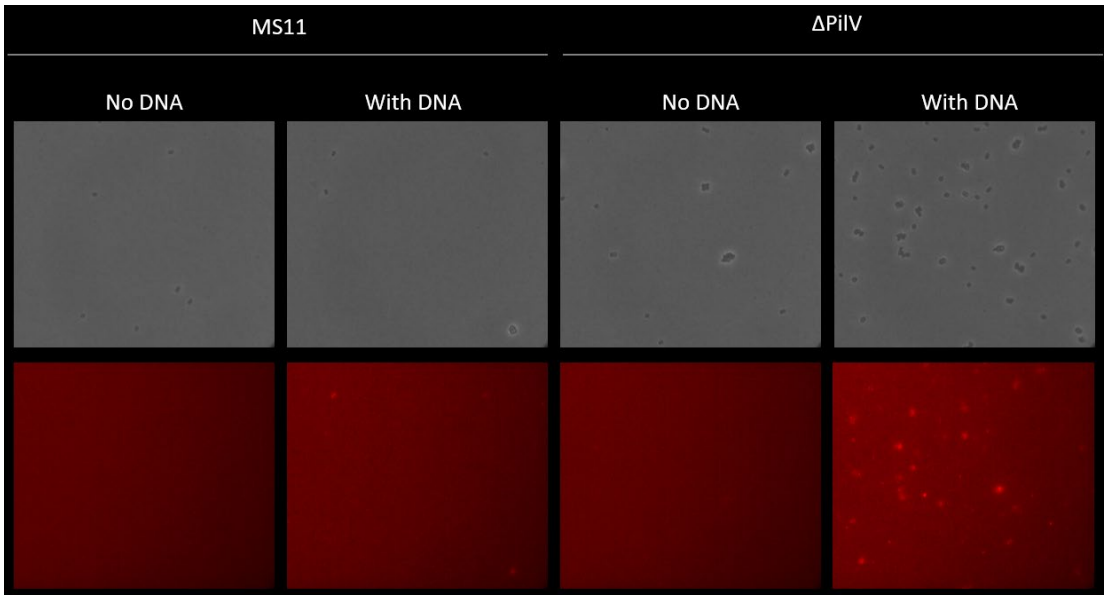


*Figure 3.24 An example of DNA uptake assay images*

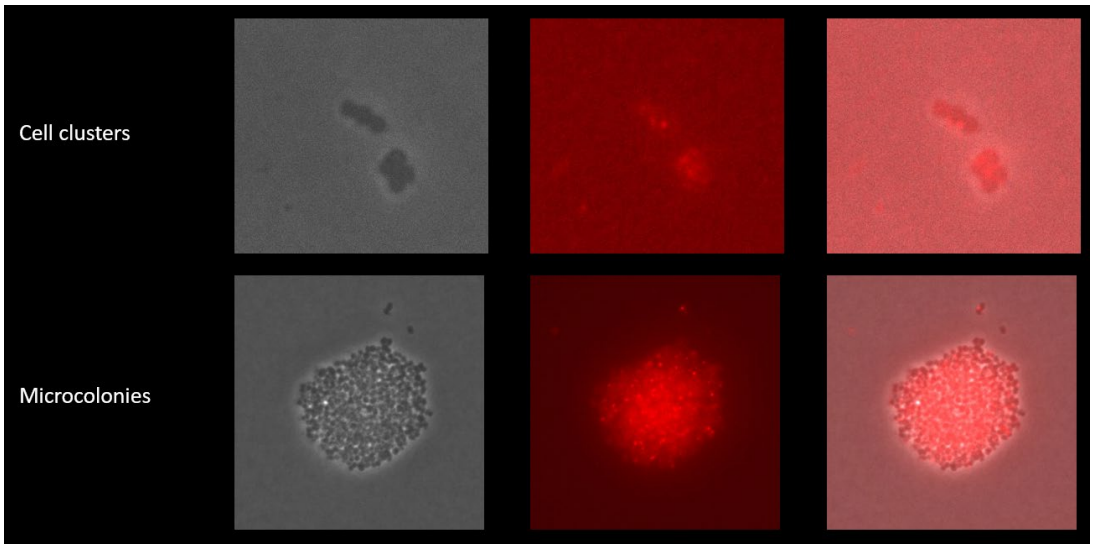


*Figure 3.25 A few examples of the different types of cells imaged during DNA uptake assay*

### 3.3.3.2 ROI determination

During image analysis, we intend to capture the signal from all of the cell body but our acquisition for the fluorescent channel is at 300ms, 20% power with 2x2 binning. This means there will be scattering if there's any DNA molecule signal at the edge of the cell body. We tested two methods to define the region of interest (ROI): i) circle method and ii) cluster method.

Through our investigation, we concluded that cluster method provide us with a better signal-to-noise ration for DNA uptake (Figure 3.26). For detailed investigation, see Study I: ROI Determination.

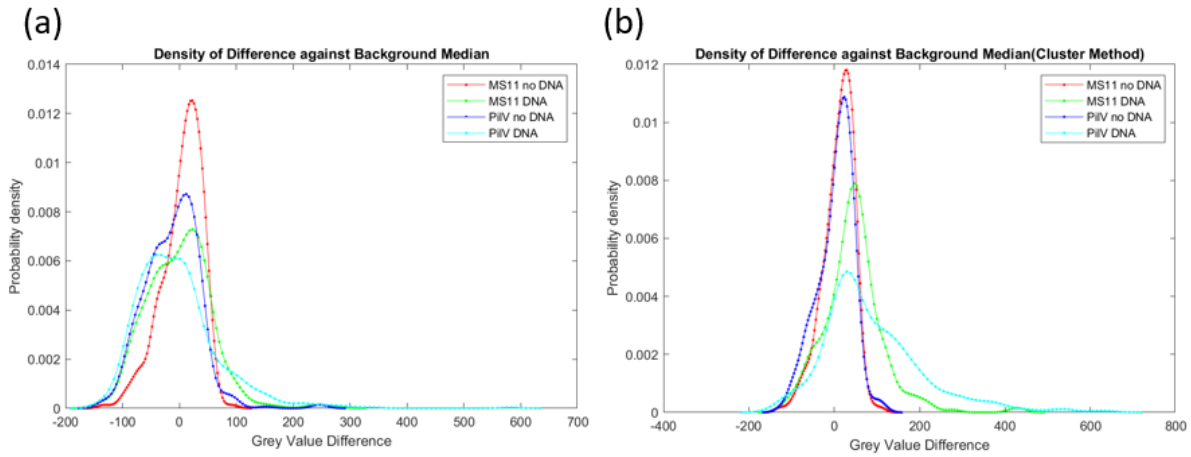


*Figure 3.26 Probability density of Grey Value Difference against Background Median using (a) circle Method and (b) cluster method*

### 3.3.3.3 Puncta Analysis

From our analysis in Section 3.3.3.2, it seems that other than obtaining information about the mean signal intensity in cell clusters, there might be important information based on pixel distribution. In other words, some of the DNA fluorescence signals stayed as puncta, and this information could be diluted if we average the values of all pixels in the ROIs. Therefore, we intend to implement a workflow to analyse the puncta quantitively. However, during the process of image acquisition and analysis, we face the issue of uneven illumination from the microscope light source. This effect is apparent in the fluorescence channel. While we could not use a corrected version for intensity measurement, it is crucial for puncta analysis since the shady corners will affect the results when we try to put a threshold on the image. For initial tests on small sample sizes, puncta analysis was done using the Find Maxima function in Fiji. However, this method was poorly documented in Fiji documentation and is difficult to translate into corresponding MATLAB commands. To overcome this issue, we employ another existing Fiji plug-in, BaSiC. BaSiC is a tool that can be used to correct uneven illumination. The tool implements image correction based on low-rank and sparse decomposition[288]. Sometimes, this tool utilizes time-lapse images to correct temporal drift, but in our case, we feed the tool with a few negative control samples to correct for the consistent uneven illumination imposed by our equipment.

In our setting, we took images of the control set without DNA and extracted a few copies of the fluorescent channels accordingly. These images are then arranged into stacks and run through the BaSiC plug-in to estimate the Dark Field, D(x) and Flat Field, S(x). Since all of our analysis is done through MATLAB, we deploy the correction through the formula provided by BaSiC developer [288].

$$I^{means}(x) = I^{true}(x) \times S(x) + D(x)$$

The corrected version of each image is then used for puncta analysis. It is important to note that since our analysis for mean intensity relies on actual pixel value, we did not use the corrected image for intensity analysis. Instead, we only used the corrected image for puncta analysis, in which the sole goal was to identify puncta and localized heightened pixel values. Our workflow for BaSiC image correction is illustrated in Figure 3.27.

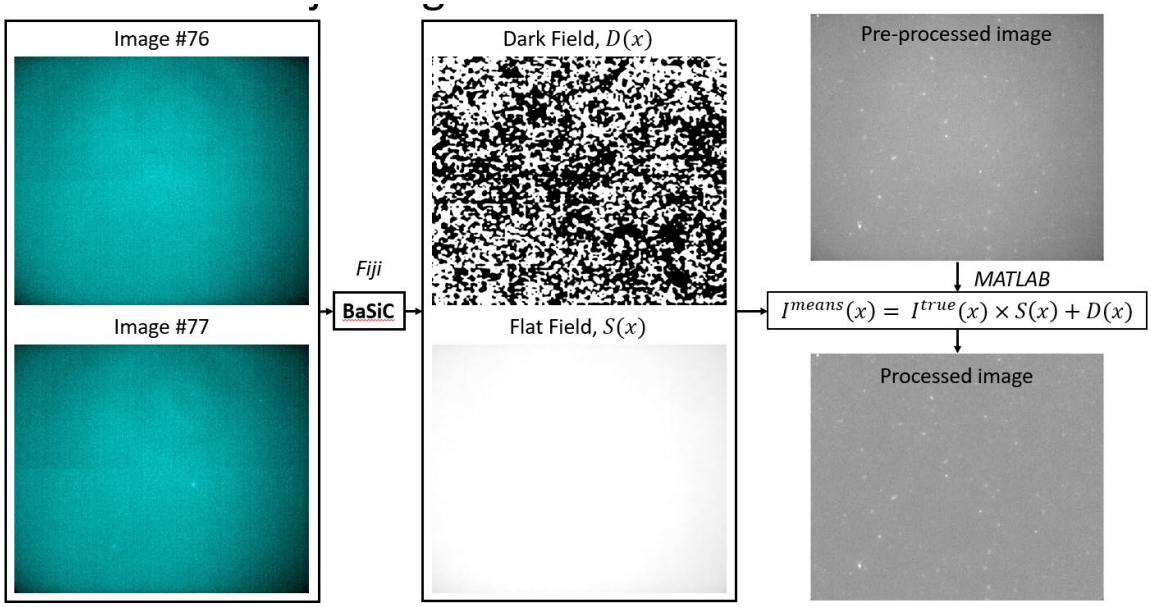


*Figure 3.27 Illustration of workflow correcting uneven illumination with BaSiC*

As a preliminary test, we also tested another correction method by applying a median filter on the image before thresholding. Since we try to ensure we can image cell clusters that are not aggregated (ideally single or double cells), the cells in our images are sparse. With the improvement of excess DNA signal, we can be sure that most of the pixels in our images are backgrounds. Using a median filter, medfilt2, we averaged the pixel value in each image based on their neighbours' median value, hence flattening any unevenness in the image.

By comparing the two correction methods, the BaSiC method is more reliable in that the puncta detected through this method is more comparable to what is analyzed from Find Maxima in Fiji. Moreover, the BaSiC method also presents a higher signal-to-noise ratio, seeing no puncta detected in the 'no DNA' set compared to those from the medfilt2 method.

In summary, these optimisation series aim to streamline a workflow to analyze the images used to quantify DNA uptake and dynamics in GC. Through optimization, the workflow is set, as

seen in Figure 3.28. We start by taking images in a brightfield and fluorescent channel (depending on the fluorophore used). Fluorescent channel images from the Control group (wild-type *N. gonorrhoeae* with no DNA) were used to generate Dark Field and Flat Field images through the BaSiC plug-in in Fiji. The cell clusters, as the region of interest (ROI), are detected through thresholding from brightfield and a mask is created. The mask is used on the fluorescent channel to detect the intensity of each ROI. Information about these ROIs was collected using MATLAB's 'regionprops' function, including Mean Intensity, Max Intensity, Centroid, and Pixel Values. This information is later used to analyze the dynamics of DNA molecules in these ROIs. During calculations for intensity, we set the median grey value of the images as 'background'. Conversely, the fluorescent images were also corrected using 'Dark Field' and 'Flat Field, ' and filtering was applied afterwards. The processed image was then thresholded to detect high-intensity pixels across the image, which is our intended 'puncta'. These detected puncta were presented as coordinates that we matched back to the labelled ROI previously. From this result, we can summarise the number of puncta in each ROI.

With the adjustments described in this Chapter, we successfully implemented a specific workflow to perform image analysis to determine the intensity and puncta resulting from DNA molecules.

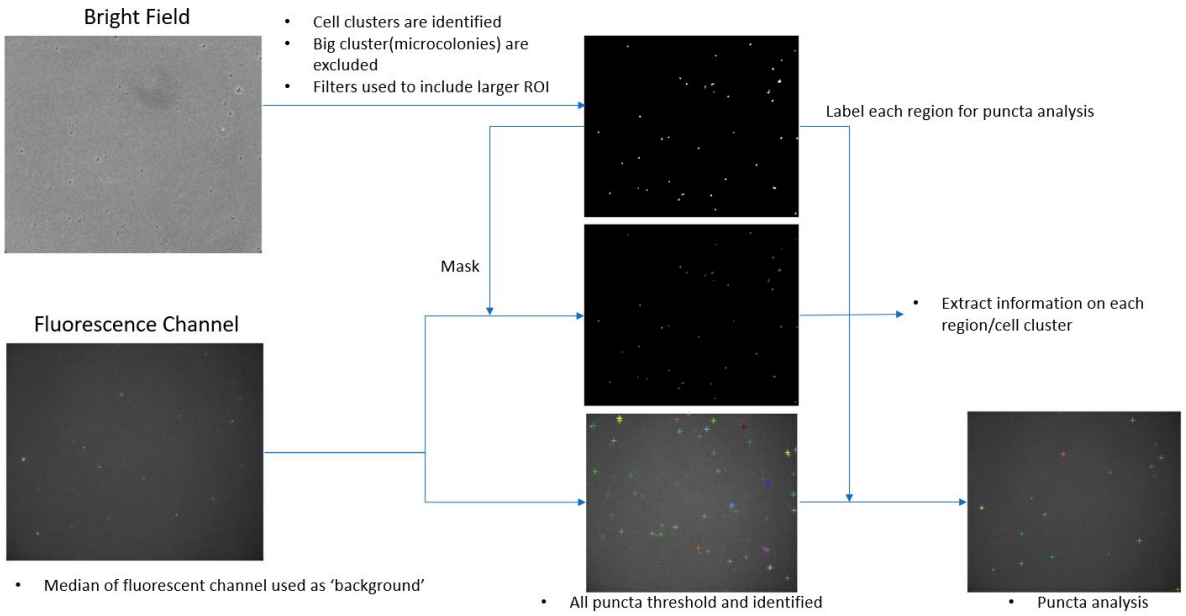


*Figure 3.28 Illustration of the entire image analysis workflow both for ROI signal intensity analysis and puncta analysis*

### 3.3.3.6 DNA Localization

When we started our study with labelled Type IV Pili, as mentioned, our goal was to capture the moments in which Type IV Pili binds to DNA molecules, retracts, and eventually transports the DNA across the cell body for recombination till expression. As displayed in Section 3.2.3.3, this event was rarely captured in our experimental set-up due to biological reasons or equipment limitations. What was not expected was the observation of the oscillation of DNA molecules around the cell body and the heterogeneity of DNA molecules after they are taken

up into the cell. This probes our interest to localize the DNA molecules in these experiments so that we can understand what is happening at a molecular level. We set out to develop a method to localize DNA molecules based on our experimental setup.

We manually cropped out the area with individual cells during the DNA localisation image analysis and saved them as files using Fiji. Using each of these files, we first perform an image processing step to help with the thresholding of the image. After that, the cell body is identified. Using code provided by Raphaël Candelier, we recognise each of the cells in each frame and assign an orientation based on their image moments properties. With a set orientation, we aligned the cells accordingly based on the z-stack we desired (whether in a certain time frame or different cells). With that, we overlapped the oriented images and produced an image with the mean value of these stacks. The workflow for DNA localization is illustrated in Figure 3.29.

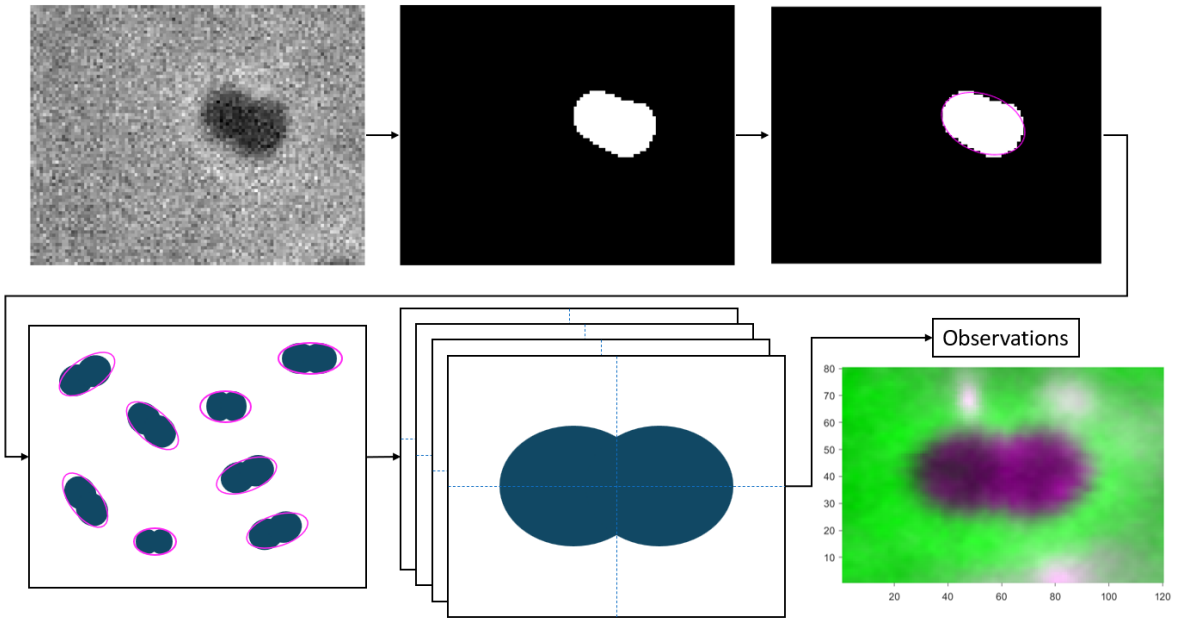


*Figure 3.29 The process of bacteria identification and alignment for DNA localization study*

## 3.4 Quantification of Pili Retraction Events

### 3.4.1 Background and Motivation

Section 3.2 presents the technique to follow pili retraction activities through visualization of Type IV Pili. However, there are a few caveats in that technique. In the pili labelling technique, we target the major pilin, PilE, for maleimide dye-labelling. Therefore, while our observations encompass most pili activities, we cannot rule out there might be blind spots in this observation. Moreover, pili labelling techniques look at pili activities mostly in what we described as 'exploration' mode. Due to the experimental setup, bacteria cells are sandwiched between an agar pad and a glass slide, allowing the pili to extend and retract as long as it can squeeze between the space. This also means that our measurements from this technique belong to pili activities when Type IV Pili are mostly not bound to any known substrate. Another crucial point

in this technique is illustrating pili activities at a single-cell level. Therefore, it is evident that we have a gap to fill. During natural growth, *N. gonorrhoeae* will start to form microcolonies depending on their incubation time, and this ability depends on its Type IV Pili activity. Another nature of Type IV Pili is its adherence to substrates; it is still debatable if these interactions affect the mechanics of these polymers. We explored different techniques to understand Type IV Pili mechanics to fill this gap.

There are many techniques in the field to study the mechanics of pili, each with advantages and limitations. Some known techniques include magnetic or optical tweezers[289,290], atomic force microscopy (AFM)[291,292], beads[293,294], surface shear stress measurement[295,296], and the usage of elastomeric micropillars[297,298]. Some of these techniques have the limitation of non-native measuring conditions. For example, the cells are not grown in certain conditions or in a native form like microcolonies. In this section, we are adding a layer of understanding to Type IV Pili activities on top of the analysis obtained from previous sections.

This section illustrated our studies on Type IV Pili retraction activities through polyacrylamide-based hydrogel micropillars[299]. We utilized an existing system that had been reported and calibrated before[297]. Using the current system as a foundation, we developed a similar system with DNA molecule-coating to explore the possibility of studying DNA molecule-specific pili activities. With these systems, this thesis also aims to ameliorate the analysis method by reducing as much noise and biases as possible. On top of our much-automatized analysis, we can extract more information and gear our analysis to study different aspects of pili activities.

In this study, we significantly reduce selection bias during analysis by considering all pillars within the selected region and its sample size. On top of that, we showed the possibility of measuring interaction-specific pili retractions. Our calculations extracted information such as pili activities per microcolonies across time, distance away from the microcolonies in which these events occur, and mechanical properties of each retraction. This study will give us a different angle on studying Type IV Pili and a deeper understanding of how pili behave with varying stages of cell and coating substrates.

### 3.4.2 Materials and Methods

#### 3.4.2.1 Transform DNA (tDNA) preparation

All tDNA was prepared with the same protocol as Chapter 2. Information on any mentioned tDNA used in this study can be found in the tDNA List.

#### 3.4.2.2 Coverslip activation

Both sides of each coverslip were passed through a Bunsen burner flame and let cool before being placed on a parafilm that was lined on a glass pan. 1 ml of 0.1M NaOH was added to each coverslip, and the excess solution was removed. The coverslips were left to airdry overnight until crystals formed on the surface. After that, 3-(aminopropyl)trimethoxysilane (APTES) was added to the entire surface and left to sit for 5 minutes. 3-(aminopropyl)trimethoxysilane was removed after, and the coverslips were immersed in water for 5 minutes. Each coverslip was washed with de-ionized water before being transferred to a

coverslip holder. The coverslip holder was then placed in a beaker with de-ionized water. The coverslips were immersed for 5 minutes. The water was replaced with 0.5% glutaraldehyde in PBS for 30 minutes. The volume used was enough to cover all of the coverslips. Afterwards, the coverslips were rinsed three times with de-ionized water to remove excess glutaraldehyde. The washed coverslips were let dry overnight under the hood and ready to be used.

#### 3.4.2.3 Hydrogel pillar preparation

The fabrication of the silica mould was described in the literature [297]. The moulds used in this study are either '21pillars' or 'beta pillars'. Both moulds produce equidistant micropillars (3um, measuring from the centre of one pillar to another). The difference between '21pillars' and 'beta pillars' is the height of the pillars, which are 6 µm and 12 µm, respectively. This dimension difference produces micropillars with different stiffness and hence spring constant. The spring constant for '21pillars' and 'beta pillars' are 240 pN/µm and 25 pN/µm, respectively. The moulds were plasma-cleaned for 5 minutes to fabricate the micropillars. When the mould was cleaned, the hydrogel master mix was prepared as follows: 250 µl of 20% Acrylamide, 25 µl of 2% Bis-acrylamide, 2.5 µl of 10% Ammonium persulfate, and 0.25 µl of Tetramethylethylenediamine (TEMED). 18ul of the master mix was pipetted on each activated coverslip (the abovementioned volume is suitable for preparing six micropillar sets at once). The mix was then covered with silicon mould and left to sit at room temperature for 30 minutes. After checking that the hydrogel was successfully set, the silicon mould was carefully removed, with the hydrogels submerged in 50 mM HEPES pH 7.4. Now layered with hydrogels, the coverslips were placed in 50 mM HEPES pH 7.4 in a 6-well plate. The buffer was then removed, and 80 µl of Sulfo-SANPAH (N-Sulfosuccinimidyl-6-(4'-azido-2'nitrophenylamino) hexanoate) solution (1 mM in 50 mM HEPES Buffer pH 7.4) was pipetted onto each hydrogel. The mixture was left to crosslink using a UV-linker for 5 minutes. This process was repeated for the second time before washing excess Sulfo-SANPAH with HEPES buffer. Hydrogels were ensured to be in solution at all times to prevent dehydration. These hydrogels were immediately used for DNA-coating or other coating to minimize the hydrolysis of the ester groups. The silicon moulds used in the experiment were immediately cleaned using 70% ethanol and blown dry.

#### 3.4.2.4 DNA-coating on micropillars

Aminated DNA fragments were prepared to a concentration close to 20 ng/µl (roughly 2 µg is sufficient to cover a surface area of one hydrogel, and each reaction is 100 µl) in the desired buffer. This study tested a few buffers: water, PBS, and Tris-HCl pH8. 100 µl of prepared DNA solution was pipetted on top of a piece of parafilm in a container. Coverslips with crosslinked hydrogel were then placed face down on top of these DNA droplets. The reaction was incubated at 37°C for one hour. After one hour of incubation, the coverslips were removed and placed in 6-well plates filled with 1ml of water. The hydrogels were washed three times with water before being stored at 4°C or used for the experiment.

#### 3.4.2.5 Carboxylated beads-coating on micropillars

100 µl of poly-L-lysine (30 ug/ml in PBS) was pipetted on top of a piece of parafilm in a container. Coverslips with crosslinked hydrogel were then placed face down on the poly-L-

lysine droplets. The reaction was incubated at 37°C for one hour. After the incubation, the coverslips were removed from the parafilm and washed three times in water. Then, 100 µl of 0.02 mm fluorescent carboxylated beads (FluoSpheres Carboxylate-Modified Microspheres from Invitrogen) was pipetted on top of a piece of parafilm in a container. Carboxyl latex beads, 4% w/v 0.02 µm, beads from Invitrogen can also be used if no coating verification is needed. The coverslips with hydrogel were placed face down on these carboxylated beads droplets. The reaction was then incubated in the dark at room temperature for an hour. After the incubation, the coverslips were removed and placed in 6-well plates filled with 1ml of water. The hydrogels were then washed three times with water before being stored in water at 4°C or being used for the experiment.

#### 3.4.2.6 DNA-labelling for crosschecking

We labelled the DNA with YOYO-1 iodide (Invitrogen) to check for the success of DNA binding on micropillars. After micropillars were prepared and checked, they were washed with 1x PBS or GCB to simulate experiment settings. Micropillars were then washed three times before YOYO-1 solution (1:1000 to 1:10000 in water) was added. The reaction was incubated in the dark for 30 minutes before observation.

#### 3.4.2.7 Microscopy for DNA-coating inspection

DNA-coated micropillars were inspected under the microscope using two approaches: i) DNA fragments amplified using fluorescently-tagged oligo, and ii) DNA labelled with YOYO-1 iodide. Epifluorescence microscopy (Nikon Ti) was used where DNA fragments tagged with TAMRA were observed at excitation and emission wavelengths of the TxsRed channel. Meanwhile, YOYO-1 iodide labelling was observed at excitation and emission wavelengths of the GFP channel. For comparison, fluorescent carboxylated bead coating was observed using the same wavelengths as YOYO-1 iodide. Exposure time and power were adjusted accordingly.

#### 3.4.2.8 Image acquisitions

Micropillar images used for coating verification were taken using a 100x objective lens, while micropillar videos taken for analysis were taken using a 60x objective lens. For micropillar videos, videos were taken with a DIC setting at 10 Hz.

#### 3.4.2.9 Pili retraction on micropillars analysis methods

Studying the mechanical properties of pili retraction using pili retraction does not stop at the experimental steps. Most information gathered at this point is qualitative until the micropillar videos are processed and analyzed. The first line of action is to identify and track the pillars that moved and extract movement information from there. In this Section, we developed and compared two methods for pillar tracking and analysis: i) Manual – a method that has been pioneered and established by Nicolas Biais and Ingrid Spielman, and ii) Automated – an effort to improve on the previous method through collaborative work with Nicolas Biais and Raphaël Candelier in the Laboratoire Jean Perrin. The reason for the comparison was not to put one method against another but to look for a workflow that allowed us to reduce as much bias as possible and fully extract all information through the least experimental effort, optimizing the

research process. The details of each method are described as follows and will be discussed in the concurring Results section.

*Manual*

In this method, the Nano_Tracking plug-in in ImageJ was used. For every pillar chosen, the image of the pillar was set as the 'target'. The image of the 'target' is processed and inverted as described in the literature. With this processing, the peak of the image is identified as the 'centre of the pillar'. Then, the 'target' is searched through the time series within a selected ROI to detect the 'centre of pillar' movement across time, which returns an output of the X and Y coordinates of the pillars through the time frame. After that, these coordinates are used for analysis in MATLAB using the 'plotpillar.m' code. Here, a reference pillar was necessary as the 'non-moving pillar. In every analyzed video, one reference pillar was manually selected using the same ImageJ plug-in. During the MATLAB operation, simple vector calculations were made to calculate the movement of the interested pillar relative to the reference pillar, a non-moving pillar. Any drift or instability in the video can be roughly nullified. With the calculation, the movement of pillars in terms of distance (x) against time can be plotted. From there, each pili retraction force and speed is hand-selected and calculated based on the height and slope of the peak.

*Automated*

In this method, all pillars in the image are taken into account. A frame in the video was used as the reference image. This image was processed and inverted to identify the centre of each pillar. The centres of all pillars were then tracked through all time frames of the video to detect their displacement. The displacements are plotted, and events are defined based on the events' amplitude and shape. Any events were calculated based on the difference in displacement within a selected time window. Through optimization, we have set a threshold to account for potential noise contributed by drifts in the image. Information on events can be extracted based on several filters and parameters. With this method, we also developed a graphical user interface that allows for specific pillar selection and pili retraction event filtering.

### 3.4.3 Results

#### 3.4.3.1 Micropillars

Type IV Pili in *N gonorrhoeae* has multiple functions and can have many biological impacts. Due to its nature as a dynamic polymer, it is often studied for its mechanical properties[182,291,300,301]. This Section will describe our work in understanding the mechanics of Type IV Pili using hydrogel micropillars. In our set-up, we employed polyacrylamide-based hydrogel micropillars that are of micron size. The utilization of hydrogel micropillars to

measure forces in biological systems is not new[299,302–304]. The usage of this micropillar system in *N. gonorrhoeae* is also not new either. It was established and developed in this lab before.

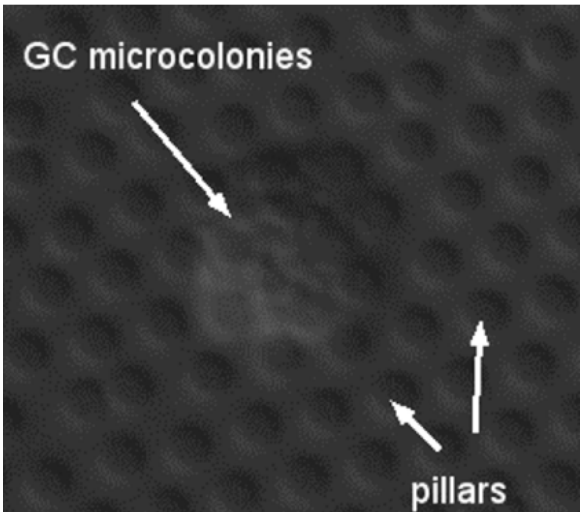


*Figure 3.30 Image showing N. gonorrhoeae microcolonies sitting on micropillars and how each pillar can be observed for their displacements*

With the micropillars, we can seed bacteria on top of these micropillars. Bacteria can be seeded as single cells or microcolonies (Figure 3.30). When bacteria interact with the substrate on these micropillars and can bind to them using Type IV Pili, any pili retraction can be monitored by capturing the aerial view of the micropillar carpet. We can calibrate each micropillar's stiffness given the material properties and the micropillar's dimension. This work was done previously by the lab using magnetic tweezers. With this information, any displacement captured can be converted into information like the force and speed of the pili retraction. One caveat of this technique is that it captures only the pili retraction mechanics and not the pili extension (Figure 3.31).

In our study, we intend to optimize the protocol and expand the potential of this methodology. Since this study aims to study DNA uptake and its dynamics, we also revisited this technique to modify it for DNA-associated study of Type IV Pili. Therefore, in this Section, we will discuss our work **for (a) improvement on pillar analysis** and **(b) construction of DNA-coated micropillars.**

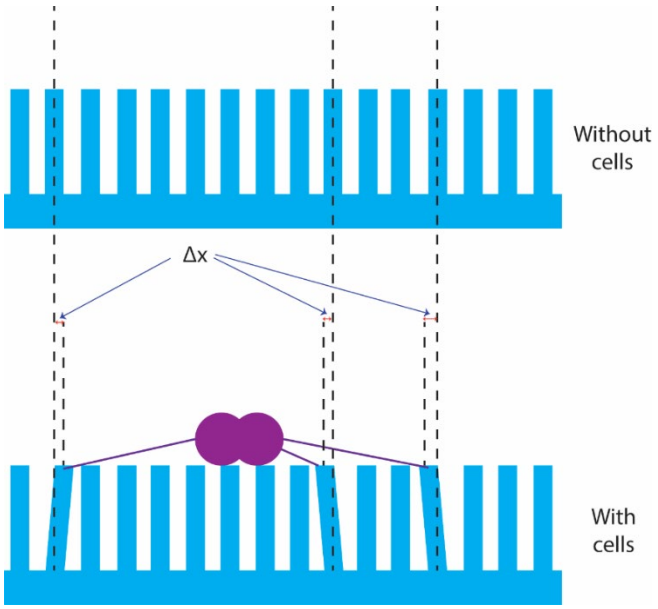


*Figure 3.31 A side-view schematic of micropillars and the measurement of bacteria pili retractions*

### 3.4.3.2 Streamlining pili retraction event analysis

Here, we intend to compare the two analysis methods: i) *Manual* and ii) *Automated*. The procedure for each method was stated in Section 3.4.2.9. The ***Manual* method** was first developed and has been robustly used long before this study. In this method, for every video taken for analysis, a reference pillar is selected by eye for its inactivity. Then, a few active pillars are selected by eye if any displacement is observed. Each pillar is then processed and tracked using the Nano_Tracking plug-in for their displacement within the selected ROI (Figure 3.32). The tracking of the pillar displacement relies on the fact that the videos are taken using Differential Interference Contrast (DIC) microscopy. Because of that, each pillar has a bright and shadowy side. Processing and mapping the grey value in a selected kernel around the pillar will give us a peak, which will be defined as the centre of the pillar[305]. With this detected peak, cross-correlation was made between this peak and any peak that occurred in a region of interest (ROI), determining the coordinates of the peak in each time frame. Then, the coordinates of active pillars are mapped against the coordinates of a reference pillar to remove any possible drift background movement in the video. This gives us information on the amount of displacement the peak has made across time, and we can calculate the force and speed of the pili retraction based on the slope and amplitude of the displacement.

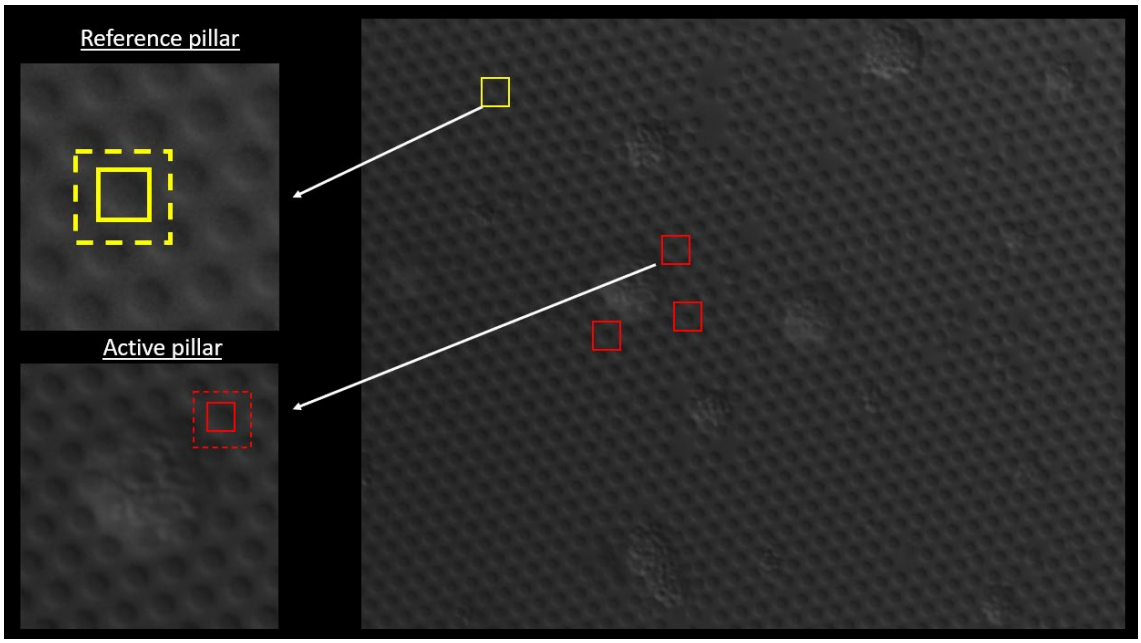


*Figure 3.32 An example of how pillars are selected in the Manual method. Reference pillar (yellow solid box) tracked within ROI (yellow dashed box), and all Active pillars (red solid box) hand-picked and tracked within each ROI (red dashed box)*

This workflow presents some disadvantages. For example, due to the high demand for manual selection, around 15 active pillars are selected in each video. This greatly reduces the sample size and is not efficient given the amount of information one should be able to extract from this video. Moreover, users might impose selection bias when picking the pillars with more obvious movement and sample size. Due to these reasons, time-to-time crosschecks between users are also required for analysis in the manual methods. To overcome these possible biases, we seek to automatize this process.

In the ***Automated*** **method**, we aim to eliminate as much bias as possible while retaining the accuracy of analysis. Therefore, we have to start with a robust pillar detection system across the whole field of view. In the *Manual* method, a kernel is defined around each pillar; hence, there was no complication in differentiating bacteria from pillars. In the *Automated* method, this can pose a problem. We imposed the same image processing to produce the peak for each pillar and used watershed to define each pillar's kernel. This process was looped over all pillars. Once the pillars can be detected, pillar tracking can be performed across the entire time frame. There are NaNs in some of the trajectories due to situations such as moving colonies on top of the pillar at a certain period of time. These trajectories will be removed by default or noted. When the trajectories are saved, the displacements can be mapped out, and events are defined based on the shape of the displacement. To do that, we first have to define what an 'event' is. In the automated method, we eliminate the potential noise or drift after trajectories are mapped. The amount of drift can be detected easily and accounted for (Figure 3.33). With this methodology, we are able to track each pillars and their trajectories. On top of that, any non-specific drifts resulting from image acquisition can be corrected.

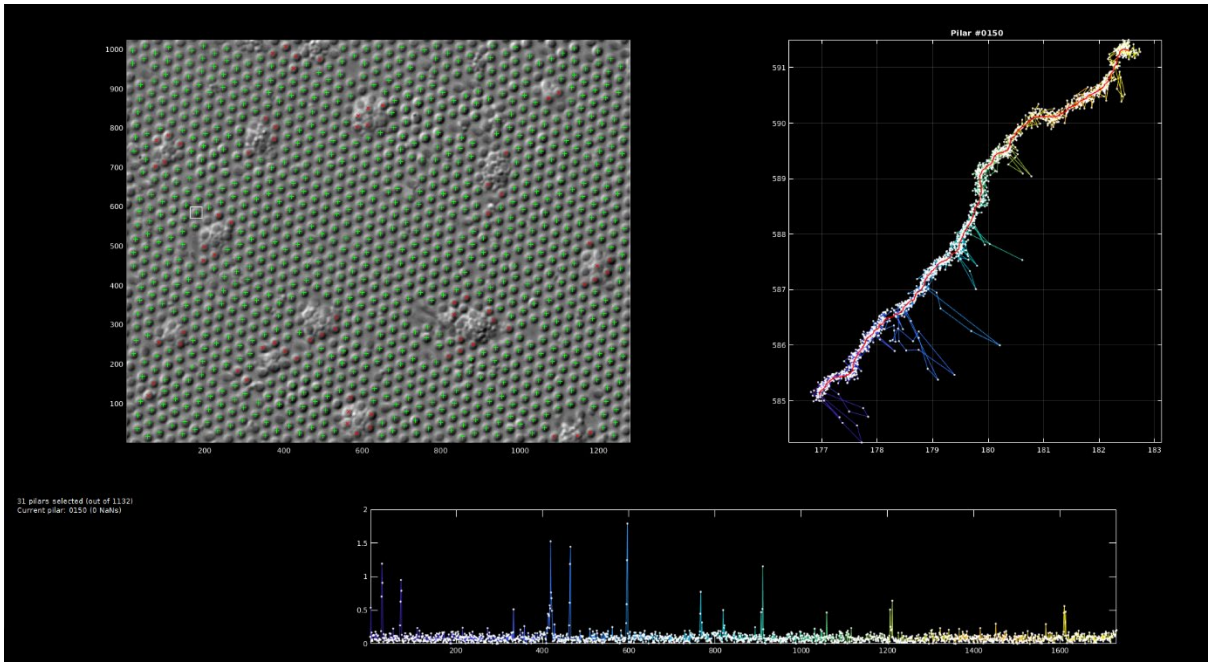


*Figure 3.33 An example of the trajectory of one pillar (top right) and the displacement detected (bottom)*

With agreeable parameters to analyze the pillar data, we put the *Automated* method to the test by comparing it with the *Manual* method. The first few tries comparing both methods with the same video returned significantly different observations. We recorded weaker and slower retraction events in the Automated method, shifting the overall mean to a smaller value than those recorded using the *Manual* method. When investigated in detail by crosschecking with manual methods and closely checking the pillar video, we concluded that some of these weaker and slower retractions are actual events. This is a good demonstration of the selection biases that may have occurred in the *Manual* method.

| 21pillars | betapillars |
|---|---|
| Chosen filter:<br>Slope: 0-inf<br>Amp: *default*-inf<br>Ramp duration: 0-inf<br>Saturation duration: 0.1/1-inf<br>Number of points: 5-inf<br>Decay time: 0-inf | Chosen filter:<br>Slope: 0-inf<br>Amp: *default*-inf<br>Ramp duration: 0-inf<br>Saturation duration: 1-inf<br>Number of points: 7-inf<br>Decay time: 0-inf |

*Figure 3.34 Finalized benchmark to use in for micropillar assay*

Another possibility of noise contributing to these weaker and slower displacements may come from the slight movement of micropillars being immersed in the medium. We took several videos of micropillars with no bacteria seeded to correct this artefact and ran an analysis to detect any 'retraction'. We did this routine for our test with '21pillar' and 'betapillar'. Using information from these control videos, we identified a few candidate parameters to filter the events. After considering all factors, we decided to set the new parameter filter, as shown in Figure 3.34.

Using these filters, we looked at the events detected in selected videos with bacteria. With the new parameters, we still see a larger pool of weaker retraction events in '21pillar', but we can capture most of the stronger retraction events. Regarding speed, we can capture faster retractions. These missed retractions from the *Manual* method match with what we observed in the labelled pili experiment. There, we observed that while longer pili are visible during pili labelling, there are many shorter and quicker pili activities around the cells. We think these smaller displacement events are most likely omitted during the *Manual* method. For 'betapillar', we can observe the new parameter can fit the calculation from the *Automated* to the *Manual* method nicely (Figure 3.35). These improvements in the analysis workflow make us more confident in extracting as much information from our videos as possible. Reassured, we continued our workflow by optimizing the protocol.

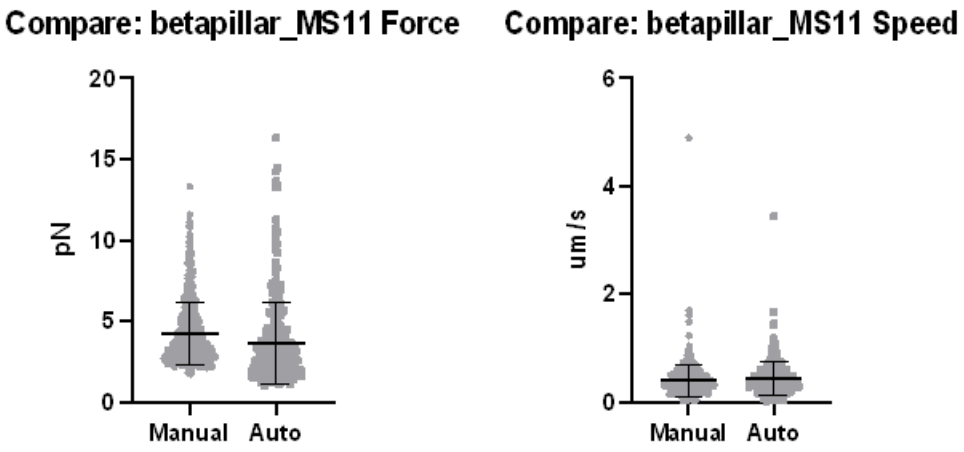


*Figure 3.35 Betapillar: comparison between the Manual method and the Automated method with different filtered parameters*

Although we recovered most of the discrepancy between the *Automated* method and the *Manual* method, we noticed that the *Automated* method usually misses out on pili retraction events that are very strong and fast. This is noticeable because these kinds of displacements

will be heavily selected in the m*anual* method. We later discovered how these events are missing in the *Automated* method. For example, we chose one particular pillar here, Pillar #0333 in the *Automated* method and P9[708,940] in the *Manual* method (Figure 3.36). It shows the detected events on the same micropillar using the *Automated* and *Manual* methods. All of the events detected are accounted for until around time frame 3700 (blue box). This type of retraction pattern can be described as 'Step', in which the pili stay pulling on the same pillar for an extended time. When that happens, we usually detect them as strong pulls in the *Manual* method. However, this information is missing due to the way we detect events in the Automated method, using a time window to slide across the time frame to detect events based on the difference in displacement. Our time window thus far is set at 80 frames. During a 'Step, ' the micropillar was continuously pulled. Other than the initial change in amplitude, the calculation could not differentiate the displacement otherwise. Nonetheless, it is good to be reminded that these events are not the majority among pili retraction events. Therefore, our method still captured most of the meaningful pili retraction events.

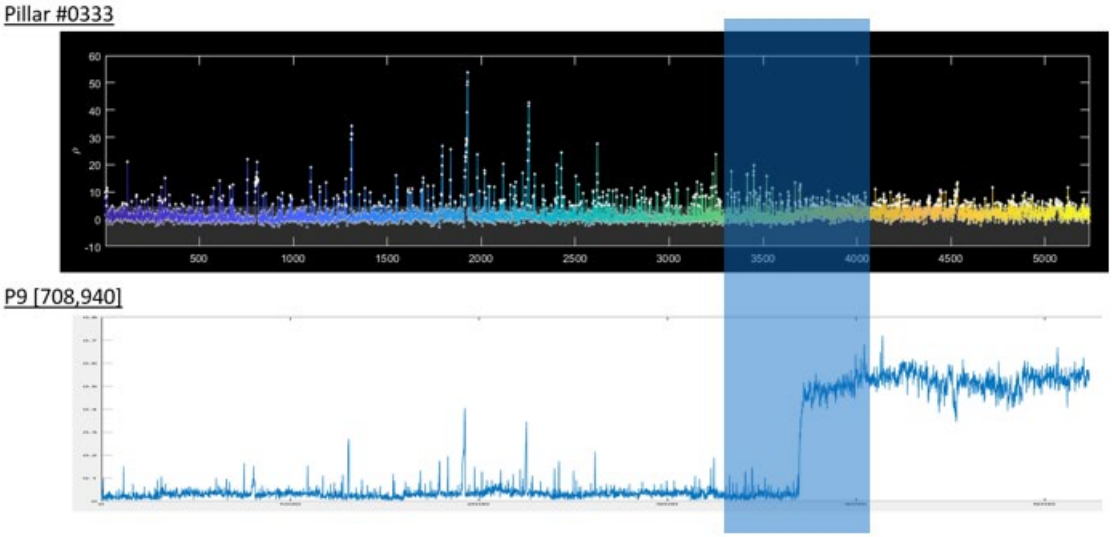


*Figure 3.36 Example of 'Step' event that can be missed in the Automated method*

### 3.4.3.3 Construction of DNA-coated micropillars

Next, we aim to modify the micropillar system for DNA uptake study. We would like to measure the mechanical properties of Type IV Pili when interacting specifically with DNA molecules. During the course of this study, it occurred to us that most of the Type IV Pili studies in *N. gonorrhoeae* assumed that all pili expressed outside the *N. gonorrhoeae* cell body are equal, as one type of Type IVa Pili. However, we observe pili of different lengths and dynamics through our study in Section 3.2.3.1. We commenced our study with a few questions in mind:

- Does all pili outside of *N. gonorrhoeae* cell body interact with DNA molecules or are involved in DNA uptake?
- Do the mechanical properties of the pili interacting with DNA molecules differ from pili that interact with non-specific substrates?

- Does the different pili lengths observed in Section 3.2.3.1 have any significant connection with DNA uptake?

Taking advantage of the pre-existing protocol for micropillar fabrication, we modified a protocol to switch the coating of micropillars to DNA. In our system, we used Sulfo-SANPAH as a hetero-bifunctional crosslinker. It has an amine-reactive N-hydroxysuccinimide (NHS) ester and a photoactivatable nitrophenyl azide. The nitrophenyl azide side will be crosslinked to the acrylamide with the help of UV light activation, while the NHS-ester side will be crosslinked to our substrate. In the original micropillar system, we crosslinked the NHS-ester with the amine group of Poly-L-Lysine (Figure 3.37). For the process of constructing DNA-coated micropillars, instead of layering Poly-L-Lysine that cross-links to hydrogel through Sulfo-SANPAH, we used DUS DNA fragments amplified with aminated oligos on one end; the other end bears a DUS sequence. The amine group from these DNA fragments can then react with Sulfo-SANPAH (Figure 3.37). During the coating process, we considered the persistent length of dsDNA, which is around 150bp (~50 nm)[306] and provided a sufficient material to cover all hydrogel surfaces for coating. The other consideration is the optimal buffer for the crosslinking reaction and storing. For the crosslinking reaction, we tried with 0.091M sodium tetraborate decahydrate (NaB) pH8.5 buffer, 1xPBS (based on its physiological relevance and protocol for Poly-L-Lysine) and water (based on the protocol for carboxylated beads coating).

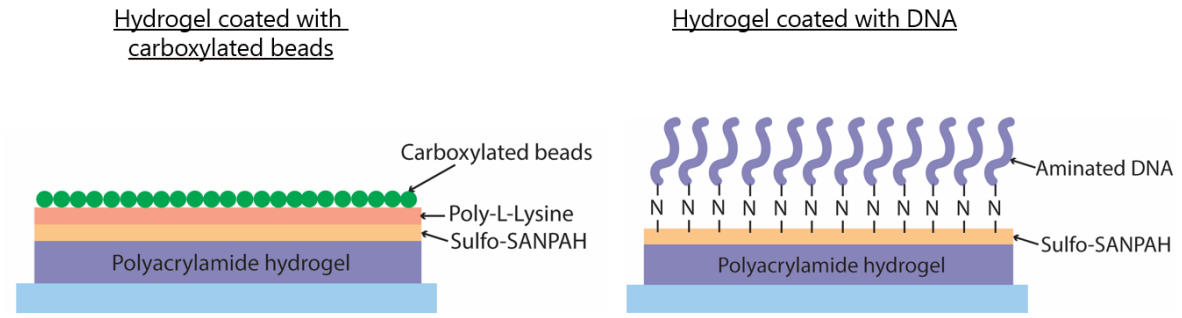


*Figure 3.37 An illustration of the coating layer in polyacrylamide hydrogel coated with carboxylated beads and DNA molecules*

To monitor our coating quality, we employ another fluorophore to visualize coating, TAMRA-DNA. TAMRA-DNA fragments were amplified from DUS DNA using an aminated oligo on one end and a TAMRA-tagged oligo on the other end that contained one DUS sequence. It became evident quickly that the NaB buffer was not optimal for our procedure, with no obvious DNA coating on the surface. On the other hand, we can observe coated fluorescent DNA for reactions using water. Our procedure concluded that performing the coating procedure in water produces the best signal. We also tested the strength of the coating by washing the surface of the micropillar with GCB+ to simulate actual experiments but visualize the fluorescence again after a second wash in 1xPBS was done. We couldn't visualize the fluorescence in GCB+ due to the high autofluorescence of the GCB medium. Similar to the coating of fluorescently-labelled carboxylated beads in xix, we also see a drop in fluorescence after washes with 1xPBS for DNA-coated micropillars (xx), indicating non-specific binding can occur, and it is worth taking note in future coating protocol. To further confirm the coating, we also probe the DNA

with another nucleic acid dye, YOYO-1 iodide. After the procedure, we observe the colocalization of the signal in both the green channel (detecting YOYO-1 iodide) and the red channel (detecting TAMRA) (Figure 3.38). It is worth noting that the coating of the micropillars does not seem as homogenous as those of carboxylated beads. This can be due to the DNA structure in this condition. Moreover, it is expected for the fluorescence signal to be lower than that of carboxylated beads since there's only one TAMRA tagged to each strand of DNA fragments. In conclusion, we can conclude that the coating of DNA molecules on micropillars was successful.

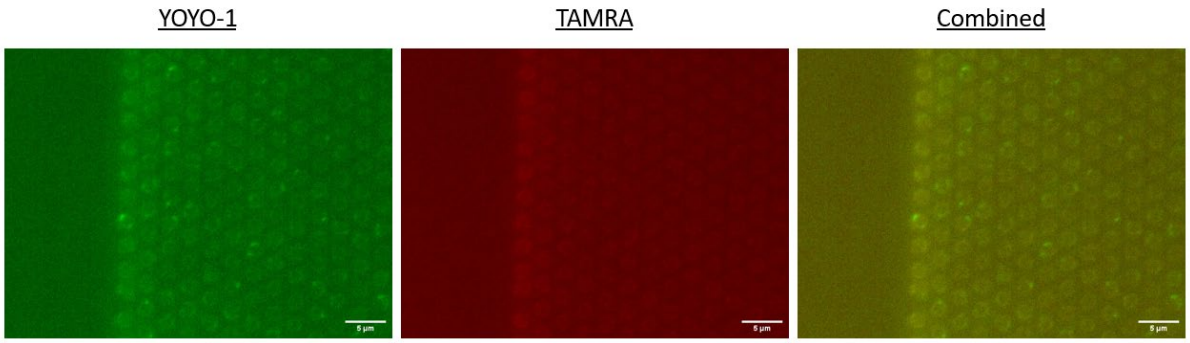


*Figure 3.38 An examination of the DNA-coating of micropillars through localization with TAMRA-probed DNA and YOYO-1 iodide DNA dye*

## 3.5 Discussion

In this chapter, we introduced various tools we developed during the course of this dissertation. In addition to molecular biology tools we introduced in Chapter 2, we also need tools to study DNA uptake and transformation at a single-cell or microcolony level. With that we developed a series of tool for each step.

At first, we intended to improve our acquired image resolution and quality by removing as much noise or autofluorescence as possible. Optimally, we aim to acquire image that allow convenience for image analysis. Therefore, we **optimized the medium** used for microscopy in *N. gonorrhoeae*. During this study, we explored the possibility in developing defined medium for *N. gonorrhoeae* for microscopy. We selected a chemically defined medium from the literature that is available in liquid culture form, GW medium. Our modified GW solid medium seems to work well for supporting growth in *N. gonorrhoeae*, but it seems to alter their colony morphology and possible the cell physiology. We also explored reducing the granularity in the common GCB agar for better image quality and reduce potential autofluorescence. Our attempt to remove and replace the starch content commonly found in GCB solid medium but not liquid medium revealed an interesting requirement for *N. gonorrhoeae*. This knowledge seems to escape most of the literature and not fully studied.

Next, to study DNA uptake live, we would like to **visualize DNA and Type IV Pili** at their dynamic form. With that, we showed that we can label the Type IV Pili using PilE cysteine mutants. Together with labelled DNA, we can observe the dynamics of Type IV Pili and their interaction with the DNA molecules. Despite our expectation of observing pili extending and

retracting together with DNA molecules, we observed more oscillating movements of DNA molecules around the cell body. Colocalization of DNA molecules with any long pili is rare. We suspect these pulling events may be rare in nature or the technical limitations of our acquisition equipment. For better image quality in this experiment, we also employ an anti-bleaching agent supplemented in the agar pad. This helped with pili activities detection.

Other than having capturing DNA-interacting pili events, we also used the labelled DNA molecules to set up a **DNA uptake assay**. One of the goals of this thesis is to dissect the DNA transformation pathway. In Chapter 2, we developed quantitative protocols for DNA transformation. Using DNA uptake assay, we can decouple the earlier part of the pathway. In this assay, we streamlined the workflow experimentally to obtain the most suitable images for analysis. Then, we also developed image analysis workflow for quantitations.

The other way of studying the role of Type IV Pili in DNA uptake also involve understanding the mechanical nature of Type IV Pili. In this aspect, we utilized the **hydrogel micropillar** setup that existed before this thesis. In this thesis, we improved the analysis workflow by including **automation** in the detection section. With this improvement, we reduce biases in our tracking progress and successfully observed many pili retraction events that we did not notice prior to this. On top of that, we also modified the micropillar to suit the study of DNA-related interaction by constructing the **DNA-coated micropillars**. In this section, we showed successful coating of the material.

All these techniques, together with molecular biology tools developed in Chapter 2, has been optimized and renewed across time. They are later used in several occasion in this thesis to study different aspects of *N. gonorrhoeae*, especially in DNA transformation topics.

# Chapter 4 : Type IV Pili and associated proteins (I): PilV

## 4.1 Background and Motivation

DNA uptake studies in *N. gonorrhoeae* are heavily linked to Type IV Pili. However, in *N. gonorrhoeae*, it can be a challenge to dissect the role of Type IV Pili in the DNA uptake process because of their multifunctional properties. A few Type IV Pili and their associated proteins are identified through studies that play potential roles in DNA uptake or transformation. Some of the examples are ComP[159,165,230,307,308] for their association with DNA uptake sequence (DUS), and ComE[118,165,307,309] for their binding activity with DNA molecules. Other than that, among minor pilin mutants, ΔPilV has been frequently used in DNA transformation studies in literature due to its enhanced competence phenotype.

In most cases, DNA transformation studies illustrate DNA transformation or uptake process through proteins such as ComP and ComE due to their positive effect on DNA uptake and transformation. However, it is interesting that in *N. gonorrhoeae*, a Type IV Pili minor pilin is reported to play an antagonistic role in the process of DNA uptake, PilV. Unfortunately, most studies used ΔPilV as a tool to enhance DNA uptake and transformation signal. There is a lack in the characterisation of ΔPilV and the understanding of the role of PilV in Type IV Pili.

In this chapter, we systematically characterise the phenotype and behaviour of ΔPilV. On top of that, we provide a detailed comparison between wild type and ΔPilV in terms of DNA uptake. Our study discovered some insights that are immensely critical in understanding PilV's role and bacterial regulation during DNA uptake.

## 4.2 Materials and Methods

### 4.2.1 Bacterial strains used and culture conditions

The strains used in this study can be found in the Bacteria Strains. Strains construction based on techniques developed in Chapter 2. We use a protocol similar to Chapter 2 and Chapter 3 to culture bacteria. Agar pads used in the microscope study are prepared with GCB+ Liquid added with 1.13% electrophoresis-grade agarose and 0.1% soluble starch or 1% potato starch.

### 4.2.4 DNA labelling

DNA labelling techniques have been described in Chapter 3.

### 4.2.5 DNA uptake assay

Bacteria were swabbed from overnight agar plate culture and resuspended in the transform medium. A bacteria solution of $OD_{600}$ of 0.7 was prepared using the transform medium. In each reaction, 67ul of transform medium was added with 10ul of the $OD_{600}$ 0.7 bacteria stock. In this reaction, labelled tDNA was added to the final concentration of 1ng/ul. A few time points are chosen depending on experiments, usually at 0.25h, 1h, 2h, and 3h. At each time point, cells

were taken and disrupted for 2min. Then the cells were treated with 1ug/ml of DNAse I at 37°C for 15min while still incubated with 5% $CO_2$. The list of tDNA used in this study can be found in the tDNA List. The oligos used in this study can also be found in the Oligos List.

### 4.2.6 Aggregation assay

Bacteria were swabbed from overnight agar plate culture and resuspended in GCB Liquid medium. A bacteria solution of $OD_{600}$ of 0.7 ($5 \times 10^8$ CFU/ml) were prepared. In a 6-well cell culture plate, 1ml of GCB+ was added. 100ul of the $OD_{600}$ 0.7 bacteria solution was added to each well. The culture was mixed well before incubating at 37°C with $CO_2$ for 3h. After 3h, the culture plates were taken out of the incubator and observed under a 20x inverted microscope.

### 4.2.7 Competence assay

Bacteria were swabbed from overnight agar plate culture and resuspended in GCB Liquid medium. A bacteria solution of $OD_{600}$ of 0.0007 was prepared. In each reaction, 10ul of cells from these stock solutions were used with 500ng of tDNA. The entire volume of the reaction was then spotted on a GCB agar plate and left to air dry. After drying, the plates were incubated at 37°C with $CO_2$ for 16h. After incubation, the spot where the transformation occurred was resuspended in GCB liquid with a swab, and 10x serial dilutions were prepared from it. These dilutions were later spotted on a non-selective plate (GCB agar plate) and a selective plate (GCB agar plate with 3ug/ml nalidixic acid). The plates were left to air dry and then incubated at 37°C with $CO_2$ until colonies were visible enough for counting.

### 4.2.10 Pili preparation for western blot

Bacteria were swabbed from overnight agar plates and resuspended in GCB. The next day, the bacteria were resuspended in 1ml of 50mM CHES buffer, pH 9.5. Cells were disrupted for 2 min. All conditions were normalised using the same starting $OD_{600}$, and a cell stock was prepared. Around 20ul of this solution is stored as the 'whole cell fraction'. The cells were spun down at 18k g for 5 min. The cell pellet was resuspended in 500ul of CHES buffer for SDS-PAGE as 'cell pellet fraction'. The supernatant was collected and ultracentrifuged further at 50000 g for 90 min. After that, the supernatant was removed, and the pellet was resuspended in the CHES buffer and labelled as the 'pili fraction'.

### 4.2.11 SDS-Polyacrylamide gel electrophoresis (SDS-PAGE), Western Blot and Detection

20% denaturing polyacrylamide gel was prepared and used for SDS-PAGE. An appropriate amount of pili fraction protein was used in each experiment. Samples were added with the appropriate amount of 4x Laemli buffer. Around 10ul of the samples were loaded for gel electrophoresis.

The protein was transferred to nitrocellulose membranes through wet transfer. Blots were blocked with 5% milk in TBST for 15 min. Then, they were probed with primary antibody (α-SM1 mouse monoclonal antibody (1:1000) in TBST), incubated at 4°C overnight, shaking at

80 rpm. On the second day, the primary antibody was removed, and membranes were washed with TBST three times, five minutes each. Membranes were then probed with a secondary antibody, an anti-mouse (1:10000) horseradish peroxidase (HRP) antibody, for an hour at room temperature. After incubation, the secondary antibody was removed, and blots were washed three times with TBST, five minutes each. After the final wash, the blots were kept in TBS buffer before being detected with Enhanced Chemiluminescence (ECL) substrate.

For detection, the chemiluminescence signal was detected on the blot using Pierce ECL Western Blotting substrate, following its user guide. The blots were exposed for an appropriate time, depending on the antibody used.

## 4.3 Results

### 4.3.1 Characterisation of ΔPilV Strains

In Chapter 3, part of our experiments confirmed and aligned with the reported phenotype of ΔPilV, which is enhanced DNA uptake. While this phenotype provides convenience to the study of DNA uptake, it is important to understand the role of PilV to understand better this phenotype and how it could shape our understanding of Type IV Pili biogenesis and regulation and its effect on competence. However, comprehensive studies on ΔPilV are still very limited despite the wide usage of this mutant for DNA uptake study. Therefore, we decided to characterise ΔPilV to provide some insights into the role of this minor pilin.

#### 4.3.1.2 ΔPilV colony morphology is slightly different

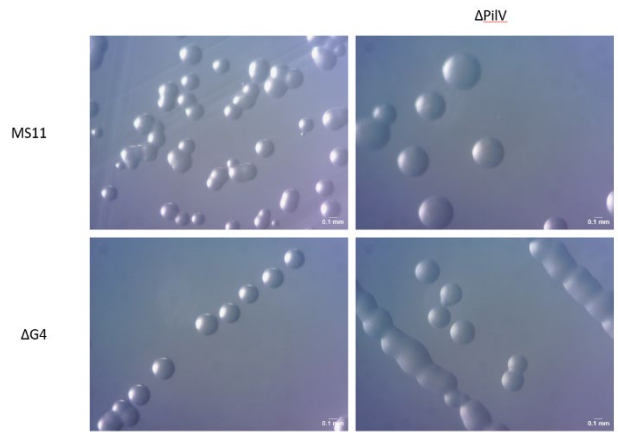


*Figure 4.1 Colony morphology of ΔPilV strains compared to two parental strains, MS11 and ΔG4*

We characterized the colony morphology of ΔPilV strains. We looked at two parental strains, MS11 and ΔG4, and their ΔPilV mutants. From both strains, the ΔPilV mutants tend to have flatter colonies (Figure 4.1). Colony morphology in *N. gonorrhoeae* can sometimes provide information about the strains by presenting pilus-dependent colony morphotypes. The morphology could result from the interactions between bacteria within a colony. Since Type IV Pili are one of the main mediators between *Neisseria gonorrhoeae* bacteria with the environment and one another, colony morphology could be affected by the strain's pili interactions. With our observations, a flatter colony could indicate the lack of interaction in ΔPilV strains. Such a possibility can align with a previous study showing PilV's role in adhesion to human epithelial cells.

#### 4.3.1.3 ΔPilV aggregates differently from MS11 or associated parent strains

Microcolony formation assay can be an indirect way to gain insight into the dynamics of pili. This is due to the fact that microcolony formation or aggregation assay can assess the effect of

these mutations on one of the main pili functions. In our experiments, we examined the microcolonies formation at 3h in a few strains: MS11 (wild type), N400 WT3 (a *ΔrecA* strain used to prevent pilin antigenic variation through recombination), and ΔG4 (MS11 with the guanidine quadruplex structure upstream of *pilE* gene replaced with a Kanamycin cassette to reduce pilin antigenic variation). These strains are used as a wild-type control for PilE mutant experiments, which will be studied in Section 5.3.3. In this experiment, we observed all three wild-type strains can similarly form microcolonies. The ΔPilV mutants of these wild-type strains still form microcolonies (Figure 4.2). However, the extent of the microcolony formation is affected (Figure 4.2). Generally, the microcolonies formed by ΔPilV mutants are further apart and do not adhere to the bottom of the well and the wild types. A slight tapping motion disrupts the microcolony attachment from the bottom of the well in ΔPilV mutants. To examine the microcolonies' formation quantitatively, we compute the nearest neighbour distance between microcolonies in each condition (xxii). The analysis allows us to quantitatively assess what we observed qualitatitvely by eye.

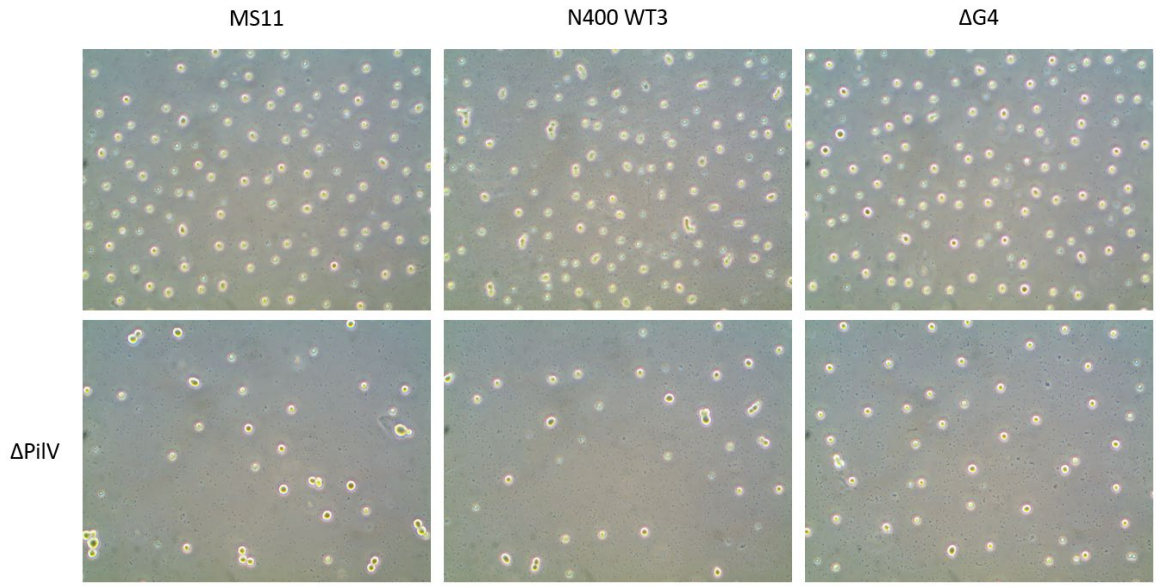


*Figure 4.2 3h microcolony formation assay for MS11, N400 WT3, and ΔG4 with their ΔPilV counterparts*

Since ΔPilV mutants showed slight defects in microcolony formation, we are interested in looking at their aggregation dynamics in detail. To do that, we study microcolony formation in MS11 and MS11 ΔPilV from the start of culture till the 3-hour time point. To ensure our observations are not affected by growth differences or differences in the way bacteria mutants settle at the bottom of the culture well, we devise 'No Spin' and 'Spin' protocols and consider the bacterial growth for the first two hours. The 'No Spin' and 'Spin' protocols differ because 'No Spin' allows the inoculated bacteria to interact in the liquid before settling at the bottom of the well. In contrast, the 'Spin' culture was centrifuged to force the bacteria to settle at the bottom of the well since the start of the culture. In both 'No Spin' and 'Spin' protocols, ΔPilV mutants have slight defects in microcolonies formation (Figure 4.3). Another interesting observation is that in the 'Spin' protocol, in which the bacteria culture starts with all bacteria settled at the bottom of the well, MS11 can start interacting immediately with one another.

Meanwhile, MS11 ΔPilV mutants showed lesser interaction with each other at the start. Moreover, at the end of the 3-hour timepoint, when the culture well plates were tapped slightly, MS11 microcolonies remained adhered to the bottom of the well. However, MS11 ΔPilV microcolonies are quick to detach. Type IV Pili are the majority of extracellular appendages that interact with the environment and other bacteria. Type IV Pili enable *Neisseria gonorrhoeae* to perform twitching motility, and this, together with adherence to another *N. gonorrhoeae* bacteria, leads to the formation of microcolonies. In short, microcolony formation results from bacterial interactions due to factors like pili adhesion, pili retraction mechanics and potentially pili length. Therefore, from this observation, we can conclude that ΔPilV leads to lesser adhesion to the substrate that can usually be adhered strongly by pili. This result aligns with the postulated role of PilV in adhesion reported in the literature[158].

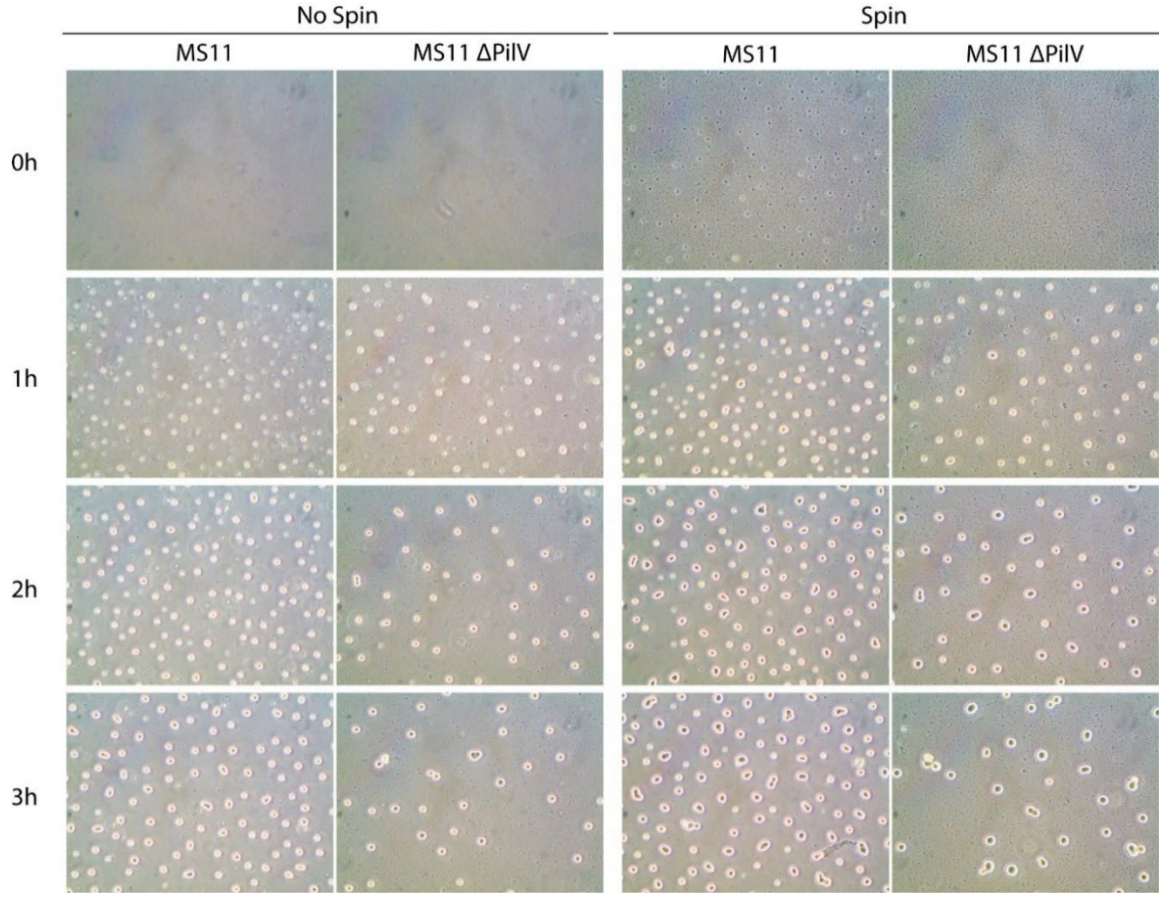


*Figure 4.3 Microcolonies formation comparison between MS11 and MS11 ΔPilV in 'No Spin' and 'Spin' protocol across 3 hours*

To exclude the doubt about any growth difference, we did not observe any growth differences throughout the first two hours of culture (see xxiii). From our study on bacterial growth in liquid culture after inoculation, it is also evident that *N. gonorrhoeae* took longer than 3h to enter the exponential growth phase. Hence, the growth observed within these two hours is expected to be stable.

### 4.3.1.4 ΔPilV enhances competence regardless of the parent strain

One of the characterisations includes looking into ΔPilV's enhanced competence phenotype as reported in the literature[164]. In our experiment, we transformed strains MS11, N400 WT3, and ΔG4 and their ΔPilV mutants with the same amount of transformed DNA (tDNA), similar to the procedure reported in 32. We then compute their transformation efficiencies by looking at the fold change difference between ΔPilV mutants and their respective parental strains. Our results show that all ΔPilV mutants have improved transformation efficiency compared to their parent strain regardless of genetic background (Figure 4.4). This observation matches what is reported in the literature.

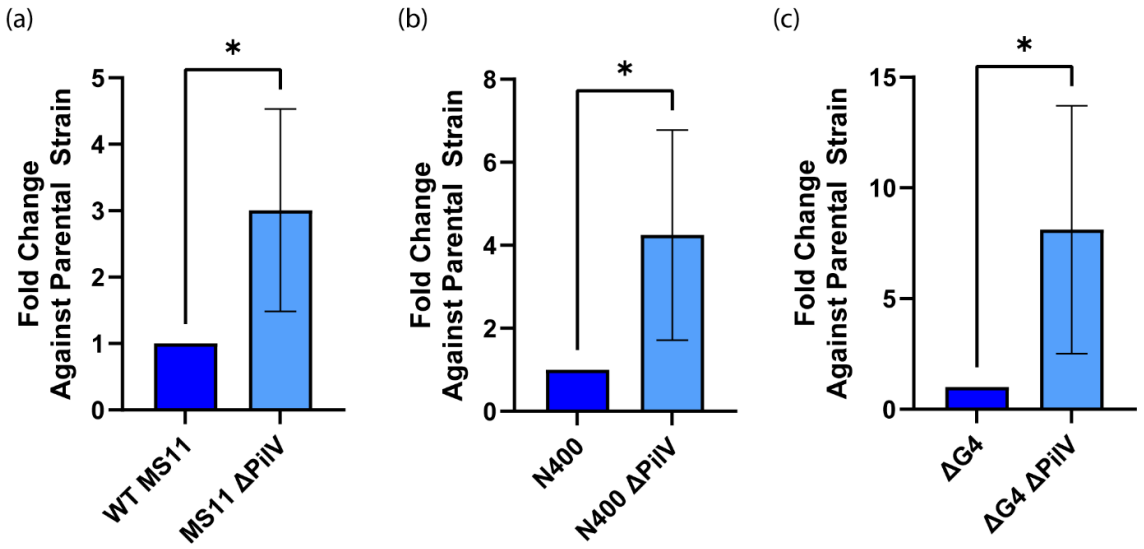


*Figure 4.4 Transformation efficiency of ΔPilV strains compared to their parent strains: (a) MS11, (b) N400 WT3, and (c) ΔG4. Student t-test was used to calculate significance.*

### 3.3.3.4 DNA uptake shows ΔPilV take up more DNA

Following our observations of ΔPilV mutants' enhanced competence phenotype in Section 4.3.1.4, we would like to investigate the part of DNA transformation pathway that ΔPilV is affected. We have used the fluorescence single molecule microscopy assays presented in Chapter 3 towards this goal. We hypothesised that since PilV is a minor pilin and is known to play an antagonistic role to ComP in DNA binding[164], enhanced competence most likely results from enhanced DNA uptake into the cell body rather than downstream pathways like DNA transport and recombination. To initiate such investigation, we first ensure we reproduce the enhanced DNA uptake phenotype through increased DNA fluorescence signal reported in the literature[165]. To ensure the robustness of our **DNA Uptake Assay**, we also included a few key pili mutants in our study: wild-type **MS11, ΔPilE, ΔPilT and ΔPilV**. This is because DNA uptake goes hand-in-hand with Type IV Pili in *N. gonorrhoeae.* We study DNA uptake at 3h for experimental practicality and to observe the maximum signal.

Before quantitative analysis, under the microscope, we can observe a good but small signal in MS11 and a really good signal in ΔPilV (Figure 4.5). However, in the condition for ΔPilE, we observe an obvious fluorescence signal. While this is not fitting to the canonical understanding of Type IV Pili being the major player in DNA uptake, this finding does fit with some of our

preliminary work in transformation. In some of our preliminary work, when incubated with a high amount of tDNA, though minimal compared to the Wild Type, the degree of transformation of ΔPilE is always higher than ΔPilT. Combining both observations, it suggests that while PilT or pili retraction is crucial for DNA uptake, the lack of retraction probably blocked the secretion channel PilQ, and hence, there was no passive entrance of DNA molecules in ΔPilT. We also think that the result from ΔPilE may be due to a few reasons. The lack of PilE might lead to a lack of pili, leaving the secretion channel hollow. These empty spaces may allow the passive entrance of DNA molecules. However, given the strength of the signal, it is hard to pinpoint if this is indeed a passive process. The other possible reason is that PilE may not be the sole leading player in DNA uptake.

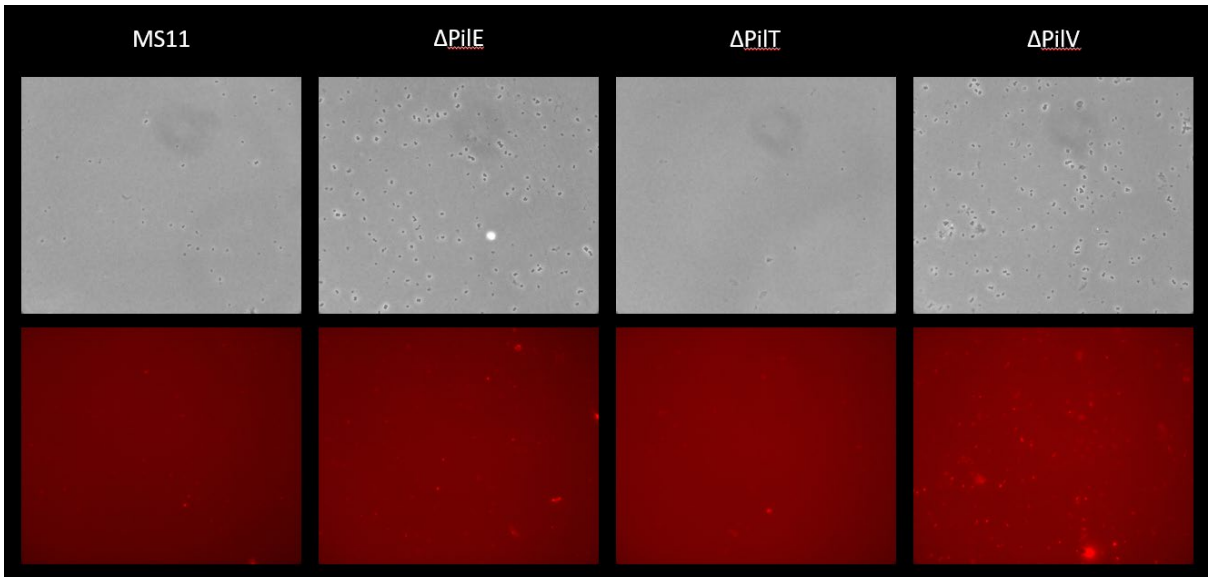


*Figure 4.5 An example of the DNA uptake images in MS11, ΔPilE, ΔPilT and ΔPilV*

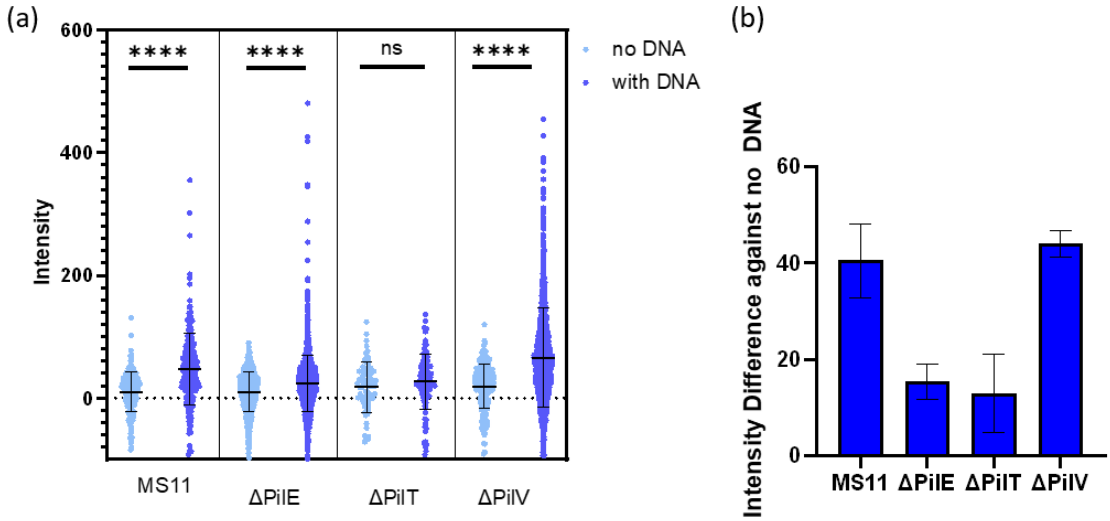


*Figure 4.6 (a) Fluorescence signal intensity in the whole population between different pili mutants (b) Summary of fluorescence intensity signal compared to 'no DNA' data set*

For quantitative analysis, we measured the fluorescence intensity and puncta of the cell clusters. Before we look into ΔPilV, we ensured what we observed on microscope for ΔPilE and ΔPilT is true. Student t-test on populations between 'no DNA' and 'with DNA' in all pili mutants, there is a significant difference for MS11, ΔPilE and ΔPilV. This statistical analysis confirmed our observations and speculations about ΔPilE's ability to take up DNA (Figure 4.6).

Similarly, we observed much higher and varied fluorescence intensity in ΔPilV 'with DNA' population (Figure 4.6). It is worth noting that there is heterogeneity in fluorescence signal among the populations of all strains, with the variation being bigger in ΔPilV. Such heterogeneity may explain why sometimes not all cells are transformed, but more investigation is needed to clarify this. Taken together, however, when compared to the signal from the 'no DNA' population, the fluorescence intensity shows that MS11 and ΔPilV have a more significant difference, while ΔPilE and ΔPilT are low in signal (Figure 4.6).

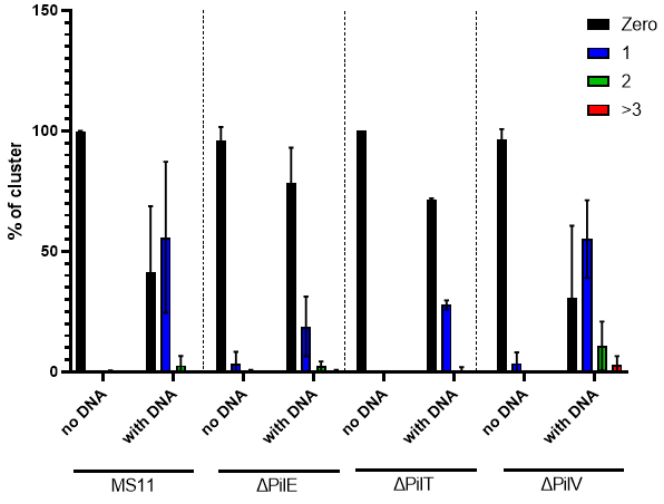


*Figure 4.7 Puncta analysis for pili mutants during DNA uptake assay*

The average fluorescence signal per cluster in might miss information like accumulation or aggregation of DNA molecules at one spot. Therefore, we performed puncta analysis on these strains. Our puncta analysis shows that MS11 ΔPilV also has a higher percentage of clusters with puncta (Figure 4.7). Moreover, although MS11 ΔPilV has a similar percentage of clusters with one puncta, it has a higher percentage of clusters with more than one puncta, as shown in clusters with 2 or >3 puncta. This result suggests that ΔPilV strains enhanced competence first by taking up more DNA than a wild type. On top of that, these excess DNA molecules most likely accumulated more in the cell. For other pili mutants, the number of clusters with puncta is low in ΔPilE and ΔPilT. The puncta in ΔPilT could be attributed to the fact that ΔPilT tends to form larger aggregates (Figure 4.8), which, during the process of DNase treatment and wash, even with the intervention of disruption, give rise to some non-specific DNA molecule binding.

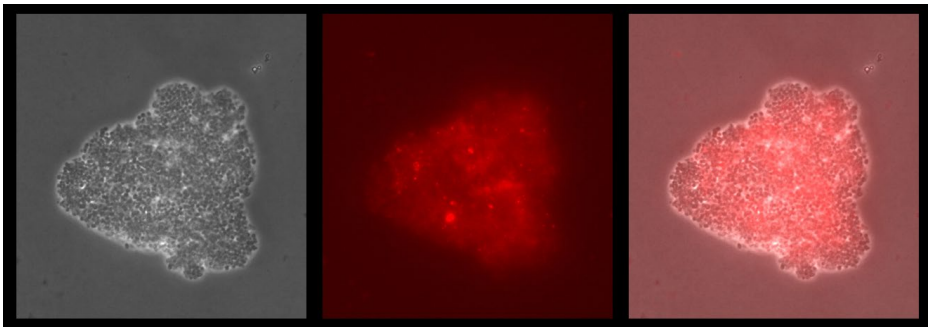

*Figure 4.8 An example of ΔPilT aggregation that can lead to extracellular DNA signal not being eliminated completely*

#### 4.3.1.5 DNA uptake and transformation dynamics in ΔPilV strains

We examined their dynamics across three hours in both aspects, a common time point used in the liquid transformation described in Chapter 2.

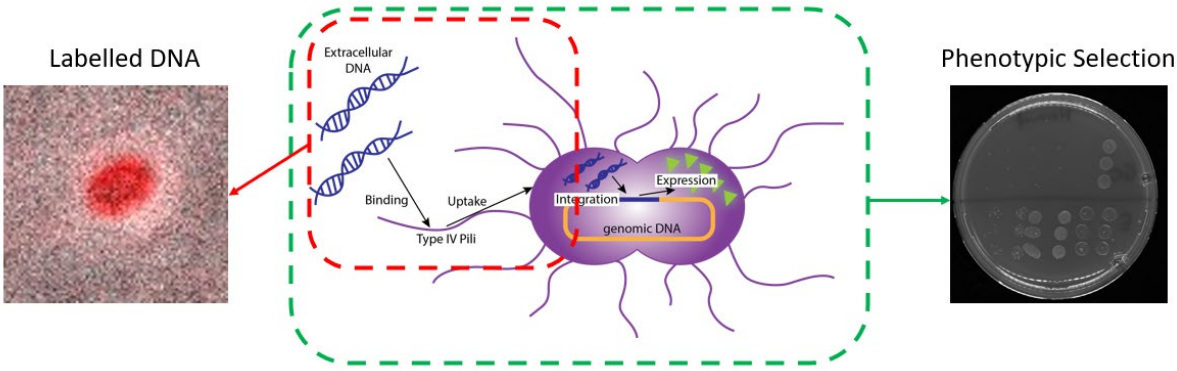


*Figure 4.9 Illustration of the two methods used to uncouple DNA uptake and DNA transformation*

*Labelled DNA Uptake Assay*

In our Labeled DNA uptake assay to study the dynamics across three hours, we observe the same heterogeneity of fluorescence signal among the population, similar to the previous experiment (Figure 4.10). In all time points, ΔPilV has higher signal intensity than the Wild Type. However, when we analyse the dynamics pattern between MS11 and MS11 ΔPilV, they share the same DNA uptake pattern (Figure 4.10). DNA uptake, signified by the fluorescence signal intensity, increases rapidly between 0.25h and 1h. After that, the process slows down into a plateau.

This observation is aligned with a reported study in which when the bacteria were pre-incubated with DNA molecules, subsequent tests in DNA uptake slowed down earlier than bacteria not pre-incubated with DNA molecules[165]. These observations agree with the hypothesis that a finite space in periplasmic space holds the DNA molecule after uptake. Moreover, this also suggests that the process of DNA uptake till transformation is spatially and temporally separated. This result also aligns with DNA translocation studies in *N. gonorrhoeae*[118], *Vibrio cholerae*[111], and most likely *Bacillus subtilis*[286,310–312]. Most likely, there is a bottleneck in transporting DNA molecules from periplasmic space to cytoplasm. However, at this stage of the experiment, it cannot be concluded if the limitation in DNA uptake is due to the limitation of periplasmic or cytoplasmic space.

What is also striking in this study is that the dynamics we observed are independent of the high amount of labelled DNA taken up in MS11 ΔPilV. This observation could suggest that although MS11 ΔPilV has the same DNA uptake dynamic as MS11, there are some differences between the two in the periplasmic or cytoplasmic space organisation.

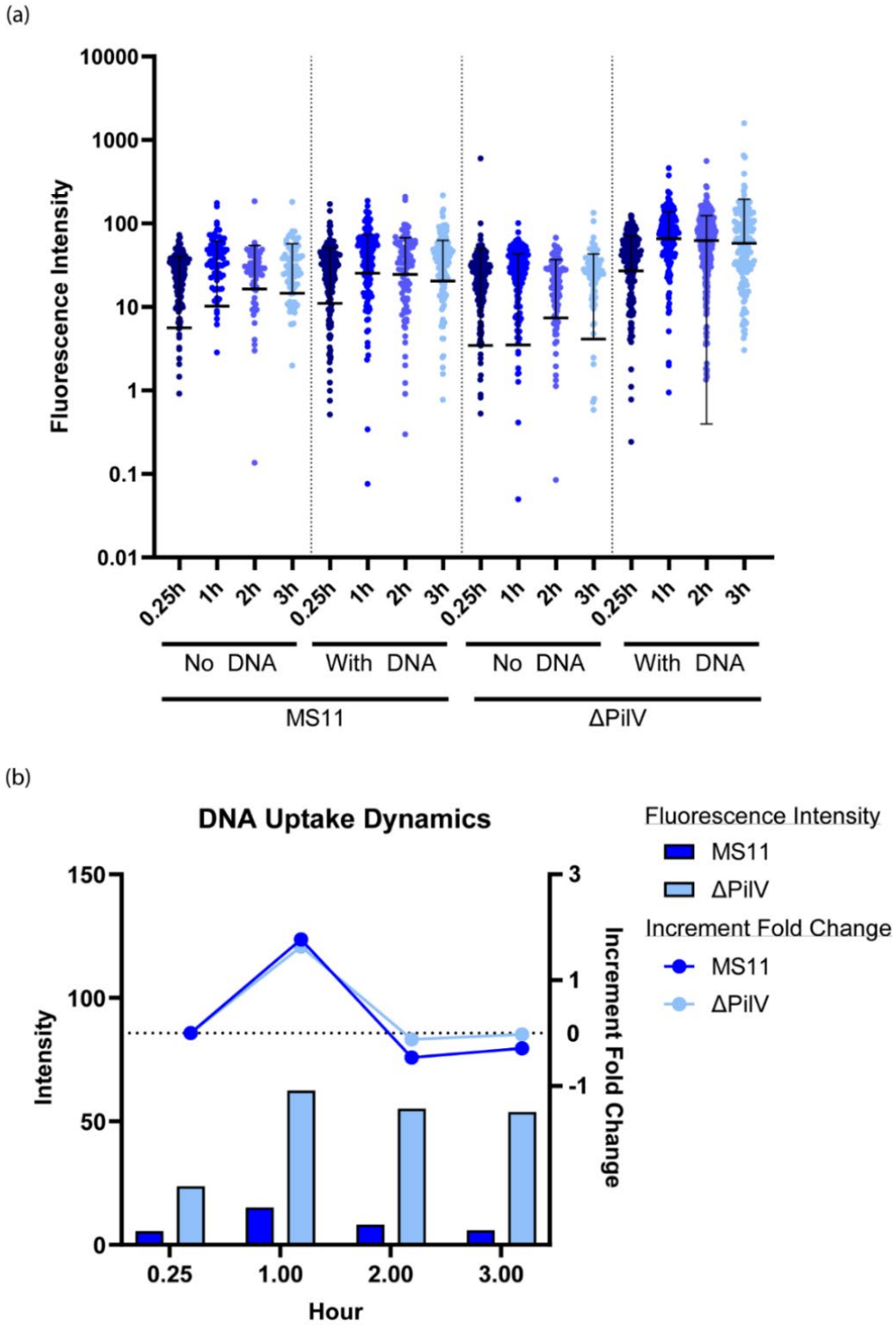


*Figure 4.10 (a) Fluorescence signal intensity per detected clusters in MS11 and MS11 ΔPilV across 3h, with or without labelled DNA (b) Bar (left axis) Averaged fluorescence signal reflected in (a), Line (right axis): Increment fold change of fluorescence signal across time.*

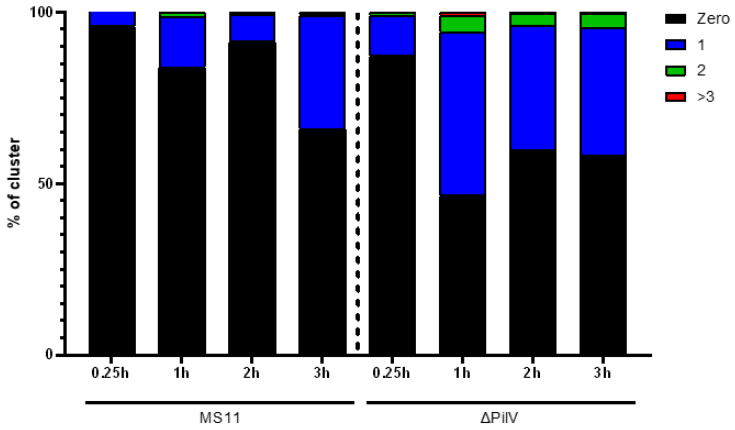


*Figure 4.12 Puncta analysis for DNA uptake assay cell clusters in MS11 and MS11 ΔPilV across 3h indicating the percentage of the cluster with zero (black), one (blue), two (green), and more than three (red) puncta*

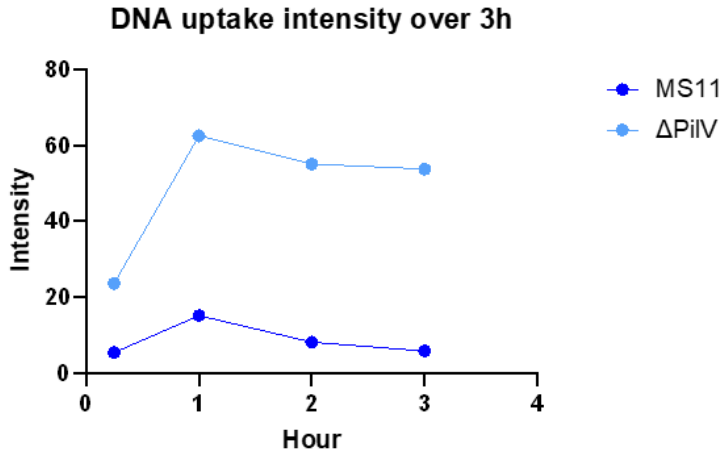


*Figure 4.11 Intensity (after removing background) of cell clusters in DNA uptake assay across 3h for MS11 and ΔPilV*

We also did a puncta analysis of these sets of data and images (Figure 4.12). This analysis will provide us with another dimension of information. For instance, the data we get from Figure 4.10 summarised the DNA uptake signal as a mean intensity. This means that we might lose some signals, especially if they are weak and the dynamic range is narrow. Fortunately, we observed a similar pattern of DNA uptake in puncta analysis. We observed a bigger portion of the ΔPilV population with puncta across all time points. The percentage of the population with puncta also increases across 3 hours for both MS11 and ΔPilV. We noticed the emergence of a population with more than one puncta in both strains. Interestingly, this population reduced in MS11 after two hours, while in ΔPilV, it reduced but maintained around 50% (Figure 4.11).

Other than such analyses, we also wondered if the DNA uptake assay time can affect the percentage of the population that takes up DNA. From our analysis presented in Figure 4.10, we realised that cell DNA fluorescent signals are heterogeneous, even on a population level. This means that there is a variability in the amount of DNA taken up in the cells, and there is also a variability in the uptake from cell to cell in a population. This can reflect our DNA transformation assay, which, given that we put in a certain amount of cells is not always all of them that become a positive transformant. In the case of DNA uptake assay, to reduce bias from the background signal in the 'noDNA' experiment, we define our threshold at the mean of the 'noDNA' cell cluster intensity plus its standard deviation for each time point. Then, we calculated the difference between the fluorescence signal in the 'with DNA' set (normalised against their own background intensity) and this threshold. As a result, we have the intensity in each cell cluster based on this definition of DNA uptake (Figure 4.13a). As we can observe from the graph, this calculation pushed several of the data values to negative. As an interpretation, any data point with a value above 0 is considered to have taken up DNA molecule. Armed with this definition, we calculated the percentage of the population that takes

up DNA at each time point (Figure 4.13b). Interestingly, we observed a constant percentage of the population in MS11 with DNA signal. The ΔPilV has a higher percentage of its population with a 'positive' cell cluster than MS11. What is striking is that this percentage is not constant in ΔPilV. Instead, the percentage increased at 1h and then started to slow down after that. This is interesting to note that indeed ΔPilV seems to change the population DNA uptake dynamics.

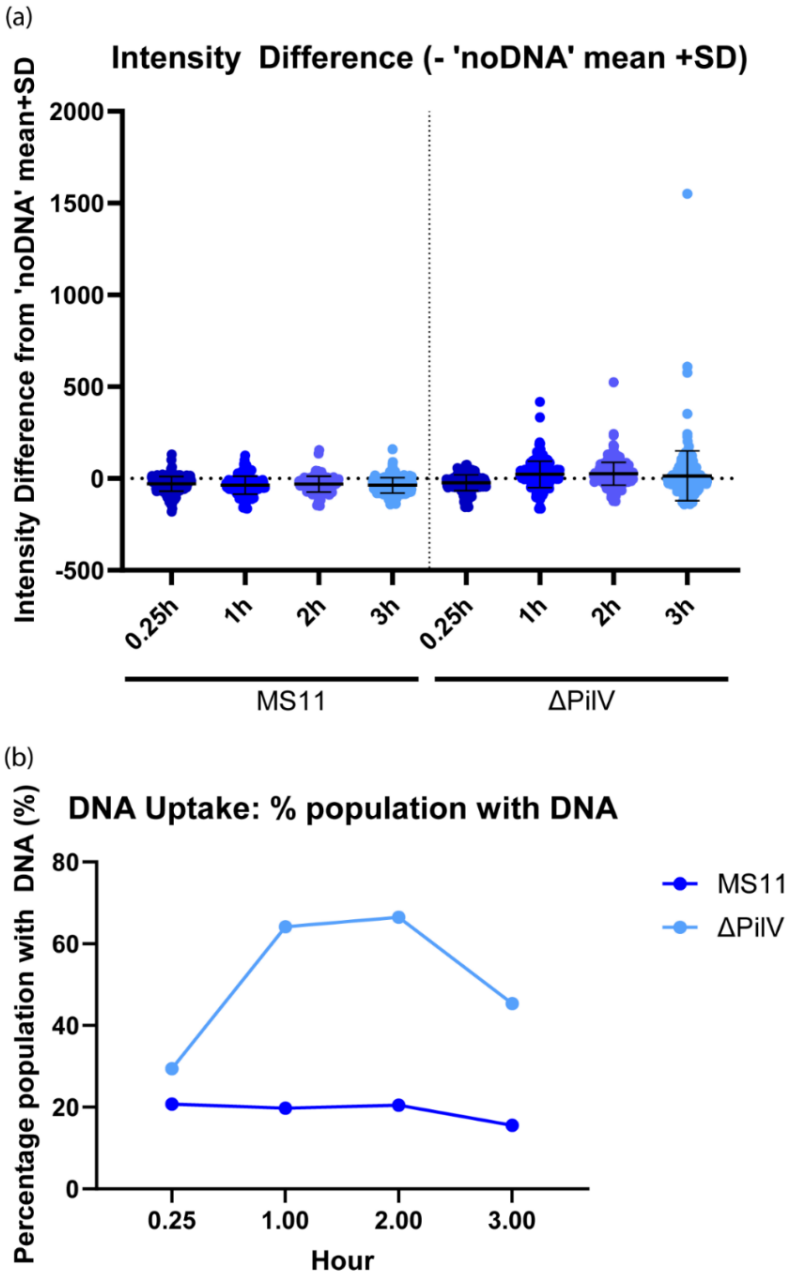


*Figure 4.13 Examining the percentage of the population in MS11 and ΔPilV that take up DNA: (a) intensity of cluster after deducting background defined as the mean of 'noDNA' with standard deviation (b) summary of the percentage of the population that takes up DNA*

*DNA Transformation Assay*

Next, we compare our labelled DNA uptake dynamics across three hours with macroscopic DNA transformation. With that, we conducted a similar experiment, except that instead of

taking labelled DNA fluorescence signal as readout, we used successful transformants as readout. To do that, we performed liquid transformation, as described in Chapter 2, with tDNA that can confer nalidixic acid resistance. After each time point, the cells were spotted on non-selective GCB agar and selective nalidixic acid plates. After allowing the transformants to grow, the colony-forming units were counted and analysed. In this experiment, we observed similar increment of transformation efficiencies at earlier timepoint (Figure 4.14). However, ΔPilV showed a higher increment in transformation efficiencies especially after 3h. Interestingly, the overall dynamics of transformation seems to be similar between both strains, noting both strains plateau after 4h (Figure 4.14).

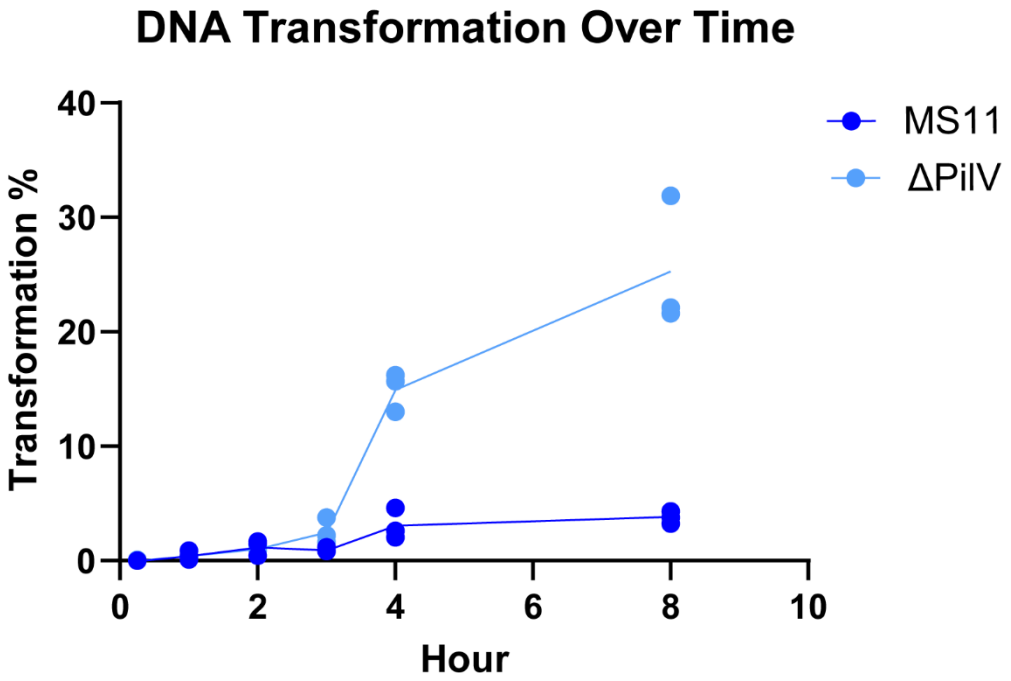


*Figure 4.14 Transformation efficiencies of MS11 and MS11 ΔPilV across 8 hours*

The similar pattern across three hours observed in both DNA Uptake Assay and DNA Transformation Assay shows that DNA uptake and transformation share the same dynamics within this given condition. Furthermore, in both methods, MS11 and MS11 ΔPilV also displayed similar dynamics. These observations pose some questions. We now know that MS11 and ΔPilV have the same DNA uptake and transformation dynamics, and the fact that the only difference was the increased amount of DNA uptake in MS11 ΔPilV. Given that you only need one copy of transform DNA to be incorporated into genomic DNA, how does the high amount of DNA taken up translate into enhanced competence in a population?

We looked closely at our DNA transformation dynamics data to answer this question. We realise that even though DNA transformation dynamics peak at 1h, when you take into account the percentage of transformed bacteria, this percentage increases over time, similar to that of MS11. However, at a later time point (3h), There is a plateau in the increment of transformant percentage in MS11, whereas, in MS11 ΔPilV, this trend has not slowed down (Figure 4.15). Given that we know MS11 and MS11 ΔPilV do not differ from each other with growth rate,

especially within the first 3h, the enhanced competence as a population may be due to a higher reservoir of DNA taken up in ΔPilV.

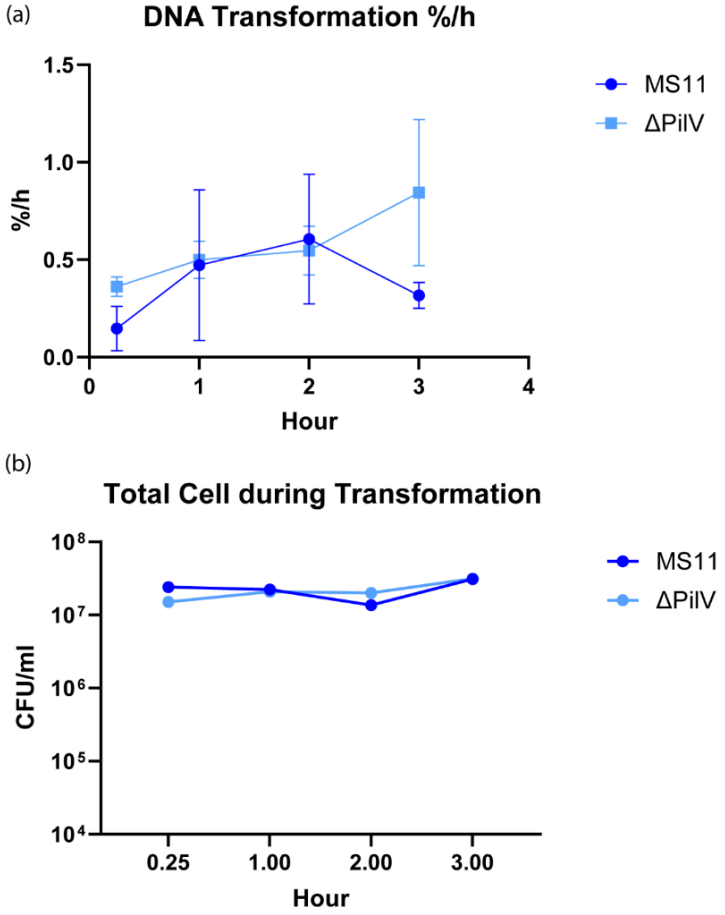


*Figure 4.15 (a) Cumulative transformation % per hour calculated from data in DNA transformation assay across 3h (b) total cell during transformation assay across 3h for MS11 and ΔPilV*

### 4.3.1.6 The role of PilV in inhibiting DNA uptake is downstream of PilT and ComP

Other than the role of PilV in DNA uptake using ΔPilV mutant, we also looked into the phenotype of its combination strains. This include ΔPilV, ΔPilT, ΔComP, ΔPilV ΔPilT, and ΔPilV ΔComP. We selected PilT and ComP as the candidates to asses as combination strains due to their known involvement in Type IV Pili retractions and DNA uptake. In this study, we conclude that PilT is still dominant in Type IV Pili dynamics compared to ComP and PilV. This means that pili functions such as retractions and microcolony formation still depend highly on pili retraction resulting from the PilT function. Between ComP and PilV based on the DNA transformation assay, it seems that our result points to ComP being more dominant than PilV. These results are aligned with what is hypothesised or reported in the literature [164] (For details, check Study III: A study on ΔComP, ΔPilV and ΔPilT combination strains).

### 4.3.1.7 DNA molecules localisation and dynamics are different in ΔPilV

The previous observations lead to a fundamental question. Assuming polyploidy in the *N. gonorrhoeae* genome is deemed existing but rare, introducing a point mutation through transformation will require only one mutant tDNA template. Wild Type and ΔPilV have the same uptake and transformation dynamics over the first three hours, and they do not differ

significantly in doubling time. In this case, if there was no bottleneck within the pathway from DNA uptake till recombination, ΔPilV taking up more DNA molecules should not lead to more progeny with positive transformants. We suspect a bottleneck within this pathway, and ΔPilV increased the probability of one of the pathways biologically or stochastically. Since we noticed more DNA puncta in ΔPilV, we hypothesised that the DNA molecule dynamics after entering the cell may provide some information. To investigate further, we look at DNA molecule localisation and dynamics.

*DNA localisation*

With the technique described in Chapter 3, we performed the DNA localization study under two conditions: (a) **Immediate** – live imaging of interaction between bacteria and DNA molecule within the first five minutes in contact and (b) **Long-term** – static images of cells after DNA uptake assay of 3 hours.

In the **Immediate** setting (Figure 4.16), bacteria cells were incubated with labelled tDNA molecules and imaged immediately for 5 minutes. This setup does not involve DNase I treatment and washes, which may lead to higher background noise. In the *Immediate* setting, the localization is a mean localization of the DNA molecules in multiple cells across a 5-minute video. As a test of this analysis, we compared the localization of DNA molecules around different *N. gonorrhoeae* strains: MS11, ΔPilE, ΔPilT and ΔPilV.

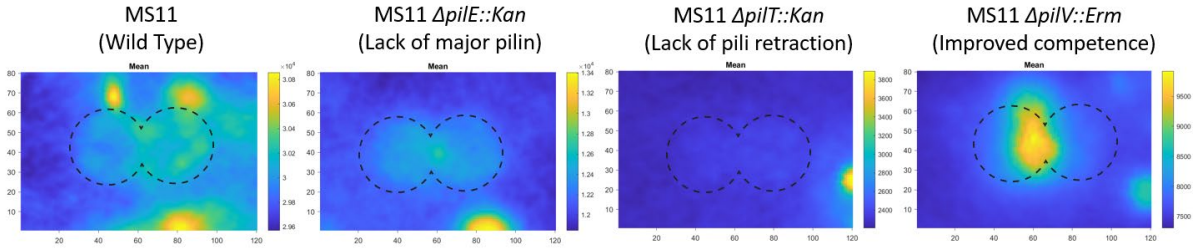


*Figure 4.16 DNA localization of DNA uptake study in pili mutant from a compilation of bacteria in a 5-minute timeframe*

As observed in the video described in Section 3.2.3.3, we observed most of the DNA molecules localized around the cell body for MS11 (Figure 4.16). Occasionally, there are a few bright spots around the cell, but those are indications of DNA molecules of high fluorescence signal. This signal could indicate an aggregate of one or more DNA molecules. The lack of DNA localization in ΔPilT fits well with the understanding that pili retraction is a major driver of the DNA uptake process. On the other hand, we observed the same anomaly with ΔPilE, in which we see DNA localization around the cell. This observation reflects exactly our observation in Section 3.3.3.4. Therefore, these two observations strengthen the theory that PilE may not be the sole player in DNA uptake. Lastly, in ΔPilV, we observe a slightly different DNA localization than MS11 (Figure 4.16). While there is some DNA localization around the cell occasionally, most of the DNA is concentrated in the middle of the cell, the septa. This observation has been reported before, but it was assumed that this is the behaviour of an enhanced DNA uptake activity[165]. We observed that the 'Immediate' setting may represent a

temporary DNA localisation within the cell. To investigate the consistency of this pattern, we collected samples for MS11 and MS11 ΔPilV from a 3h timepoint and performed a similar analysis the **Long-Term** setting.

In the **Long-term** setting (Figure 4.17), *N. gonorrhoeae* cells are incubated for 3 hours in contact with labelled tDNA, and then washed and treated with DNAse I. These cells were then mounted on the microscope, and images were taken. The DNA localisation is taken as the mean localisation of DNA molecules from multiple cells in selected images. Our **Long-term** setting experiment looked at the DNA localisation for MS11 and ΔPilV. In this setting, we observed that DNA localisation in MS11 spread more homogenously across the whole cell body. Compared to the **Immediate** setting, the mean intensity inside the cell body is also slightly higher. This means the DNA molecules taken into the periplasm have been transported into the cytoplasm or spread around the cell. This can also mean that at 3 hours, some of the DNA molecules have exceeded their turnover time in the periplasm, which has yet to be measured experimentally. In ΔPilV, we observe the same higher signal intensity inside the cell body, signalling the transport of DNA molecules into the cytoplasm. Yet, the accumulation of fluorescence signal at the septa does not cease at 3 hours.

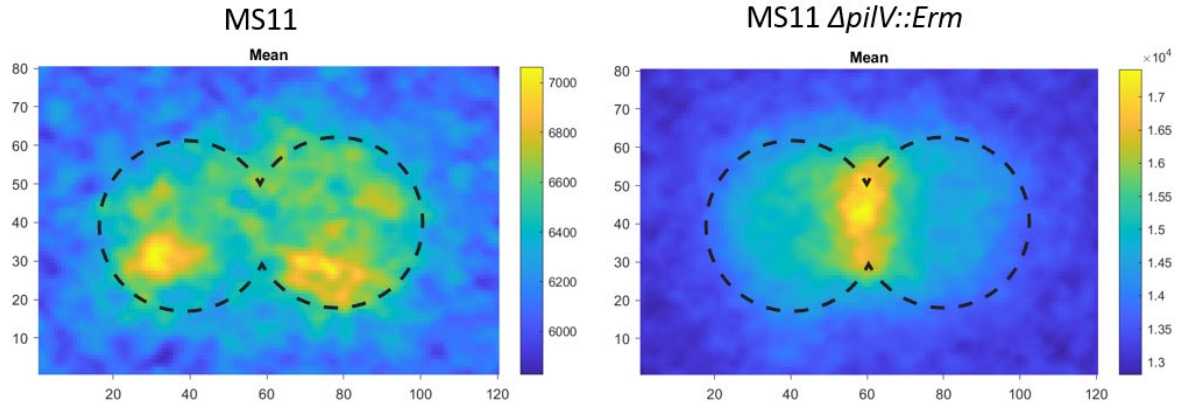


*Figure 4.17 DNA localisation of MS11 and ΔPilV after 3h of incubation with labelled DNA*

Overall, the **Long-term** setting observation seems to match observations from the *Immediate* settings, giving confidence that the DNA localisation we observed in both time points is not random and is most likely regulated. Our result shows an excellent visualisation of DNA localisation in pili mutants at 5-minute and 3-hour intervals. Moreover, it also shows an interesting phenomenon for ΔPilV that is not extensively studied. From the result, we can interpret that DNA molecules stay in the periplasm after being taken up by the cell. After some time, the DNA molecules are slowly distributed homogenously across the cell body. However, in MS11 ΔPilV, even after some of the DNA molecules were distributed across the cell body, DNA molecules still accumulate near the septa region. With this data, it is still insufficient to conclude if such accumulation is due to a slower turnover of DNA molecules into the cytoplasm, a heightened amount of DNA molecules taken up into the periplasm or a directional flow forcing the accumulation of DNA molecules at the septa region of the cell. Whether this key difference leads to increased competence phenotype in ΔPilV is still debatable. Therefore, we

continued our investigation in a similar setting by looking at the dynamics of DNA molecules after entering the cell body.

*DNA molecules dynamics*

To investigate the dynamics of DNA molecules within the cell body after uptake, we captured time-lapse images of the bacteria across two hours. Since we know from previous experiments that DNA uptake saturates after 3h, we captured the video after 3h incubation, after removing excess DNA molecules by washing and DNAse I treatment. With that, we will start with the highest possible DNA fluorescence signal and track their trajectories afterwards.

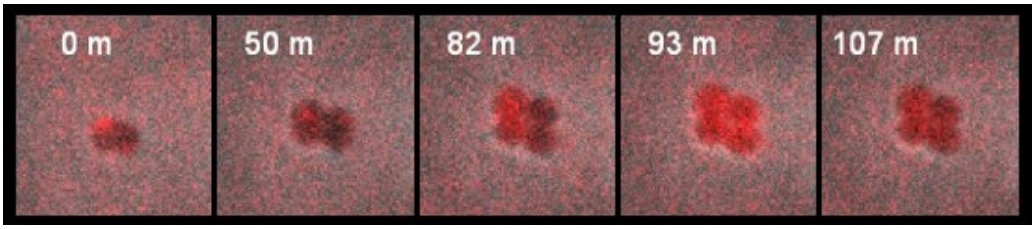


*Figure 4.18 Labelled DNA dynamics in MS11 across 2h*

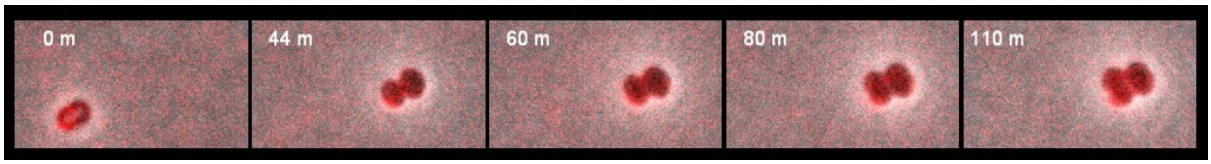


*Figure 4.19 Labelled DNA dynamics in MS11 ΔPilV across 2h*

Across these two hours, we observed some critical differences between MS11 and MS11 ΔPilV. We noted that the DNA fluorescence signal in MS11 will oscillate and then start spreading across the cell body (Figure 4.18), whereas, in MS11 ΔPilV, we observed strong DNA fluorescence signal oscillating around the cell, presumably at the periplasmic space for a longer time (Figure 4.19). We selected some cells for analysis to ensure what we observed by eye was true. In the analysis, we identify the cell area, examine the fluorescence signal across time, and extract parameters like total, maximum, minimum, and mean intensity of the selected region of interest. Our analysis shows that MS11 cells generally increase their total intensity together with all other parameters (maximum, minimum, and mean intensity) (xxiv, xxv, xxvi). This shows that the spread of the fluorescence signal is indeed homogenous across the cell cluster. However, in MS11 ΔPilV, although it also has an increase in total fluorescence intensity, there were no big fluctuations in the mean, maximum and minimum intensity (xxiv, xxv, xxvi). This could be explained by the bright fluorescence signal in the periplasm staying the same although they oscillate. Another interesting observation through analysis is that MS11 ΔPilV seems to be observed to lyse more often than MS11. However, our experimental setup and analysis do not allow for a controlled quantification of this phenomenon. With this observation, we hypothesised that the membrane integrity of MS11 ΔPilV may differ from MS11.

One of the extra observations we capture is the secretion of DNA. Although not frequently observed, we captured instances in which the DNA signal that was wrapped around the cell periplasm left the cell body area near the septa during cell division (Figure 4.20). We can see

from pixel analysis of the cell cluster region that the total pixel intensity did not change across the time frame. Still, the maximum value increased when the signal appeared to shift outside of the cell (xxvii). The secretion of chromosomal DNA by the Type IV Secretion System (T4SS) in *N. gonorrhoeae* has been reported and studied in the literature[313–315]. The secretion of single-stranded DNA (ssDNA) through T4SS during early *N. gonorrhoeae* biofilm formation has also been reported[316]. In this case, what we observed most likely occurred through the same secretion system. However, further studies should be done to confirm this.

Overall, these observations confirmed what we hypothesised during our DNA localisation analysis. ΔPilV showed different DNA uptake dynamics through increased cellular uptake and DNA molecule dynamics. The DNA molecules tend to stay longer in the periplasm, which could lead to the accumulation of DNA fluorescence signal at the septa through biological or stochastic reasons. This critical change to the DNA molecules dynamic in the cell may be a factor in its increased competence phenotype.

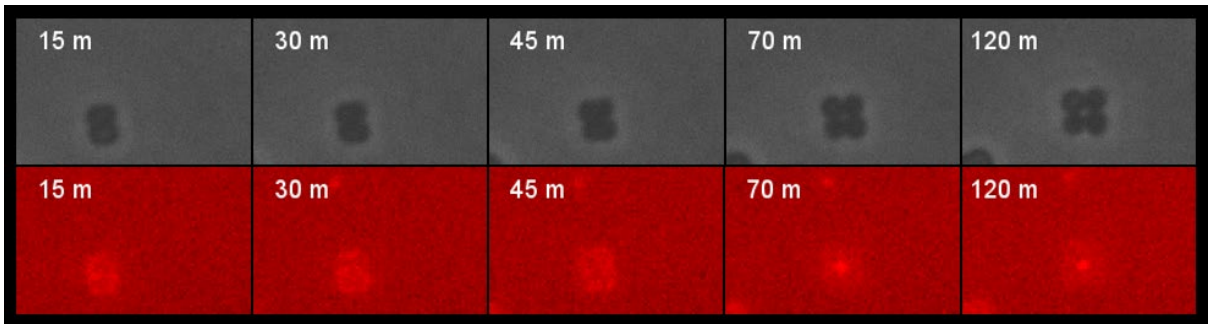


*Figure 4.20 Example of possible DNA secretion*

### 4.3.2 Pili retraction mechanical properties of ΔPilV Strains

#### 4.3.2.1 Pili retraction profile on micropillars

Other than assessing ΔPilV in their DNA uptake phenotype through labelled DNA, we turned to investigate the pili retraction profile of ΔPilV. Before we start characterizing pili retraction profile with ΔPilV or any DNA-related pili retractions, we first established both of our **carboxylated bead-coated** and **DNA-coated micropillars**.

During our preliminary study, we did not have a good resolution of **DNA-molecule interacting pili retractions profile** on '21pillar' (xxviii). We consistently observed lesser events on DNA-coated pillars compared to carboxylated beads-coated pillars, which could be due to coverage concentration. Nonetheless, for better resolution, we proceed with the less stiff 'betapillar'. We first tested our system with Wild Type MS11.

On 'betapillar' micropillars, the pili retraction mechanics usually adapted to a lower force. In our study, we still see more pili retraction events on carboxylated beads-coated micropillars. On top of that, we can also observe that given the same condition, the pili retraction force and speed are weaker and slower on DNA-coated micropillars (Figure 4.21). We did observe that when we inoculated more cells (50 µl of $OD_{600}$ 0.7 in 500 ml GCB+) at longer hours (5h) when microcolonies were formed, we could observe stronger pili retractions but still slower pili

retractions (Figure 4.21). When we used the usual cell number (25 µl of $OD_{600}$ 0.7 in 500 ml GCB+) at 5h, we observed slower and weaker pili retractions even with the presence of $MgSO_4$, a medium closer to liquid transformation (Figure 4.21). These results suggest that the amount of cells or the cell growth stage does affect the pili retraction mechanics, although given the same conditions, pili interacting with DNA molecules are of the weaker and slower retraction populations.

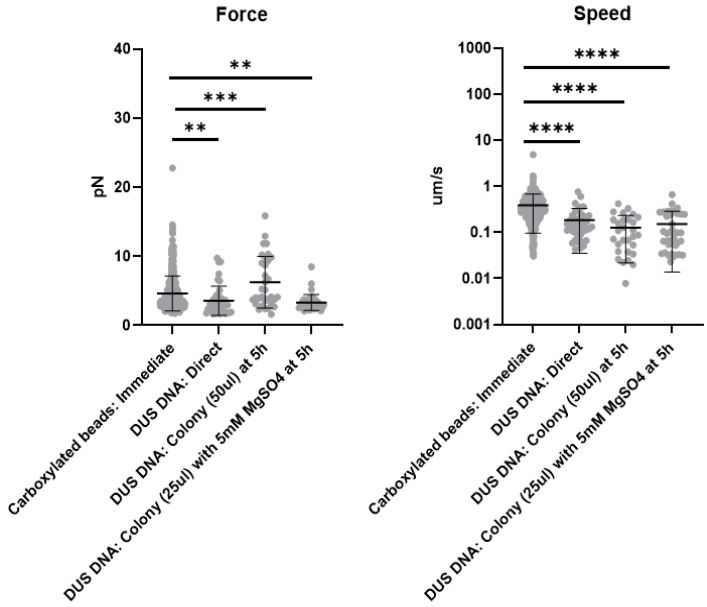


*Figure 4.21 Comparison of MS11 pili retraction (a) force and (b) speed on 'betapillar'*

*Table 3.1 Small sampling to check on the coating comparison between different substrates through events per microcolonies*

| | Microcolonies # | Total Events | Events/Microcolony |
|---|---|---|---|
| **MS11** | | | |
| 21-carboxy | 3 | 271 | 90 |
| 21-DNA | 2 | 40 | 20 |
| Beta-carboxy | 6 | 1370 | 228 |
| Beta-DNA | 3 | 115 | 38 |
| **ΔPilV** | | | |
| Beta-carboxy | 4 | 794 | 199 |
| Beta-DNA | 3 | 170 | 57 |
| **ΔComP** | | | |
| Beta-carboxy | 3 | 728 | 243 |
| Beta-DNA | 3 | 73 | 24 |

Since we observe a discrepancy between the amount of pili retractions on pillars with different coating, we suspect it is not rational to compare numbers directly from the two types of pillar. The discrepancy may be due to the surface binding site concentration of the different molecules. To ensure both types of micropillar are useful for measurement on their own, we designed an experiment to test the coverage. Using MS11 (Wild Type), ΔPilV (enhanced competence), and

*Table 3.2 Average events/microcolony ratio between carboxylated beads-coated micropillars and DNA-coated micropillars in different strains or micropillars dimension*

| | **Carboxy:DNA** |
|---|---|
| **MS11-21** | 4.5 |
| **MS11-beta** | 6 |
| **ΔPilV-beta** | 3.5 |
| **ΔComP-beta** | 10.1 |

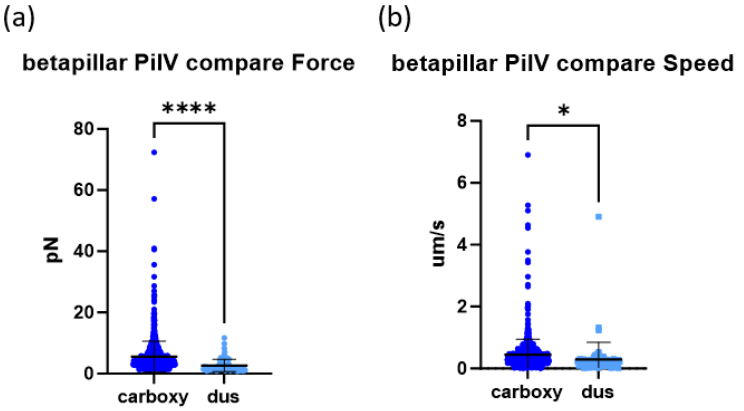


*Figure 4.22 Comparison of MS11 ΔPilV pili retraction profile on betapillar between carboxylated beads coat and DNA-DUS coating*

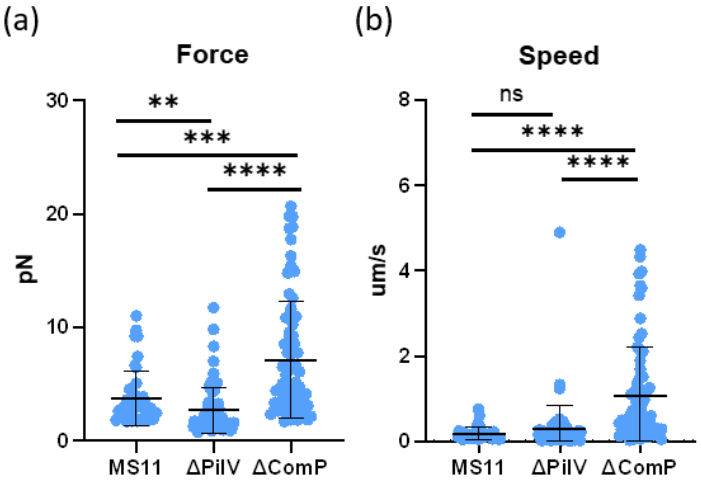


*Figure 4.23 Pili retraction profile of different strains on 'betapillar' DNA-coated pillar: (a) force and (b) speed*

ΔComP (reduced competence), we measured their events per microcolonies on micropillars with different coating (Table 3.1). Since this is a control experiment, we selected only a few microcolonies. With these data, we compared the ratio of events per microcolony on the three different strains. Our results show that the ratio of events per microcolonies on carboxylated beads coating versus DNA coating (carboxy:DNA) is lower in ΔPilV compared to Wild Type, while ΔComP shows the opposite (Table 3.2). This suggests that, given the bacteria present a certain amount of pili retraction events, more DNA-specific activities are observed in the enhanced competence strain, ΔPilV, and the opposite is true for ΔComP. We conclude that although we could not make an absolute comparison between the different coatings, we could use the ratio to understand the Type IV Pili dynamics and activities in different bacteria strains. This also points out that the available binding site per area for Type IV Pili in different substrate coating is most likely the contributor to the large difference in pili retraction events recorded.

With our system set up, we compared the pili retraction profile for MS11 ΔPilV on 'betapillars' coated with carboxylated beads or DNA. We could characterise that pili retractions for MS11 ΔPilV are weaker and slower on DNA-DUS coated betapillars (Figure 4.23).

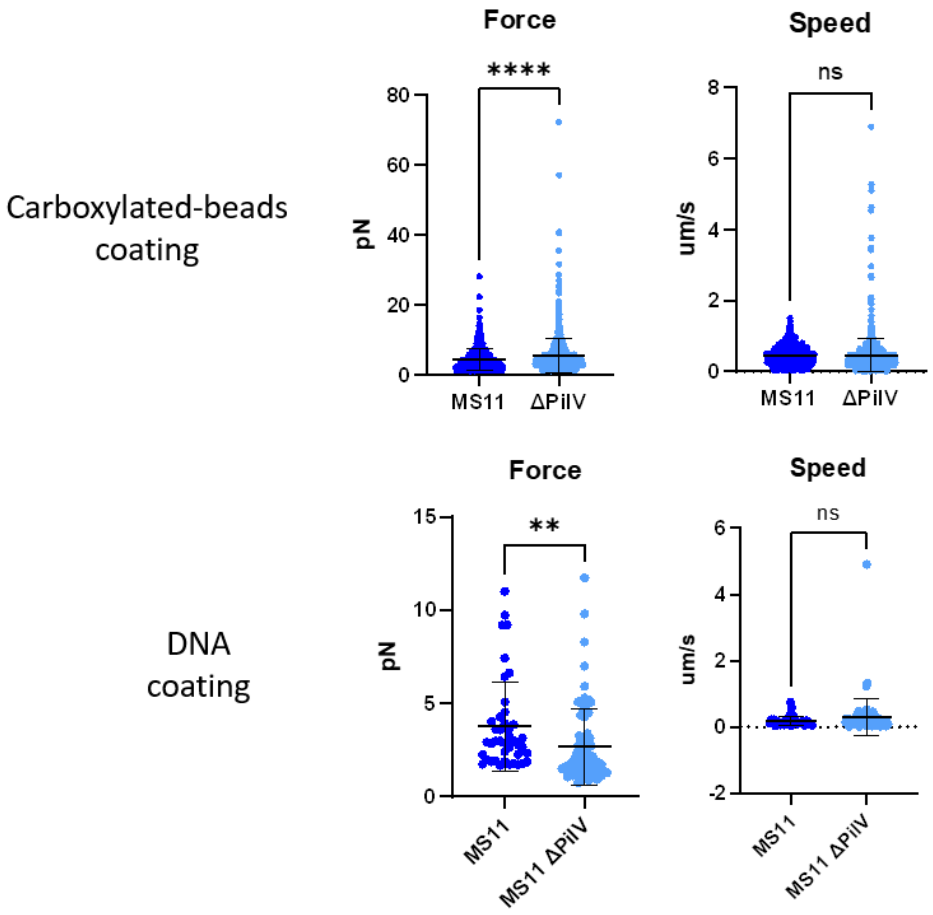


*Figure 4.24 Comparison of pili retraction (i) Force and (ii) Speed between MS11 and MS11 ΔPilV on 'betapillar' coated with (a) carboxylated beads and (b) DUS-DNA*

When compared between MS11 and MS11 ΔPilV, we observed that the pili retraction speed does not differ regardless of the coating (Figure 4.24). Force-wise, MS11 ΔPilV tends to have stronger pulls than MS11 on carboxylated beads coated 'betapillars' but weaker pulls than MS11 on DUS-DNA coated betapillars. In all cases, MS11 ΔPilV tends to have bigger variation for its retraction profile than in MS11. When we compared MS11, ΔPilV, and ΔComP on DNA-coated 'betapillar', we noticed that ΔComP tend to have stronger and faster pili retractions. Overall, in the context of pili retractions related to DNA molecules, ΔPilV, that takes up more DNA seems to have **weaker but faster pili retractions** than that of MS11.

### 4.3.2.2 Pili retraction events distance analysis

Other than investigating the force and speed of pili retractions, we noticed that there was a high frequency of pili retraction events near or at the periphery of microcolonies, whereas those far away tend to occur occasionally. This observation is even more extreme on DNA-coated micropillars when most events were observed close to the microcolonies on '21pillar'. To prove this observation is true, we performed **distance analysis**. We calculated the distances in which these events occur corresponding to a manually-defined centre of the microcolonies (Figure 4.25) and mapped out their nature. We included a bigger area around the microcolonies for preliminary pili retraction event distance population analysis. Since Type IV Pili in *N.*

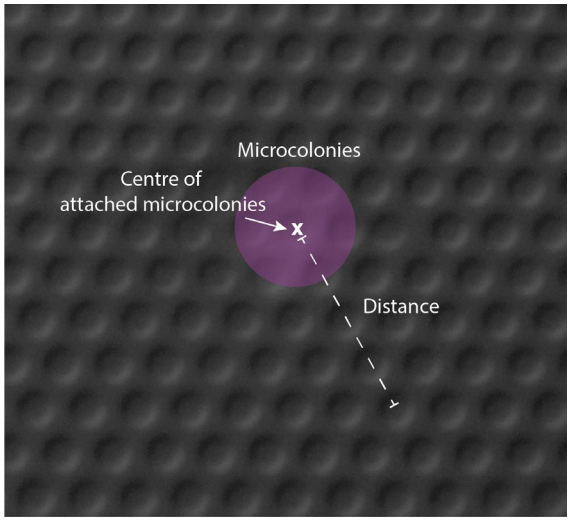


*Figure 4.25 An illustration of how the distances of events were defined and calculated*

*gonorrhoeae* are reported to reach up to 30 µm in length[297], it is good to note that events recorded further than that are possibly artefacts recorded from nearby microcolonies.

In both '21pillar' and 'betapillar' for MS11, we observed higher proportion of pili retraction events occurring near the microcolonies (Figure 4.26). This observation is more obvious on DNA-DUS coated 'betapillar'. In addition to that, we observed the same trend for ΔPilV and ΔComP (xxx). We did note that ΔPilV actually has more events further away from the microcolony on DNA-coated micropillars.

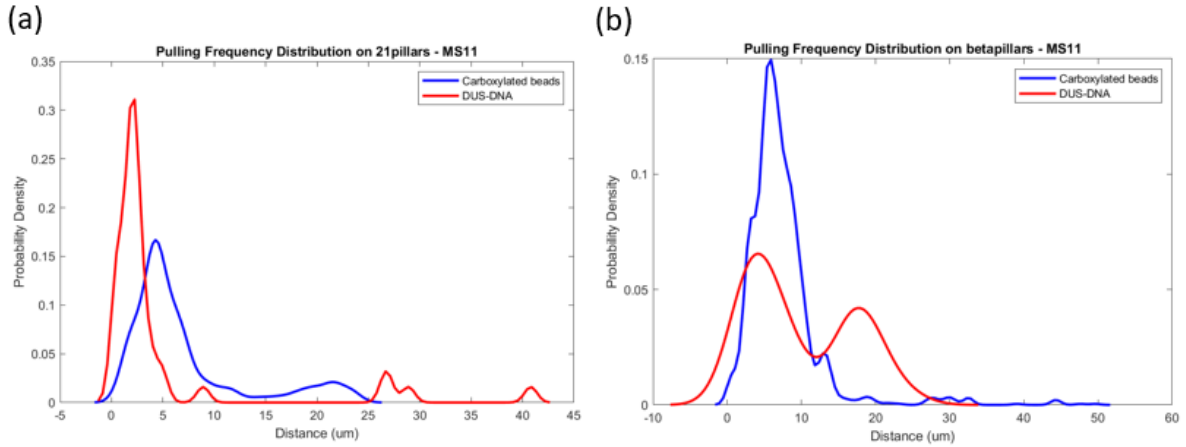


*Figure 4.26 MS11 pili retraction events profile on carboxylated beads-coated (blue) and DNA-coated (red) '21pillar' against distance on: (a) '21pillar' and (b) 'betapillar'*

For better study on ΔPilV and DNA-related pili retractions, we analyzed pili retraction for **MS11, ΔPilV, and ΔComP** on micropillars with different coating. When we compared all three strains on **carboxylated beads-coated pillars** (Figure 4.27), the spread of ΔPilV is broader than the rest in terms of the distance of the events. In contrast, ΔComP has a much narrower range. These results align with the fact that PilV is reported to play a role in adhesion. We suspect that the defect in securing a strong binding to the substrate renders ΔPilV Type IV Pili to explore further than the rest. It is also interesting to see that ΔComP pili retraction events distance profile is narrower than the Wild Type. We hypothesise that this can be due to the lack of ComP leading to more adhesion-based pilin being shuttled into the Type IV Pili, hence securing better binding. Interestingly, this will also raise the question of better binding, which may not necessarily mean better DNA binding and competence.

On **DNA-coated pillars** (Figure 4.28), we can observe the two distinct populations of pili retraction events, **long-distance** and **short-distance**. This is an interesting observation since we similarly noted the long and short pili activity during pili labelling experiment. According

to observations, the short-distance events mostly occur underneath the microcolonies. One thing worth noting is how, in ΔPilV and ΔComP, the long-distance population peaks are smaller compared to the Wild Type. When we compare between ΔPilV and ΔComP, ΔPilV seemed to have a much higher short-distance to long-distance pili event ratio. However, ΔPilV still seems to have a much broader spread of the distance in which the pili retractions take place.

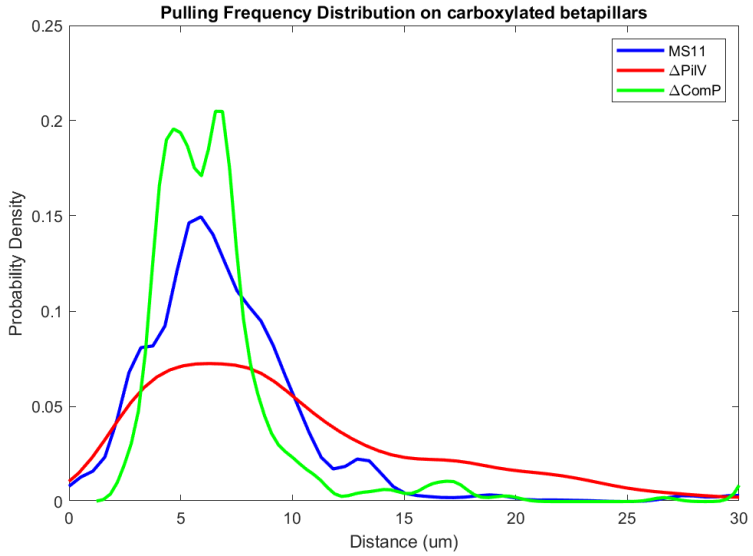


*Figure 4.27 Probability distribution of pili retraction events on carboxylated beads-coated 'betapillar' in terms of distance from the centre of the microcolony for MS11, ΔPilV and ΔComP*

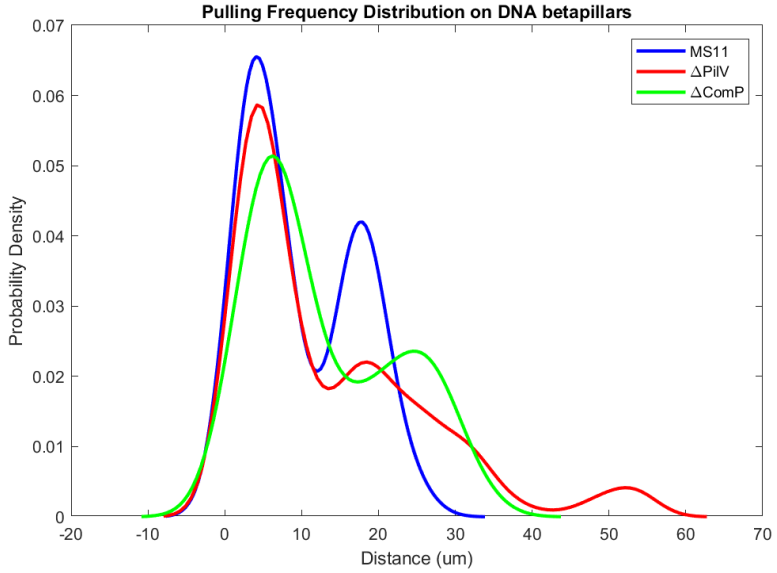


*Figure 4.28 Probability distribution of pili retraction events on DNA-coated 'betapillar' in terms of distance from the centre of the microcolony for MS11, ΔPilV and ΔComP*

To provide a bigger picture, we mapped the relationship between force, speed, and distance for each strain on different pillars (Figure 4.29). We can conclude that long-distance retraction events are usually not the strongest or fastest pulls on carboxylated beads-coated pillars. Meanwhile, the spread for force and speed across distance is wider on DNA-coated pillars. We also observed that on DNA-coated pillars, ΔPilV and ΔComP tend to have more long-distance retractions that pull faster. ΔComP can be seen as having a more scattered pattern for the speed versus force relationship.

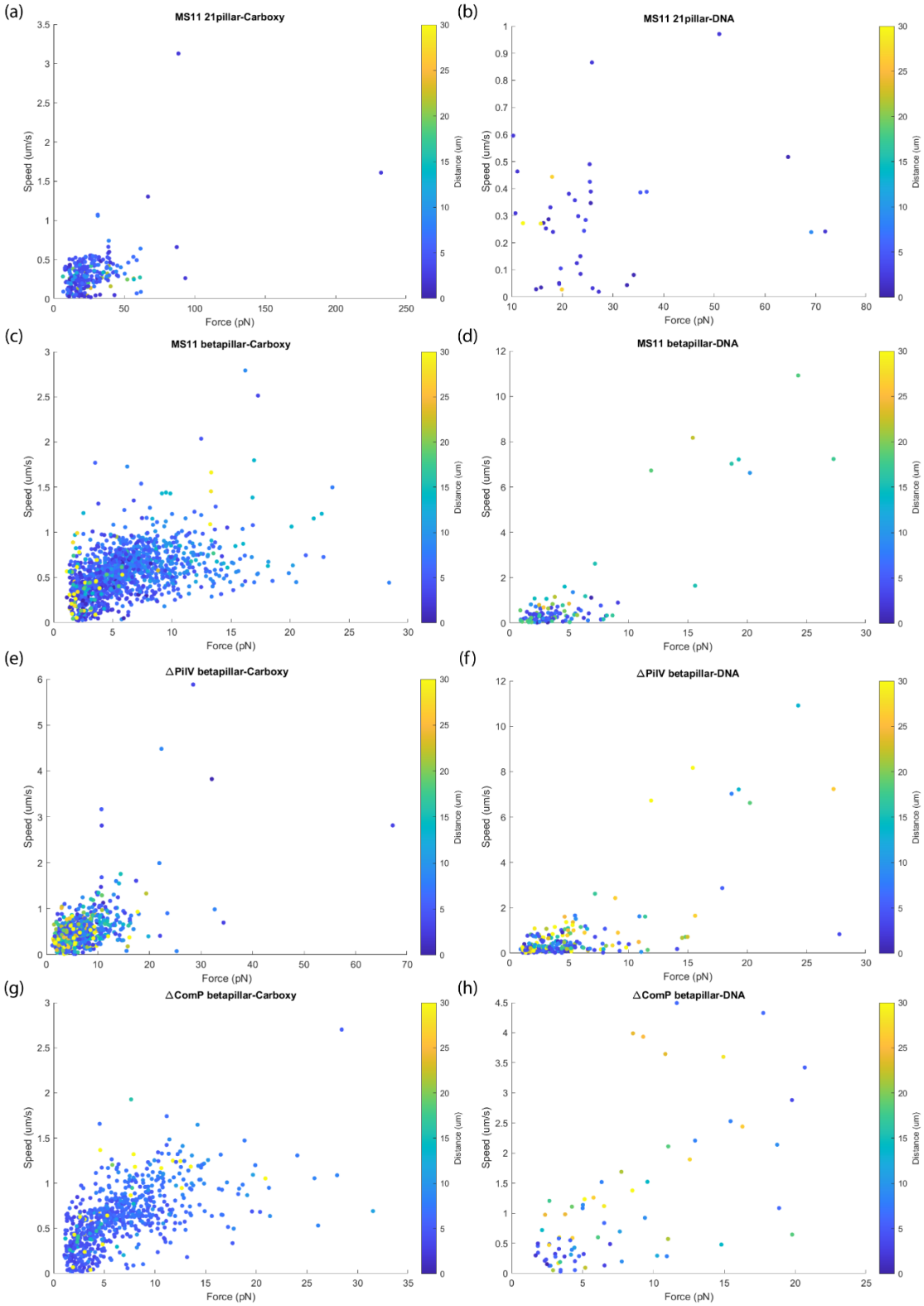


*Figure 4.29 Plot illustrating the relationship between pili retraction event force (x-axis), speed (left y-axis), and distance (right y-axis) for: MS11 on '21pillar' (a) carboxylated beads-coated (b) DNA-coated, and all strains on 'betapillar' as follow: carboxylated beads-coated pillar for (c) MS11, (e) ΔPilV, and (g) ΔComP, and DNA-coated pillar for (d) MS11, (f) ΔPilV, and (h) ΔComP.*

#### 4.3.2.3 Categorical pulling events characterization

After getting a rough idea of the pili retraction profile concerning distance, we decided to characterize these events in detail. We artificially defined short- and long-distance pili retraction events based on our previous observations. Here, we defined pili retraction events that occurred at 0 – 15 µm as 'Short' and 15 – 30 µm as 'Long' distance. With this definition, we categorized these events accordingly and looked at differences in their mechanical properties. Since we discovered the coating coverage of the surface substrate may be the reason leading to lesser pulling events on DNA-coated micropillar, we only compare the 'Short' and 'Long' distance populations within the experiments with the same surface coating.

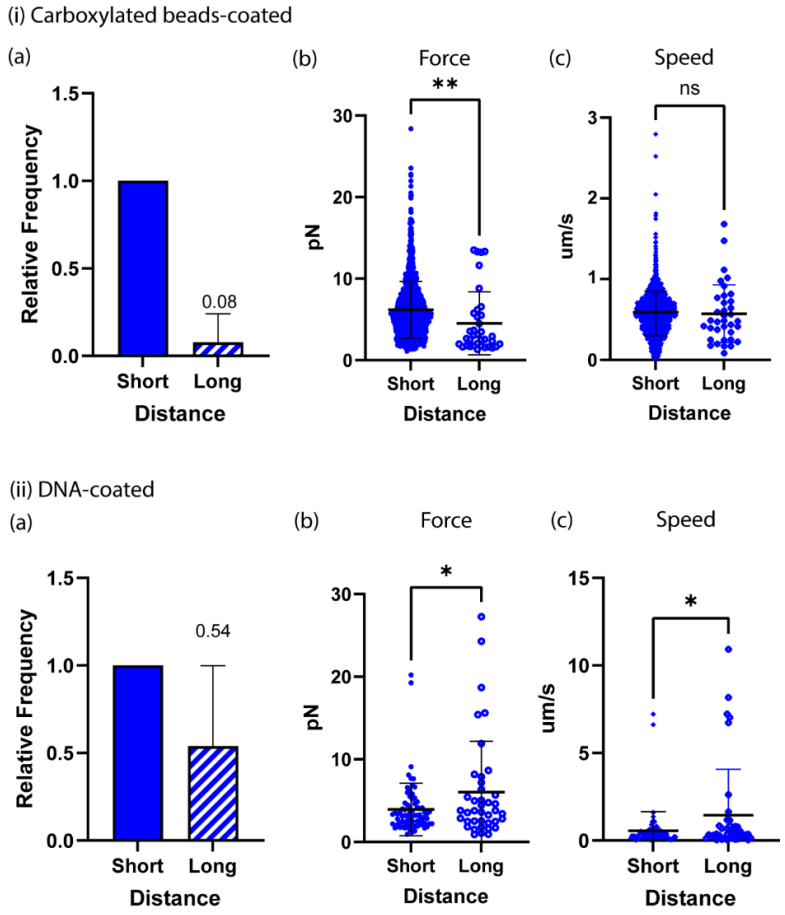


*Figure 4.30 Breakdown of pili retraction profile for MS11 on 'betapillar' with (i) carboxylated beads-coating and (ii) DNA-coating, detailing the (a) relative frequency, (b) force, and (c) speed of Short and Long distance pili retraction events*

For data extracted from MS11 on '21pillar' (xxxi), we observed that on both types of coating, the frequency of 'Long' distance events is around 10% of 'Short' distance events. There was no significant difference between the two populations regarding the force exerted on carboxylated beads-coated micropillars, but the speed of the 'Long' population is slower. We couldn't conduct any statistics on the DNA-coated micropillars due to the small sample size. When we look at MS11 on 'betapillar' (Figure 4.30), we still see the frequency of 'Long' distance events at around 10% of 'Short' distance events. However, we noted a shift in the ratio of DNA-coated micropillars. This fits with what we observed in the pooled results. Nonetheless, the 'Short' events pulled stronger than 'Long' on carboxylated beads-coated micropillars, with

no significant difference in their speed. On DNA-coated micropillars, the mechanics were shifted. The 'Long' distance events are more robust and faster than the 'Short' distance events.

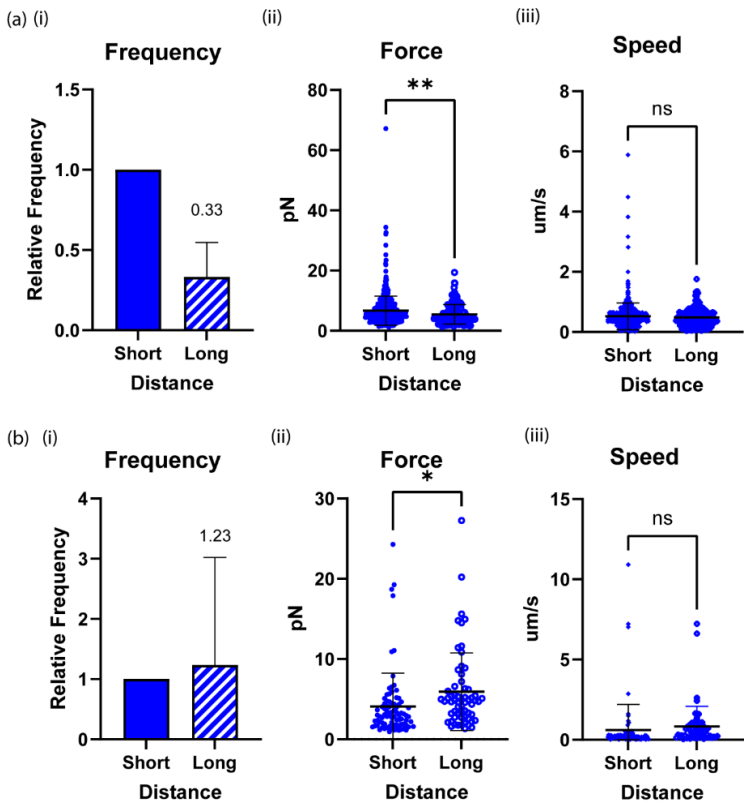


*Figure 4.31 Detailed profile of MS11 ΔPilV pili retraction event on (a) carboxylated beads coated betapillar and (b) DUS-DNA coated betapillar: (i) The relative frequency between short and long pili retraction events (ii) The force profile between short and long*

For both ΔPilV and ΔComP, the 'Long' and 'Short' distance profile looks similar. On both carboxylated beads-coated and DNA-coated pillars, there was no significant difference in the change in speed for the long-distance and short-distance pili retraction events (Figure 4.31 and Figure 4.32). However, the force of these retractions differs significantly. Both ΔPilV and ΔComP show stronger pull for short-distance retraction on carboxylated beads-coated pillars, while they show weaker pull for short-distance retractions on DNA-coated pillars (Figure 4.31 and Figure 4.32). What strikes in our analysis is **the frequency of short-distance and long-distance pili retraction events**. In both MS11 and ΔComP, we have roughly the same proportion regarding the population, but we have a slight difference in ΔPilV. Nonetheless, our data sampling in this study may not be statistically relevant to conclude anything.

We compiled and compared some of these data in a few different situations. First, we were curious if there is any significant difference between the pili mechanics on other coatings. Our previous study showed that pili retractions on DNA-coated pillars are slower and weaker, mainly when the difference could be observed on 'betapillar'. On 'betapillar' (xxxiii), we noted that the weaker pulls on DNA-coated pillars can only be observed from the short-distance pool in both MS11 and ΔPilV. On the other hand, when we compared the speed, the long-distance pool in both strains had a higher speed on DNA-coated pillars.

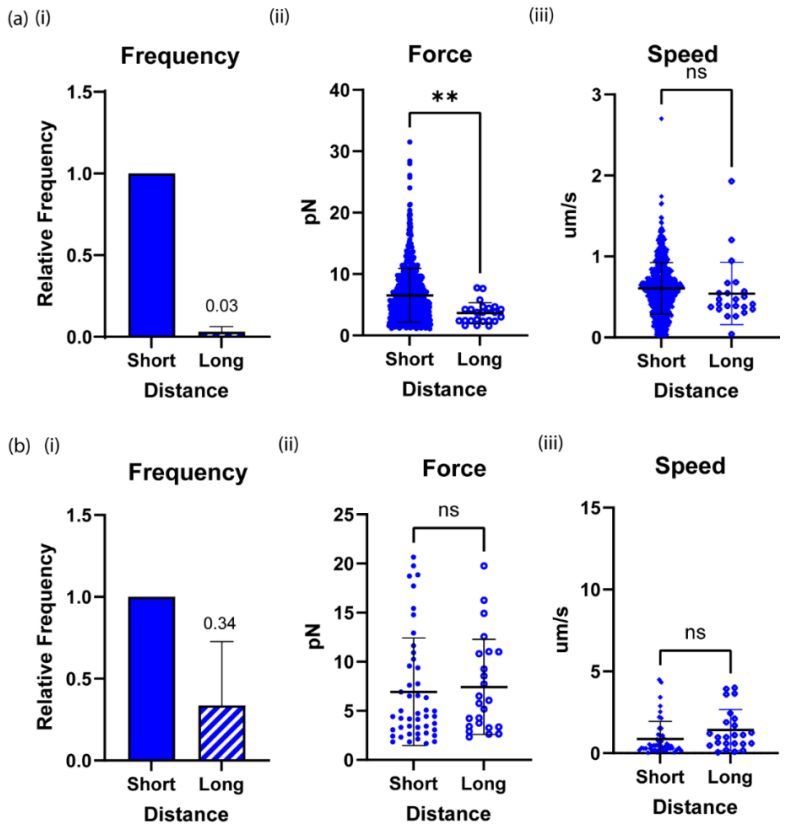


*Figure 4.32 Detailed profile of MS11 ΔComP pili retraction event on (a) carboxylated beads coated betapillar and (b) DUS-DNA coated betapillar: (i) The relative frequency between short and long pili retraction events (ii) The force profile between short and long*

After that, we proceed to compare the distance analysis between strains. We separated the same data pool to compare MS11 and ΔPilV (Figure 4.33) and then between MS11, ΔPilV, and ΔComP (Figure 4.34). There is no scientific reason for this separation except that it makes visualising the analysis easier. Overall, it is safe to say that if there is any difference in significance among the pool of pili events between the strains, they are primarily **short-distance** pili retraction events. This observation suggests some regulations on the pili mechanics in the cell, which might be altered in the mutants. It is also interesting to note that given how **ΔPilV can take up more DNA yet we don't see any significant changes with their pili dynamics**.

### 4.3.3 PilE protein profile in ΔPilV

At this point, we understand that PilV, as a minor pilin, most probably affect a certain property of the Type IV Pili in *N. gonorrhoeae*. At the same time, we also suspect that removing PilV alters the periplasmic dynamics regarding DNA uptake. We could also assess the difference in Type IV Pili with ΔPilV, the PilE protein profile in ΔPilV strains. This is a simple investigation of the expression or localisation of the major pilin, PilE. Using our pili preparation protocol, we collected three different fractions: whole cell fraction, sheared pili fraction and cell pellet fraction. The cells were resuspended in CHES buffer and normalised based on $OD_{600}$. The representation of the location of the pili collected is illustrated in Figure 4.47.

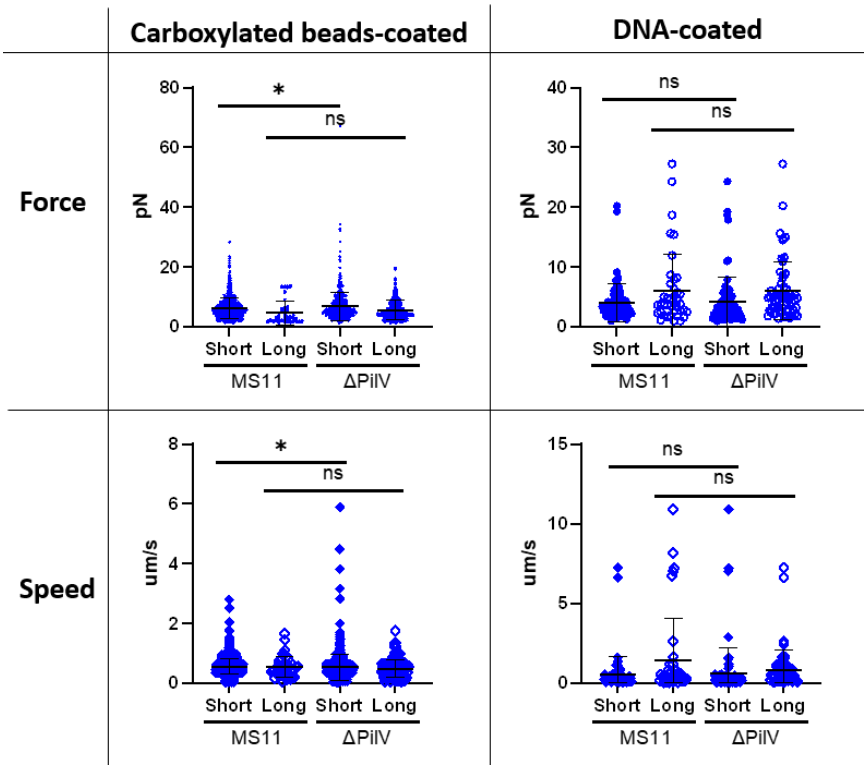


*Figure 4.33 Comparison between MS11 and ΔPilV for their pili retraction profile using distance analysis*

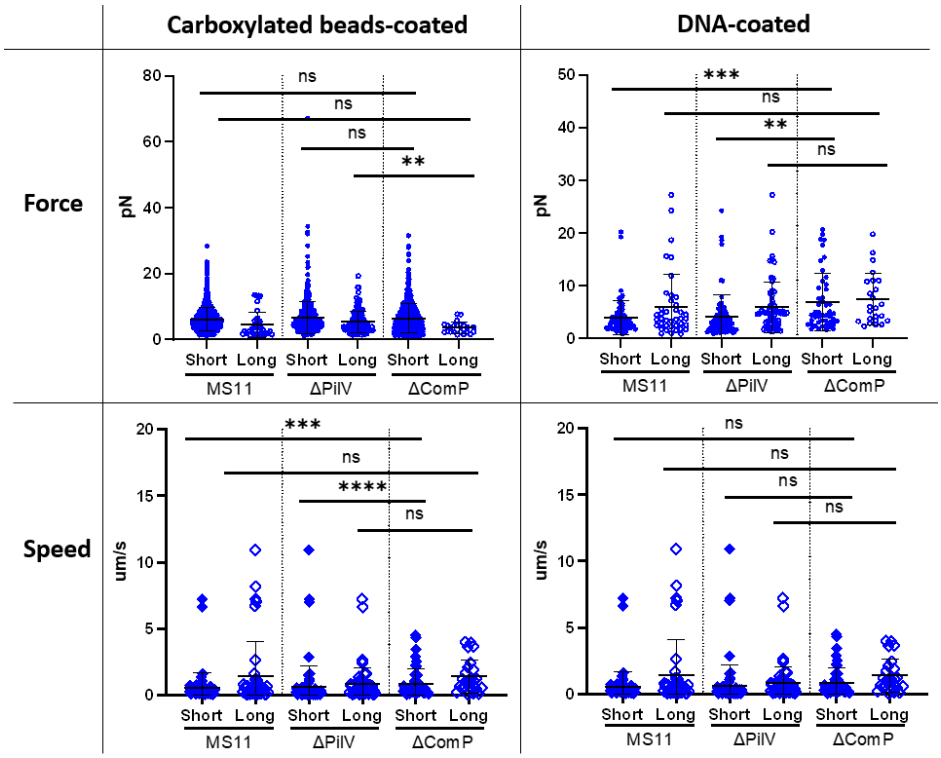


*Figure 4.34 Further comparison between MS11, ΔPilV, and ΔComP for their pili retraction profile using distance analysis*

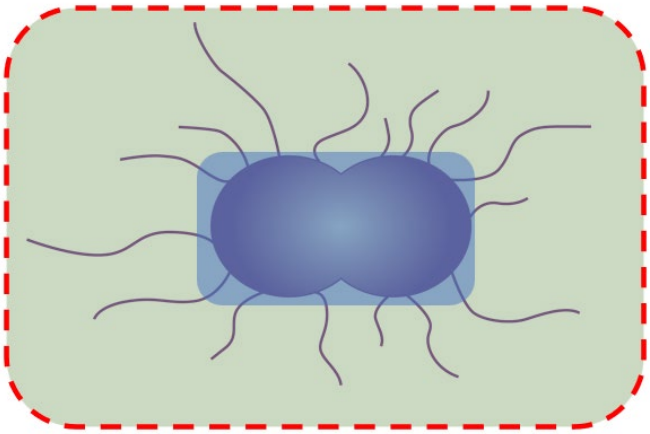

*Figure 4.35 Three different fractions are collected: whole cell (dashed red line region), sheared pili (green region), and cell pellet (blue region).*

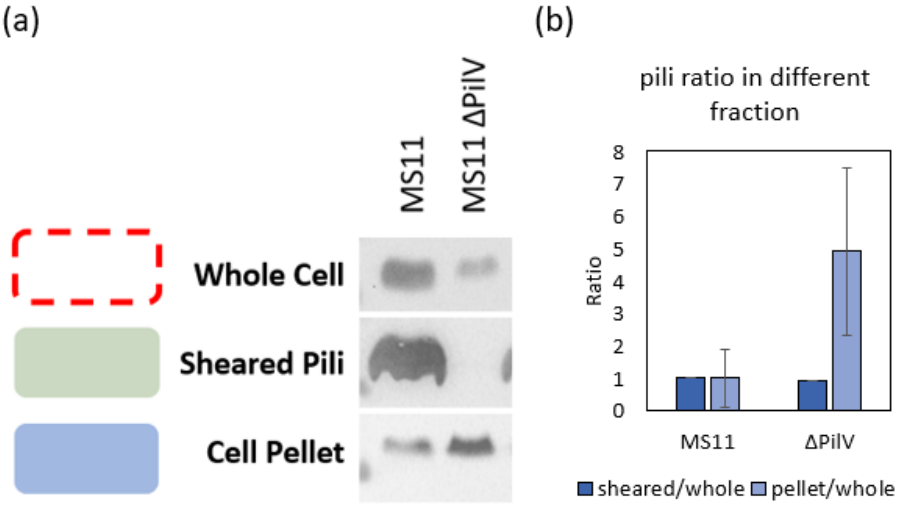


*Figure 4.36 (a) Western blot probing SM1 region of PilE in different samples collected from MS11 and MS11 ΔPilV and (b) its quantitative analysis. Quantitative analysis was taken from triplicate experiments.*

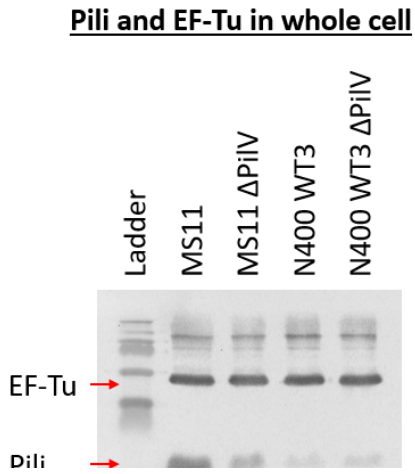


*Figure 4.37 Western blot probing for EF-Tu and SM1 (PilE) in parent strain and their PilV mutants*

After SDS-PAGE and western blot, we probe the blot with antibodies detecting the SM1 region of PilE. In this experiment, we saw a decrease in PilE in MS11 ΔPilV strain compared to MS11, as seen in the whole cell fraction. With this observation, it is expected that in the sheared pili fraction, MS11 ΔPilV also contains lesser PilE (Figure 4.36). However, when we look at the cell pellet fraction, we can see a similar or greater amount of PilE in MS11 ΔPilV. The similar or more amount of PilE in cell pellet fraction varies in repeats, probably due to the stability of PilE during sample preparation. To ensure reproducibility and significance, we quantify the sheared/whole PilE ratio and cell

pellet/whole PilE ratio. From this observation, it is interesting that removing PilV alone leads to a lower PilE. PilV knockout could affect the PilE level through lower expression or higher degradation. Our current resources' experimental setup makes it difficult to conclude which pathway was involved. To further prove that the expression of PilE in the whole cell was true, we also probed for EF-Tu as a loading control (Figure 4.37).

This result suggests that removing PilV can affect either PilE expression or stability. Not only that, this is also one of the results that hinted at the possible role of PilV as a PilE trafficker, either directly or indirectly.

### 4.3.4 PilE mutation reveals possible PilV interaction

#### 4.3.4.1 ΔPilVs of PilE mutants do not aggregate

Our studies on DNA uptake and transformation in *N. gonorrhoeae* led us to discover the peculiar differences between ΔPilV and Wild Type. Our systematic characterisation of PilV eventually leads us to discover more of its role when we intend to visualise the pili activity of ΔPilV. In Chapter 3, we mentioned the PilE mutants, which allowed us to visualise Type IV Pili in their dynamic nature through fluorescence maleimide dye labelling. Our prior study brought us two successful strains, K9C and C7G, with N400 WT3 as background, that label well and behave like the Wild Type regarding growth and phenotype. We also reconstituted these mutations in a ΔG4 background, T132C and T138C. One of our main concerns with K9C and C7G is that these constructs removed potentially functional 3'-end sequences that were not known to be important during construction. It is reported that disruption to some of the DNA sequences at this site will lead to reduced PilE expression. While we showed in Section 3.2.3.2 that having less PilE expression in K9C and C7G helped with better visualisation, we did our studies in both constructs for comparison and cross-checking.

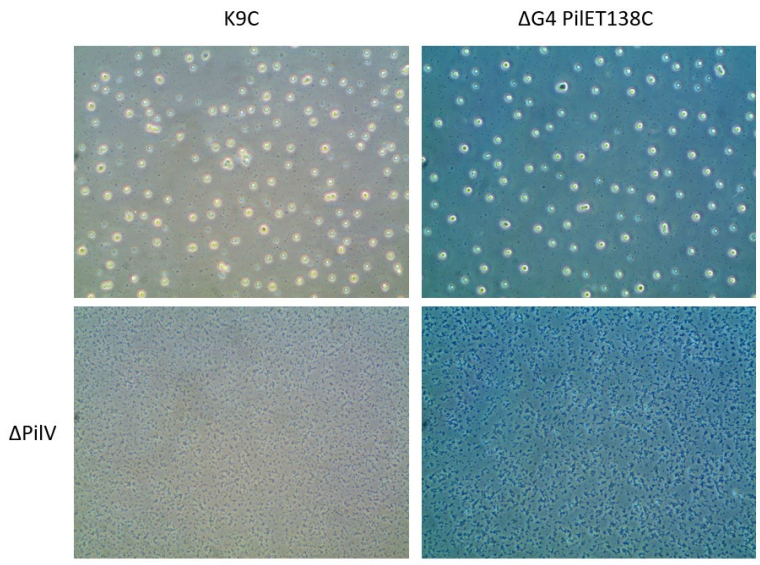


*Figure 4.38 Microcolony formation assay for PilE mutants K9C and ΔG4 PilET138C with their PilV mutants*

The microcolony assay is the first experiment that hinted at the potential of using PilE mutants to study PilV. Section 5.3.1.3 noted that ΔPilV microcolonies are more spaced than the Wild Type. Although this observation was peculiar, this only means that removing PilV affects pili function partially. In the following experiment, we will only show results from K9C and T138C (both are the same mutation in different genetic backgrounds). Though, we observed similar results in C7G and T132C. Our results showed that K9C and T138C do not differ from Wild Type regarding microcolony formation. However, when we removed PilV from these strains, their ability to aggregate was

obliterated (Figure 4.38). Even though we can see a slightly bigger aggregation in T138C than in K9C, none can form the signature microcolonies we observed in MS11 ΔPilV. The difference we observed in T138C and K9C was probably due to the different PilE expression levels in the two strains. The fact that the only difference between PilV mutants that aggregate and those that do not is the point mutations in PilE hinted that PilV function is closely linked to PilE. This result suggests that PilV could interact with PilE, which would affect pili functions.

### 4.3.4.2 ΔPilV of PilE mutants has flatter colonies

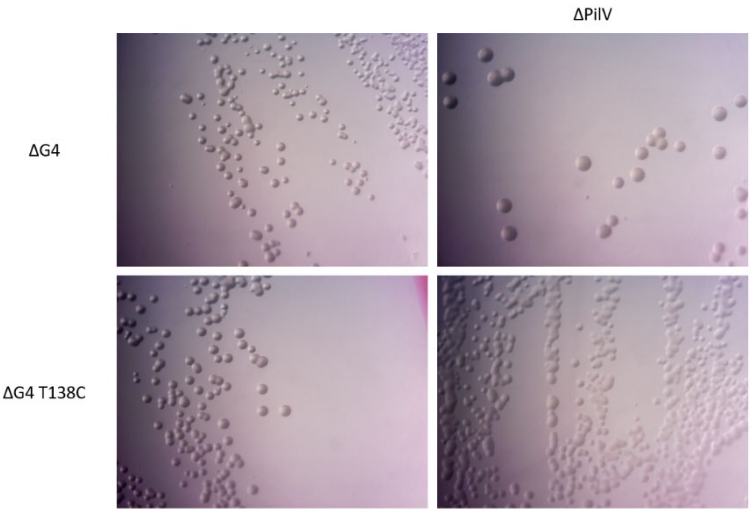


*Figure 4.39 Colony morphology of PilV mutants of ΔG4 and ΔG4 PilET138C*

We were curious to see if this seemingly 'loss-of-pili-function' we observed in the microcolony assay also means they present a colony morphology similar to strains that lose their pili functions. Typically, strains that lost pili function, for example, non-piliated colonies, have flatter colonies. In our case, we noted that MS11 ΔPilV colonies are flatter (Figure 4.39). This is roughly the same with ΔG4 ΔPilV. However, the extent of the flatness was greater in T138C ΔPilV. Nonetheless, neither colony morphology is similar to that of non-piliated colonies. This suggests that, for some reason, even though the pili function was severed, it is not totally annulled.

### 4.3.4.3 ΔPilVs of PilE mutants still have enhanced competence despite severed pili function

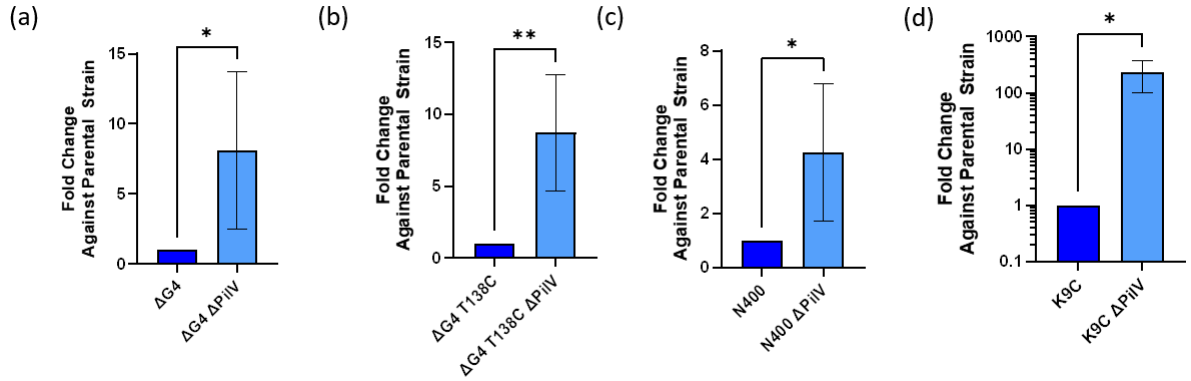


*Figure 4.40 Transformation efficiencies of ΔPilV and their parent strains in (a) ΔG4, (b) ΔG4 PilET138C, (c) N400, and (d) N400 K9C*

Another crucial consequence for *N. gonorrhoeae*, when they lose their pili function, is their competence. As we are probably familiar with by now throughout this thesis, Type IV Pili's involvement in DNA uptake is ineligible. When any assay for a mutant strain hints at a loss in pili function, for example, microcolony formation, it usually also means the mutants are

probably defective in taking up DNA. We are curious to see that ΔPilV enhanced competence still stands when their pili function is severely affected due to PilE mutation. Our study tested the transformation efficiency on ΔPilV variants of ΔG4, ΔG4 PilET138C, N400, and N400 K9C. Interestingly, their ΔPilVs showed enhanced competence in all cases despite what we observed in other assays (Figure 4.40). Note that in N400 K9C, the significant increase in competence may rely more on the induction of IPTG for the RecA level. This result is also interesting because it shows that more tests should be taken into account to assess pili function and competence: loss of microcolony formation ability does not equal total loss of pili function and also does not equal loss of competence.

#### 4.3.4.4 ΔPilVs of PilE mutants take up more DNA

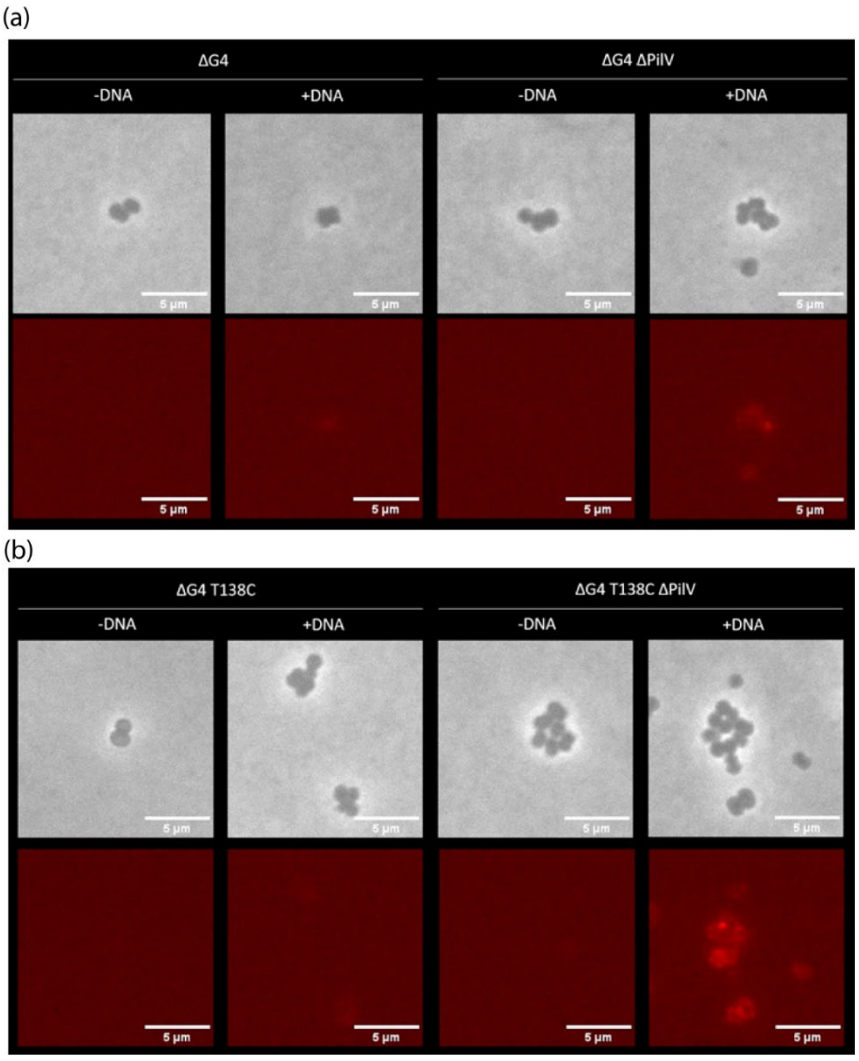


*Figure 4.41 Cell cluster observation for DNA uptake assay in ΔPilV of (a) ΔG4 and (b) T138C*

In conjunction with what we observed in DNA transformation, we wondered if this observation would be consistent with DNA uptake. We performed a similar DNA uptake assay on ΔG4 and T138C and their ΔPilV variants. Before performing any analysis, we observed the uptake phenotype through images. Our first perception confirmed that ΔPilV mutants of both ΔG4 and T138C indeed have increased DNA uptake compared to their parent strain (Figure 4.41).

Interestingly, we also noted that the DNA uptake level seems higher in T138C ΔPilV. The same can be observed at each cell cluster (Figure 4.42). To ensure what we observed by eye is true, we performed image analysis on these data.

Our image analysis showed that what we observed by eye was correct. ΔPilV mutants consistently take up more DNA than their parent strain regardless of their PilE type (Figure 4.42). Moreover, the increase in DNA uptake for T138C ΔPilV compared to T138C is bigger than ΔG4 ΔPilV compared to ΔG4. Given that we know that T138C ΔPilV has a defective pili function in other tests, it is impressive to note that it not only does not affect its ΔPilV enhanced competence phenotype, but it is also still possible to take up more DNA.

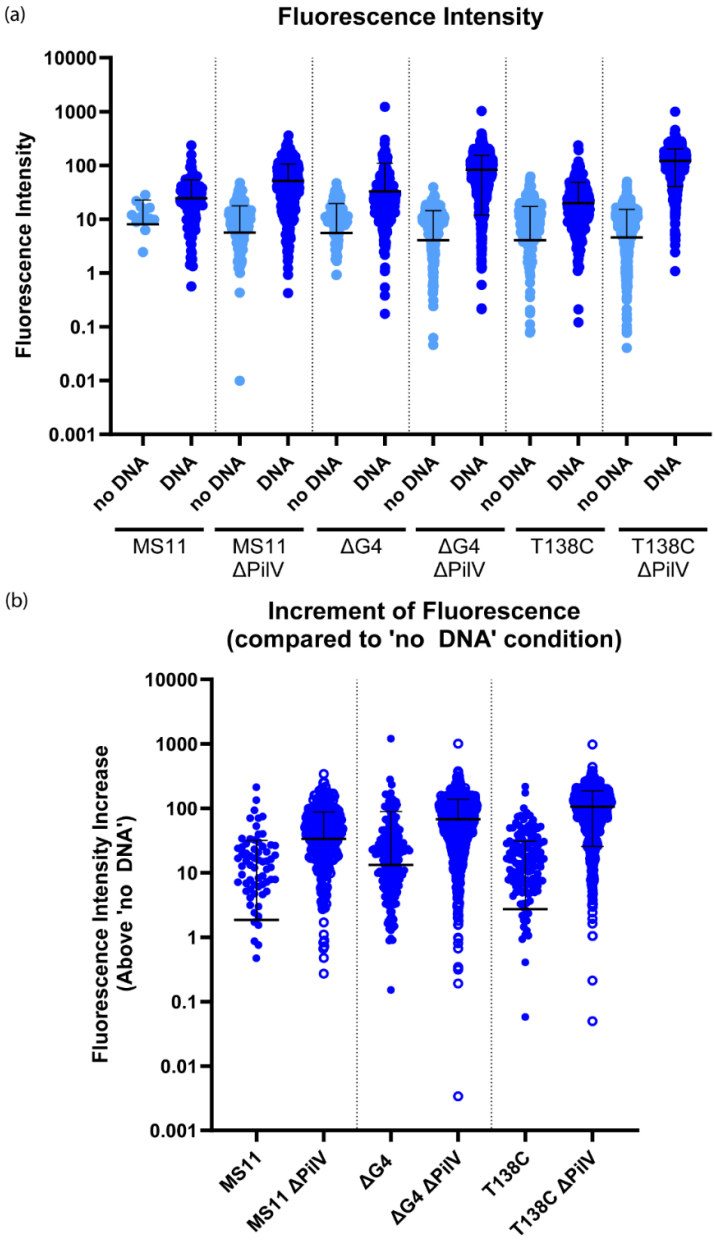


*Figure 4.42 Image analysis of DNA uptake assay for ΔG4 and T138C and their ΔPilV mutants: (a) fluorescence intensity and (b) intensity difference against 'noDNA'*

### 4.3.4.5 PilE protein profile of ΔPilVs of PilE mutants

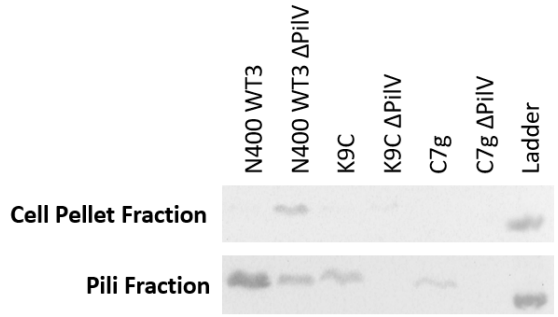


*Figure 4.43 Western blot probing PilE for K9C and C7G and their ΔPilV mutants*

Following up on all the information we gathered so far, it seems that despite the loss of pili function at forming microcolonies, ΔPilVs in PilE mutants did not differ much in phenotype in terms of DNA uptake and transformation. Next, we decided to investigate if we can observe the same trend in Wild Type in terms of the localisation of PilE. At first, we looked at the cysteine mutants constructed from N400, K9C and C7G and their ΔPilVs (Figure 4.43). Our western blot probing PilE showed a weak signal. We still see roughly the same trend in which the PilE level was reduced in ΔPilV in the whole cell and pili fraction. We also note the disproportionate accumulation of PilE in cell pellets in ΔPilV on top of the already low PilE level as a whole. However, this blot also shows how PilE expression is affected in K9C and C7G due to the perturbation at the 3'-end of the *pilE* gene. To ensure what we observe is consistent and related to ΔPilV, we tried the cysteine mutants constructed on ΔG4.

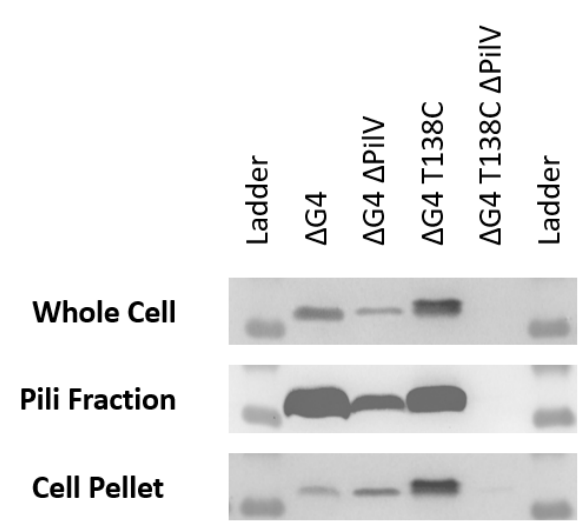


*Figure 4.44 Western blot probing PilE for ΔG4 and ΔG4 PilET138C and their ΔPilV strains*

Our blot with strains constructed on ΔG4 showed a good PilE level comparable to that of MS11 (Figure 4.44). We can note that the PilE level in ΔG4 T138C is comparable to ΔG4. What is worth noting is that we can start to see incomplete processing of PilE in ΔG4 T138C with the extra larger band. In ΔG4 ΔPilV, we observed the same pattern as in MS11 ΔPilV. In ΔG4 T138C ΔPilV, we note that the overall PilE level was severely affected. We also tried to reverse what we observed in an IPTG-inducible system, but our current construct was leaky; hence, we could not make any concrete advancement through that experiment. Nonetheless, given the low level of PilE (almost undetected), we still see some signal at the cell pellet fraction. This strengthens our hypothesis that PilV plays a significant role in localising PilE and shuttling PilE into the pili.

### 4.3.4.6 Pili retraction behaviour of ΔPilV of PilE mutants

When we tried to inspect how the cysteine mutant and its ΔPilV change their pili dynamics, we used carboxylated beads-coated micropillars to examine the difference. In T138C, we recorded pili retractions comparable to the Wild Type. This is something reported before by Kan et al.(unpublished) in K9C and C7G. In T138C, we still see the same thing, knowing that the different amounts of PilE do not contribute to the mechanical properties of pili retraction in

these strains. Perhaps they might contribute to different frequencies of pili retractions, but this will require further investigation. In T138C ΔPilV, as expected, we did not see the aggregation into microcolonies (Figure 4.45).

On top of that, T138C ΔPilV also does not record any pili retractions. This is interesting because we could see the bacteria cells attaching and settling on micropillars, meaning some minimal binding is available on the cell surface or any available pili. Even in Section 4.3.2.2, we note that ΔPilV and its combination mutants in MS11 background still can record some pili retractions. These results suggest that removing PilV aggravated pili biogenesis when presented with the PilE point mutation. The lack of pili retraction also aligns very well with our western blot result of reduced PilE level.

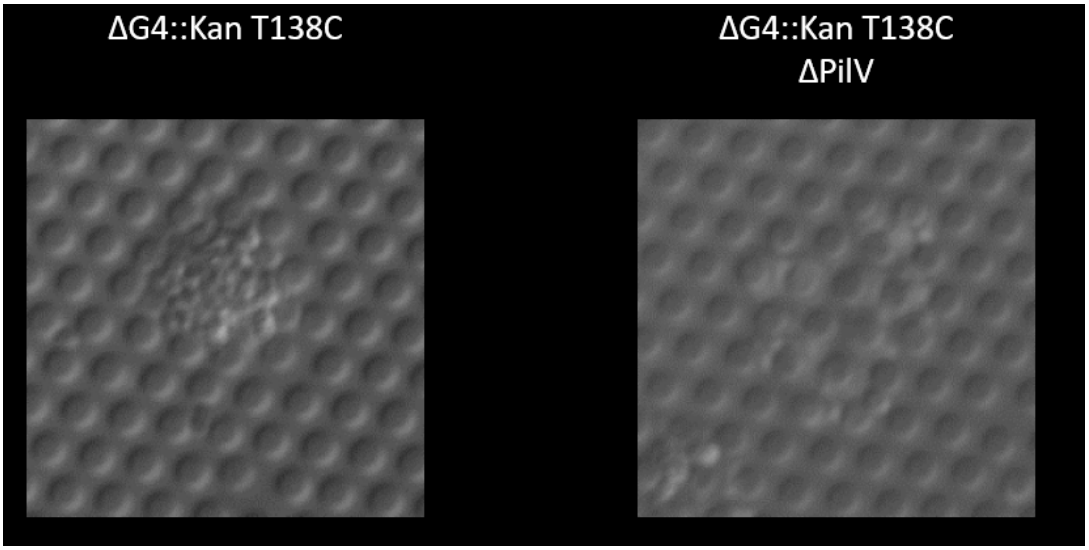


*Figure 4.45 T138C and T138C ΔPilV on micropillars*

#### 4.3.4.7 Pili labelling reveals the importance of short pili

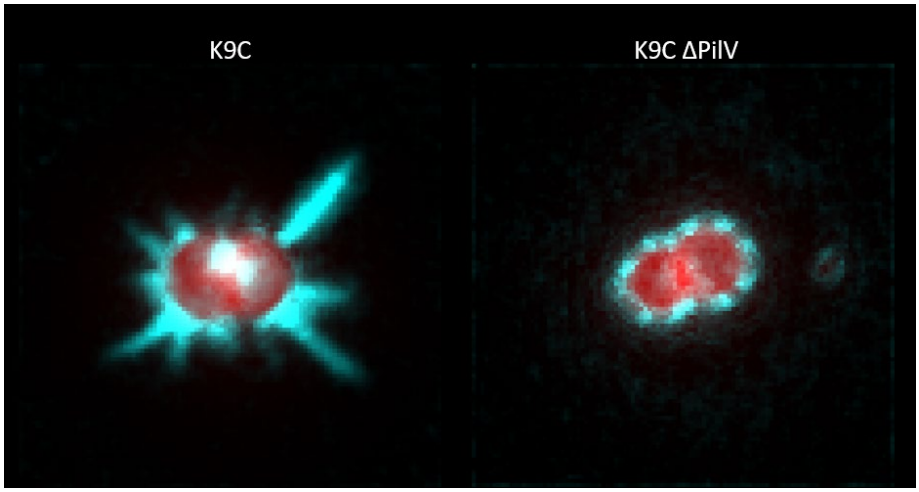


*Figure 4.46 Summary of the most prominent pili activity in K9C and K9C ΔPilV*

With all the information at hand, we highly suspect that labelled pili for cysteine mutants and their ΔPilV strains will be informative. We tested on K9C, K9C ΔPilV, T138C, and T138C ΔPilV. We noticed that the image quality from T138C images was not great. This is largely

contributed by the larger amount of pili in ΔG4. In this case, we realise the reduced PilE level in K9C was, in fact, a blessing in disguise. By eye, we noticed that the pili activity in K9C/T138C is more active than in their ΔPilV. However, we will need further analysis to prove that.

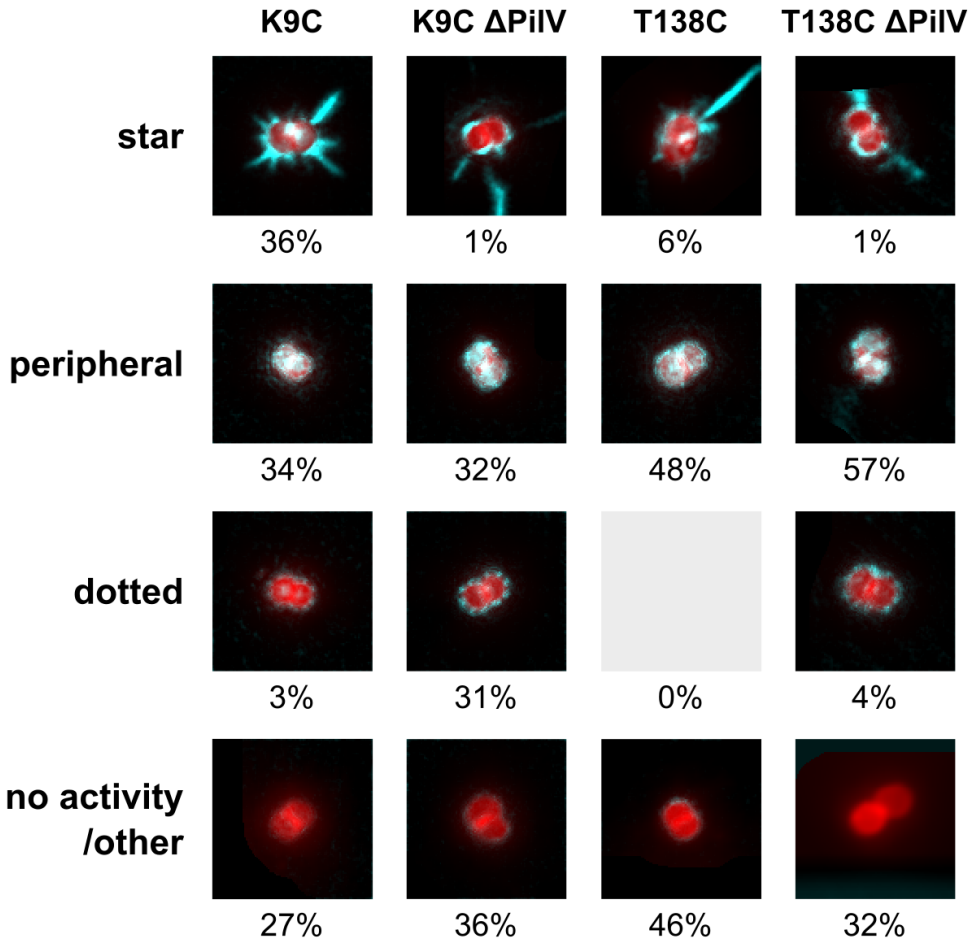


*Figure 4.47 Summarises the type of pili activities and their rough distribution in each strain. From the left column, we have K9C, K9C ΔPilV, 'kv' that is the same as K9C ΔPilV, T138C, and T138C ΔPilV*

With that, we did most of our detailed analysis in K9C and K9C ΔPilV. This pili activity analysis was done with the help of Raphaël Candelier. The change in pixel intensity over time was normalised against the standard deviation to define the amount of changes in intensity over time. Our image analysis is staggering because we summarised that in K9C, we observed more cells that presented nicely extending and retracting pili activity, represented by the sunshine-like spikes around the cell body (Figure 4.46). Whereas in K9C ΔPilV, more of the cells still have some pili activities, but the activity region is closer to the cell body, represented by the halo around the cell. Interestingly, these activities near the cell body also tend to occur at specific points, shown as dots around the cell body. When we map the proportion of cells in our image data set that present different pili activities, we note there is a consistent 'peripheral' activity (Figure 4.47). The major change we notice between K9C/T138C and their ΔPilV is the drop in 'star' activity and the increase in 'dotted' activities.

This result is significant as it is one of the first glimpses into regulating Type IV Pili in *N. gonorrhoeae*. The drop in average pili length in K9C/T138C ΔPilV led to shorter pili activities. The fact that these strains still have enhanced competence proved that these short pili are sufficient to support and even result in enhanced competence. With that, it is possible that perhaps short pili are more efficient in DNA uptake than long pili. This also opens the question that long pili could either not be that efficient in DNA uptake or more on facilitating in bringing DNA molecules closer to the cell body that uptake. The observation of 'dotted' activity was also possibly observable when the pili were short compared to in 'star' activity. There are few possibilities that the pili activities accumulate as dots. When the pili is short, it might lead to a higher turnover of PilE shuttling into the pili. This activity could attract most of the PilE around the PilQ and hence show specific high-activity regions. The other possibility is that the PilQs that are active are somehow stochastically spaced, and not all of them are active simultaneously. This is hypothesised due to the rough estimation of active dots being lower than the reported concentration of PilQ on the *N. gonorrhoeae* cell surface.

### 4.3.5 Structural predictions of PilV and Type IV Pili

Thanks to the findings from multiple assays and also the aid of PilE cysteine mutants, we unravel some interesting roles of PilV. However, there are still details about PilV and its involvement with pili biogenesis that we cannot pinpoint for several reasons. These reasons can be due to a lack of time, resources and expertise. Another way we decided to attempt before concluding our study is to explore predictions and build a hypothetical model for the convenience of future researchers. In this case, we turned to one of the popular open-source resources available during this study, Alpha Fold.

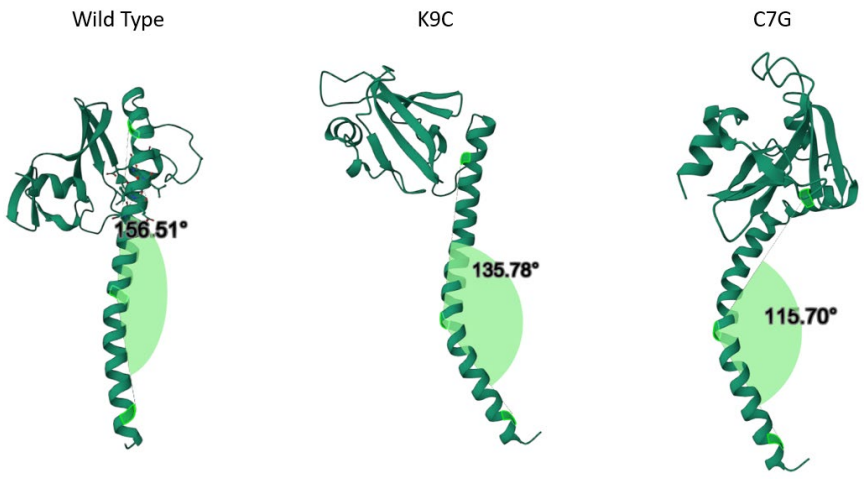


*Figure 4.48 Measurement of alpha helix hydrophobic region in PilE of Wild Type, K9C, and C7G*

We venture this artificial intelligence program with basic parameters for this particular study. Even though AlphaFold might not always predict the correct protein structure, it can still provide us with valuable information about the relative structure and interaction between different proteins. This is exactly what our studies can provide while we fully understand the limitations of such an approach. Our studies show that although ΔPilV affects pili functions,

we observed varying degrees of severity to which the removal of PilI affects pili function depending on the genetic background (MS11 and our cysteine mutant strains K9C and C7G). The fact that one point mutation in PilE for these mutants is sufficient to exaggerate the influence of PilV shows that we might find a big difference between these mutants. To try to come up with an explanation, we predicted the structure of PilE in MS11, K9C and C7G. Since the structure of PilE is more or less known and understood through literature, AlphaFold will have enough prior information to predict the structure confidently.

In our prediction for PilE, we noticed that there were indeed some structural differences for K9C and C7G. The most obvious difference comes from the N-terminal alpha-helical transmembrane region. K9C and C7G seem to have bigger angle banding of helices compared to Wild Type PilE (Figure 4.48). To measure quantitatively the bending, we selected three amino acids along the alpha helix structure and measured the angle between them (Figure 4.63). Our measurement showed the severity of bending is higher in C7G (Figure 4.64). This prediction seems promising since we see a similar trend in PilE expression in these mutants in Section 4.3.4.5.

Further, we decided to investigate how these structural differences interact with PilV since these ΔPilV mutants of these PilE mutants showed a severed pili function compared to the Wild Type. To investigate that, we utilised the multimer prediction option in AlphaFold. Given the structural differences between the point mutation PilE mutants, when predicted as multimer with PilV, they have similar structural predictions as the wild-type PilE. We can see from the prediction that the N-terminal alpha-helical transmembrane region aligned well with those of PilVs in all three cases (Figure 4.49).

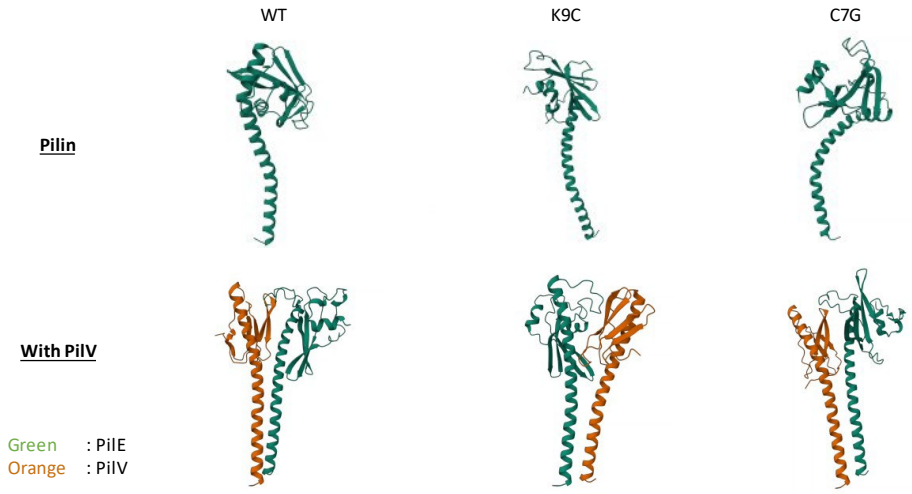


*Figure 4.49 AlphaFold prediction of PilE protein in Wild Type, K9C (T138C), and C7G (T132C), and multimer prediction of respective PilE with PilV protein*

This result suggests that if these predictions are right, the point mutations we introduced to PilE affected the PilE protein's tertiary structure, especially in the N-terminal hydrophobic region. This might mean that this change can affect the embedding or the mobility of PilE in the membrane. The fact that the prediction with PilV showed good alignment between the two

probably means PilE and PilV are good at interacting with each other, and this interaction may be useful for some pathways. Please note that when predicted with other minor pilin, ComP, major and minor pilins can also align pretty well, except for PilC. We should also note that what was known in the literature about pilin-pilin interaction is that pilin-pilin interaction in the pili is, in fact, not totally symmetrical. A study in *N. meningitidis* finds that after processing, the N-terminal end of a second pilin will interact at the 5$^{th}$ Glutamic acid (Glu5) of the first pilin subunit [152]. With that, if any interaction that we expect, such as that in Figure 1.65, occurs, it should occur while the pilins are embedded in the membrane.

### 4.3.6 Hypothetical model

With the information we obtained from experimental data and structural prediction, we gathered some insights and formulated a hypothetical model of the role of PilV. We proposed a model in which PilE interacts with PilV prior to Type IV Pili biogenesis. This is based on our microcolony formation experiment and PilE localisation check results. To recap, PilE mutants, C7G and K9C, with one point mutation in PilE, show an aggravated microcolony formation defect when PilV was removed. The fact that these mutants behaved like wild type before the removal of PilV shows that the effect from point mutation exaggerated the impact of ΔPilV. On top of that, we gathered that ΔPilV has a reduced pili function and yet takes up more DNA. This means that PilV plays a role in pili biogenesis, though not essential. The understanding of how it takes up more DNA will be discussed further. The fact that ΔPilV has the same DNA uptake and transformation dynamics yet takes up more DNA and produces more positive transformants hinted that in ΔPilV, the extraneous amount of DNA taken up may have been stored and subsequently transported into the cytoplasm for integration across generations.

Using all the information we gathered, we proposed the following model:

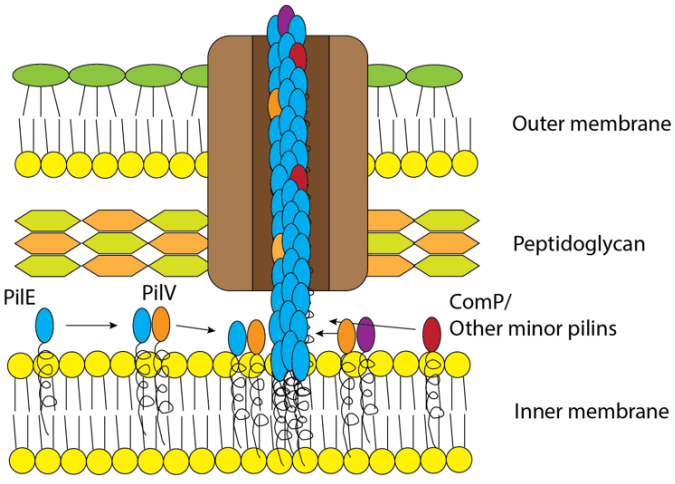


*Figure 4.50 Hypothetical model of pilin-pilin interaction in Wild Type*

In **Wild Type** (Figure 4.50), PilE and PilV most probably interact before Type IV Pili assembly. During Type IV Pili assembly or biogenesis, PilV-PilE interaction may facilitate the shuttling of PilE into the pili more efficiently. Therefore, without PilV, pili functions are severed but not nullified. At the same time, other minor pilins may not necessarily need to interact with PilV for assembly; therefore, assemble into the pili occasionally. The regulation of major/minor pilin composition in Type IV Pili and the mechanism of action of PilV-PilE interaction are still a mystery and are beyond this laboratory's expertise.

To strengthen this model, studies are showing that ΔPilV mutants showed a different PilE modification population in *Neisseria gonorrhoeae*. The study hypothesised that PilV is probably the minor pilin that brings PilE close to the necessary enzyme to modify PilE properly. In Wild Type, the study found a higher population of PilE modified with phosphoethanolamine (PE), while in ΔPilV, there was a higher population of phosphocholine (PC)-modified PilE instead[160–162]. They hypothesised that such different PilE modifications could play a role in PilE localisation in *N. gonorrhoeae*. These hypotheses fit nicely with our observations.

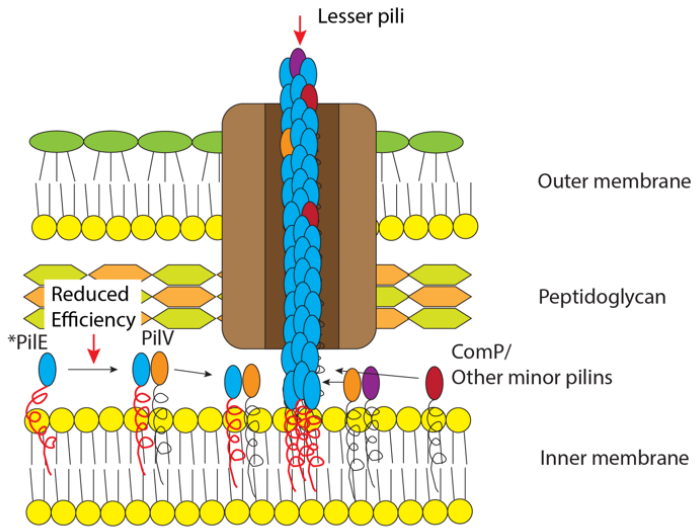


*Figure 4.51 Hypothetical model of pilin-pilin interaction in Pilin mutants*

In our study, we are lucky to chance upon mutants that revealed the importance of PilV through **PilE mutants**. We observed that introducing point mutations in PilE does not present any obvious phenotypic change. However, when the point mutation is present with ΔPilV, the pili functions are greatly affected. Through our structural predictions of wild-type and mutant PilE, we understood that given the mutations were introduced near the 'lollipop' protein-protein interaction domain, there was an effect on the hydrophobic alpha helix structures. This could have meant that PilE mutants may have a problem embedding into the inner membrane. However, our pili mutant ΔG4 T138C shows that this should not be the case. ΔG4 T138C did not significantly reduce PilE at the pili fraction unless ΔPilV is introduced. With that, although we might not be able to quantitatively show any effect in the embedding of PilE in PilE mutants, we can be sure that it does not cause any significant problem. Given the multimer prediction between PilE and PilV, it seems that these two pilins can interact very well with each other and even structurally correct the defects in mutant PilE. With that, we proposed that they could still interact due to the interaction between PilE and PilV, albeit the structural difference in mutant PilE (Figure 4.51). The possible trade-off could be that in mutant PilE, more energy is needed to sustain these interactions, leading to reduced efficiency. However, there was no significant aggravation in pilin function since PilE and PilV can interact despite the structural differences.

In **ΔPilV mutants**, there are two cases: (i) in wild-type background and (ii) in PilE mutants.

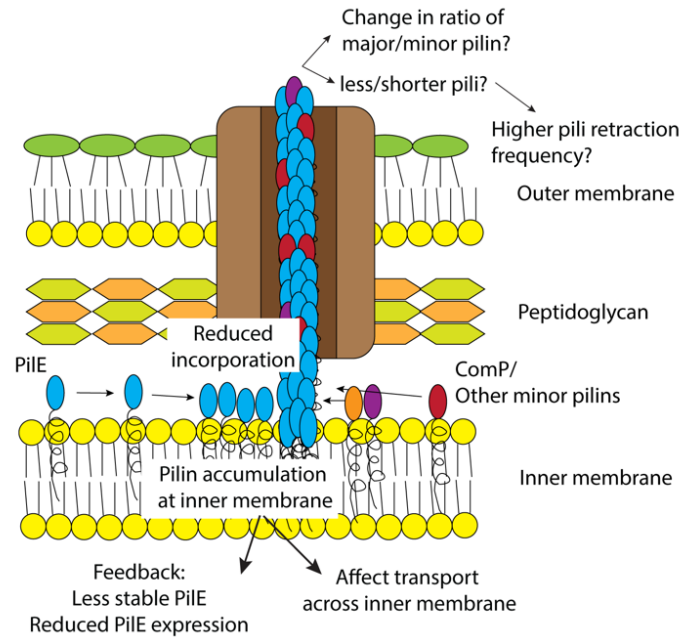


*Figure 4.52 Hypothetical model of pilin-pilin interaction in ΔPilV with wild-type PilE*

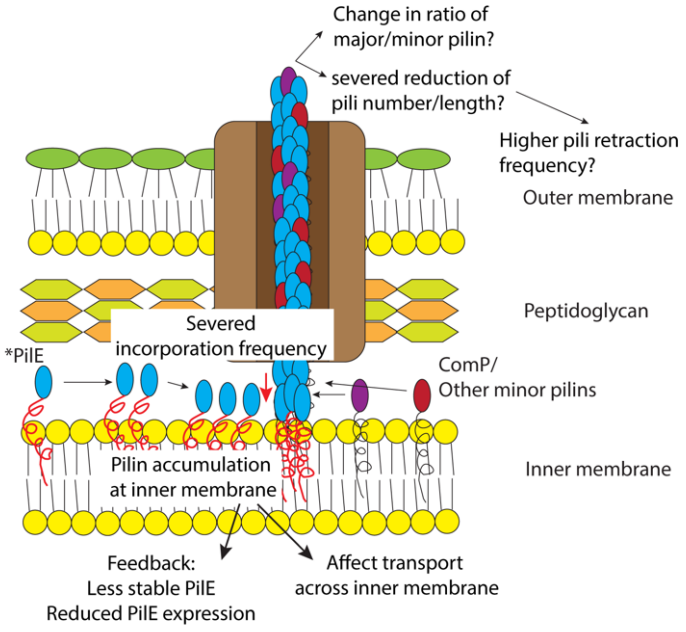


*Figure 4.53 Hypothetical model of pilin-pilin interaction in ΔPilV with mutant PilE*

In **wild-type background strains** (Figure 4.52), there was no PilV for PilE to interact. Such lack of interactions may lead to different modifications of PilE or localisation of PilE. Therefore, even though there were still residual pili functions, most of the PilE were not successfully shuttled into Type IV Pili. This might lead to crowding of PilE in the inner membrane. Not only that, such crowding may also lead to lower PilE in cell pellet fraction through these possibilities: (i) negative feedback loop on PilE expression, (ii) instability of excess or 'wrongly-modified' PilE, or (iii) higher degradation of excessive PilE.

In the **PilE mutant's background** (Figure 4.53), the severity of ΔPilV was aggravated since the neutralising effect of PilE-PilV interaction on mutant PilE does not exist anymore. With that, mutant PilE could not incorporate effectively into Type IV Pili. Not only that, in both cases, we observed that ΔPilV has enhanced competence, both in DNA uptake and transformation. In our model, we proposed a few mechanisms to explain this. First, the reduced efficiency in PilE incorporation into Type IV Pili in the absence of PilV may provide a higher chance for other minor pilins to be incorporated into Type IV Pili. Since there is a study that shows that the effect of ΔComP overrides ΔPilV [164], and in our results, we also observed the same thing. This means that not all pilin interacts similarly to PilV as in PilE. In ΔPilV, the incorporation of PilE may be reduced compared to other minor pilins. With that, other minor pilins might have a stronger binding preference to DNA molecules, for example, ComP, that are shuttled into Type IV Pili. A higher ratio of another minor pilin might change the way Type IV Pili binds to the substrate, leading to a higher uptake of DNA. Second, our experiments showed that pili retraction dynamics in

ΔPilV tend towards higher frequency simultaneously. Although a more detailed investigation entails, this also provides an insight into the relationship between pili biogenesis and its function. We hypothesised that since ΔPilV may have reduced efficiency in incorporating PilE, the major pilin, into Type IV Pili, it may change the regulation of pili biogenesis. With such a higher frequency of pili retraction, it makes sense that it will also create more opportunities to pick up more DNA molecules from the extracellular environment. This is especially useful especially if the pili formed in ΔPilV tend to be shorter. Hence, the cycle of taking up DNA molecules will be faster, too.

## 4.4 Discussion

In this chapter, we initially intended to use ΔPilV to study DNA transformation in *N. gonorrhoeae.* Despite the limited studies and understanding of the role of PilV in Type IV Pili and *N. gonorrhoeae*, ΔPilV has been constantly used as a strain in DNA uptake studies due to its enhanced competence phenotype. While we proceeded with our DNA transformation study, we cautiously characterised ΔPilV simultaneously.

During characterization, we found that although ΔPilV **does not remove pili functions entirely**, it shows some phenotypes hinting at a slight alteration in the Type IV Pili function. ΔPilV has flatter colonies on agar plates and aggregates differently from the Wild Type. Nonetheless, these potential reductions in pili functions did not prevent ΔPilV from having the enhanced competence phenotype.

Consistent with the literature, ΔPilV **transforms DNA better and takes up more DNA** than their parent strains. Since there is a potential discrepancy between enhanced competence and DNA uptake, we break down the process by comparing two methods to study DNA uptake and successful DNA transformation. Using these protocols, we discovered that the Wild Type and ΔPilV showed **similar DNA uptake and transformation dynamics**. During DNA uptake, ΔPilV takes up more DNA than the Wild Type, but similar to the Wild Type, the increase in DNA signal in the cell quickly plateau after 1h. Wild Type and ΔPilV showed similar positive transformants for the first two hours of incubation with DNA molecules in the DNA transformation. In summary, the most efficient DNA transformation or uptake in retrospect to time occurs **within the first hour** in contact with the DNA molecule. However, the enhanced competence phenotype we saw in ΔPilV only surface at later times showing a continuing incorporation of DNA.

In most cases, one successful recombination will allow the bacteria to become a positive transformant. Given that both MS11 and ΔPilV do not differ significantly with their doubling time, taking up more DNA does not exactly explain why, as a population, ΔPilV will have more percentage of positive transformants after a longer period. This result suggests a **subsequent import and recombination of DNA from the excess DNA taken up by ΔPilV**. Our DNA localization study strengthened this hypothesis. We observed that DNA molecules in ΔPilV tend to localize longer at the periplasm of the cell and septa area. It seems that **periplasm has coincidentally acted as a DNA reservoir** for subsequent DNA transformation later in cell life

or cell division. Our DNA localization study also showed some interesting observations, such as possible **retraction-independent DNA uptake in ΔPilE** and the **secretion of DNA molecules** into the extracellular environment in our experiment setting.

We also characterized the ΔPilV pili retraction profile using micropillars. On our micropillar system, we observed **two populations of pili retraction** events, "Long-distance" and "Short-distance". This observation is an excellent callback to our observation of two types of Type IV Pili on *N. gonorrhoeae* with labelled pili in Chapter 3. Our pili retraction profiles showed that **DNA-interacting pili retractions are generally slower and weaker than** those interacting with carboxylated beads. The difference between MS11, ΔPilV and ΔComP also tends to be more significant at the "Short-distance" pili events. ΔPilV also seems to have a higher proportion of "Long-stance" pili retraction, which we suspect was due to ΔPilV being also reported to reduce its adhesion ability. As a whole, however, the differences did not result in drastic changes in the pili dynamics. This could be because minor pilin constitutes a small portion of the Type IV Pili polymer. Next, when we probe how ΔPilV affects PilE, we found that PilV most likely plays **a role in trafficking PilE**. We noticed a drop in PilE detected in ΔPilV, possibly due to possible downregulation of PilE expression or degradation of PilE. On top of that, most of the PilE in ΔPilV did not make it into the pili fraction.

Our understanding on PilV became more concrete when we discovered our PilE cysteine mutants showed aggravated loss of pili function with a ΔPilV background. This proves that **PilE most likely interact with PilV** either directly or indirectly. Interestingly, although our PilE mutant with ΔPilV showed deteriorated pili function in microcolony formation and pili retraction, that did not affect their enhanced competence phenotype**. Regardless of the mutation on PilE, their ΔPilVs still take up more DNA and transform better than their parent strain**. This observation goes against the common metric we used to assess pili function: good microcolony formation equals good pili function and good competence. This observation will be a great reminder that it is important to assess a few aspects of Type IV Pili before concluding their pili functions, and these functions could well be decoupled under certain circumstances. When we labelled the pili for these mutants, we observed a significantly lower population of ΔPilV with long pili. **Most pili activities on PilE mutant ΔPilV stay near the cell surface**. Literature shows that ΔPilV also changes the posttranslational modification landscape of PilE, suggesting that this alteration might lead to pili instability or PilE localization[317]. This alignment with others' findings gave our hypothesis more confidence in formulating a hypothetical model. Our AlphaFold prediction suggested that PilE-PilV interaction may be able to counter the structural defect caused by the point mutation in PilE. Thus, we proposed a **hypothetical model** on the role of PilV in pili biogenesis and how it leads to enhanced DNA uptake.

In this chapter, we discovered a plethora of exciting information about Type IV Pili. The fact that we realize that **short surface pili in Type IV Pili are enough to enhance DNA uptake** means that the long pili most likely play a much different role. It also makes sense that short pili is more efficient for DNA uptake. Short pili also means that the pili's turnover is higher, probably leading to a higher chance of pulling DNA molecules into the cell body. The

interesting thing about this discovery is that in other systems with competence pili, their competence pili are usually short and near the cell surface[114,276,312,318–321]. Our findings showed that the discovery of short pili and their efficiency in DNA uptake may not be a coincidence but a successful evolutionary result.

# Chapter 5 : Type IV Pili and associated proteins (II)

## 5.1 PilC C-terminal peptide and its structural importance in PilC-dependent T4P biogenesis

### 5.1.1 Background and Motivation

Given its tight relation with the T4P function, competence should be an aspect where PilC could play an important role. Peculiarly, this is one of the lesser-studied aspects of PilC. Thus far, its involvement was proven when expression of PilC2 in trans or the addition of purified PilC could rescue DNA uptake deficiency in PilC1 PilC2 double mutant in *N. gonorrhoeae*[167]. As expected, piliation is essential in tandem with PilC for competence[167]. Given this observation, we know PilC is part of the mechanism resulting in competence, yet no study could uncouple these two processes while studying it. Therefore, this facet of PilC is a knowledge gap, and more studies remain to be done to pursue this investigation.

### 5.1.2 Materials and Methods

#### 5.1.2.1 Strains used and culture conditions

Strains (both *Neisseria gonorrhoeae* and *Neisseria elongata*) used in this study can be found in the Bacteria Strains. We use a similar protocol to culture *N. gonorrhoeae* and *N. elongata*, as reported in Chapter 2.

#### 5.1.2.2 Peptide synthesis and preparation

The sequences of peptides were selected and sent to Proteomics, IBPS (Institut de Biologie Paris-Seine) for synthesis. The synthesised peptides were then prepared into stocks of 1mg/ml. Synthesised peptides used in this study:

Table 5.1 Peptides synthesised for this study and their respective peptide sequences

| Peptide | Peptide Sequence |
|---|---|
| **Gono** | CGIKRLSWREVFF |
| **Elong** | NSVRRISWREIF |
| **Meningo** | GMKRISWREVFF |
| **Sicca** | CGLQRISWRELFF |
| **Scrambled** | RIENSRVSIFWR |

#### 5.1.2.3 Aggregation Assay

Aggregation assay in *N. gonorrhoeae* was mentioned in Chapter 4. For *N. elongata,* 100ul of $OD_{600}$ of 0.4 ($5 \times 10^8$ CFU/ml) cells were used instead. For conditions with synthesised peptide, the synthesised peptide was added at 1:1000 dilution. After 3h (for *N. gonorrhoeae*) or 4h (for *N. elongata*), the culture was removed from the incubator and observed under a light microscope to observe the formation of microcolonies or aggregates.

#### 5.1.2.4 Competence Assay

Both *N. gonorrhoeae* and *N. elongata* used the same protocol. Liquid transformation similar to what was described in Chapter 2 was used as the competence assay in this study. The peptides are supplemented for the whole procedure until the selection part for the supplementation of synthesised peptides. The cell suspension was diluted into 5 10x dilutions for competence quantification and plated on non-selective and selective plates.

For competence assay on agar, Spot Transformation, similar to Chapter 2 was done by drying DNA and peptide (if needed) on the agar first, and then bacteria was spread on top of the dried spot. During selection, the growth on the spot was then spread on appropriate agar plates.

#### 5.1.2.5 SDS-Polyacrylamide Gel electrophoresis (SDS-PAGE), Western Blot and Detection

The procedure is described in Chapter 4. The only difference is we used α- Nel pilin rabbit polyclonal antibody (1:1000 in TBST) as the primary antibody and anti-rabbit (1:10000) horseradish peroxidase (HRP) antibody as the secondary antibody.

#### 5.1.2.6 Transmission Electron Microscopy

Cells were grown according to the protocol for aggregation assay. After 3h of growth, cells were gently flushed with pre-existing media to detach them from the bottom of the well. 10ul of cells were placed on a parafilm. Then, a cleaned grid was placed on the droplet for 5 minutes. After that, the grid was dabbed and placed onto a 1% glutaraldehyde solution for 5 min. The grid was then passed quickly in water, and excess fluid was removed with a soft paper towel. Then, the samples were coated with 1% uranyl acetate for 3 min. The grid with samples was then loaded into the Transmission Electron Microscope 200kV (2100HC, JEOL) for observation.

### 5.1.2 Results

#### 5.1.2.1 C-terminal peptide partially restores cell aggregation phenotype in ΔPilC mutant

Previous studies have shown the supply of purified PilC can restore the piliation and pili function in ΔPilC. In our study, we intend to investigate if the supplement of the C-terminal peptide of PilC is sufficient in restoring piliation in ΔPilC. One of the reasons that this study took place stems from valuable discussions between the lab and collaborator Vladimir Pelicic, from Laboratoire de Chimie Bactérienne (LCB), CNRS, Marseille. Prior studies and predictions suggest that there is an evolutionary relation between the C-terminal end of PilC and each *Neisserial* species. On top of that, since PilC is also known as adhesion, it is intriguing when one of the structural predictions showed PilC to match with the Type IV Pili biogenesis complex, PilH, PilI, PilJ, and PilK[322–324]. These studies set the foundation for this study.

Since *N. gonorrhoeae* has two copies of PilCs, of which each function and significance are unknown, we decided to perform most of our studies in *N. elongata*. Part of the reason also includes resource availability to perform experiments in facilities with the right Biosafety levels.

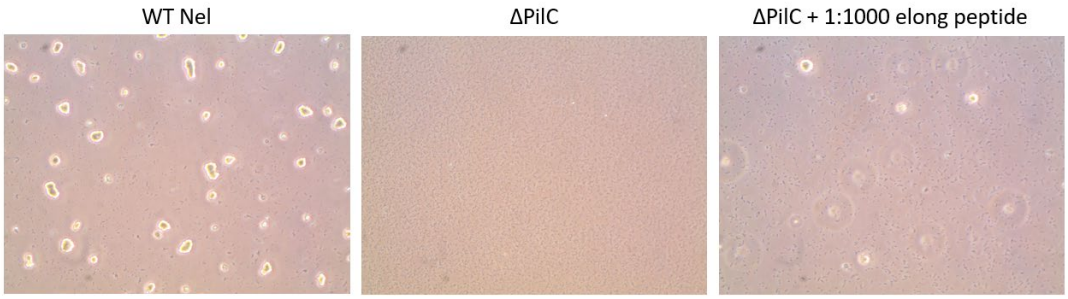


*Figure 5.1 External incubation of C-terminal peptides partially restores cell aggregation phenotype*

As we mentioned, microcolony formation has been used as an assessment for pili function in Chapter 4. We used the same test to assess pili functions in ΔPilC. Previous studies have reported the lack of pili observed in ΔPilC mutant, and only pili near the membrane was observed[179]. This could explain the lack of cell aggregation. To test if the C-terminal peptide of PilC is enough to restore this phenotype, we incubated ΔPilC mutant together with the C-terminal peptide. We have tested on separate experiments to ensure the peptides do not affect the survival of either wild type or ΔPilC mutant. In our study, we observed cell aggregation in the culture containing ΔPilC mutant and C-terminal peptide (Figure 5.1). However, we noted that the aggregation level restored by the C-terminal peptide is not on the same level as those of wild type. Since the cell aggregation phenotype is linked to the function of Type IV pili, this observation suggests the possibility of C-terminal peptides restoring the pili function. For the record, a similar observation has been made in our *N. gonorrhoeae* experiments.

### 5.1.2.2 C-terminal peptide restores competence in ΔPilC mutant in a dose-dependent manner

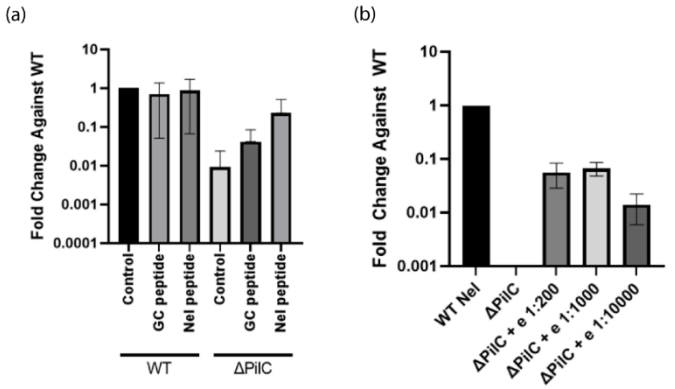


*Figure 5.2 (a)The addition of the C-terminal peptide of GC origin or Elong origin improves the competence of ΔPilC mutant (b) The effect of C-terminal peptide of Elong origin can restore the competence of ΔPilC mutant in a dose-dependent manner*

The other way we assess the restoration of pili function is through competence. Given what we learned in Chapter 5, this will complement our observation with aggregation assay. Literature reported that ΔPilC's competence was entirely nullified. In our study, we saw transformation efficiency in ΔPilC that is close to none or near the lower end of our detection. Its transformation efficiency is at least 2 logs lower than that of a wild type. In our study, we observe an improvement of competence when we incubate ΔPilC mutant with the C-terminal peptide of GC origin or Elong origin (Figure 5.2). The better improvement of the C-terminal peptide of *N. elongata* origin points towards the possibility of specificity or structural compatibility of the C-terminal peptide with the potential target. On top of that, when the concentration of C-terminal peptide is titrated, the effect is dose-dependent, saturating at around 1:200 dilution. This suggests that this peptide probably has a corresponding target, and all sites have been bound or interacted at a saturated concentration.

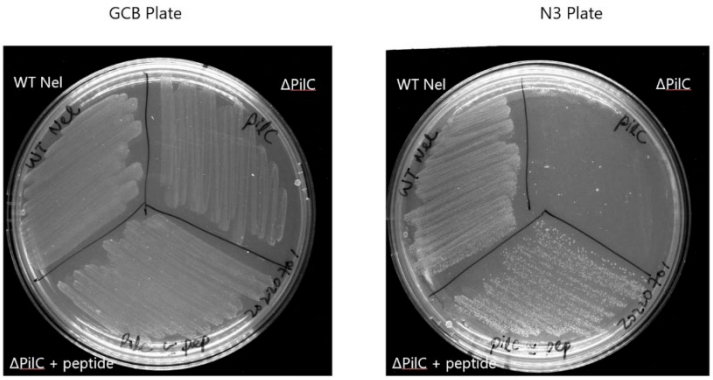


*Figure 5.3 Competence assay for ΔPilC and peptide supplementation on solid medium*

Next, we tested competence on a solid medium to strengthen our observation from previous experiments and remove the possibility of peptide aiding the diffusion of DNA molecules in a liquid medium. We did Spot Transformation with or without supplementation of peptide. After that, the growth was selected on appropriate agar plates, and we observed a noticeable improvement in transformation ability in ΔPilC supplemented with peptide, even in this transformation protocol (Figure 5.3).

### 5.1.2.3 There is sequence/structural specificity of C-terminal peptides in its effect

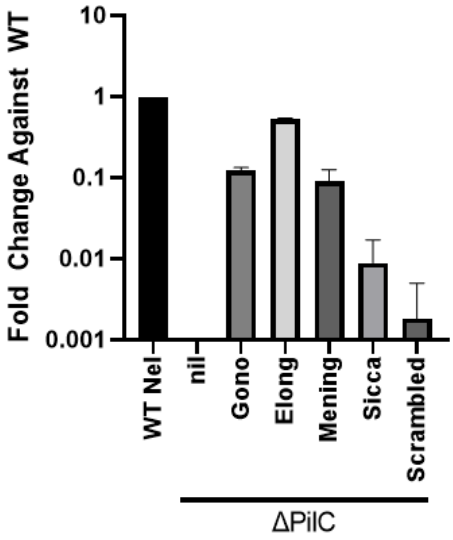


*Figure 5.4 The improvement of competence in ΔPilC mutant with C-terminal peptides of different species origins*

Since one of the earlier hypotheses that kickstarted this study was based on a structural prediction of PilC with the pili biogenesis complex, we wondered if the restoration of pili function and piliation can be sequence or structurally specific, especially based on PilC C-terminal peptide sequences from other Neisserial species. We synthesised peptides with the C-terminal sequence of PilC from a few species within the Neisseria family, *N. gonorrhoeae*, *N. elongata*, *N. meningitidis*, and *N. sicca*. We also included a randomly scrambled sequence from *N. gonorrhoeae* PilC as a control. With these synthesised peptides, we utilised a competence assay to study the effect of these peptides on the restoration of pili function in ΔPilC mutant since this assay is also quantitative. As expected, the peptide of *N. elongata* origin (labelled Elongata here) has the best effect on pili function restoration in Elongata ΔPilC (Figure 5.4). There are also different degrees of competence restoration among samples supplemented with different peptides. Next to peptides of Elongata origin, Gonorrhoeae and Meningitidis origin were second best in restoring competence. Peptides of Sicca origin fair the least among those from the *Neisseria* family, and the 'Scrambled' restored the least competence, slightly at the edge of detection.

We used AlphaFold to predict the structure of these peptide sequences (xxxv). It is worth noting that most of them share a similar structure when not predicted with any interacting molecule. Most of them are unstructured from the N-terminus and end with an alpha-helical structure neat to the C-terminus. This alpha-helical structure will be untangled in previous predictions and interact with the pili biogenesis complex. This prediction makes sense since these are all PilCs

from the same Type IV Pili system within the same bacteria family. Coincidentally, when we analyse the sequences through sequence alignment and their phylogenetic closeness (xxxvi), the pattern of closeness corresponds to how well these peptides restore competence. As shown in Fig 4b, other than 'Scrambled', the sequence from Elongata is closest to those of gonorrhoeae and meningitidis and furthest from Sicca. This observation strengthens the reasoning that the restoration of piliation most likely depends on sequence and structural specificity.

### 5.1.2.4 Supplementation of PilC C-terminal peptide restores Type IV Pili

With the results from all the experiments, it is obvious that the external peptide supplementation restores pili function defects in ΔPilC regarding cell aggregation and competence. However, we would like to know if these restorations resulted from the restoration of pili and, if yes, to what extent is the restoration. For that, we investigated the effect of peptide supplementation on pili protein. For that, we used two techniques: western blot and transmission electron microscopy.

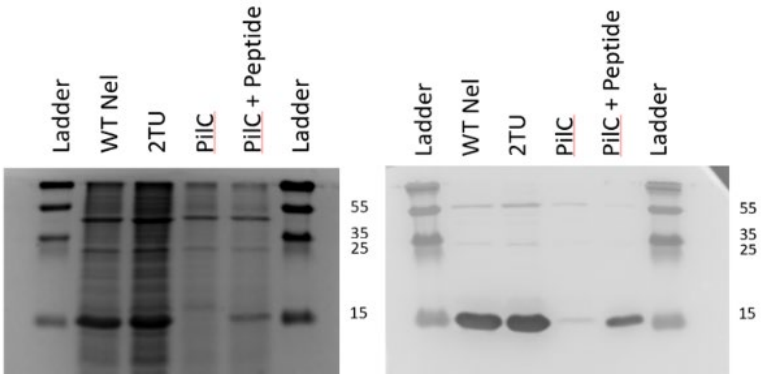


*Figure 5.5 Coomassie-stained gel (left) and western blot (right) probing Elongata pilin from liquid culture collected after four hours of incubation*

We first tested pili samples collected from growth on a solid medium supplemented with peptide for **western blot**. This is because this was the lab's sole protocol at that time. We realise it is difficult to get a consistent result because we noticed sometimes we can still detect traces of pilin protein in ΔPilC, and we could not see our hyperpiliated strain, 2TU, having a higher pilin level. Later on, we decided to develop a pili collection in a condition more consistent with the experiments in which we observed the effect of external peptide supplementation in the liquid medium. At first, we coated 6-well plates with agar and then added liquid before collection of cells for pili preparation. With these experiments, we later observed the recovery of pilin protein in the pili fraction when ΔPilC was supplemented with peptides (xxxvii). We also collected cells and prepared pili from a 4-hour culture in the liquid medium (Figure 5.5). In this case, we can indeed observe an apparent restoration of pilin protein in the pili fraction. We still observe a minute amount of pilin in ΔPilC. This could be because ΔPilC can still express pili, but their pili are not stable when retraction is present. Therefore, we might be detecting some of the remnants that escaped when the pili disintegrate during retraction. It is also worth noting that pilins are expressed at the same level as in the Wild Type from the cell pellet result. This result shows that pilin is expressed similarly among the strains on a protein level, but in ΔPilC, piliation did not occur or occurred at a lower level. When supplemented with C-terminal PilC peptides, piliation was indeed restored.

Now that our western blot results showed the recovery of pilin in pili fraction when ΔPilC was supplemented with peptides, we wondered if it restored the pili the same way. One of the methods we can use to observe the extent or the type of piliation restored is **Transmission Electron Microscopy** (Figure 5.6). In this case, we collected cells from a four-hour culture in the liquid medium. As reported in the literature, no pili was observed in the ΔPilC mutant. When incubated together with synthesised PilC C-terminal peptides, pili were observed. This is a piece of strong evidence showing the restoration of pili by the external supplementation of PilC C-terminal peptides. It is worth noting that these observations were done after only 4h of incubation of ΔPilC mutant with the peptide that is only 12 amino acids at the C-terminal of a protein that is originally 1342 amino acids long.

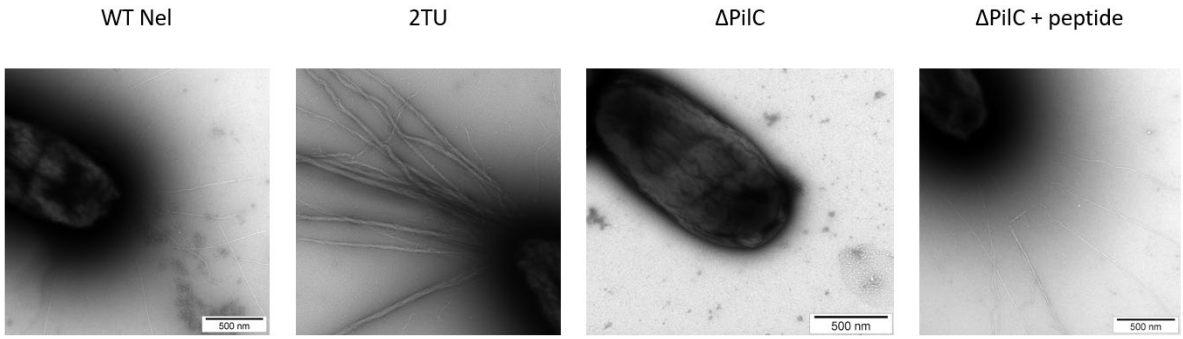


*Figure 5.6 Transmission electron microscopy images of Neisseria elongata (a) Wild type (b) 2TU (c) ΔPilC and (d) ΔPilC with C-terminal peptide*

To verify our finding and understanding, we performed a small study with truncated PilC (PilCtrunc), ΔPilK and combination with ΔPilT. The study can be found in Study IV: Studies using truncated PilC and ΔPilK.

## 5.2 Effect PilD-dependent PilE modifications on GC Competence

### 5.2.1 Background and Motivations

Because of the dual function of PilD as both a peptidase and a methyltransferase, further investigations intended to uncouple its two functions to better study each of them. These studies also aim to use this information to unravel PilD structure-function relationship. Based on the conserved residues in prepilin peptidase across species, several cysteine residues were identified, and mutations were tested in *Pseudomonas aeruginosa*: residue 17, 72, 75, 97 and 100 [187,325]. There seems to be no difference in the expression level of PilD except C72S[325]. When tested in vitro, substituting a cysteine residue at 72 and 75 has a lesser effect on its peptidase activity than substituting at 97 and 100[325]. However, substitution at any of these residues decreases methyltransferase activity[325]. Another study showed substitution at Glycine95 gives a significant decrease in methyltransferase activity, while substitution at Lysine96 has varying effects on methyltransferase activity[188]. Surprisingly, both mutants do not significantly change their peptidase activity[188]. Another study identified the active sites of PilD-like protein in Vibrio cholerae, Type-IV prepilin peptidase (TFPP). Being a bilobed aspartate protease that is unlike any other protease, the active site pairs of aspartic acids of the two TFPPs in *Vibrio cholerae*

are found at positions 125 and 189 of TcpJ and 147 and 212 of VcpD. What is interesting is that these corresponding aspartate residues are completely conserved throughout this extensive peptidase family[326]. Overall, these studies showed some meaningful structure-function relationships of PilD. However, it does not conclusively elucidate the effect of PilD on pilin.

The role of PilD may be linked with multiple systems in the cell membrane. Incomplete maturation of pilin by pilD mutant leads to the accumulation of prepilin in the membrane of cyanobacterium *Synechocystis sp.*[327]. The same phenomenon has been reported in *Pseudomonas aeruginosa*[186]. Moreover, this accumulation further triggers the degradation of SecY translocase and YidC insertase, implying a downstream effect on membrane protein translocations[327]. The study suggested a link between prepilin toxicity and lagged glycosylation of the pilin protein in PilD mutant, leading to growth arrest[327]. From this literature, it is interesting to put into perspective that the processing of pilin can indirectly lead to other physiological effects in the cell, highlighting the interconnectedness of all these systems.

Meanwhile, studies on *Neisseria gonorrhoeae* prepilin peptidase surfaced slightly later than those of *Pseudomonas aeruginosa*, and the quest to understand PilD has extended across different species due to its ubiquity[185,190]. Its ability to perform similar functions across species suggests its importance in pili biogenesis[187]. However, studies of PilD in vivo of *N. gonorrhoeae*, especially that of uncoupling the two main functions, peptidase and methyltransferase, are still minimal. On top of that, the lagged glycosylation of pilin in PilD mutant from cyanobacterium raises the question of PilD's other role in regulating pili assembly[327]. In this study, it will be in our interest to investigate PilD's role in prepilin processing and how it affects pili biogenesis or any of its functions, including competence, our main interest in this thesis. We have used the genomic tools developed in Chapter 2 to be able to dissect the effect of PilD processing on PilE using PilD mutants. Our study finds that mutations at Cysteine72 and Glycine93 amino acids alone do not affect its peptidase activity. However, a double mutant (PilDC72SG93S) and a mutant replacing Isoleucine134 with methionine confer a lower pilin yield outside the cell. The pilin in these two mutants seemed to be unprocessed as well. At the same time, this study shows that PilD mutants alter post-translational modifications on PilE. Our preliminary investigation suggests that PilD may be involved in PilE-processing functions other than peptidase and methyltransferase. These alterations shifted the Type IV Pili retraction dynamics but do not alter natural transformation.

### 5.2.2 Materials and Methods

#### 5.2.2.1 Strains used and culture conditions

The strains used in this study are listed in the Appendix. The growth and culture conditions are similar to what is mentioned in Chapter 2.

#### 5.2.2.2 Strains construction

Strain constructions are performed as described in Chapter 2. All tDNA used in this study or for strain constructions can be found in the Bacteria Strains. Oligos used in this study or for strain constructions can be found in the Oligos List.

#### 5.2.2.3 Pili preparation

Overnight cultures of bacteria were swabbed from GCB agar plate and resuspended in 1ml of 50 mM CHES buffer, pH9.5 or 50 mM ammonium bicarbonate, pH7.4. Ammonium bicarbonate buffer was especially used for sample preparation intended for Matrix Assisted Laser Desorption Ionization - Time of Flight (MALDI-TOF). After normalising bacteria cells against $OD_{600}$, stocks were prepared with the appropriate buffers. The cell solution was disrupted for 2 min. The cells were spun down at 18k g for 5 min. The supernatant was collected and ultracentrifuged at 50000 g for 90 min at 4°C. After that, the supernatant was removed, and the pellet was resuspended in the appropriate buffer (either CHES or ammonium bicarbonate buffer) and labelled as pili fraction.

#### 5.2.2.4 SDS-Polyacrylamide Gel electrophoresis (SDS-PAGE), Western Blot and Detection

The procedure is described in Chapter 4. In this study, we also used α-GCpilin polyclonal rabbit antibody (1:1000) as the primary antibody and α-rabbit horseradish peroxidase antibody (1:10000) as the secondary antibody.

#### 5.2.2.5 Protein Preparation for MALDI-TOF

Protein sample concentrations were measured using BCA Protein Assay and diluted to a stock of approximately 20uM. For better results, we used custom-made chromatographic microcolumns filled with a mixture of C8 and C18 beads in Eppendorf GELoader micropipette tips to desalt and concentrate the protein sample[328]. The stationary phase was equilibrated with 1% TFA, and then samples were added to 1% TFA before binding to the stationary phase. Protein was eluted with Sinapinic acid (SA).

#### 5.2.2.6 In-gel Trypsin Digestion

The pili samples were run and separated through SDS-PAGE as described above for sample preparation. After SDS-PAGE, the polyacrylamide gel was stained with Coomassie Blue. After de-staining or washing with clean water, the gel was recuperated. The bands showing protein of the right size were excised and cut into small pieces. The Coomassie blue stain was then washed out through washes of acetonitrile. After the stain was washed out and the gel was dehydrated, the sample was reduced with 10mM DTT in ammonium bicarbonate and incubated for 45 min at 56°C in a water bath. After incubation, the samples were taken out to cool down. Then, the cysteines were alkylated using iodoacetamide (IAA) in ammonium bicarbonate. The reaction was left to incubate for 30 min at room temperature. After incubation, excess IAA was removed, and a volume of 10 mM of DTT was added again to kill the alkylation process. The samples were washed multiple times with acetonitrile to eliminate excess DTT and IAA. After the gel was dehydrated, trypsin in ammonium bicarbonate was added to the sample while it was on ice. The reaction was left on ice for 45 min to let the trypsin seep through and hydrate the gel. After 45 min, the reaction was placed at 37°C overnight for digestion. The next day, the samples were centrifuged, and the supernatant was recovered for the downstream process.

#### 5.2.2.7 Matrix-Assisted Laser Desorption Ionisation - Time of Flight (MALDI-TOF)

The samples were mixed with matrices before being left dry on the target plate. Matrices tested in our study include α-Cyano-4-hydroxycinnamic acid (HCCA) and Sinapinic Acid (SA).

Dilutions were optimised to obtain optimal spectrometry. Once ready, plates were loaded onto MALDI-TOF (Appareil Bruker, Autoflex IV). Spectrometry results were analysed on FlexAnalysis.

### 5.2.3 Results

#### 5.2.3.1 Characterisation of PilD mutants

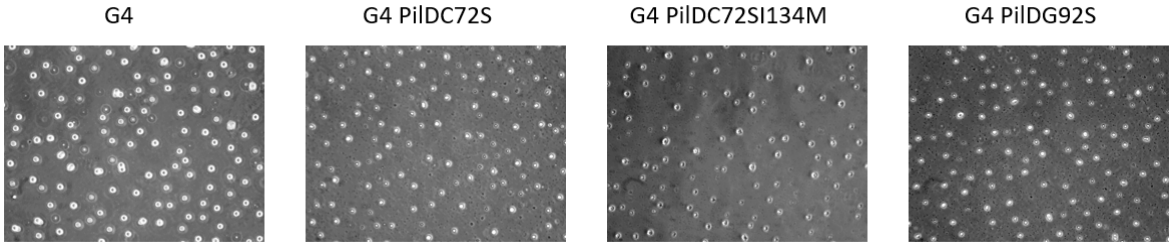


*Figure 5.7 Aggregation assay of PilD mutants*

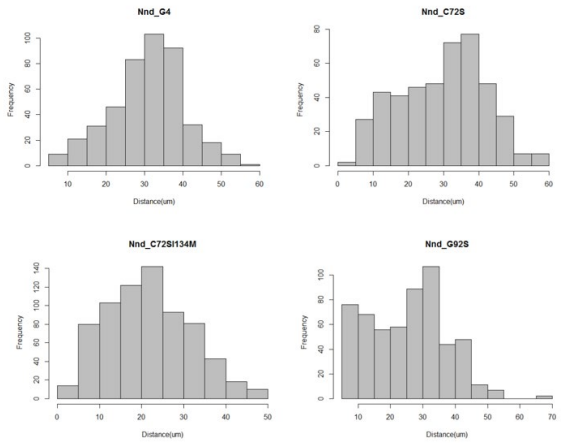


*Figure 5.8 Distribution of microcolonies nearest neighbour distance (nnd) in PilD mutants*

To decouple the two known functions of PilD (methyltransferase and prepilin peptidase), we obtained, through discussion with collaborator Katrina Forest from the University of Wisconsin-Madison, some potential amino acids as targets. These are based on her experience and also available literature from Type IV Pili in other bacteria species. The two targets we found interesting are **Cysteine72 and Glycine93**. These amino acids are selected based on sequence alignment with PilD from *Pseudomonas aeruginosa*. We also built our mutants on an ΔG4 strain to prevent artefacts from pilin antigenic variation. Through strain construction, we obtained **C72S, G93S** and **C72SG93S** mutants. We also obtained a **C72SI134M** through unintended mutation. Our aggregation assay showed no obvious defects in these PilD mutants (Figure 5.7). Nearest neighbour distance (nnd) analysis (Figure 5.8) also confirms no big difference in how these mutants aggregate.

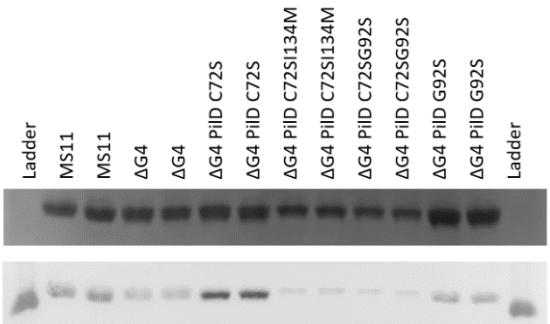


*Figure 5.9 Pili profile of PilD mutants: (a) Coomassie-stained gel and (b) western blot probed with α-SM1 antibody*

#### 5.2.3.2 PilD mutants present differing pili profile

To examine the primary function of PilD mutants, we turned to look at their effect on pilin. Given PilD's canonical function as pilin peptidase and methyltransferase, we expect to see disruption in these functions in the mutant strains. Surprisingly, the observation proved to be more multifaceted than we thought. Given that the cell number collected was normalised,

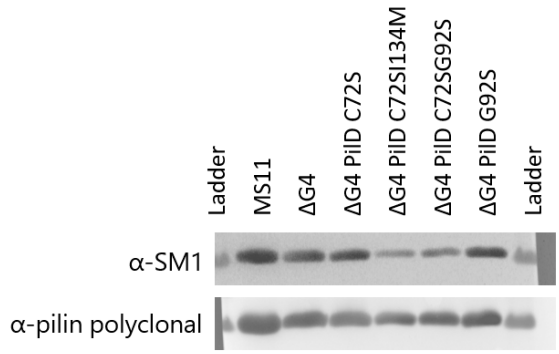


*Figure 5.10 Western blot of pili from PilD mutants probed with different antibodies*

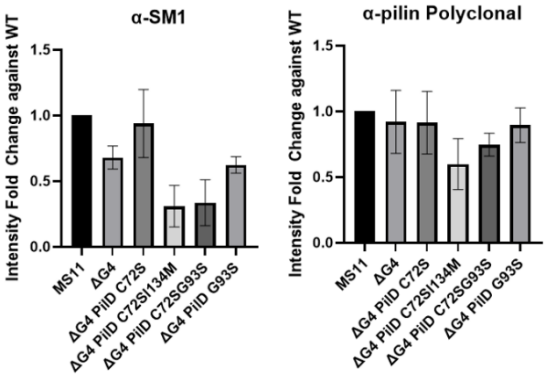


*Figure 5.11 Quantification of the intensity for both western blot in the previous figure*

these strains did not produce the same amount of pilin. On Coomassie-stained gel (Figure 5.9), we could observe slight differences in pilin sizes in C72SI134M and C72SG93S, which was expected since PilD is a peptidase. Therefore, any perturbation in peptidase function will lead to uncleaved pilins. However, pilin from C72S and G93S differ from neither the background strain ΔG4 nor wild-type MS11.

Interestingly, when probed with primary antibody against the SM1 region of PilE (EYYLN) (xxxviii), the pili profile looks different from what we observed on Coomassie-stained gel (Figure 5.9). We note that C72S pilin showed a higher signal, while G93S showed roughly a similar signal level as ΔG4. C72SI134M and PilDC72SG93S, as expected from the already lower pilin in Coomassie, showed the least signal. Since it is a primary antibody probing a specific region of PilE, we turned to detect PilE with a polyclonal antibody against PilE.

Our immunoblot of PilD mutants with polyclonal antibody against PilE showed less variation in pilin detection, reflecting what was observed in Coomassie-stained gel (Figure 5.10). Our quantitative analysis of the blot confirms this observation (Figure 5.11). This result suggests that during immunoblot with antibodies probing specific regions of PilE, some changes in the PilE protein could protect the protein from being detected. The fact that this was done in denaturing conditions also means that structural changes due to protein folding did not contribute to this difference. The other explanation we could provide is that some modifications on the protein prevent anti-SM1 antibodies from binding effectively to these PilE proteins. Literature has reported the ability of modification-recognizing (i.e. phosphocholine-recognizing) recognizing PilE but not the other way round[162].

### 5.2.3.3 MALDI-TOF

During our initial attempt to analyse our pili fraction proteins in MALDI-TOF, we tested two matrices, HCCA and SA. SA gave us a better resolution in differentiating the peaks (xxxix). From our MALDI-TOF spectra (Figure 5.12), there are peaks corresponding to pilin at m/z +1. There are common peaks between MS11, ΔG4 and C72S at 17740.511, 17859.171, and 17822.493. What is intriguing is the bump around 18000, which is abundant in MS11 and C72S alike. The peak at 17740.511 also shifted slightly to 17729.948 in C72S. In G93S, the 17729.948 peak was not observed, but we see a smaller peak at 17621.356 (Figure 5.12). However, the double mutants (C72SI134M and C72SG93S) spectra were not resolved for

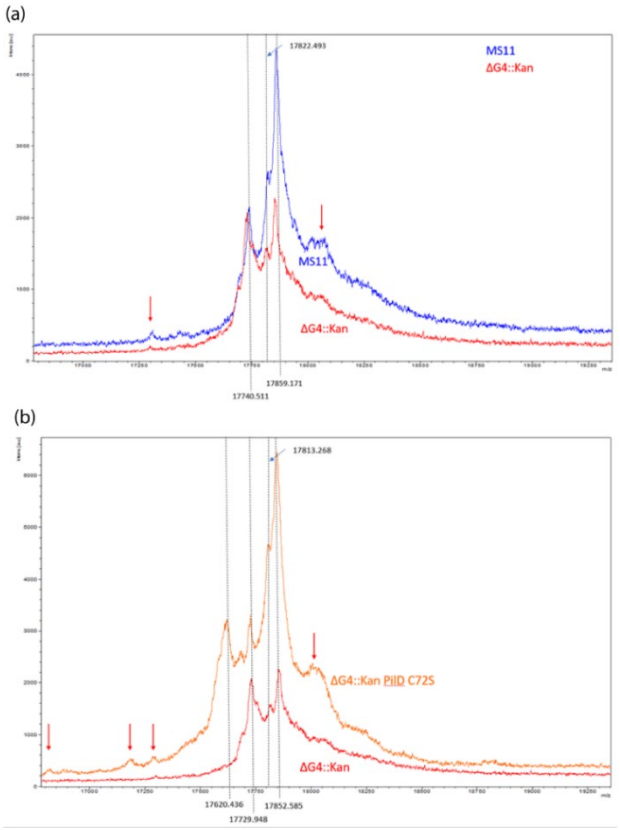


*Figure 5.12 Differences between the m/z of pilin*

several reasons. It could be that the lesser pilin we observed already meant a less stable pilin or that the pilin in these mutants could not reflect in the MALDI-TOF effectively. Initially, we wondered if this could be due to the buffer we used to extract pili fraction, CHES buffer pH9.4. To ensure we have a compatible buffer, we used one that was commonly used in the facility and was also reported in the literature for T4P in *Pseudomonas aeruginosa* [329]. We confirmed again with the pili profile when pili were extracted in this buffer and ensured they showed the same result as in the CHES buffer. In our MALDI-TOF spectrometry, we still observe a similar trend; therefore, it seems this study has to be furthered to reach any conclusion. However, since it is a preliminary study, we decided to focus on the single mutants that show some difference in the spectra and proceed to look at potential sites from which such difference in m/z came.

### 5.2.3.4 In-gel Trypsin Digestion

Our subsequent investigation involved cleaving these pilins to look for the fragments in which any modification is involved. To do that, we used in-gel trypsin digestion to digest the pilins. The digested peptide was then loaded to run on MALDI-TOF again to identify the fragments. In this study, we focused on MS11, G4 and C72S (Figure 5.13). In our results, we MALDI-TOF spectrometry on the reflector and linear mode. Our analysis showed no significant difference between the peaks in reflector mode. However, we can observe differences in the linear mode. This indicates that the fragment that shows a mass difference is fragile and could not fly during the reflector mode. It is difficult to accurately identify the mass in a linear mode since it reflects the average mass. Nonetheless, we did a preliminary analysis of the available data.

Since we observed different detection signals through western blots probed with different antibodies, we deduced that the modification could be near or on the SM1 sequence. The smallest fragment predicted for trypsin digestion containing EYYLN is SAVTEYYLNHGK at 1382.5152. When we check on the spectra at this m/z, we indeed find the peak with varying height. However, we are careful not to quantify based on the peak height; instead, we look at multiple other peaks to look at the consistency of the ratio of the peak. We observed varying ratios of the peak. For example, we see more in MS11 for some peaks, while some were more in C72S. Taken together, we conclude that PilD mutations alter the modifications of PilE

populations, but due to the lack of expertise, it is not conclusive. In the future, we would like to perform MS/MS on these fragments to identify them.

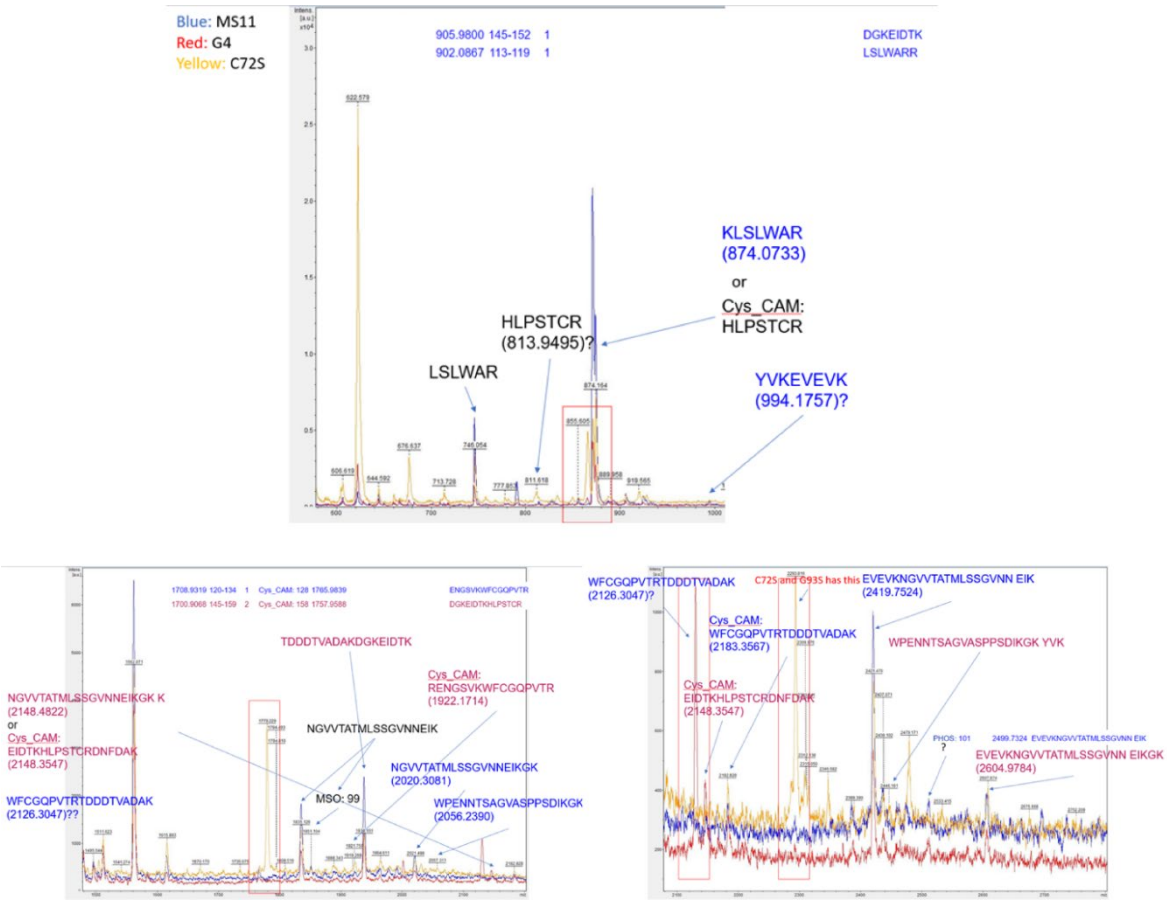


*Figure 5.13 In-gel trypsin digested pilin in linear mode MALDI-TOF shows differences in the m/z of fragments in PilD mutants*

### 5.2.3.5 The effect of PilD mutations on T4P retraction dynamics

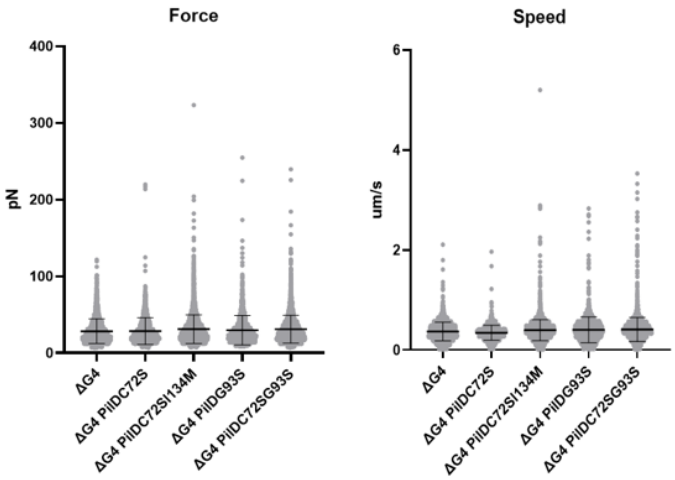


*Figure 5.14 Pili retraction profile of PilD mutants: Force (left) and Speed (right)*

Since we observed unidentified modifications on T4P in PilD mutants, we suspect these modifications could impact the pili dynamics. There are known post-translational modifications in T4P in *N. gonorrhoeae* that can moderately affect the attraction force between the bacteria and alter the microcolonies' material properties[330]. We wonder if these PilD mutants will also change the pili retraction properties. To test this, checked the PilD mutants' pili mechanical properties using the micropillar

assay described in Chapter 3. Our investigation of T4P retraction dynamics showed subtle differences between the mutants (Figure 5.14). Although the mean of the pili retraction force and speed are quite similar (T- i and T- iii), student t-test analysis on our dataset showed that they have slight changes in the population distribution (T- ii and T- iv). Nonetheless, these differences are very minute. In conclusion, we can see no major effect of PilD-dependent PilE modification on pili retraction dynamics. This, together with our spectrometry data, suggests a possibility that these modifications or changes that we saw were not large-scale. In another term, modifications of PilE resulting from PilD mutation probably did not affect the majority of the Type IV Pili. Therefore, the collective effect was not apparent by ratio when we studied the pili at a macro scale.

#### 5.2.3.6 The effect of PilD-processing PilE modification on GC competence

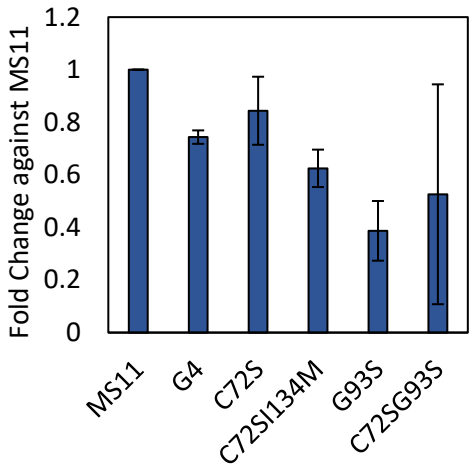


*Figure 5.15 Competence of PilD mutants*

Our competence assay on PilD mutants reflects what we observed in other experiments. From our experiment, it seems there was no significant difference in the change of competence in these mutants (Figure 5.15). When there is a defect in DNA uptake, the different fold-change of competence can go up to 10 or more fold differences. In the case of PilD, the most significant decrease in transformation efficiency was around a 2.5-fold change in G93S. The more interesting observation would be the trend of competence level corresponds nicely to our western blot probed with SM1 antibody, which might hint at some mechanisms at play. Most probably, since the modification did not occur globally on all pilin in the pili, it did not affect the competence significantly. Nonetheless, we thus conclude that PilD-dependent PilE modifications do not affect competence significantly. The results suggest that there is more to be considered when studying T4P since the pili seems more like a plethora of pilin than a population of identical pilin.

## 5.3 Discussion

From the previous Chapter, we learn that understanding Type IV Pili can be a complex task. It is important to be aware of their dynamic and polymeric nature and, at the same time, their connection to many processes in the cells partly due to their multifunctionality. In this Chapter, we explored two features of Type IV Pili and how they affect processes such as pili biogenesis and competence.

In the first Section, we used **external supplementation of PilC C-terminal peptide** to reveal some interesting aspects of Type IV Pili biogenesis. In this study, we reproduced, in a different way, the observation in literature in which supplementation of PilC proteins in ΔPilC is enough to regain the loss of pili. Interestingly, our study shows that the loss of pili in ΔPilC can also be rescued with just peptide as short as 15 amino acids of the C-terminal peptide of PilC. This

means that just the small stretch of the peptide sequence is enough to interact with an essential part of the machinery in securing stable pili. This process also seems to occur near the cell surface, given that external supplementation of peptide or protein seems to rescue defective pili phenotype in ΔPilC. This result is **an interesting addition to our observation with ΔPilV in Chapter 4.** Previously, we found that good competence can be achieved with short pili, which could be a factor for enhanced competence. In this Chapter, we showed that the stability of pili provided by PilC is probably crucial for the whole operation of pili, given that ΔPilC will still try to produce pili, but they could not extend further due to instability during retraction. In this ΔPilC study, we can deduce that some short fragments of pili reach the surface and react with the external supplemented peptide before ensuring stable pili formation. We made a structural prediction between PilC, PilV and PilE but were not able to observe the PilE-PilV interaction we see in Chapter 4 between PilC-PilE or PilC-PilV. Nonetheless, these short pili near the secretin are not enough to lead to competence. Through this, we can be sure that in the case of ΔPilV, the act of pili extending and retracting and their turnover in and out of PilQ probably lead to their enhanced competence phenotype. Moreover, the fact that this act can be achieved through external supplementation also opens some possibilities for external intervention targeting Type IV Pili during application.

In the second Section, we looked at the effect of **PilD-dependent pilin processing on Type IV Pili**. This study was initially meant to decouple the bifunctional prepilin peptidase, PilD, studying it in detail from a structure-function perspective. During this study, we discovered that mutation on PilD modified PilE in more aspects than we imagined. Other than the peptidase activity, we observed other possible modifications in PilE. Interestingly, we did not observe a total alteration in PilE processing or modification, hinting there is more than one straightforward pathway in PilE or pilin processing before pili assembly. This heterogeneity in pilin processing can be detected in our study, and yet it also does not affect too much of the Type IV Pili mechanical properties as a whole. This shows that the regulation of pilin processing and pili assembly is pretty robust and modulated. This result also helped us to suspect the role of PilV back in Chapter 4. With a wild-type PilD, we can already see a difference in pilin accumulation in the cell membrane, showing that there are more pathways in play before pili assemble into the pili. From Chapter 4, we also got to know **of PilV's potential role in maintaining certain pilin modification landscapes in the pili.** This suggests the that **pilin-pilin interactions** (either between major pilins or among all pilins) can be a pre-requisite for many **pre-processing or modifications** during the biogenesis process.

# Chapter 6 : DNA Uptake in *Neisseria* species interaction

It is naïve to assume the totality of bacterial behaviour based solely on single species bacteria culture. Bacteria exist as a community, mostly co-habiting with other species. Bacteria interaction in this community adds to the complexity of bacteria life. More often, different populations of bacteria may need to strategize for survival, perhaps through positive interaction (mutualism or commensalism) or negative interaction (predation or competition)[6,7,315,331]. Though limited in literature, positive and negative interactions between commensal and pathogenic *Neisseria* have been reported.

Bacterial evolution drives the diversity in the bacteria community and provides several mechanisms of action in these interactions. The influence of **horizontal gene transfer** among bacteria populations or communities on the emergence of antibiotic resistance has been recognized for some time. Combined with spontaneous mutation, horizontal gene transfer facilitates the heterogeneity of bacterial population genomics. Acquisition of genes conferring antibiotic resistance means enhancing the chance of population survival when encountering antibiotics, whether it is produced by other co-habiting bacteria or human intervention. On top of this, in *Neisseria* species, **DNA uptake** has been reported as a mechanism of *N. gonorrhoeae* killing by *N. elongata*[332]. However, there remains some gap in understanding the exact mechanism of this killing. There is no clear indication of the key step in the **DNA transformation process** that caused this killing.

Hence, we are interested in understanding the implication of this interaction as yet a **new role for competence** in *N. gonorrhoeae*. To do that, we reproduced the same interaction under our experimental conditions and tested several systems to probe the specific DNA transformation steps. During our investigation, we surmised that the interaction may not be directly related to DNA transformation and proposed a few other possible explanations for this phenomenon.

## 6.2 Materials and Methods

### 6.2.1 Strains used and culture conditions

Strains (both *Neisseria gonorrhoeae* and *Neisseria elongata*) used in this study can be found in the Bacteria Strains. We use a similar protocol to culture *N. gonorrhoeae* and *N. elongata*, as reported in Chapter 2.

### 6.2.2 Killing Assay

To perform a killing assay, required cells were swabbed from a GCB agar plate in which they were grown overnight at 37°C with 5% $CO_2$ and resuspended in a GCB liquid medium. A stock of $OD_{600}$ 0.7 was prepared. In a 6-well culture plate, 1 ml of GCB liquid medium supplemented with Supplements I and II were added. In each well, 100ul of $OD_{600}$ 0.7 cells were added. If it is a condition with one type of bacteria, 100ul was used entirely. If it was an interaction condition, 50ul of each cell was added. The ratio of the cells changes according to experiments and will be stated in the results section. In the supernatant/nutrient study, the supernatant was

added to the culture accordingly, mixed well and left for incubation at 37°C with 5% $CO_2$. Timepoints chosen to investigate the killing effect were chosen based on each experiment, usually as 0h, 6h, 24h, and 30h. The culture was recovered entirely during time points, including scraping adhering cells at the bottom of the well. The cells were then prepared into 10x serial dilutions and spotted on agar plates for CFU counting. The agar plates were GCB agar (for growth of all strains), LB agar (to select for *N. elongata* growth) and GCB agar with VCN supplement (to select for *N. gonorrhoeae* growth). After spotting, the plates were left to air dry before incubating at 37°C with 5% $CO_2$ overnight. The growth was observed and quantified the next day.

### 6.2.3 SDS-PAGE and Staining

The procedure is described in Chapter 5. For detection, the gel was washed briefly with clean water and then stained with GC Colloidal Coomassie Stain (Bio-Rad Laboratories) according to manufacturer recommendations.

### 6.2.4 Transposon-5 (Tn-5) mutagenesis library screening

An *N. gonorrhoeae* Tn-5 mutagenesis library was obtained (This is a library established by Jingbo Kan for another study). By using the stock of Tn-5 library, the bacteria were lawned on a GCB Agar Plate and incubated overnight at 37°C with 5% $CO_2$. The bacteria were then resuspended in a GCB Liquid medium, and a stock of $OD_{600}$ 0.7 was prepared. On the other hand, an overnight culture plate of WT *N. elongata* was also resuspended in GCB Liquid medium, and a stock of $OD_{600}$ 0.4 was prepared. In a 6-well culture plate, 1ml of GCB Liquid with supplements was prepared. In each well, 50ul of *N. gonorrhoeae* and WT *N. elongata* stock each was added. At the same time, a control well with WT *N. gonorrhoeae* and WT *N. elongata* were prepared. The cultures were then incubated for 30 hours at 37°C with 5% $CO_2$. After 30h, the entirety of the culture was scraped off the well and disrupted. The cultures were then centrifuged to reduce the volume of liquid to around 100ul. These reactions were then plated on VCN selection plates. The plates were incubated for another day at 37°C with 5% $CO_2$. Any growth observed on the VCN selection plates the next day was then collected for further analysis.

### 6.2.5 Identification of mutation in Tn-5 library mutants

The mutation in selected Tn-5 mutants is identified by using Random Amplification of Transposon Ends (RATE) described in a published protocol[333]. Three steps of amplification were involved in this method. For all amplification, Taq polymerase mix was used. For the first amplification, the inverse PCR primer Inv-2 was used, and each of the colonies was selected and resuspended in water to be used as the template. The reaction was heated at 95°C for 5 minutes. After that, the amplification was done with 30 cycles as such: 95°C 30 seconds, 55°C 30 seconds, and 72°C 3 minutes. After that, a second amplification was done with 30 cycles as such: 95°C 30 seconds, 55°C 30 seconds, and 72°C 3 minutes. After that, a third round of amplification was done with 30 cycles as such: 95°C 30 seconds, 55°C 30 seconds, and 72°C 2 minutes. The resulting reactions from the amplification were checked on DNA agarose gel

electrophoresis. The reaction was then cleaned up and sent for sequencing using the sequencing primer KAN-2 FP-1.

### 6.2.6 Disc and Agar Inoculation Test

To examine whether molecules exert the killing effect, we turned to a disc test and an alternative agar inoculation test. For the **disc test**, we first prepare the test samples. The first set of test samples is direct extraction from *N. elongata*. An overnight culture plate of *N. elongata* was resuspended in 1 ml of methanol or ethanol. The solution was then centrifuged and filtered through a 0.2 µm syringe filter to remove cell debris. In this set of experiments, we used a known GC-inhibitory extract from *Bacillus subtilis S* as a positive control (Kan J, unpublished data). We collected supernatant from a culture containing either *N. elongata* or both *N. elongata* and *N. gonorrhoeae* co-culture for the second set of test samples. The supernatant was then evaporated under the fume hood until it was around 10x more concentrated in volume. In each disc test, 10 ul of the samples were spotted on a sterile filter paper disc with a 6 mm diameter. The disc was then air-dried for a while. At the same time, on a GCB agar plate, WT *N. gonorrhoeae* MS11 was lawned evenly on a GCB agar plate. After that, the disc was placed on top of the lawn. The plates were then incubated overnight at 37°C with 5% $CO_2$. The plates were observed the next day for any inhibition of growth. WT *N. gonorrhoeae* MS11 was lawned evenly on a GCB agar plate for **the agar inoculation test**. On an overnight culture plate of WT *N. elongata*, a swab was used to get some of the growth, which was then spotted lightly on top of the lawn of MS11. The plate was then incubated overnight at 37°C with 5% $CO_2$. The plates were observed the next day for any inhibition of growth.

## 6.1 Results

### 6.1.1 Killing of *N. gonorrhoeae* by *N. elongata* in liquid medium

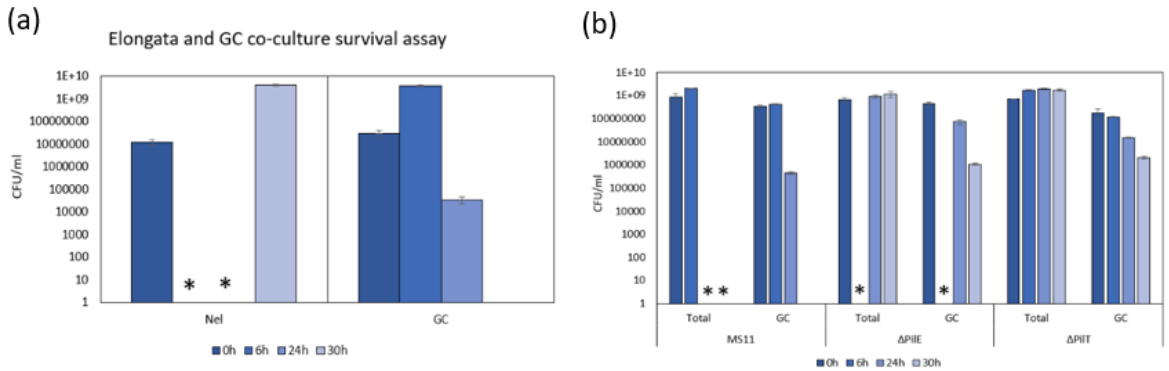


*Figure 6.1 (a) Killing of N. gonorrhoeae in Nel-GC co-culture (b) Killing assay with GC pili mutants. * means Too-Many-To-Count.*

We were curious about the role of DNA uptake in *N. gonorrhoeae* and *N. elongata* co-culture reported in the literature[332]. Due to the use of two different bacteria, we will also refer to *N. gonorrhoeae* as **GC** and *N. elongata* as **Nel**. In our study, we observed the same phenomenon. Our result (Figure 6.1) showed that Nel's growth was not affected up to 30h. However, there is

a decline in GC growth between 6h and 24h. The cell number recorded is lower than what we observed if GC was cultured by itself. Next, we repeated the same killing assay with GC pili mutants, ΔPilE and ΔPilT. These mutants are known to be defective in DNA transformation. Therefore, it seems fitting that ΔPilE and ΔPilT survive the killing assay, aligning with what is reported in the literature. *Note: * represents samples that are 'Too Many To Count'(TMTC)*

### 6.1.2 Growth space and nutrient as possible factors

While our findings from the previous Section match the literature well, given the multifunctional nature of Type IV Pili, survival of ΔPilE and ΔPilT in killing assay may not necessarily mean it is DNA uptake-dependent. We intend to test if the killing phenomenon still occurs when we increase the space in which the bacteria interact by performing the killing assay in 1ml and 2ml of liquid culture. On top of that, we tested a combination between GC, Nel, and Nel ΔPilT. This will also allow us to see if a lack of pili retraction or DNA uptake works in both directions or only from the GC side. Instead of tracking all time points, we also collected cells from 24 hours or 30 hours to ensure we could observe killing if it was present. Our result shows that in 2ml, the killing effect is reduced. We also know from this result that having a pili defect from the Nel side does not impede killing (Figure 6.2). Overall, in a 2 ml culture, cells will have more space to grow and less interaction between bacteria, and if there are secreted substances, they will be more diluted than in a 1 ml culture. This result suggests that the killing may also depend on the culture's growth space and available nutrients.

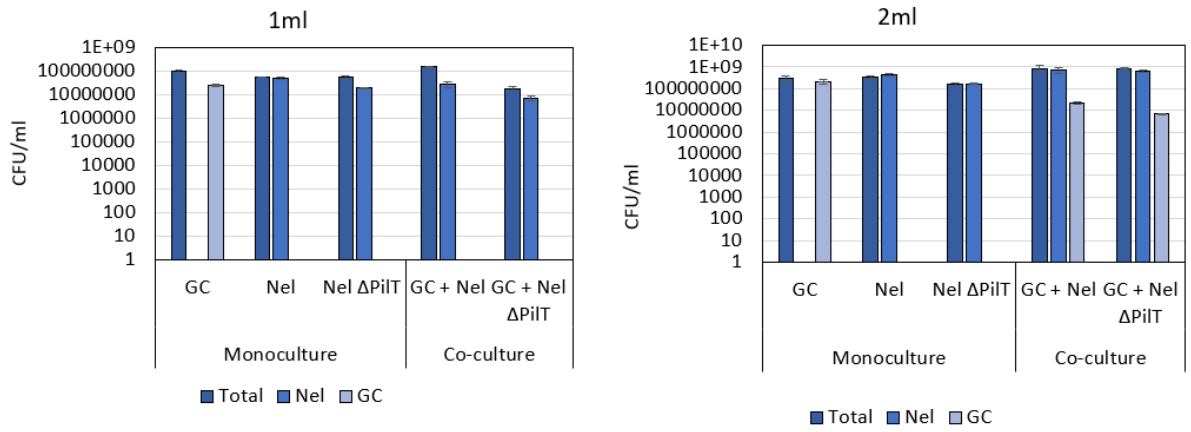


*Figure 6.2 Killing assay for monoculture and co-culture between GC, GC ΔPilT, Nel and Nel ΔPilT in different volumes of medium: 1ml (left) and 2ml (right)*

With that, we hypothesize there are a few possibilities for the killing mechanism through the culturing media: i) nutrient constraint and ii) secreted anti-GC molecules. We incubated *N. gonorrhoeae* with supernatant from overnight culture to investigate this hypothesis. The control was grown in fresh GCB media.

At first, we performed the killing assay by replacing the media either with 50% or 100% of the overnight culture medium of Nel or GC/Nel co-culture. With these, if any secreted molecules result from Nel or co-culture, we should observe the killing of GC. Our result observed poorer growth for GC in culture involving any overnight culture supernatant Figure 6.3). We observe

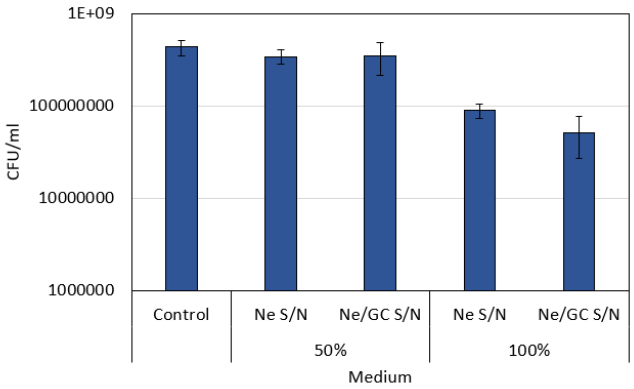


*Figure 6.3 Killing assay survival using different medium supernatant*

a dose-dependent manner where when 100% of the supernatant was replaced with overnight culture, GC growth was the poorest. To check if this observation was the result of depleted nutrients in overnight culture supernatant, we repeated a similar experiment with PBS as control. All culture conditions used 50% fresh GCB or fresh PBS (except the GCB Control).

Our results showed that the drop in survival we observed may be due to the lack of nutrients in the overnight culture since we observe the same magnitude of growth in those replaced in PBS as those with overnight culture (Figure 6.4). Also, if any killing factor is secreted or released in the media, then the magnitude of death or growth in GC should be comparable between the two groups. With this, we can conclude that killing factor most likely was not released in the media. This conclusion is further strengthened by the observation that supernatant from Elongata culture or a mixed culture did not affect growth as much as before the culture incubated with GC. Conversely, it is interesting to note that survival of ΔPilE and ΔPilT is not of the same magnitude as the Wild Type.

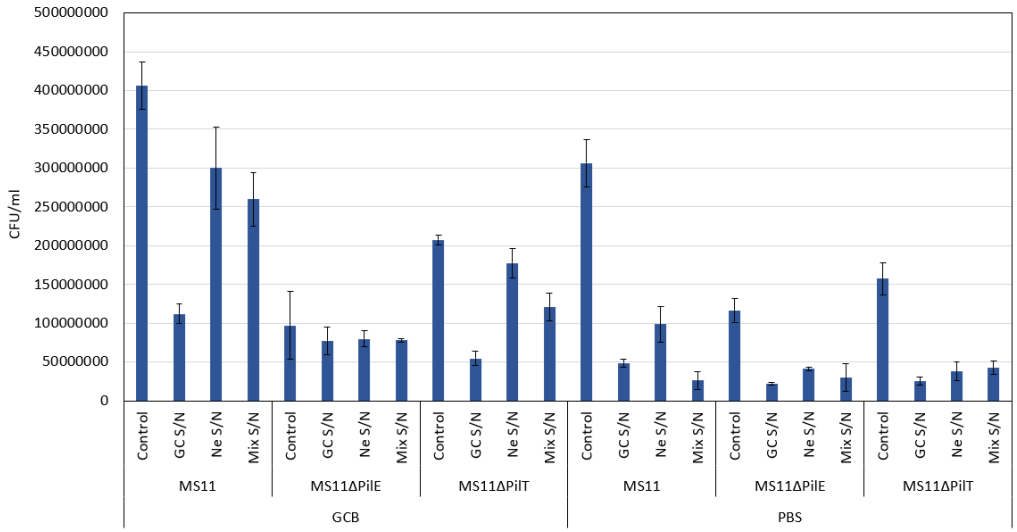


*Figure 6.4 Killing assay survival checking the effect of nutrients on 'killing'*

### 6.1.3 Possible competition behaviour in co-culture

Given that nutrients in the media can be a factor for the killing mechanism, we wonder if there will be competition behaviour between the two species during co-culture. We performed a killing assay with an asymmetrical inoculation between GC and Nel to do a preliminary test. We changed the Nel: GC ratio to 3:7 or 7:3. Our result shows that changing the inoculum

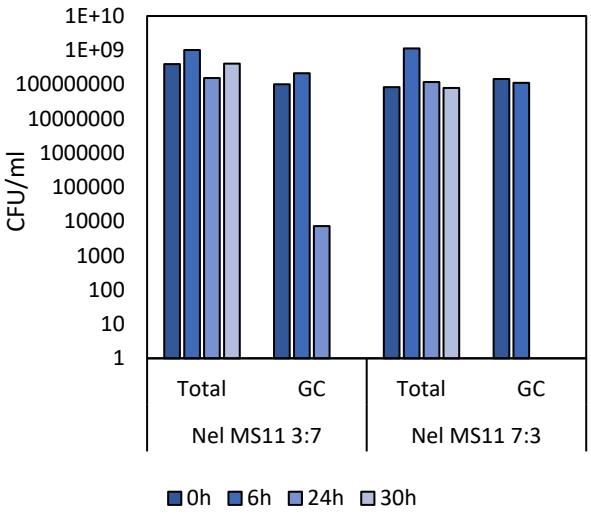


*Figure 6.6 Killing assay by varying inoculum ratio*

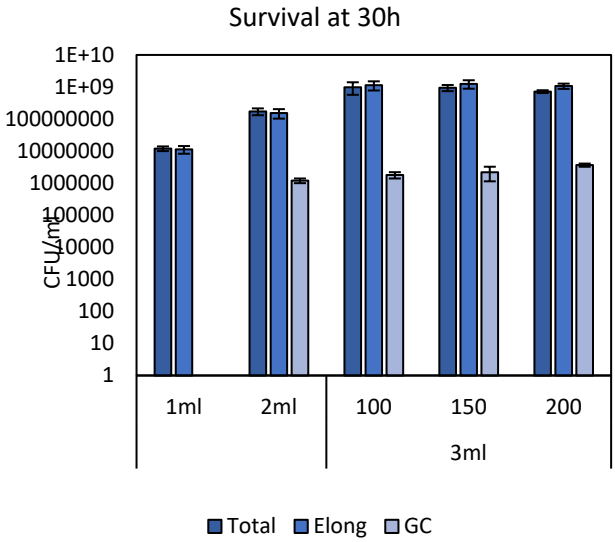


*Figure 6.5 Killing assay with different culture volume and inoculum amount*

amount does change the outcome of the killing assay, with GC surviving better when they started as the majority (Figure 6.6). This means that GC somehow established a dominating effect when they outnumbered Nel.

Since we observed that GC would survive the killing assay once we increased the liquid medium to 2ml, we also checked that increasing the culture further to 3ml would improve survival. Seeing that GC can survive better when we inoculate more of them from the start also made us wonder if the ratio between Nel:GC is important or just the inoculum size. In our experiment, we tested a killing assay in which we also inoculated 100 µl, 150 µl, and 200µl, Nel and GC each. We observed that increasing the medium volume does not improve survival (Figure 6.5). The change in inoculum size does not change the dynamic between Nel and GC, yet on each LB agar plate that is selected for just *N. elongata*, we noticed that there are flat Nel colonies in conditions in which GC survived (xl). This hinted that there is a response from the Nel side towards the presence of this *Neisserial* species in the same culture medium. However, after Nel successfully dominated the culture, in which GC did not survive, they returned to a normal colony morphology state. No significant difference was in colonies selected on VCN agar plates (for *N. gonorrhoeae*) (xli).

### 6.1.4 Competence may not be the sole mechanism

On top of the information we gathered, we would like to tackle the proposed mechanism, DNA uptake-dependent, from a different perspective. Besides using the conventional competence-defective pili mutants, we are lucky to build two examples during this study that allow us to investigate the mechanism further. They are (i) ΔPilC and external peptide supplementation (discussed in Chapter 6) and (ii) ComM (one of the competence-defective mutants we obtained).

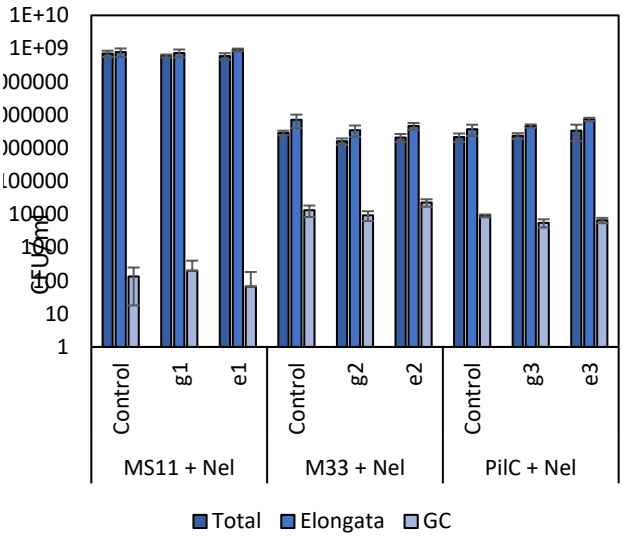


*Figure 6.7 Killing assay using ΔPilC mutants and peptide supplementation*

In our previous studies on **ΔPilC**, we discovered the recovery of competence in ΔPilC by supplementing C-terminal peptides of PilC. In that study, we discovered that the supplementation of peptide leads to the restoration of piliation and, hence, DNA uptake. In this study, we took advantage of this system to test if the killing by Nel is directly linked to DNA uptake. We used MS11 as a wild type and two different strains of ΔPilC mutant: M33 and PilC. During incubation with *N. elongata,* the co-culture was supplemented with C-terminal peptides of PilC from either *N. elongata* (e1) or *N. gonorrhoeae* (g1). In all of our conditions, although we see a drop in total CFU count, we did not see as big a difference between Nel and GC survival in ΔPilC supplemented with or without the peptide (Figure 6.7). If the killing depends on DNA uptake, we should see killing in samples supplemented with peptides. With this, we suspect that DNA uptake may not be the sole mechanism of the killing.

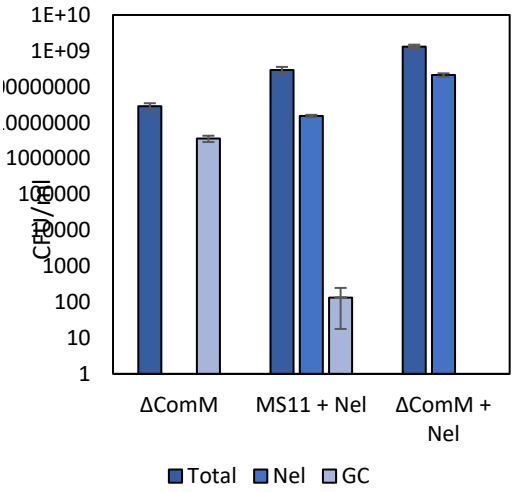


*Figure 6.8 Killing assay with ΔComM*

Another system we used to investigate this subject is using **ΔComM**. In our other study, we discovered that removing ComM does not nullify competence but can affect competence to a significant degree. Since ComM is a helicase in *N. gonorrhoeae*, the defect in competence is most likely affecting the recombination step. In our study, we realize that having some defect in competence, presumably the recombination step does not call for survival during the killing assay (Figure 6.8). Similar to the Wild Type, ΔComM could not survive the killing assay. Taken together, it seems the statement of DNA uptake-dependent killing may need further investigation.

### 6.1.5 Supernatant in Killing Assay does not contribute to the killing

At this point, we have some reservations about DNA uptake as the killing mechanism and would like to investigate if there was indeed any *N. elongata* DNA that was released into the medium, resulting in the killing as reported in the literature. Therefore, we collected culture media from 6h, 14h, 24h and 30h of mono- and co-culture of Nel and GC. These media were then checked using DNA agarose gel electrophoresis. Our DNA agarose gel detected a bright band in culture from 14h onwards in any culture that comes with *N. elongata* (Figure 6.9). The

size of the band exceeds 10kbp (which is the maximum of the used DNA ladder). Since we used SyBr Gold in this gel electrophoresis, this detected signal is of nucleic acid nature. Given the size of the molecule, we also suspect it could be the genomic DNA of *N. elongata.* However, we could not deduce anything further with this experiment.

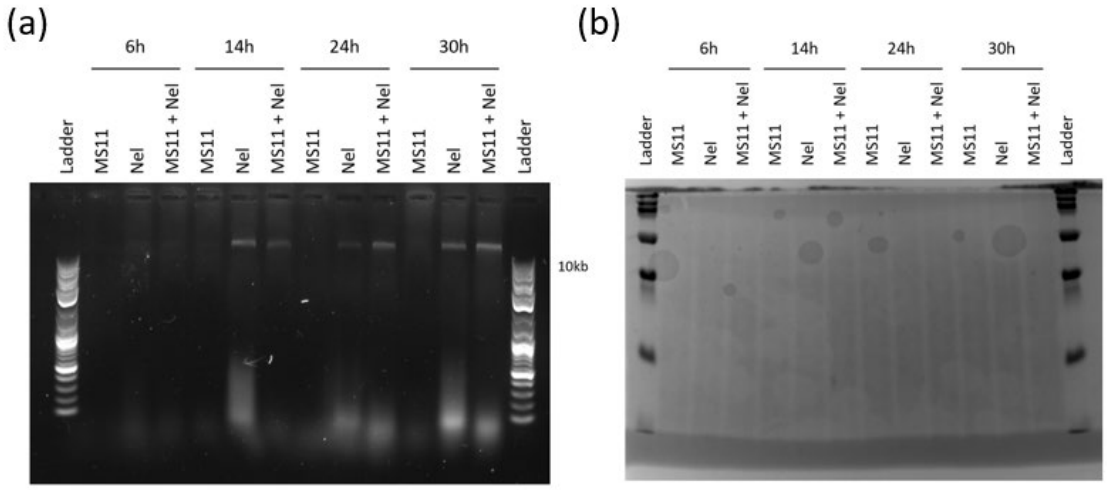


*Figure 6.9 (a) DNA agarose gel of supernatant collected from mono and co-culture at different time points (b) Concentrated fraction of collected supernatant with 3kDa MWCO*

We then continued our experiment by using some of the supernatant and concentrating with filer units (3kD MWCO). The rationale for this step is to inoculate the content of this concentrated supernatant to *N. gonorrhoeae* to show if the nucleic acid-like molecule is the cause of the killing. We did a protein gel electrophoresis to examine and check if there were any molecules we missed. However, our results showed no particular difference between the supernatants (Figure 6.9). When we added the concentrated medium into the culture containing MS11, MS11 survived even after 24/30h. This experiment confirms that the nucleic acid-like molecule is probably not the main source of killing.

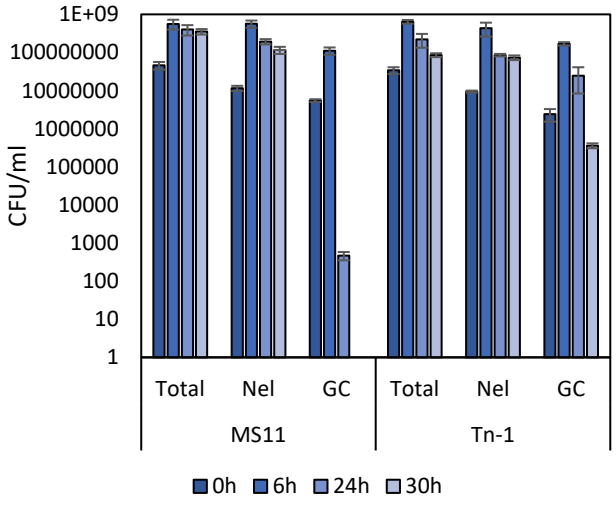


*Figure 6.10 Killing assay of Tn-1 (selected mutant from Tn-5 screening)*

### 6.1.6 Transposon-5 mutagenesis selection resulted in few mutants

The other approach we tried was to look for a potential target for this killing mechanism. One of the more conventional ways to do that is to generate a Tansposon-5 (Tn5) mutagenesis library of *N. gonorrhoeae*. With this mutagenesis library, we can use them to screen for potential mutants that could survive the killing. Tn5 screening will allow us to look for targets or better understand the nature of the killing mechanism. If DNA

uptake was indeed the primary mechanism, then we would expect to obtain mutants that are defective in DNA uptake.

In our Tn-5 mutagenesis library screening, we selected 16 colonies that survived the killing. Since these colonies are surviving colonies that came from the same pot of culture, one of the concerns was that the survival was a compound effect of multiple mutations or cooperative effects between mutants. To eliminate these possibilities, we inoculated these mutants, for example, Tn-1, in the killing assay to ensure it can reproduce survival in the assay. From our study, Tn-1 can withstand the killing even after 30h (Figure 6.10). On top of that, we also tested the competence assay on these mutants to see that not all of them are defective in competence (Figure 6.11).

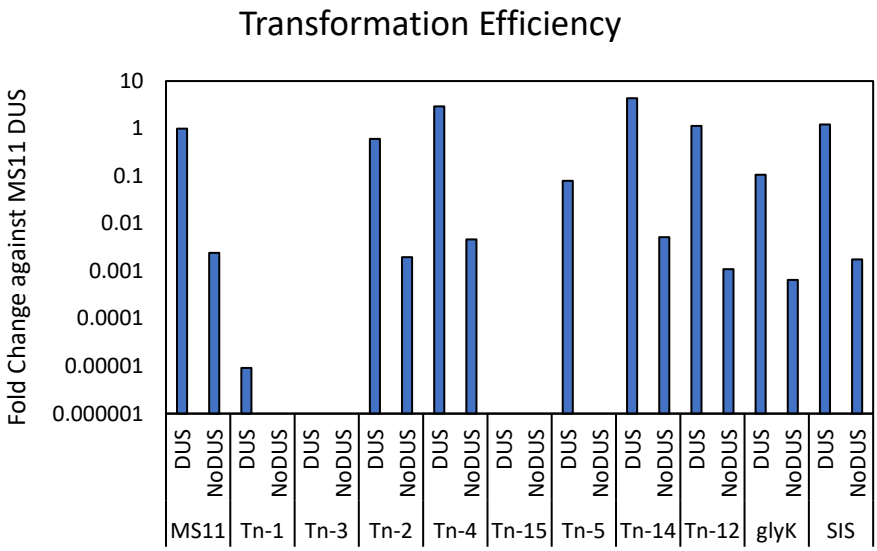


*Figure 6.11 Competence assay of selected Tn5 mutants and reconstructed mutants*

*Table 6.1 Selected Tn5 mutants that survive killing assay*

| Mutant # | Gene | Product | Genomic location |
|---|---|---|---|
| 1, 3, 6, 7, 10, 11, 13, 16 | *glyK* | Glycerate kinase | 514761 - 515875 |
| 2, 4, 8, 9 | *putP* | sodium/proline symporter PutP | 1597688 - 1599214 |
| 15 | **no name** | Na+/H+ antiporter NhaC family protein | 143429 - 141909 |
| 5 | *hexR* | Previously: SIS domain-containing protein<br>Now: DNA-binding transcriptional regulator HexR | 719022 - 719870 |
| 14 | *prmA* | L11 ribosomal protein methyltransferase | 40522 - 39635 |

Through RATE[333], the region in which mutation was introduced was identified in each mutant (Table 6.1). Surprisingly, the result does not point towards a specific target gene. However, we have a higher percentage of mutants that have a mutation at the Glycerate Kinate (*glyK*) (8 out of 16) and sodium/proline symporter (*putP*) (4 out of 16) gene. The locus of these genes in *N.*

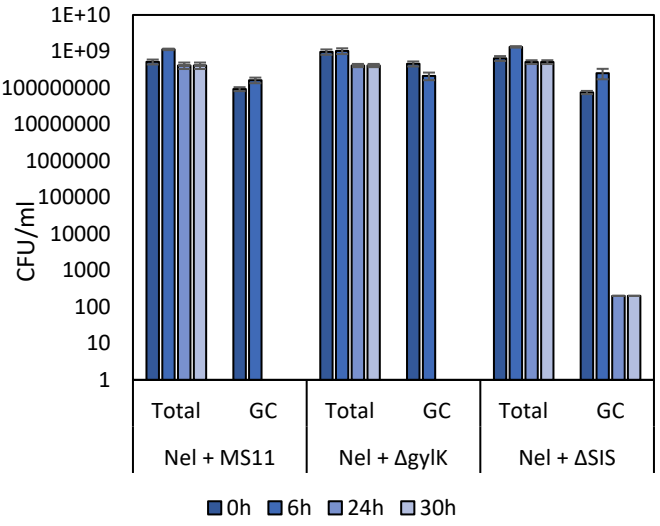


*Figure 6.12 Killing assay of reconstituted mutants, ΔglyK and ΔSIS*

*gonorrhoeae* genome can be found in the Tn5 mutagenesis library screening mutants locus. This observation provides us with some interesting information. We did not notice a consistent target for all the screening, meaning that the killing mechanism does not specifically target one gene. Instead, most of the mutations are in genes that are more likely metabolic-related than competence-related. This is good evidence that the killing mechanism may not entirely be DNA uptake-dependent and may be related to competition for essential metabolites.

Furthermore, even when it seems that the selected Tn5-mutants can survive *N. elongata* killing, it is always a concern that the effect we saw was due to unintended mutations in other sites of the genomic DNA or a polar effect from this specific mutation. The saturation of the Tn-5 mutagenesis library mutation rate could cause these effects. To ensure these mutated genes give rise to the phenotype of surviving *N. elongata* killing, we selected *glyK* and *SIS* (Figure 6.12). When we reconstituted ΔglyK and ΔSIS and checked them on killing assay, these mutants no longer survive. Therefore, the other possibility could be that the mutation in this gene affects downstream gene expression. When we check on their locus, we still observe mostly metabolic-centric genes. However, we recently found a new update on one of the downstream genes distantly related to the conjugation system. Nonetheless, we could not obtain a strong candidate through Tn5 mutagenesis library screening and could not conclude further.

### 6.1.7 Disc Test and Agar Inoculation Test

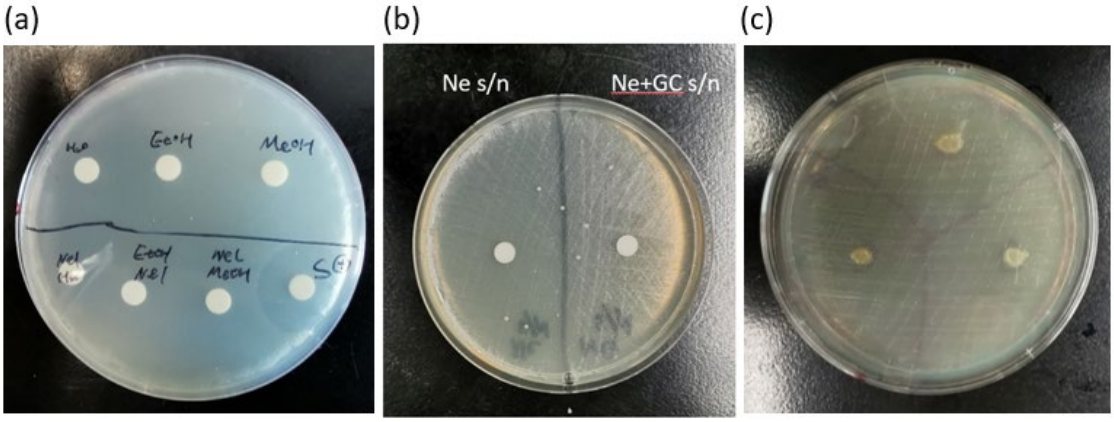


*Figure 6.13 (a) Disc test using extraction of Nel using water, ethanol or methanol. S+ is a positive control as an anti-GC in the lab (b) Disc test using mono- and co-culture supernatant (c) Inoculation of Nel in the middle of GC lawn*

The other methodology we employed to check if the killing factor is a molecule is through the disc test and an alternate test called the agar inoculation test. We have two sets of disc tests. In the first set, we utilized organic extraction of Nel through methanol and ethanol. We also have a sample of Nel in water, presumably lysed (Figure 6.13a). For the second set, we used concentrated medium from either *N. elongata* or *N. elongata* and *N. gonorrhoeae* co-culture (Figure 6.13b). Neither disc test showed any growth inhibition. For the agar inoculation test (Figure 6.13c), there was no growth inhibition of *N. gonorrhoeae* around the spot in which *N. elongata* was spotted. These observations showed that the killing factor was most likely not a small molecule. Together with previous results, it also seems that killing occurs only during liquid culture settings.

### 6.1.8 *N. gonorrhoeae* microcolonies are still intact during co-culture

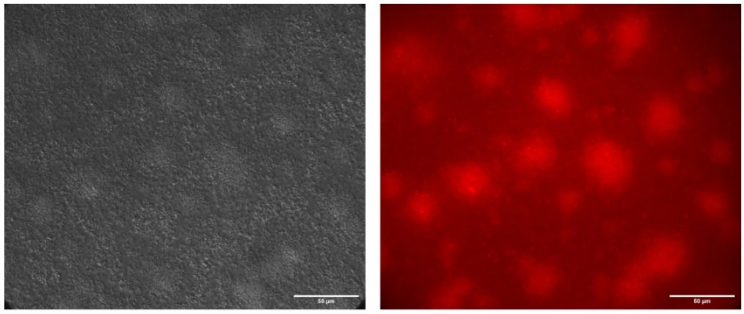

*Figure 6.14 DIC (left) and Fluorescence (right) images of 30h co-culture with Nel and GC constitutively expressing mCherry*

We turned towards microscopy to understand what happened to *N. gonorrhoeae* during the co-culture and how it died. We utilized a strain constitutively expressing mCherry under the *pilE* promoter. We kept the co-culture for 30h and observed the interaction between Nel and GC. Interestingly, we still see GC microcolonies, confirmed by the fluorescence (Figure 6.14). This is puzzling since we expected the microcolonies to disintegrate after being killed by Nel. When the culture was scraped out and selected on vancomycin selection plates, none of the GCs were viable.

### 6.1.9 Study on ATP concentration in GC and Nel

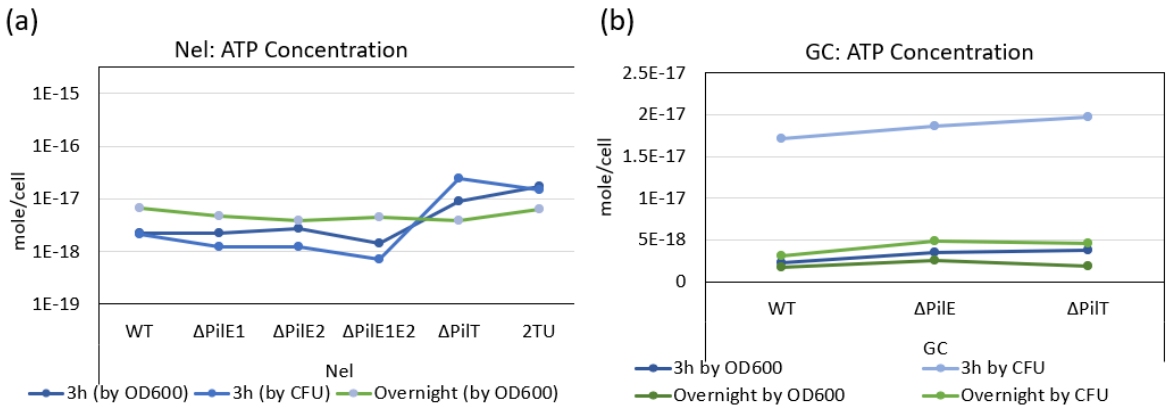


*Figure 6.15 ATP concentration in (a) Nel strains and (b) GC strains*

Another suspicion we had was that the survival of different GC strains may be due to their **metabolic state**. Although we didn't have enough resources to check their metabolic profiles, we tested an ATP assay on the strains in GC and Nel (Figure 6.15). In our experiment, it is interesting to see that there was no difference in the ATP per cell between strains in Nel, but

when the cells grow in liquid culture for three hours, we see one log difference for ΔPilT and 2TU. This makes sense since without the ATPases for pili retraction, more ATP are probably spared. However, we do not see the same in GC. Through all conditions and calculations, there seems to be no variation between strains in GC in terms of ATP per cell. This might mean that GC may possess some feedback regulation to normalize the ATP concentration in their cell even in the absence of pili retractions.

## 6.2 Discussion

In this chapter, although we started the study to determine the role of DNA uptake among *Neisserial* species, we started to suspect that this interaction and killing resulted from complex physiological factors. This study showed we can only observe the killing phenomenon in a particular condition. **The change in culture space, nutrient availability or method may help with GC survival.** The interaction altered the colony morphology of *N. elongata,* suggesting that *N. elongata* probably also responded to the presence of *N. gonorrhoeae*. It is also interesting to note that ***N. elongata*** **releases nucleic-acid-like molecules into the medium after prolonged incubation**. However, it is inconclusive if the content in the supernatant is potent enough to kill GC.

Regarding DNA uptake as the killing mechanism, we showed two examples other than pili mutants that implied that **DNA uptake may not be the primary mechanism**. The fact that we recovered no competence-defective mutant through Tn5 mutagenesis library screening also supports this. We also observed that **GC microcolonies do not disintegrate even after death in co-culture**. Our study points towards cell metabolism that leads to GC killing. However, we did not note any difference in ATP level in GC strains. We suggest that more studies should be done to prove this hypothesis.

# Chapter 7 : Conclusions and Perspectives

## 7.1 Conclusion

Natural transformation was discovered as early as 1928, but its exact mechanism and dynamics have not been fully elucidated to date. This thesis contributes to this body of knowledge from the perspective of the role of Type IV Pili in DNA transformation in *Neisseria gonorrhoeae*.

We first proposed useful **molecular biology techniques** in Chapter 2. With that we proposed a quantitative approach to DNA transformation study. On top of that, we contributed to the molecular biology field of *N. gonorrhoeae* a series of cloning techniques and strategies. These advancements will not only allow us to understand the basic molecular mechanisms of DNA transformation, but also opens up potential application in genetic engineering and treatment applications. We next developed **tools for microscopy** in DNA uptake study in Chapter 3. This study allows us to discover the importance of culture media development in *N. gonorrhoeae*. On top of that, we developed several assays that help us study DNA transformation and Type IV Pili, using uptake assay and micropillar system. With the tools, we can differentiate DNA uptake from transformation during analysis.

With the help of the developed tools, we study a few candidates: PilV, PilC, and PilD. Throughout the thesis, we discovered possible regulation of Type IV Pili and how this regulation can affect DNA uptake. We discovered that ΔPilV affects the translocation of PilE and lead to lesser and shorter pili. With that, we also discovered that shorter pili are most likely the more efficient way the bacteria can take up DNA. Therefore, ***N. gonorrhoeae* has probably evolved to accommodate its multi-function Type IV Pili by regulating the different types of pili expressed on its cell surface**. Discovering the role of near-cell surface pili in DNA uptake also shows that **several pili biogenesis events can occur at the cell surface**, especially when proven in our study in ΔPilC. It is also interesting to note that our studies on minor pilin result in changes in phenotype, yet they do not necessarily alter the pili retraction mechanics. In our PilV study, we learn about the impact of posttranslational modification of pilin on PilE localization. And yet, together with PilD mutants, we discovered that **Type IV Pili may not be as homogenous as we thought as a polymer**. Besides comprising major and minor pilins, it also encompasses pilins with different posttranslational modification landscapes. While under our study, the alteration in this landscape did not affect any of the pili retraction mechanics, showing the robustness and versatility of Type IV Pili as a polymer.

We close our thesis with a small study on the interaction of commensal and pathogenic *Neisseria* within the context of DNA uptake. Although we could not conclude from this study, it will be a great open question to those interested in dreaming of the vast opportunity DNA transformation study can bring to this field.

## 7.2 Perspective

This thesis brings several interesting aspects of DNA transformation and Type IV Pili in *N. gonorrhoeae*. At the end of the study, we also open up more questions and possible avenues for future research. For example, it will be interesting to ponder the impact of pili structures on their functionality. Do the long and short pili cooperate in getting tasks done for the bacteria? What is the purpose of posttranslational modification in pilin, and how does the cell regulate them? These are all worth questioning, and we are confident that someone somewhere in this world is trying to crack.

As a continuation of this study, we have a few recommendations.

**To further elucidate the role of PilV**, it would be helpful to investigate the protein-protein interaction between PilE an d PilV. Some of the possible methods we would suggest will be to studying PilV with a background with a point mutation at the Glu5 of PilE or an in vitro pulldown assay. Another way to identify if PilV's effect on pilin is the change in PilE posttranslational modification, is by performing pulse-chase experiments examining PilE modifications with inducible PilV. It will also be interesting to study the effects of pili length on DNA molecule mobility around cell body. This can be a great topic for numerical simulations. More studies should also be done to detail the DNA molecule activity inside the cell.

Since this thesis encompass a few aspects of DNA transformation in *N. gonorrhoeae*, there are several other recommendations in which we incorporated in each chapter's discussion. Finally, we hope this thesis convinced you that DNA transformation is interesting and ignited your curiosity after this read!

# Bibliography


1. Centers for Disease Control and Prevention (U.S.). *Antibiotic Resistance Threats in the United States, 2019*. https://stacks.cdc.gov/view/cdc/82532 (2019) doi:10.15620/cdc:82532.
2. Walsh, C. & Wencewicz, T. *Antibiotics: Challenges, Mechanisms, Opportunities*. (John Wiley & Sons, 2020).
3. Bader, J., Mast-Gerlach, E., Popović, M. K., Bajpai, R. & Stahl, U. Relevance of microbial coculture fermentations in biotechnology. *J. Appl. Microbiol.* **109**, 371–387 (2010).
4. Canon, F., Nidelet, T., Guédon, E., Thierry, A. & Gagnaire, V. Understanding the Mechanisms of Positive Microbial Interactions That Benefit Lactic Acid Bacteria Co-cultures. *Front. Microbiol.* **11**, (2020).
5. McLean, J. S. Advancements toward a systems level understanding of the human oral microbiome. *Front. Cell. Infect. Microbiol.* **4**, (2014).
6. Stubbendieck, R. M., Vargas-Bautista, C. & Straight, P. D. Bacterial Communities: Interactions to Scale. *Front. Microbiol.* **7**, (2016).
7. Xu, P. Dynamics of microbial competition, commensalism, and cooperation and its implications for coculture and microbiome engineering. *Biotechnol. Bioeng.* **118**, 199–209 (2021).
8. Hutchings, M. I., Truman, A. W. & Wilkinson, B. Antibiotics: past, present and future. *Curr. Opin. Microbiol.* **51**, 72–80 (2019).
9. Alberts, B. *Molecular Biology of the Cell*. (Garland Science, New York, 2014).
10. Neu, H. C. The Crisis in Antibiotic Resistance. *Science* **257**, 1064–1073 (1992).
11. Richter, J. H. ALBERT NEISSER Centenary of Birth 1855—January 22—1955. *AMA Arch. Dermatol.* **71**, 92–94 (1955).
12. Bosch, F. & Rosich, L. The Contributions of Paul Ehrlich to Pharmacology: A Tribute on the Occasion of the Centenary of His Nobel Prize. *Pharmacology* **82**, 171–179 (2008).
13. Williams, K. The introduction of 'chemotherapy' using arsphenamine – the first magic bullet. *J. R. Soc. Med.* **102**, 343–348 (2009).
14. Ehrlich, P. *The Experimental Chemotherapy of Spirilloses*. (Rebman, 1911).
15. Kawamura, I. Sahachiro Hata (1873-1938) and his contributions to the birth of antimicrobial chemotherapy. *J. Infect. Chemother.* **29**, 546–548 (2023).
16. Dowling, H. F. Comparisons and Contrasts Between the Early Arsphenamine and Early Antibiotic Periods. *Bull. Hist. Med.* **47**, 236–249 (1973).
17. Denyer, S. P., Hodges, N. A. & Gorman, S. P. Pharmaceutical Microbiology. (2004).
18. Zaffiri, L., Gardner, J. & Toledo-Pereyra, L. H. History of Antibiotics. From Salvarsan to Cephalosporins. *J. Invest. Surg.* **25**, 67–77 (2012).
19. Fleming, A. On the Antibacterial Action of Cultures of a Penicillium, with Special Reference to their Use in the Isolation of B. influenzæ. *Br. J. Exp. Pathol.* **10**, 226–236 (1929).
20. Abraham, E. P. *et al.* FURTHER OBSERVATIONS ON PENICILLIN. *The Lancet* **238**, 177–189 (1941).
21. Chain, E. *et al.* PENICILLIN AS A CHEMOTHERAPEUTIC AGENT. *The Lancet* **236**, 226–228 (1940).
22. Brack, P. Norman Heatley: the forgotten man of penicillin. *The Biochemist* **37**, 36–37 (2015).
23. Hamilton-Miller, J. M. T. Dr Norman Heatley. *J. Antimicrob. Chemother.* **53**, 691–692 (2004).

24. Moberg, C. L. Penicillin's forgotten man: Norman Heatley. *Science* **253**, 734–735 (1991).
25. Ho, N. C. Introduction to Emerging Areas in Bioengineering. in *Emerging Areas in Bioengineering* 3–20 (John Wiley & Sons, Ltd, 2018). doi:10.1002/9783527803293.ch1.
26. Short, B. Antibacterial warfare: The production of natural penicillin and the search for synthetic penicillin during the second world war. *J. Mil. Veterans Health* **29**, 36–42 (2021).
27. Currie, G. M. Pharmacology, Part 1: Introduction to Pharmacology and Pharmacodynamics. *J. Nucl. Med. Technol.* **46**, 81–86 (2018).
28. Bush, K. *et al.* Tackling antibiotic resistance. *Nat. Rev. Microbiol.* **9**, 894–896 (2011).
29. Munita, J. M. & Arias, C. A. Mechanisms of Antibiotic Resistance. in *Virulence Mechanisms of Bacterial Pathogens* (eds. Kudva, I. T. et al.) 481–511 (ASM Press, Washington, DC, USA, 2016). doi:10.1128/9781555819286.ch17.
30. Yoneyama, H. & Katsumata, R. Antibiotic Resistance in Bacteria and Its Future for Novel Antibiotic Development. *Biosci. Biotechnol. Biochem.* **70**, 1060–1075 (2006).
31. Barrett, T. C., Mok, W. W. K., Murawski, A. M. & Brynildsen, M. P. Enhanced antibiotic resistance development from fluoroquinolone persisters after a single exposure to antibiotic. *Nat. Commun.* **10**, 1177 (2019).
32. Høiby, N., Bjarnsholt, T., Givskov, M., Molin, S. & Ciofu, O. Antibiotic resistance of bacterial biofilms. *Int. J. Antimicrob. Agents* **35**, 322–332 (2010).
33. Lewis, K. Persister cells, dormancy and infectious disease. *Nat. Rev. Microbiol.* **5**, 48–56 (2007).
34. Lewis, K. Multidrug tolerance of biofilms and persister cells. *Curr. Top. Microbiol. Immunol.* **322**, 107–131 (2008).
35. Mah, T.-F. Biofilm-specific antibiotic resistance. *Future Microbiol.* **7**, 1061–1072 (2012).
36. Wood, T. K., Knabel, S. J. & Kwan, B. W. Bacterial Persister Cell Formation and Dormancy. *Appl. Environ. Microbiol.* **79**, 7116–7121 (2013).
37. Unemo, M. & Shafer, W. M. Antimicrobial Resistance in Neisseria gonorrhoeae in the 21st Century: Past, Evolution, and Future. *Clin. Microbiol. Rev.* **27**, 587–613 (2014).
38. Blomquist, P. B., Miari, V. F., Biddulph, J. P. & Charalambous, B. M. Is gonorrhea becoming untreatable? *Future Microbiol.* **9**, 189–201 (2014).
39. Ohnishi, M. *et al.* Is Neisseria gonorrhoeae Initiating a Future Era of Untreatable Gonorrhea?: Detailed Characterization of the First Strain with High-Level Resistance to Ceftriaxone ▿ . *Antimicrob. Agents Chemother.* **55**, 3538–3545 (2011).
40. Kenyon, C., Laumen, J. & Manoharan-Basil, S. Choosing New Therapies for Gonorrhoea: We Need to Consider the Impact on the Pan-Neisseria Genome. A Viewpoint. *Antibiotics* **10**, 515 (2021).
41. Brives, C. & Pourraz, J. Phage therapy as a potential solution in the fight against AMR: obstacles and possible futures. *Palgrave Commun.* **6**, 1–11 (2020).
42. Lin, D. M., Koskella, B. & Lin, H. C. Phage therapy: An alternative to antibiotics in the age of multi-drug resistance. *World J. Gastrointest. Pharmacol. Ther.* **8**, 162–173 (2017).
43. Pirnay, J.-P. Phage Therapy in the Year 2035. *Front. Microbiol.* **11**, (2020).
44. Bucheli, J. E. V., Fugaban, J. I. I., Holzapfel, W. H. & Todorov, S. D. Combined Action of Antibiotics and Bacteriocins against Vancomycin-Resistant Enterococci. *Microorganisms* **10**, 1423 (2022).
45. Gradisteanu Pircalabioru, G. *et al.* Bacteriocins in the Era of Antibiotic Resistance: Rising to the Challenge. *Pharmaceutics* **13**, 196 (2021).
46. Nami, Y. *et al.* Probiotics or antibiotics: future challenges in medicine. *J. Med. Microbiol.* **64**, 137–146 (2015).
47. Silva, D. R. *et al.* Probiotics as an alternative antimicrobial therapy: Current reality and future directions. *J. Funct. Foods* **73**, 104080 (2020).

48. C, S. *et al.* Advances and perspectives for antimicrobial peptide and combinatory therapies. *Front. Bioeng. Biotechnol.* **10**, 1051456 (2022).
49. Rima, M. *et al.* Antimicrobial Peptides: A Potent Alternative to Antibiotics. *Antibiot. Basel Switz.* **10**, 1095 (2021).
50. Foo, J. L., Ling, H., Lee, Y. S. & Chang, M. W. Microbiome engineering: Current applications and its future. *Biotechnol. J.* **12**, 1600099 (2017).
51. Kali, A. Human Microbiome Engineering: The Future and Beyond. *J. Clin. Diagn. Res. JCDR* **9**, DE01–DE04 (2015).
52. Shapiro, B. J. How clonal are bacteria over time? *Curr. Opin. Microbiol.* **31**, 116–123 (2016).
53. Arnold, B. J., Huang, I.-T. & Hanage, W. P. Horizontal gene transfer and adaptive evolution in bacteria. *Nat. Rev. Microbiol.* **20**, 206–218 (2022).
54. Goyal, A. Horizontal gene transfer drives the evolution of dependencies in bacteria. *iScience* **25**, 104312 (2022).
55. Hall, R. J., Whelan, F. J., McInerney, J. O., Ou, Y. & Domingo-Sananes, M. R. Horizontal Gene Transfer as a Source of Conflict and Cooperation in Prokaryotes. *Front. Microbiol.* **11**, (2020).
56. Lee, I. P. A., Eldakar, O. T., Gogarten, J. P. & Andam, C. P. Bacterial cooperation through horizontal gene transfer. *Trends Ecol. Evol.* **0**, (2021).
57. Boto, L. Horizontal gene transfer in evolution: facts and challenges. *Proc. R. Soc. B Biol. Sci.* **277**, 819–827 (2009).
58. Emamalipour, M. *et al.* Horizontal Gene Transfer: From Evolutionary Flexibility to Disease Progression. *Front. Cell Dev. Biol.* **8**, (2020).
59. Sun, D. Pull in and Push Out: Mechanisms of Horizontal Gene Transfer in Bacteria. *Front. Microbiol.* **9**, 2154 (2018).
60. Beltran, L. C. *et al.* Archaeal DNA-import apparatus is homologous to bacterial conjugation machinery. *Nat. Commun.* **14**, 666 (2023).
61. Lederberg, J. & Tatum, E. L. Gene Recombination in Escherichia Coli. *Nature* **158**, 558–558 (1946).
62. Avery, O. T., MacLeod, C. M. & McCarty, M. STUDIES ON THE CHEMICAL NATURE OF THE SUBSTANCE INDUCING TRANSFORMATION OF PNEUMOCOCCAL TYPES. *J. Exp. Med.* **79**, 137–158 (1944).
63. Davis, B. D. Nonfiltrability of the agents of genetic recombination in Escherichia coli. *J. Bacteriol.* **60**, 507–508 (1950).
64. Lederberg, J., Cavalli, L. L. & Lederberg, E. M. Sex Compatibility in Escherichia Coli. *Genetics* **37**, 720–730 (1952).
65. Johnson, C. M. & Grossman, A. D. Integrative and Conjugative Elements (ICEs): What They Do and How They Work. *Annu. Rev. Genet.* **49**, 577–601 (2015).
66. Filloux, A. A Variety of Bacterial Pili Involved in Horizontal Gene Transfer. *J. Bacteriol.* **192**, 3243–3245 (2010).
67. Virolle, C., Goldlust, K., Djermoun, S., Bigot, S. & Lesterlin, C. Plasmid Transfer by Conjugation in Gram-Negative Bacteria: From the Cellular to the Community Level. *Genes* **11**, 1239 (2020).
68. Zinder, N. D. & Lederberg, J. GENETIC EXCHANGE IN SALMONELLA. *J. Bacteriol.* **64**, 679–699 (1952).
69. Schneider, C. L. Bacteriophage-Mediated Horizontal Gene Transfer: Transduction. in *Bacteriophages* (eds. Harper, D., Abedon, S., Burrowes, B. & McConville, M.) 1–42 (Springer International Publishing, Cham, 2017). doi:10.1007/978-3-319-40598-8_4-1.
70. The Nobel Prize in Physiology or Medicine 1958. *NobelPrize.org* https://www.nobelprize.org/prizes/medicine/1958/summary/.

71. Griffith, F. The Significance of Pneumococcal Types. *J. Hyg. (Lond.)* **27**, 113–159 (1928).
72. Dawson, M. H. THE TRANSFORMATION OF PNEUMOCOCCAL TYPES. *J. Exp. Med.* **51**, 123–147 (1930).
73. Dawson, M. H. & Sia, R. H. P. IN VITRO TRANSFORMATION OF PNEUMOCOCCAL TYPES. *J. Exp. Med.* **54**, 681–699 (1931).
74. Dubnau, D. DNA Uptake in Bacteria. *Annu. Rev. Microbiol.* **53**, 217–244 (1999).
75. Johnston, C., Martin, B., Fichant, G., Polard, P. & Claverys, J.-P. Bacterial transformation: distribution, shared mechanisms and divergent control. *Nat. Rev. Microbiol.* **12**, 181–196 (2014).
76. Kulkarni, R. *et al.* Roles of Putative Type II Secretion and Type IV Pilus Systems in the Virulence of Uropathogenic Escherichia coli. *PLoS ONE* **4**, e4752 (2009).
77. Blokesch, M. Natural competence for transformation. *Curr. Biol.* **26**, R1126–R1130 (2016).
78. Finkel, S. E. & Kolter, R. DNA as a Nutrient: Novel Role for Bacterial Competence Gene Homologs. *J. Bacteriol.* **183**, 6288–6293 (2001).
79. Abe, K., Nomura, N. & Suzuki, S. Biofilms: hot spots of horizontal gene transfer (HGT) in aquatic environments, with a focus on a new HGT mechanism. *FEMS Microbiol. Ecol.* **96**, fiaa031 (2020).
80. Bárdy, P. *et al.* Structure and mechanism of DNA delivery of a gene transfer agent. *Nat. Commun.* **11**, 3034 (2020).
81. Dubey, G. P. & Ben-Yehuda, S. Intercellular Nanotubes Mediate Bacterial Communication. *Cell* **144**, 590–600 (2011).
82. Lang, A. S., Zhaxybayeva, O. & Beatty, J. T. Gene transfer agents: phage-like elements of genetic exchange. *Nat. Rev. Microbiol.* **10**, 472–482 (2012).
83. Jose, P. P., Vivekanandan, V. & Sobhanakumari, K. Gonorrhea: Historical outlook. *J. Skin Sex. Transm. Dis.* **2**, 110–114 (2020).
84. Tulchinsky, T. H. & Varavikova, E. A. A History of Public Health. *New Public Health* 1–42 (2014) doi:10.1016/B978-0-12-415766-8.00001-X.
85. Kolmer, J. A. & Brown, C. P. Complement-Fixation in Gonococcus Infections. *J. Infect. Dis.* **15**, 6–21 (1914).
86. Chacko, C. W. & Nair, G. M. Chacko-Nair egg-enriched selective medium in the diagnosis of pathogenic Neisseriae. *Br. J. Vener. Dis.* **44**, 67–71 (1968).
87. Gould, R. G., Kane, L. W. & Mueller, J. H. On the Growth Requirements of Neisseria Gonorrhoeae. *J. Bacteriol.* **47**, 287–292 (1944).
88. Mueller, J. H. & Hinton, J. A Protein-Free Medium for Primary Isolation of the Gonococcus and Meningococcus. *Exp. Biol. Med.* **48**, 330–333 (1941).
89. Vedder, E. B. Starch Agar, A Useful Culture Medium. *J. Infect. Dis.* **16**, 385–388 (1915).
90. Stuart, R. D. The Diagnosis and Control of Gonorrhoea by Bacteriological Cultures. *Glasg. Med. J.* **27**, 131–142 (1946).
91. Ebright, J. R. *et al.* Evaluation of Modified Stuart's Medium in Culturettes ® for Transport of Neisseria gonorrhoeae. *Sex. Transm. Dis.* **9**, 45–47 (1982).
92. Ng, L.-K. & Martin, I. E. The laboratory diagnosis of Neisseria gonorrhoeae. *Can. J. Infect. Dis. Med. Microbiol.* **16**, 15–25 (2005).
93. Kirkcaldy, R. D., Weston, E., Segurado, A. C. & Hughes, G. Epidemiology of Gonorrhea: A Global Perspective. *Sex. Health* **16**, 401–411 (2019).
94. Green, L. R., Cole, J., Parga, E. F. D. & Shaw, J. G. Neisseria gonorrhoeae physiology and pathogenesis. in *Advances in Microbial Physiology* vol. 80 35–83 (Elsevier, 2022).
95. Walker, E., van Niekerk, S., Hanning, K., Kelton, W. & Hicks, J. Mechanisms of host manipulation by Neisseria gonorrhoeae. *Front. Microbiol.* **14**, 1119834 (2023).

96. Virji, M. Pathogenic neisseriae: surface modulation, pathogenesis and infection control. *Nat. Rev. Microbiol.* **7**, 274–286 (2009).
97. Mahapure, K. & Singh, A. A Review of Recent Advances in Our Understanding of Neisseria gonorrhoeae. *Cureus* **15**, e43464.
98. Griffiss, J. M. *et al.* The immunochemistry of neisserial LOS. *Antonie Van Leeuwenhoek* **53**, 501–507 (1987).
99. Griffiss, J. M. *et al.* Lipooligosaccharides: The Principal Glycolipids of the Neisserial Outer Membrane. *Rev. Infect. Dis.* **10**, S287–S295 (1988).
100. Mubaiwa, T. D. *et al.* The sweet side of the pathogenic Neisseria: the role of glycan interactions in colonisation and disease. *Pathog. Dis.* **75**, ftx063 (2017).
101. Muenzner, P. & Hauck, C. R. Neisseria gonorrhoeae Blocks Epithelial Exfoliation by Nitric-Oxide-Mediated Metabolic Cross Talk to Promote Colonization in Mice. *Cell Host Microbe* **27**, 793-808.e5 (2020).
102. Potter, A. D. & Criss, A. K. Dinner date: *Neisseria gonorrhoeae* central carbon metabolism and pathogenesis. *Emerg. Top. Life Sci.* ETLS20220111 (2023) doi:10.1042/ETLS20220111.
103. Seifert, H. S. Location, Location, Location—Commensalism, Damage and Evolution of the Pathogenic Neisseria. *J. Mol. Biol.* **431**, 3010–3014 (2019).
104. Johnson, M. B. & Criss, A. Resistance of Neisseria Gonorrhoeae to Neutrophils. *Front. Microbiol.* **2**, (2011).
105. Stohl, E. A., Dale, E. M., Criss, A. K. & Seifert, H. S. Neisseria gonorrhoeae Metalloprotease NGO1686 Is Required for Full Piliation, and Piliation Is Required for Resistance to H2O2- and Neutrophil-Mediated Killing. *mBio* **4**, e00399-13 (2013).
106. Chen, A. & Seifert, H. S. Structure-Function Studies of the Neisseria gonorrhoeae Major Outer Membrane Porin. *Infect. Immun.* **81**, 4383–4391 (2013).
107. Liu, Y., Liu, W. & Russell, M. W. Suppression of host adaptive immune responses by Neisseria gonorrhoeae: role of interleukin 10 and type 1 regulatory T cells. *Mucosal Immunol.* **7**, 165–176 (2014).
108. Dubnau, D. & Blokesch, M. Mechanisms of DNA Uptake by Naturally Competent Bacteria. *Annu. Rev. Genet.* **53**, 217–237 (2019).
109. Matthey, N. & Blokesch, M. The DNA-Uptake Process of Naturally Competent Vibrio cholerae. *Trends Microbiol.* **24**, 98–110 (2016).
110. Veening, J.-W. & Blokesch, M. Interbacterial predation as a strategy for DNA acquisition in naturally competent bacteria. *Nat. Rev. Microbiol.* **15**, 621–629 (2017).
111. Seitz, P. & Blokesch, M. DNA Transport across the Outer and Inner Membranes of Naturally Transformable Vibrio cholerae Is Spatially but Not Temporally Coupled. *mBio* **5**, e01409-14 (2014).
112. Hamilton, H. L. & Dillard, J. P. Natural transformation of *Neisseria gonorrhoeae* : from DNA donation to homologous recombination: Natural transformation of *Neisseria gonorrhoeae*. *Mol. Microbiol.* **59**, 376–385 (2006).
113. Mell, J. C. & Redfield, R. J. Natural Competence and the Evolution of DNA Uptake Specificity. *J. Bacteriol.* **196**, 1471–1483 (2014).
114. Piepenbrink, K. H. DNA Uptake by Type IV Filaments. *Front. Mol. Biosci.* **6**, 1 (2019).
115. Chen, I. & Dubnau, D. DNA uptake during bacterial transformation. *Nat. Rev. Microbiol. 2004 23* **2**, 241–249 (2004).
116. Berry, J.-L. & Pelicic, V. Exceptionally widespread nanomachines composed of type IV pilins: the prokaryotic Swiss Army knives. *FEMS Microbiol. Rev.* **39**, 134–154 (2015).
117. Facius, D., Fussenegger, M. & Meyer, T. F. Sequential action of factors involved in natural competence for transformation of Neisseria gonorrhoeae. *FEMS Microbiol. Lett.* **37**, 159–164 (1996).

118. Hepp, C. & Maier, B. Kinetics of DNA uptake during transformation provide evidence for a translocation ratchet mechanism. *Proc. Natl. Acad. Sci.* **113**, 12467–12472 (2016).
119. Obergfell, K. P. & Seifert, H. S. Mobile DNA in the Pathogenic *Neisseria*. *Microbiol. Spectr.* **3**, 3.1.07 (2015).
120. Hepp, C., Gangel, H., Henseler, K., Günther, N. & Maier, B. Single-Stranded DNA Uptake during Gonococcal Transformation. *J. Bacteriol.* **198**, 2515–2523 (2016).
121. Chaussee, M. S. & Hill, S. A. Formation of Single-Stranded DNA during DNA Transformation of *Neisseria gonorrhoeae*. *J. Bacteriol.* **180**, 5117–5122 (1998).
122. Sharma, D. K., Misra, H. S., Bihani, S. C. & Rajpurohit, Y. S. Biochemical Properties and Roles of DprA Protein in Bacterial Natural Transformation, Virulence, and Pilin Variation. *J. Bacteriol.* **205**, e00465-22 (2023).
123. Beyene, G. T., Kalayou, S., Riaz, T. & Tonjum, T. Comparative proteomic analysis of Neisseria meningitidis wildtype and dprA null mutant strains links DNA processing to pilus biogenesis. *BMC Microbiol.* **17**, 96 (2017).
124. Mortier-Barrière, I. *et al.* A Key Presynaptic Role in Transformation for a Widespread Bacterial Protein: DprA Conveys Incoming ssDNA to RecA. *Cell* **130**, 824–836 (2007).
125. Duffin, P. M. & Barber, D. A. DprA is required for natural transformation and affects pilin variation in Neisseria gonorrhoeae. *Microbiology* **162**, 1620–1628 (2016).
126. Giltner, C. L., Nguyen, Y. & Burrows, L. L. Type IV Pilin Proteins: Versatile Molecular Modules. *Microbiol. Mol. Biol. Rev.* **76**, 740–772 (2012).
127. Van Gerven, N., Waksman, G. & Remaut, H. Chapter 2 - Pili and Flagella: Biology, Structure, and Biotechnological Applications. in *Progress in Molecular Biology and Translational Science* (ed. Howorka, S.) vol. 103 21–72 (Academic Press, 2011).
128. Craig, L. & Li, J. Type IV pili: paradoxes in form and function. *Curr. Opin. Struct. Biol.* **18**, 267–277 (2008).
129. Ellison, C. K., Whitfield, G. B. & Brun, Y. V. Type IV Pili: dynamic bacterial nanomachines. *FEMS Microbiol. Rev.* **46**, fuab053 (2022).
130. Melville, S. & Craig, L. Type IV Pili in Gram-Positive Bacteria. *Microbiol. Mol. Biol. Rev.* **77**, 323–341 (2013).
131. Persat, A. *et al.* The Mechanical World of Bacteria. *Cell* **161**, 988–997 (2015).
132. Kühn, M. J. *et al.* Two antagonistic response regulators control Pseudomonas aeruginosa polarization during mechanotaxis. *EMBO J.* **42**, e112165 (2023).
133. Kühn, M. J. *et al.* Mechanotaxis directs Pseudomonas aeruginosa twitching motility. *Proc. Natl. Acad. Sci. U. S. A.* **118**, e2101759118 (2021).
134. Mordue, J., O'Boyle, N., Gadegaard, N. & Roe, A. J. The force awakens: The dark side of mechanosensing in bacterial pathogens. *Cell. Signal.* **78**, 109867 (2021).
135. Webster, S. S., Wong, G. C. L. & O'Toole, G. A. The Power of Touch: Type 4 Pili, the von Willebrand A Domain, and Surface Sensing by Pseudomonas aeruginosa. *J. Bacteriol.* **204**, e00084-22 (2022).
136. Craig, L., Forest, K. T. & Maier, B. Type IV pili: dynamics, biophysics and functional consequences. *Nat. Rev. Microbiol.* **17**, 429–440 (2019).
137. Laurenceau, R. *et al.* A Type IV Pilus Mediates DNA Binding during Natural Transformation in Streptococcus pneumoniae. *PLoS Pathog.* **9**, e1003473 (2013).
138. Kirchner, L. & Averhoff, B. DNA binding by pilins and their interaction with the inner membrane platform of the DNA transporter in Thermus thermophilus. *Biochim. Biophys. Acta BBA - Biomembr.* **1864**, 183818 (2022).
139. Depelteau, J. S., Brenzinger, S. & Briegel, A. Bacterial and Archaeal Cell Structure. in *Encyclopedia of Microbiology (Fourth Edition)* (ed. Schmidt, T. M.) 348–360 (Academic Press, Oxford, 2019). doi:10.1016/B978-0-12-809633-8.20679-1.

140. Jacobsen, T., Bardiaux, B., Francetic, O., Izadi-Pruneyre, N. & Nilges, M. Structure and function of minor pilins of type IV pili. *Med. Microbiol. Immunol. (Berl.)* **209**, 301–308 (2020).
141. Higashi, D. L. *et al.* Dynamics of Neisseria gonorrhoeae Attachment: Microcolony Development, Cortical Plaque Formation, and Cytoprotection. *Infect. Immun.* **75**, 4743–4753 (2007).
142. Hockenberry, A. M., Hutchens, D. M., Agellon, A. & So, M. Attenuation of the Type IV Pilus Retraction Motor Influences Neisseria gonorrhoeae Social and Infection Behavior. *mBio* **7**, e01994-16 (2016).
143. Howie, H. L., Glogauer, M. & So, M. The N. gonorrhoeae Type IV Pilus Stimulates Mechanosensitive Pathways and Cytoprotection through a pilT-Dependent Mechanism. *PLOS Biol.* **3**, e100 (2005).
144. Taktikos, J., Lin, Y. T., Stark, H., Biais, N. & Zaburdaev, V. Pili-Induced Clustering of N. gonorrhoeae Bacteria. *PLOS ONE* **10**, e0137661 (2015).
145. Berry, J.-L. *et al.* Structure and Assembly of a Trans-Periplasmic Channel for Type IV Pili in Neisseria meningitidis. *PLoS Pathog.* **8**, e1002923 (2012).
146. Siewering, K. *et al.* Peptidoglycan-binding protein TsaP functions in surface assembly of type IV pili. *Proc. Natl. Acad. Sci. U. S. A.* **111**, E953–E961 (2014).
147. Biais, N., Ladoux, B., Higashi, D., So, M. & Sheetz, M. Cooperative Retraction of Bundled Type IV Pili Enables Nanonewton Force Generation. *PLoS Biol.* **6**, e87 (2008).
148. Hockenberry, A. M., Post, D. M. B., Rhodes, K. A., Apicella, M. & So, M. Perturbing the acetylation status of the Type IV pilus retraction motor, PilT, reduces Neisseria gonorrhoeae viability. *Mol. Microbiol.* **110**, 677–688 (2018).
149. McCallum, M. *et al.* Multiple conformations facilitate PilT function in the type IV pilus. *Nat. Commun.* **10**, 5198 (2019).
150. McCallum, M., Burrows, L. L. & Howell, P. L. The Dynamic Structures of the Type IV Pilus. *Microbiol. Spectr.* **7**, 7.2.02 (2019).
151. Wang, F. *et al.* Cryoelectron Microscopy Reconstructions of the Pseudomonas aeruginosa and Neisseria gonorrhoeae Type IV Pili at Sub-nanometer Resolution. *Structure* **25**, 1423-1435.e4 (2017).
152. Kolappan, S. *et al.* Structure of the Neisseria meningitidis Type IV pilus. *Nat. Commun.* **7**, 13015 (2016).
153. Kilmury, S. L. N. & Burrows, L. L. Type IV pilins regulate their own expression via direct intramembrane interactions with the sensor kinase PilS. *Proc. Natl. Acad. Sci.* **113**, 6017–6022 (2016).
154. Kuchma, S. L. & O'Toole, G. A. Surface-Induced cAMP Signaling Requires Multiple Features of the Pseudomonas aeruginosa Type IV Pili. *J. Bacteriol.* **204**, e00186-22 (2022).
155. Reardon, P. N. & Mueller, K. T. Structure of the Type IVa Major Pilin from the Electrically Conductive Bacterial Nanowires of Geobacter sulfurreducens*. *J. Biol. Chem.* **288**, 29260–29266 (2013).
156. Parge, H. E. *et al.* Structure of the fibre-forming protein pilin at 2.6 Å resolution. *Nature* **378**, 32–38 (1995).
157. Parge, H. E. *et al.* Biochemical purification and crystallographic characterization of the fiber-forming protein pilin from Neisseria gonorrhoeae. *J. Biol. Chem.* **265**, 2278–2285 (1990).
158. Winther-Larsen, H. C. *et al. Neisseria gonorrhoeae* PilV, a type IV pilus-associated protein essential to human epithelial cell adherence. *Proc. Natl. Acad. Sci.* **98**, 15276–15281 (2001).

159. Wolfgang, M., van Putten, J. P. M., Hayes, S. F. & Koomey, M. The comP locus of Neisseria gonorrhoeae encodes a type IV prepilin that is dispensable for pilus biogenesis but essential for natural transformation. *Mol. Microbiol.* **31**, 1345–1357 (1999).
160. Vik, Å. *et al.* Type IV Pilus Assembly Proficiency and Dynamics Influence Pilin Subunit Phospho-Form Macro- and Microheterogeneity in Neisseria gonorrhoeae. *PLoS ONE* **9**, e96419 (2014).
161. Hegge, F. T. *et al.* Unique modifications with phosphocholine and phosphoethanolamine define alternate antigenic forms of Neisseria gonorrhoeae type IV pili. *Proc. Natl. Acad. Sci. U. S. A.* **101**, 10798–10803 (2004).
162. Aas, F. E. *et al.* Neisseria gonorrhoeae Type IV Pili Undergo Multisite, Hierarchical Modifications with Phosphoethanolamine and Phosphocholine Requiring an Enzyme Structurally Related to Lipopolysaccharide Phosphoethanolamine Transferases. *J. Biol. Chem.* **281**, 27712–27723 (2006).
163. Barnier, J. P. *et al.* The minor pilin PilV provides a conserved adhesion site throughout the antigenically variable meningococcal type IV pilus. *Proc. Natl. Acad. Sci. U. S. A.* **118**, (2021).
164. Aas, F. E., Løvold, C. & Koomey, M. An inhibitor of DNA binding and uptake events dictates the proficiency of genetic transformation in Neisseria gonorrhoeae: mechanism of action and links to Type IV pilus expression. *Mol. Microbiol.* **46**, 1441–1450 (2002).
165. Gangel, H. *et al.* Concerted Spatio-Temporal Dynamics of Imported DNA and ComE DNA Uptake Protein during Gonococcal Transformation. *PLoS Pathog.* **10**, e1004043 (2014).
166. Imhaus, A. & Duménil, G. The number of *Neisseria meningitidis* type IV pili determines host cell interaction. *EMBO J.* **33**, 1767–1783 (2014).
167. Rudel, T. *et al.* Role of pili and the phase-variable PilC protein in natural competence for transformation of Neisseria gonorrhoeae. *Proc. Natl. Acad. Sci.* **92**, 7986–7990 (1995).
168. Boyle, E. C. & Finlay, B. B. Bacterial pathogenesis: exploiting cellular adherence. *Curr. Opin. Cell Biol.* **15**, 633–639 (2003).
169. Rudel, T., Putten, J. P. M., Gibbs, C. P., Haas, R. & Meyer, T. F. Interaction of two variable proteins (PilE and PilC) required for pilus-mediated adherence of Neisseria gonorrhoeae to human epithelial cells. *Mol. Microbiol.* **6**, 3439–3450 (1992).
170. Rudel, T., Scheuerpflug, I. & Meyer, T. F. Neisseria PilC protein identified as type-4 pilus tip-located adhesin. *Nature* **373**, 357–359 (1995).
171. Kirchner, M. & Meyer, T. F. The PilC adhesin of the Neisseria type IV pilus - binding specificities and new insights into the nature of the host cell receptor: Neisseria type IV pilus receptor. *Mol. Microbiol.* **56**, 945–957 (2005).
172. Lambden Paul, R., Robertson Janet, N. & Watt Peter, J. Y. 1981. The Preparation and Properties of α and β Pili from Variants of Neisseria gonorrhoeae P9. *Microbiology* **124**, 109–117 (1981).
173. Virji, M. & Everson, J. S. Comparative virulence of opacity variants of Neisseria gonorrhoeae strain P9. *Infect. Immun.* **31**, 965–970 (1981).
174. Jonsson, A. B., Nyberg, G. & Normark, S. Phase variation of gonococcal pili by frameshift mutation in pilC, a novel gene for pilus assembly. *EMBO J.* **10**, 477–488 (1991).
175. Jonsson, A.-B., Ilver, D., Falk, P., Pepose, J. & Normark, S. Sequence changes in the pilus subunit lead to tropism variation of Neisseria gonorrhoeae to human tissue. *Mol. Microbiol.* **13**, 403–416 (1994).
176. Morand, P. C., Tattevin, P., Eugene, E., Beretti, J.-L. & Nassif, X. The adhesive property of the type IV pilus-associated component PilC1 of pathogenic Neisseria is supported by the conformational structure of the N-terminal part of the molecule. *Mol. Microbiol.* **40**, 846–856 (2001).

177. Nassif, X. *et al.* Roles of pilin and PilC in adhesion of Neisseria meningitidis to human epithelial and endothelial cells. *Proc. Natl. Acad. Sci.* **91**, 3769–3773 (1994).
178. Morand, P. C., Drab, M., Rajalingam, K., Nassif, X. & Meyer, T. F. Neisseria meningitidis differentially controls host cell motility through PilC1 and PilC2 components of type IV Pili. *PloS One* **4**, e6834 (2009).
179. Morand, P. C. *et al.* Type IV pilus retraction in pathogenic Neisseria is regulated by the PilC proteins. *EMBO J.* **23**, 2009–2017 (2004).
180. Taha, M.-K. *et al.* Pilus-mediated adhesion of Neisseria meningitidis: the essential role of cell contact-dependent transcriptional upregulation of the PilC1 protein. *Mol. Microbiol.* **28**, 1153–1163 (1998).
181. Leighton, T. L., Buensuceso, R. N. C., Howell, P. L. & Burrows, L. L. Biogenesis of Pseudomonas aeruginosa type IV pili and regulation of their function. *Environ. Microbiol.* **17**, 4148–4163 (2015).
182. Webster, S. S. *et al.* Force-Induced Changes of PilY1 Drive Surface Sensing by Pseudomonas aeruginosa. *mBio* **13**, e03754-21 (2022).
183. Orans, J. *et al.* Crystal structure analysis reveals Pseudomonas PilY1 as an essential calcium-dependent regulator of bacterial surface motility. *Proc. Natl. Acad. Sci. U. S. A.* **107**, 1065–1070 (2010).
184. Kehl-Fie, T. E., Miller, S. E. & St Geme, J. W. Kingella kingae expresses type IV pili that mediate adherence to respiratory epithelial and synovial cells. *J. Bacteriol.* **190**, 7157–7163 (2008).
185. Nunn, D. N. & Lory, S. Product of the Pseudomonas aeruginosa gene pilD is a prepilin leader peptidase. *Proc. Natl. Acad. Sci.* **88**, 3281–3285 (1991).
186. Strom, M. S., Nunn, D. N. & Lory, S. A single bifunctional enzyme, PilD, catalyzes cleavage and N-methylation of proteins belonging to the type IV pilin family. *Proc. Natl. Acad. Sci. U. S. A.* **90**, 2404–2408 (1993).
187. Lory, S. & Strom, M. S. Structure-function relationship of type-IV prepilin peptidase of Pseudomonas aeruginosa – a review. *Gene* **192**, 117–121 (1997).
188. Pepe, J. C. & Lory, S. Amino Acid Substitutions in PilD, a Bifunctional Enzyme ofPseudomonas aeruginosa. *J. Biol. Chem.* **273**, 19120–19129 (1998).
189. Nunn, D., Bergman, S. & Lory, S. Products of three accessory genes, pilB, pilC, and pilD, are required for biogenesis of Pseudomonas aeruginosa pili. *J. Bacteriol.* **172**, 2911–2919 (1990).
190. Dupuy, B. & Pugsley, A. P. Type IV prepilin peptidase gene of Neisseria gonorrhoeae MS11: presence of a related gene in other piliated and nonpiliated Neisseria strains. *J. Bacteriol.* **176**, 1323–1331 (1994).
191. Helaine, S., Dyer, D. H., Nassif, X., Pelicic, V. & Forest, K. T. 3D structure/function analysis of PilX reveals how minor pilins can modulate the virulence properties of type IV pili. *Proc. Natl. Acad. Sci.* **104**, 15888–15893 (2007).
192. Bally, M., Ball, G., Badere, A. & Lazdunski, A. Protein secretion in Pseudomonas aeruginosa: the xcpA gene encodes an integral inner membrane protein homologous to Klebsiella pneumoniae secretion function protein PulO. *J. Bacteriol.* **173**, 479–486 (1991).
193. Strom, M. S., Nunn, D. & Lory, S. Multiple roles of the pilus biogenesis protein pilD: involvement of pilD in excretion of enzymes from Pseudomonas aeruginosa. *J. Bacteriol.* **173**, 1175–1180 (1991).
194. Hagblom, P., Segal, E., Billyard, E. & So, M. Intragenic recombination leads to pilus antigenic variation in Neisseria gonorrhoeae. *Nature* **315**, 156–158 (1985).
195. Seifert, H. S., Ajioka, R. S., Marchal, C., Sparling, P. F. & So, M. DNA transformation leads to pilin antigenic variation in Neisseria gonorrhoeae. *Nature* **336**, 392–395 (1988).

196. Hill, S. A., Woodward, T., Reger, A., Baker, R. & Dinse, T. Role for the RecBCD Recombination Pathway for *pilE* Gene Variation in Repair-Proficient *Neisseria gonorrhoeae*. *J. Bacteriol.* **189**, 7983–7990 (2007).
197. Hill, S. A., Morrison, S. G. & Swanson, J. The role of direct oligonucleotide repeats in gonococcal pilin gene variation. *Mol. Microbiol.* **4**, 1341–1352 (1990).
198. Hill, S. & Grant, C. Recombinational error and deletion formation in Neisseria gonorrhoeae: a role for RecJ in the production of pilE L deletions. *Mol. Genet. Genomics 2001 2666* **266**, 962–972 (2002).
199. Sparling, P. F., Cannon, J. G. & So, M. Phase and Antigenic Variation of Pili and Outer Membrane Protein II of Neisseria gonorrhoeae. *J. Infect. Dis.* **153**, 196–201 (1986).
200. Haas, R. & Meyer, T. F. The repertoire of silent pilus genes in neisseria gonorrhoeae: Evidence for gene conversion. *Cell* **44**, 107–115 (1986).
201. Haas, R., Veit, S. & Meyer, T. f. Silent pilin genes of Neisseria gonorrhoeae MS11 and the occurrence of related hypervariant sequences among other gonococcal isolates. *Mol. Microbiol.* **6**, 197–208 (1992).
202. Hamrick, T. S., Dempsey, J. A. F., Cohen, M. S. & Cannon, J. G. Antigenic variation of gonococcal pilin expression in vivo: Analysis of the strain FA1090 pilin repertoire and identification of the pilS gene copies recombining with pilE during experimental human infection. *Microbiology* **147**, 839–849 (2001).
203. Wachter, J., Masters, T. L., Wachter, S., Mason, J. & Hill, S. A. pilS loci in Neisseria gonorrhoeae are transcriptionally active. *Microbiology* **161**, 1124–1135 (2015).
204. Meyer, T. Pilus expression in neisseria gonorrhoeae involves chromosomal rearrangement. *Cell* **30**, 45–52 (1982).
205. Meyer, T. F., Billyard, E., Haas, R., Storzbach, S. & So, M. Pilus genes of Neisseria gonorrheae: chromosomal organization and DNA sequence. *Proc. Natl. Acad. Sci. U. S. A.* **81**, 6110–6114 (1984).
206. Lobanovska, M., Tang, C. M. & Exley, R. M. Contribution of σ70 and σN Factors to Expression of Class II pilE in Neisseria meningitidis. *J. Bacteriol.* **201**, e00170-19 (2019).
207. Cahoon, L. A. & Seifert, H. S. An alternative DNA structure is necessary for pilin antigenic variation in Neisseria gonorrhoeae. *Science* **325**, 764–767 (2009).
208. Kuryavyi, V., Cahoon, L. A., Seifert, H. S. & Patel, D. J. RecA-Binding pilE G4 Sequence Essential for Pilin Antigenic Variation Forms Monomeric and 5′ End-Stacked Dimeric Parallel G-Quadruplexes. *Structure* **20**, 2090–2102 (2012).
209. Cahoon, L. A. & Seifert, H. S. Focusing homologous recombination: pilin antigenic variation in the pathogenic Neisseria. *Mol. Microbiol.* **81**, 1136–1143 (2011).
210. Cahoon, L. A. & Seifert, H. S. Transcription of a cis-acting, Noncoding, Small RNA Is Required for Pilin Antigenic Variation in Neisseria gonorrhoeae. *PLOS Pathog.* **9**, e1003074 (2013).
211. Prister, L. L., Yin, S., Cahoon, L. A. & Seifert, H. S. Altering the *Neisseria gonorrhoeae pilE* Guanine Quadruplex Loop Bases Affects Pilin Antigenic Variation. *Biochemistry* **59**, 1104–1112 (2020).
212. Savitskaya, V. Y. *et al.* pilE G-Quadruplex Is Recognized and Preferentially Bound but Not Processed by the MutL Endonuclease from Neisseria gonorrhoeae Mismatch Repair Pathway. *Int. J. Mol. Sci.* **24**, 6167 (2023).
213. Rotman, E. & Seifert, H. S. Neisseria gonorrhoeae MutS Affects Pilin Antigenic Variation through Mismatch Correction and Not by pilE Guanine Quartet Binding. *J. Bacteriol.* **197**, 1828–1838 (2015).
214. Voter, A. F. *et al.* Antigenic Variation in *Neisseria gonorrhoeae* Occurs Independently of RecQ-Mediated Unwinding of the *pilE* G Quadruplex. *J. Bacteriol.* **202**, (2020).

215. Prister, L. L., Ozer, E. A., Cahoon, L. A. & Seifert, H. S. Transcriptional initiation of a small RNA, not R-loop stability, dictates the frequency of pilin antigenic variation in *Neisseria gonorrhoeae*. *Mol. Microbiol.* **112**, 1219–1234 (2019).
216. Ozer, E. A. *et al.* PacBio Amplicon Sequencing Method To Measure Pilin Antigenic Variation Frequencies of Neisseria gonorrhoeae. **4**, 14 (2019).
217. Elkins, C., Thomas, C. E., Seifert, H. S. & Sparling, P. F. Species-specific uptake of DNA by gonococci is mediated by a 10-base-pair sequence. *J. Bacteriol.* **173**, 3911–3913 (1991).
218. Goodman, S. D. & Scocca, J. J. Identification and arrangement of the DNA sequence recognized in specific transformation of Neisseria gonorrhoeae. *Proc. Natl. Acad. Sci. U. S. A.* **85**, 6982–6986 (1988).
219. Treangen, T. J., Ambur, O., Tonjum, T. & Rocha, E. P. The impact of the neisserial DNA uptake sequences on genome evolution and stability. *Genome Biol.* **9**, R60 (2008).
220. Mora, M., Mell, J. C., Ehrlich, G. D., Ehrlich, R. L. & Redfield, R. J. Genome-wide analysis of DNA uptake across the outer membrane of naturally competent Haemophilus influenzae. *iScience* **24**, 102007 (2021).
221. Frye, S. A., Nilsen, M., Tønjum, T. & Ambur, O. H. Dialects of the DNA Uptake Sequence in Neisseriaceae. *PLoS Genet.* **9**, e1003458 (2013).
222. Dillard, J. P. Genetic Manipulation of *Neisseria gonorrhoeae*. *Curr. Protoc. Microbiol.* **23**, (2011).
223. Duffin, P. M. & Seifert, H. S. DNA uptake sequence-mediated enhancement of transformation in Neisseria gonorrhoeae is strain dependent. *J. Bacteriol.* **192**, 4436–4444 (2010).
224. Davidsen, T. *et al.* Biased distribution of DNA uptake sequences towards genome maintenance genes. *Nucleic Acids Res.* **32**, 1050–1058 (2004).
225. Hughes-Games, A., Roberts, A. P., Davis, S. A. & Hill, D. J. Identification of integrative and conjugative elements in pathogenic and commensal Neisseriaceae species via genomic distributions of DNA uptake sequence dialects. *Microb. Genomics* **6**, (2020).
226. Spencer-Smith, R., Roberts, S., Gurung, N. & Snyder, L. A. S. DNA uptake sequences in Neisseria gonorrhoeae as intrinsic transcriptional terminators and markers of horizontal gene transfer. *Microb. Genomics* **2**, (2016).
227. Long, C. D., Madraswala, R. N. & Seifert, H. S. Comparisons between Colony Phase Variation ofNeisseria gonorrhoeae FA1090 and Pilus, Pilin, and S-Pilin Expression. *Infect. Immun.* **66**, 1918–1927 (1998).
228. Obergfell, K. P. & Seifert, H. S. The Pilin N-terminal Domain Maintains Neisseria gonorrhoeae Transformation Competence during Pilus Phase Variation. *PLOS Genet.* **12**, e1006069 (2016).
229. Berry, J. L. *et al.* A Comparative Structure/Function Analysis of Two Type IV Pilin DNA Receptors Defines a Novel Mode of DNA Binding. *Structure* **24**, 926–934 (2016).
230. Berry, J.-L., Cehovin, A., McDowell, M. A., Lea, S. M. & Pelicic, V. Functional Analysis of the Interdependence between DNA Uptake Sequence and Its Cognate ComP Receptor during Natural Transformation in Neisseria Species. *PLoS Genet.* **9**, e1004014 (2013).
231. Cehovin, A. *et al.* Specific DNA recognition mediated by a type IV pilin. *Proc. Natl. Acad. Sci.* **110**, 3065–3070 (2013).
232. Hughes-Games, A., Davis, S. A. & Hill, D. J. Direct visualization of sequence-specific DNA binding by gonococcal type IV pili. *Microbiology* **168**, (2022).
233. Seow, V. Y., Tsygelnytska, O. & Biais, N. Multisite transformation in Neisseria gonorrhoeae: insights on transformations mechanisms and new genetic modification protocols. *Front. Microbiol.* **14**, (2023).

234. Dalia, A. B. Natural Cotransformation and Multiplex Genome Editing by Natural Transformation (MuGENT) of Vibrio cholerae. in *Vibrio Cholerae* (ed. Sikora, A. E.) vol. 1839 53–64 (Springer New York, New York, NY, 2018).
235. Dalia, A. B., McDonough, E. & Camilli, A. Multiplex genome editing by natural transformation. *Proc. Natl. Acad. Sci.* **111**, 8937–8942 (2014).
236. Dalia, T. N. *et al.* Multiplex Genome Editing by Natural Transformation (MuGENT) for Synthetic Biology in *Vibrio natriegens*. *ACS Synth. Biol.* **6**, 1650–1655 (2017).
237. Trieu-Cuot, P., Poyart-Salmeron, C., Carlier, C. & Courvalin, P. Nucleotide sequence of the erythromycin resistance gene of the conjugative transposon Tn1545. *Nucleic Acids Res.* **18**, 3660–3660 (1990).
238. Mehr, I. J. & Seifert, H. S. Differential roles of homologous recombination pathways in *Neisseria gonorrhoeae* pilin antigenic variation, DNA transformation and DNA repair. *Mol. Microbiol.* **30**, 697–710 (1998).
239. Tobiason, D. M. & Seifert, H. S. Genomic Content of *Neisseria* Species. *J. Bacteriol.* **192**, 2160–2168 (2010).
240. Ramsey, M. E., Hackett, K. T., Kotha, C. & Dillard, J. P. New complementation constructs for inducible and constitutive gene expression in Neisseria gonorrhoeae and Neisseria meningitidis. *Appl. Environ. Microbiol.* **78**, 3068–3078 (2012).
241. Viollier, P. H. *et al.* Rapid and sequential movement of individual chromosomal loci to specific subcellular locations during bacterial DNA replication. *Proc. Natl. Acad. Sci.* **101**, 9257–9262 (2004).
242. Biswas, G. D., Sox, T., Blackman, E. & Sparling, P. F. Factors affecting genetic transformation of Neisseria gonorrhoeae. *J. Bacteriol.* **129**, 983–992 (1977).
243. Cehovin, A., Jolley, K. A., Maiden, M. C. J., Harrison, O. B. & Tang, C. M. Association of Neisseria gonorrhoeae Plasmids With Distinct Lineages and The Economic Status of Their Country of Origin. *J. Infect. Dis.* **222**, 1826–1836 (2020).
244. Roberts, M. C. Plasmids of Neisseria gonorrhoeae and other Neisseria species. *CLIN MICROBIOL REV* **2**, 6 (1989).
245. Sparling, P. F. Genetic Transformation of *Neisseria gonorrhoeae* to Streptomycin Resistance. *J. Bacteriol.* **92**, 1364–1371 (1966).
246. Jones, R. A., Yee, W. X., Mader, K., Tang, C. M. & Cehovin, A. Markerless gene editing in Neisseria gonorrhoeae. *Microbiology* **168**, 001201 (2022).
247. Nyongesa, S., Chenal, M., Bernet, È., Coudray, F. & Veyrier, F. J. Sequential markerless genetic manipulations of species from the Neisseria genus. *Can. J. Microbiol.* cjm-2022-0024 (2022) doi:10.1139/cjm-2022-0024.
248. Ashwini, M., Murugan, S. B., Balamurugan, S. & Sathishkumar, R. Advances in molecular cloning. *Mol. Biol.* **50**, 1–6 (2016).
249. Zou, R., Zhou, K., Stephanopoulos, G. & Too, H. P. Combinatorial engineering of 1-deoxy-D-xylulose 5-phosphate pathway using cross-lapping in vitro assembly (CLIVA) method. *PloS One* **8**, e79557 (2013).
250. Doktycz, M. J. *et al.* AFM imaging of bacteria in liquid media immobilized on gelatin coated mica surfaces. *Ultramicroscopy* **97**, 209–216 (2003).
251. Bottomley, A. L., Turnbull, L., Whitchurch, C. B. & Harry, E. J. Immobilization Techniques of Bacteria for Live Super-resolution Imaging Using Structured Illumination Microscopy. in *Bacterial Pathogenesis: Methods and Protocols* (eds. Nordenfelt, P. & Collin, M.) 197–209 (Springer, New York, NY, 2017). doi:10.1007/978-1-4939-6673-8_12.
252. Benson, R. C., Meyer, R. A., Zaruba, M. E. & McKhann, G. M. Cellular autofluorescence--is it due to flavins? *J. Histochem. Cytochem.* **27**, 44–48 (1979).

253. Müllerová, L., Marková, K., Obruča, S. & Mravec, F. Use of Flavin-Related Cellular Autofluorescence to Monitor Processes in Microbial Biotechnology. *Microorganisms* **10**, 1179 (2022).
254. Lukacs, G. L. *et al.* Size-dependent DNA Mobility in Cytoplasm and Nucleus *. *J. Biol. Chem.* **275**, 1625–1629 (2000).
255. Robertson, R. M., Laib, S. & Smith, D. E. Diffusion of isolated DNA molecules: Dependence on length and topology. *Proc. Natl. Acad. Sci.* **103**, 7310–7314 (2006).
256. Pluen, A., Netti, P. A., Jain, R. K. & Berk, D. A. Diffusion of macromolecules in agarose gels: comparison of linear and globular configurations. *Biophys. J.* **77**, 542–552 (1999).
257. Kraus, S. J. Culture Methods for Neisseria Gonorrhoea. *Arch. Androl.* **3**, 343–349 (1979).
258. Ley, H. L. & Mueller, J. H. On the Isolation from Agar of an Inhibitor for Neisseria gonorrhoeae. *J. Bacteriol.* **52**, 453–460 (1946).
259. Carifo, K. & Catlin, B. W. Neisseria gonorrhoeae Auxotyping: Differentiation of Clinical Isolates Based on Growth Responses on Chemically Defined Media. *Appl. Microbiol.* **26**, 223–230 (1973).
260. Scolea, L. J. L. & Young, F. E. Development of a Defined Minimal Medium for the Growth of Neisseria gonorrhoeae. *APPL MICROBIOL* 7 (1974).
261. Walstad, D. L., Reitz, R. C. & Sparling, P. F. Growth Inhibition Among Strains of Neisseria gonorrhoeae due to Production of Inhibitory Free Fatty Acids and Lysophosphatidylethanolamine: Absence of Bacteriocins. *Infect. Immun.* **10**, 481–488 (1974).
262. Bergsson, G., Steingrímsson, Ó. & Thormar, H. In Vitro Susceptibilities of Neisseria gonorrhoeae to Fatty Acids and Monoglycerides. *Antimicrob. Agents Chemother.* **43**, 2790–2792 (1999).
263. Morselli, S., Valente, S., Foschi, C., Marangoni, A. & Pasquinelli, G. Effect of different fatty acids on Neisseria gonorrhoeae viability. 9 (2021).
264. De La Rosa, M., Villareal, R., Vega, D., Miranda, C. & Martinezbrocal, A. Granada medium for detection and identification of group B streptococci. *J. Clin. Microbiol.* **18**, 779–785 (1983).
265. Recuero-Checa, M. A. *et al.* Chlamydia trachomatis growth and development requires the activity of host Long-chain Acyl-CoA Synthetases (ACSLs). *Sci. Rep.* **6**, 23148 (2016).
266. Wade, J. J. & Graver, M. A. A fully defined, clear and protein-free liquid medium permitting dense growth of *Neisseria gonorrhoeae* from very low inocula. *FEMS Microbiol. Lett.* **273**, 35–37 (2007).
267. Wong, T. P., Shockley, R. K. & Johnston, K. H. WSJM, a simple chemically defined medium for growth of Neisseria gonorrhoeae. *J. Clin. Microbiol.* **11**, 363–369 (1980).
268. Gregory, M. R., Gregory, W. W., Bruns, D. E. & Zakowski, J. J. Amylase inhibits Neisseria gonorrhoeae by degrading starch in the growth medium. *J. Clin. Microbiol.* **18**, 1366–1369 (1983).
269. Palace, S. G. *et al.* Identification of bile acid and fatty acid species as candidate rapidly bactericidal agents for topical treatment of gonorrhoea. *J. Antimicrob. Chemother.* **76**, 2569–2577 (2021).
270. Schoch, T. J. & Williams, C. B. Adsorption of fatty ccid by the linear component of corn starch. *J. Am. Chem. Soc.* **66**, 1232–1233 (1944).
271. Craig, L. *et al.* Type IV Pilus Structure by Cryo-Electron Microscopy and Crystallography: Implications for Pilus Assembly and Functions. *Mol. Cell* **23**, 651–662 (2006).
272. Neuhaus, A. *et al.* Cryo-electron microscopy reveals two distinct type IV pili assembled by the same bacterium. *Nat. Commun.* **11**, 2231 (2020).

273. Carbonnelle, E., Hélaine, S., Prouvensier, L., Nassif, X. & Pelicic, V. Type IV pilus biogenesis in Neisseria meningitidis: PilW is involved in a step occurring after pilus assembly, essential for fibre stability and function. *Mol. Microbiol.* **55**, 54–64 (2005).
274. Eriksson, J. *et al.* Characterization of motility and piliation in pathogenic Neisseria. *BMC Microbiol.* **15**, 92 (2015).
275. Talà, L., Fineberg, A., Kukura, P. & Persat, A. Pseudomonas aeruginosa orchestrates twitching motility by sequential control of type IV pili movements. *Nat. Microbiol.* **4**, 774–780 (2019).
276. Ellison, C. K. *et al.* Retraction of DNA-bound type IV competence pili initiates DNA uptake during natural transformation in Vibrio cholerae. *Nat. Microbiol.* **3**, 773–780 (2018).
277. Ellison, C. K., Dalia, T. N., Dalia, A. B. & Brun, Y. V. Real-time microscopy and physical perturbation of bacterial pili using maleimide-conjugated molecules. *Nat. Protoc.* **14**, 1803–1819 (2019).
278. Wegel, E. *et al.* Imaging cellular structures in super-resolution with SIM, STED and Localisation Microscopy: A practical comparison. *Sci. Rep.* **6**, 27290 (2016).
279. Banaz, N., Mäkelä, J. & Uphoff, S. Choosing the right label for single-molecule tracking in live bacteria: side-by-side comparison of photoactivatable fluorescent protein and Halo tag dyes. *J. Phys. Appl. Phys.* **52**, 064002 (2018).
280. Crissman, H. A. & Hirons, G. T. Chapter 13 Staining of DNA in Live and Fixed Cells. in *Methods in Cell Biology* vol. 41 195–209 (Elsevier, 1994).
281. Stingl, K., Müller, S., Scheidgen-Kleyboldt, G., Clausen, M. & Maier, B. Composite system mediates two-step DNA uptake into Helicobacter pylori. *Proc. Natl. Acad. Sci.* **107**, 1184–1189 (2010).
282. Cordes, T., Vogelsang, J. & Tinnefeld, P. On the Mechanism of Trolox as Antiblinking and Antibleaching Reagent. *J. Am. Chem. Soc.* **131**, 5018–5019 (2009).
283. Brickner, J. R., Garzon, J. L. & Cimprich, K. A. Walking a tightrope: The complex balancing act of R-loops in genome stability. *Mol. Cell* **0**, (2022).
284. Tobiason, D. M. & Seifert, H. S. The Obligate Human Pathogen, Neisseria gonorrhoeae, Is Polyploid. *PLoS Biol.* **4**, (2006).
285. Uphoff, S. Super-resolution microscopy and tracking of DNA-binding proteins in bacterial cells. *Methods Mol. Biol.* **1431**, 221–234 (2016).
286. Hahn, J., DeSantis, M. & Dubnau, D. Mechanisms of Transforming DNA Uptake to the Periplasm of Bacillus subtilis. **12**, 17 (2021).
287. Bender, N., Hennes, M. & Maier, B. Mobility of extracellular DNA within gonococcal colonies. *Biofilm* **4**, 100078 (2022).
288. Peng, T. *et al.* A BaSiC tool for background and shading correction of optical microscopy images. *Nat. Commun.* **8**, 14836 (2017).
289. Jass, J. *et al.* Physical Properties of Escherichia coli P Pili Measured by Optical Tweezers. *Biophys. J.* **87**, 4271–4283 (2004).
290. Santos, L. C., Munteanu, E. L. & Biais, N. An In Vitro Model System to Test Mechano-microbiological Interactions Between Bacteria and Host Cells. *Methods Mol. Biol. Clifton NJ* **1365**, 195–212 (2016).
291. Beaussart, A. *et al.* Nanoscale Adhesion Forces of Pseudomonas aeruginosa Type IV Pili. *ACS Nano* **8**, 10723–10733 (2014).
292. Miller, E., Garcia, T., Hultgren, S. & Oberhauser, A. F. The Mechanical Properties of E. coli Type 1 Pili Measured by Atomic Force Microscopy Techniques. *Biophys. J.* **91**, 3848–3856 (2006).
293. Sangermani, M., Hug, I., Sauter, N., Pfohl, T. & Jenal, U. Tad Pili Play a Dynamic Role in Caulobacter crescentus Surface Colonization. *mBio* **10**, 10.1128/mbio.01237-19 (2019).

294. Skerker, J. M. & Berg, H. C. Direct observation of extension and retraction of type IV pili. *Proc. Natl. Acad. Sci. U. S. A.* **98**, 6901–6904 (2001).
295. Koch, M. D. Pseudomonas aeruginosa distinguishes surfaces by stiffness using retraction of type IV pili. 1–9 (2022) doi:10.1073/pnas.2119434119/-/DCSupplemental.Published.
296. Palalay, J.-J. S., Simsek, A. N., Sabass, B. & Sanfilippo, J. E. Shear force enhances adhesion of Pseudomonas aeruginosa by counteracting pilus-driven surface departure. *bioRxiv* 2023.05.08.539440 (2023) doi:10.1101/2023.05.08.539440.
297. Biais, N., Higashi, D., So, M. & Ladoux, B. Techniques to Measure Pilus Retraction Forces. in *Neisseria meningitidis* (ed. Christodoulides, M.) vol. 799 197–216 (Humana Press, Totowa, NJ, 2012).
298. Ghassemi, S. *et al.* Fabrication of elastomer pillar arrays with modulated stiffness for cellular force measurements. *J. Vac. Sci. Technol. B Microelectron. Nanometer Struct.* **26**, 2549–2553 (2008).
299. Gupta, M. *et al.* Micropillar substrates: a tool for studying cell mechanobiology. *Methods Cell Biol.* **125**, 289–308 (2015).
300. Treuner-Lange, A. *et al.* Large pilin subunits provide distinct structural and mechanical properties for the Myxococcus xanthus type IV pilus. *BioRxiv Prepr. Serv. Biol.* 2023.07.22.550172 (2023) doi:10.1101/2023.07.22.550172.
301. Dufrêne, Y. F. & Persat, A. Mechanomicrobiology: how bacteria sense and respond to forces. *Nat. Rev. Microbiol.* **18**, 227–240 (2020).
302. Rahmouni, S. *et al.* Hydrogel Micropillars with Integrin Selective Peptidomimetic Functionalized Nanopatterned Tops: A New Tool for the Measurement of Cell Traction Forces Transmitted through αvβ3- or α5β1-Integrins. *Adv. Mater. Deerfield Beach Fla* **25**, 5869–5874 (2013).
303. Park, K. J. *et al.* Micropillar arrays enabling single microbial cell encapsulation in hydrogels. *Lab. Chip* **14**, 1873–1879 (2014).
304. Schoen, I., Hu, W., Klotzsch, E. & Vogel, V. Probing Cellular Traction Forces by Micropillar Arrays: Contribution of Substrate Warping to Pillar Deflection. *Nano Lett.* **10**, 1823–1830 (2010).
305. Gelles, J., Schnapp, B. J. & Sheetz, M. P. Tracking kinesin-driven movements with nanometre-scale precision. *Nature* **331**, 450–453 (1988).
306. Manning, G. S. The Persistence Length of DNA Is Reached from the Persistence Length of Its Null Isomer through an Internal Electrostatic Stretching Force. *Biophys. J.* **91**, 3607–3616 (2006).
307. Aas, F. E. *et al.* Competence for natural transformation in Neisseria gonorrhoeae: Components of DNA binding and uptake linked to type IV pilus expression. *Mol. Microbiol.* **46**, 749–760 (2002).
308. Koomey, M. Competence for natural transformation in Neisseria gonorrhoeae: a model system for studies of horizontal gene transfer. *APMIS. Suppl.* **84**, 56–61 (1998).
309. Chen, I. & Gotschlich, E. C. ComE, a Competence Protein from *Neisseria gonorrhoeae* with DNA-Binding Activity. *J. Bacteriol.* **183**, 3160–3168 (2001).
310. Krüger, N.-J. & Stingl, K. Two steps away from novelty – principles of bacterial DNA uptake. *Mol. Microbiol.* **80**, 860–867 (2011).
311. Hahn, J., Maier, B., Haijema, B. J., Sheetz, M. & Dubnau, D. Transformation Proteins and DNA Uptake Localize to the Cell Poles in Bacillus subtilis. *Cell* **122**, 59–71 (2005).
312. Zuke, J. D., Erickson, R., Hummels, K. R. & Burton, B. M. Visualizing dynamic competence pili and DNA capture throughout the long axis of Bacillus subtilis. *J. Bacteriol.* **205**, e00156-23.

313. Hamilton, H. L., Domínguez, N. M., Schwartz, K. J., Hackett, K. T. & Dillard, J. P. Neisseria gonorrhoeae secretes chromosomal DNA via a novel type IV secretion system. *Mol. Microbiol.* **55**, 1704–1721 (2005).
314. Callaghan, M. M., Heilers, J.-H., van der Does, C. & Dillard, J. P. Secretion of chromosomal DNA by the Neisseria gonorrhoeae type IV secretion system. *Curr. Top. Microbiol. Immunol.* **413**, 323–345 (2017).
315. Jakubovics, N. S., Shields, R. C., Rajarajan, N. & Burgess, J. G. Life after death: the critical role of extracellular DNA in microbial biofilms. *Lett. Appl. Microbiol.* **57**, 467–475 (2013).
316. Zweig, M. *et al.* Secreted single-stranded DNA is involved in the initial phase of biofilm formation by Neisseria gonorrhoeae. *Environ. Microbiol.* **16**, 1040–1052 (2014).
317. Schulze, E., Asai, D. J., Bulinski, J. C. & Kirschner, M. Posttranslational modification and microtubule stability. *J. Cell Biol.* **105**, 2167–2177 (1987).
318. Muschiol, S., Balaban, M., Normark, S. & Henriques-Normark, B. Uptake of extracellular DNA: Competence induced pili in natural transformation of *Streptococcus pneumoniae*. *BioEssays* **37**, 426–435 (2015).
319. Lam, T. *et al.* Competence pili in Streptococcus pneumoniae are highly dynamic structures that retract to promote DNA uptake. *Mol. Microbiol.* **116**, 381–396 (2021).
320. Muschiol, S. *et al.* Structure of the competence pilus major pilin ComGC in Streptococcus pneumoniae. *J. Biol. Chem.* **292**, 14134–14146 (2017).
321. Balaban, M. *et al.* Secretion of a pneumococcal type II secretion system pilus correlates with DNA uptake during transformation. *Proc. Natl. Acad. Sci.* **111**, (2014).
322. Pelicic, V. Mechanism of assembly of type 4 filaments: everything you always wanted to know (but were afraid to ask). *Microbiology* **169**, 001311 (2023).
323. Busch, A. & Waksman, G. Chaperone–usher pathways: diversity and pilus assembly mechanism. *Philos. Trans. R. Soc. B Biol. Sci.* **367**, 1112–1122 (2012).
324. Goosens, V. J. *et al.* Reconstitution of a minimal machinery capable of assembling periplasmic type IV pili. *Proc. Natl. Acad. Sci. U. S. A.* **114**, E4978–E4986 (2017).
325. Strom, M. S., Bergman, P. & Lory, S. Identification of active-site cysteines in the conserved domain of PilD, the bifunctional type IV pilin leader peptidase/N-methyltransferase of Pseudomonas aeruginosa. *J. Biol. Chem.* **268**, 15788–15794 (1993).
326. LaPointe, C. F. & Taylor, R. K. The Type 4 Prepilin Peptidases Comprise a Novel Family of Aspartic Acid Proteases *. *J. Biol. Chem.* **275**, 1502–1510 (2000).
327. Linhartová, M. *et al.* Mutations Suppressing the Lack of Prepilin Peptidase Provide Insights Into the Maturation of the Major Pilin Protein in Cyanobacteria. *Front. Microbiol.* **12**, 756912 (2021).
328. Sachon, E., Mohammed, S., Bache, N. & Jensen, O. N. Phosphopeptide quantitation using amine-reactive isobaric tagging reagents and tandem mass spectrometry: application to proteins isolated by gel electrophoresis. *Rapid Commun. Mass Spectrom.* **20**, 1127–1134 (2006).
329. Asikyan, M. L., Kus, J. V. & Burrows, L. L. Novel Proteins That Modulate Type IV Pilus Retraction Dynamics in Pseudomonas aeruginosa. *J. Bacteriol.* **190**, 7022–7034 (2008).
330. Zöllner, R. *et al.* Type IV Pilin Post-Translational Modifications Modulate Material Properties of Bacterial Colonies. *Biophys. J.* **116**, 938–947 (2019).
331. Hibbing, M. E., Fuqua, C., Parsek, M. R. & Peterson, S. B. Bacterial competition: surviving and thriving in the microbial jungle. *Nat. Rev. Microbiol.* **8**, 15–25 (2010).
332. Kim, W. J. *et al.* Commensal Neisseria Kill Neisseria gonorrhoeae through a DNA-Dependent Mechanism. *Cell Host Microbe* **26**, 228-239.e8 (2019).
333. Ducey, T. F. & Dyer, D. W. Rapid Identification of EZ::TN$^{TM}$ Transposon Insertion Sites in the Genome of Neisseria gonorrhoeae.

334. Chlebek, J. L., Denise, R., Craig, L. & Dalia, A. B. Motor-independent retraction of type IV pili is governed by an inherent property of the pilus filament. *Proc. Natl. Acad. Sci.* **118**, e2102780118 (2021).

# Appendix I

## Basic Information

### Culture Media

| Media | Details |
|---|---|
| GCB | GCB Liquid Medium |
| GCB+ | GCM Liquid Medium + Supplement I & II |
| GCB Agar | GCB Solid Medium + Supplement I & II |
| Transformation Medium | GCB+ with 5mM $MgSO_4$ |
| GW Medium | A chemically defined medium from Wade and Graver[266] |

Components of GCB Solid medium

| Material | Final concentration (g/L) |
|---|---|
| **Component 1: GCB Medium Base (Ingredient listed below)** | |
| Proteose Peptone No. 3 | 15.0 |
| Dipotassium Phosphate | 4.0 |
| Monopotassium Phosphate | 1.0 |
| Sodium Chloride | 5.0 |
| Corn Starch | 1.0 |
| Agar | 10.0 |
| **Component 2** | |
| Bacto Agar | 1.25 |

Components of GCB Liquid medium

| Material | Final concentration (g/L) |
|---|---|
| Liquid Medium | |
| Proteose Peptone No. 3 | 15.0 |
| Dipotassium Phosphate | 4.0 |
| Monopotassium Phosphate | 1.0 |
| Sodium Chloride | 5.0 |

### Antibiotics

| Antibiotics | Abbreviation | Concentration* |
|---|---|---|
| Kanamycin | Kan | 80 ug/ml |
| Chloramphenicol | Chl | 7.5 ug/ml |
| Erythromycin | Erm | 10 ug/ml |
| Nalidixic acid | NA | 3 ug/ml |

* if an otherwise concentration was used, it will be mentioned in the text itself

### Bacteria Strains

*N. gonorrhoeae* strains used:

| Strains | Description |
|---|---|
| MS11 | Wild type |
| ΔPilE | MS11 *ΔpilE::Erm* (Strain 306) |
| ΔPilT | MS11 *ΔpilT::Kan* |
| ΔPilV | MS11 *ΔpilV::Erm* |
| ΔPilV ΔPilT | MS11 *ΔpilV::Erm ΔpilT::Kan* |
| ΔPilV ΔComP | MS11 *ΔpilV::Erm ΔcomP::Kan* |
| ΔG4 | MS11 *ΔG4::Kan* |
| ΔG4 ΔPilV | MS11 *ΔG4::Kan ΔpilV::Erm* |
| N400 | N400 WT3 |
| N400 ΔPilV | N400 WT3 *ΔpilV::Erm* |
| K9C | N400 WT3 *pilET138C* |
| K9C ΔPilV | N400 WT3 *pilET138C ΔpilV::Erm* |
| C7G | N400 WT3 *pilET132C* |
| C7G ΔPilV | N400 WT3 *pilET132C ΔpilV::Erm* |
| M33 | MS11 *ΔpilC::Kan* |
| ΔPilC | MS11 *ΔpilC::Chl* |
| C72S | MS11 *ΔG4::Kan PilDC72S AR::Erm*<br>Obtained through co-transformation of G4 with C72S tDNA and AR::Erm |
| C72SI134M | MS11 *ΔG4::Kan PilDC72SI134M AR::Erm*<br>Obtained through co-transformation of G4 with C72S tDNA and AR::Erm but an additional mutation was identified at I134 |
| G93S | MS11 *ΔG4::Kan PilDC93S AR::Erm*<br>Obtained through co-transformation of G4 with G93S tDNA and AR::Erm |
| C72SG93S | MS11 *ΔG4::Kan PilDC72SG93S AR::Erm*<br>Obtained through co-transformation of G4 with C72SG93S tDNA and AR::Erm |

*N. elongata* strains used

| Strains | Description |
|---|---|
| WT | Wild type *Neisseria elongata glycolytica* |
| ΔComP | *ΔcomP::Kan* |
| ΔPilV | *ΔpilV::Erm* |
| ΔPilC | *ΔpilC::Kan* |
| ΔPilCtrunc | *pilCtrunc NelAR::Erm* |
| ΔPilT | *ΔpilT::Kan* |

| | |
|---|---|
| ΔPilE1 | *ΔpilE1::Kan* |
| ΔPilE2 | *ΔpilE2::Kan* |
| ΔPilE1PilE2 | *ΔpilE1E2::Kan* |
| ΔPilK | *ΔpilK::Erm* |
| ΔPilK ΔPilT | *ΔpilK::Erm ΔpilT::Kan* |
| ΔPilC ΔPilK | *ΔpilC::Kan ΔpilK::Erm* |
| ΔPilCtrunc ΔPilT | *pilCtrunc NelAR::Erm ΔpilT::Kan* |

## Oligos List

| Oligo Name | Oligo Sequence |
|---|---|
| gyrB1_MS11_F | CCTCGTCGAGGGCAACTCCGCAGGCGG |
| gyrB1_MS11_R | CCGCCTGCGGAGTTGCCCTCGACGAGG |
| GyrB1DUS | TCGTATGCCGTCTGAACCGCCGAAGTCATCATGAC |
| GyrB1Reverse | GCATTTGGCGGTAGAAGAAG |
| ResistanceF | CTCGAGGGCTTGACACTTTATG |
| ResistanceR | ATCGATGTTTAAACTTCAGACGGC |
| UpGCF | CCCCGCCAAACAAATGCCG |
| UpGCR_resistance | CATAAAGTGTCAAGCCCTCGAGGGGTATAGAGCAGAACG GATG |
| DownGCF_resistance | TCTGAAGTTTAAACATCGATCGTTTCCGCCTACCTCGAAC |
| DownGCR | CTGGAAACAGACGCAATCACG |
| AR_Erm_F | CCGTTCTGCTCTATACCCCTTAGAAGCAAACTTAAGAGTG |
| AR_Erm_R | GTTCGAGGTAGGCGGAAACGATCGATACAAATTCCCCG |
| UpGCF | CCCCGCCAAACAAATGCCG |
| UpGCR | GGGTATAGAGCAGAACGGATG |
| DownGCF | CGTTTCCGCCTACCTCGAAC |
| DownGCR | CTGGAAACAGACGCAATCACG |
| gyrB_2kbp_F | TACAAAATCTCCGGCGGCCTGCAC |
| gyrB_2kbp_R | GGTTCGACCTCGTCGCCCATCA |
| gyrB_4kbp_F | AGTTCTTTTGTCGCCACGACGAC |
| gyrB_4kbp_R | CCTGCGGTGAGCAGGAAGTTTTC |
| gyrB_6kbp_F | CAAGCGGTGCGGCATCGTCAAA |
| gyrB_6kbp_R | TGCCTCGCCTTAGCTCAAAGAGAA |
| ReadInsertGC_F | CGGCAATGATTTTCTTCCTC |
| ReadInsertGC_R | GGCTTCGATGTGCTTGAAGA |
| Insert1kbGCF | ATGGGTGCGCTGATTATGGT |
| Insert1kbGCR | AATCATGCCGTCCCAATCCA |
| ComM-Up-F | CGTAAGACACCAGTCCCAATAC |
| ComM-Up-R | ATTTCAGACGGCCTTATTCGC |
| FluoComM-fluo-F | GCGAATAAGGCCGTCTGAAATATGGTGAGCAAGGGCG |
| YFPComM-yfp-R | TCCACCTGCTCCACCTGCTCTAGACTTGTACAGCTCGTCC |
| ComM-Down-F | GCAGGTGGAGCAGGTGGATCGCTTGCCTTGGTTTACAG |
| ComM-Down-R | GACCGCAGCAGCCATTCTTG |
| ComM--525-F | CTTGTAATGTAATCGGGCGTTGC |
| ComM-787-R | CGAGTTGTTGTTGGTGGTTGG |
| deltaCidAB-Up-F | GCGAAGTGGTGCTGCGTTATCTG |

| | |
|---|---|
| deltaCidAB-Up-R | GTTGTGTGTCTGTCTTTTGACGGCGTTG |
| deltaCidAB-Down-F | GTCAAAAGACAGACACACAACACCCGTTTCAGACGGC |
| deltaCidAB-Down-R | CCGCCGTTGAAACCCGAAAAATAC |
| CidAB--153-F | AAAGTCTGAACACGCCCCGG |
| CidAB-p73-R | CAGCCATAACGGTTCTCCTTGCG |
| GCPilDC72S-Up-F | GGCAATCAGTGCCATCAGAACGGG |
| GCPilDC72S-Down-R | ATTCACCGTCCTTACGGGATGGTGC |
| GCPilDUpNewF | CGGTTCGCTTGGTGCTTCATC |
| GCPilDDownNewR | TGGTCAGGACACGCCGTATCAG |
| GCPilDC72S-Up-NR | GCGCGTATCGGCACACGGCTTTTGGGACAGCAG |
| GCPilDC72S-Down-NF | CCTGCTGTCCCAAAAGCCGTGTGCCGATAC |
| GyrB1DUS | TCGTATGCCGTCTGAACCGCCGAAGTCATCATGAC |
| TAMRA-GyrB1DUS | /TAM/TCGTATGCCGTCTGAACCGCCGAAGTCATCATGAC |
| GyrB1Reverse-N | /Am/GCATTTGGCGGTAGAAGAAG |
| GCPilDC72S-Up-F | GGCAATCAGTGCCATCAGAACGGG |
| GCPilDC72S-Down-R | ATTCACCGTCCTTACGGGATGGTGC |
| GCPilDC72S-Up-NR | GCGCGTATCGGCACACGGCTTTTGGGACAGCAG |
| GCPilDC72S-Down-NF | CCTGCTGTCCCAAAAGCCGTGTGCCGATAC |
| GCPilDG93S-F | CCTGCTCCTGCGCAGCAAATGCGCTTCCTGCCAAAC |
| GCPilDG93S-R | GCAGGAAGCGCATTTGCTGCGCAGGAGCAGGTAACTG |
| GCPilDUpNewF | CGGTTCGCTTGGTGCTTCATC |
| GCPilDDownNewR | TGGTCAGGACACGCCGTATCAG |
| gyrB_6kbp_F | CAAGCGGTGCGGCATCGTCAAA |
| gyrB_6kbp_R | TGCCTCGCCTTAGCTCAAAGAGAA |
| GyrB1DUS | TCGTATGCCGTCTGAACCGCCGAAGTCATCATGAC |
| GyrB1NoDUS | CCGCCGAAGTCATCATGAC |
| GyrB1Reverse | GCATTTGGCGGTAGAAGAAG |
| TAMRA-GyrB1DUS | /TAM/TCGTATGCCGTCTGAACCGCCGAAGTCATCATGAC |
| GyrB1Reverse-N | /Am/GCATTTGGCGGTAGAAGAAG |
| GC-PilV-UF | TCTTCTTTCACATCGTTCTCATCA |
| GC-PilV-nUR | ACACACTCTTAAGTTTGCTTCTAAGAGCAATGTGTTTCCATTTGGTTG |
| Erm_F | CTTAGAAGCAAACTTAAGAGTGTGTTGATAGTG |
| N_Erm_R | ATCGATACAAATTCCCCGTAGGC |
| GC-PilV-nDF | GCCTACGGGGAATTTGTATCGATTCCTCCGCCGAAGC |
| GC-PilV-DR | ACCCAGTTCCTCTACATCTCC |
| PilT_-156F | CGGACACCTCACGATAACG |
| pilT-p527-R | GCTGCCTTGGCTGTGGT |
| GCPilV--297-F | GCAACAGCCGACCATTTCATC |
| GCPilV-p322-R | CCACATCGCCCGCTACATTTTTATTC |
| GC-ComP_-323-F | CTTCTCCCTTGCGGCGGTAA |
| GC-ComP_p344-R | TAAGGACGGGGCTGCGATTG |

## tDNA List

| tDNA | Description |
|---|---|
| DUSgyrB1 | Amplified from MS11 *gyrB1* mutant using GyrB1DUS and GyrB1Reverse |
| gyrB1-2kbp | Amplified from MS11 *gyrB1* mutant using gyrB_2kbp_F and gyrB_2kbp_R |
| gyrB1-4kbp | Amplified from MS11 *gyrB1* mutant using gyrB_4kbp_F and gyrB_6kbp_R |
| gyrB1-6kbp | Amplified from MS11 *gyrB1* mutant using gyrB_6kbp_F and gyrB_6kbp_R |
| AR::Kan | Amplified from MS11$_{AR::Kan}$ using Insert1kbGCF and Insert1kbGCR |
| AR::Erm | Amplified from MS11$_{AR::Erm}$ using Insert1kbGCF and Insert1kbGCR |
| C72S tDNA | Up fragment was amplified from MS11 gDNA using GCPilDC72S-Up-F and GCPilDC72S-Up-NR, Down fragment was amplified from MS11 gDNA using GCPilDC72S-Down-NF and GCPilDC72S-Down-R. The assembly of both fragments are re-amplified using GCPilDUpNewF and GCPilDDownNewR. |
| G93S tDNA | Up fragment was amplified from MS11 gDNA using GCPilDC72S-Up-F and GCPilDG93S-R, Down fragment was amplified from MS11 gDNA using GCPilDG93S-F and GCPilDC72S-Down-R. The assembly of both fragments are re-amplified using GCPilDUpNewF and GCPilDDownNewR. |
| C72SG93S tDNA | Up fragment was amplified from MS11 *ΔG4::Kan PilDC72S AR::Erm* gDNA using GCPilDC72S-Up-F and GCPilDG93S-R, Down fragment was amplified from MS11 gDNA using GCPilDG93S-F and GCPilDC72S-Down-R. The assembly of both fragments are re-amplified using GCPilDUpNewF and GCPilDDownNewR. |
| AR::Erm | An erythromycin cassette containing region used for co-transformation (VY Seow et. al, in review) |
| DUS tDNA | Prepared as described in previous study (VY Seow et al, in review) |
| | |
| gyrB1-6kbp | Amplified from MS11 *gyrB1* mutant using gyrB_6kbp_F and gyrB_6kbp_R |
| DUS | Amplified from MS11 *gyrB1* mutant using GyrB1DUS and GyrB1Reverse |
| noDUS | Amplified from MS11 *gyrB1* mutant using GyrB1NoDUS and GyrB1Reverse |
| DUSgyrB1-NH2 | Amplified from MS11 *gyrB1* mutant using GyrB1DUS and GyrB1Reverse-N |
| TAMRA-DUSgyrB1-NH2 | Amplified from MS11 *gyrB1* mutant using TAMRA-GyrB1DUS and GyrB1Reverse-N |

| | |
|---|---|
| ΔpilV::Erm tDNA | Amplied from *MS11 ΔpilV::Erm* using GCPilV--297-F and GCPilV-p322-R |
| ΔcomP::Kan tDNA | Amplied from *MS11 ΔcomP::Kan* using GC-ComP_-323-F and GC-ComP_p344-R |
| ΔpilT::Kan tDNA | Amplied from *MS11 ΔpilT::Kan* using PilT_-156F and pilT-p527-R |

## Sequence alignments and phylogenetic analysis

All Major and Minor Pilins

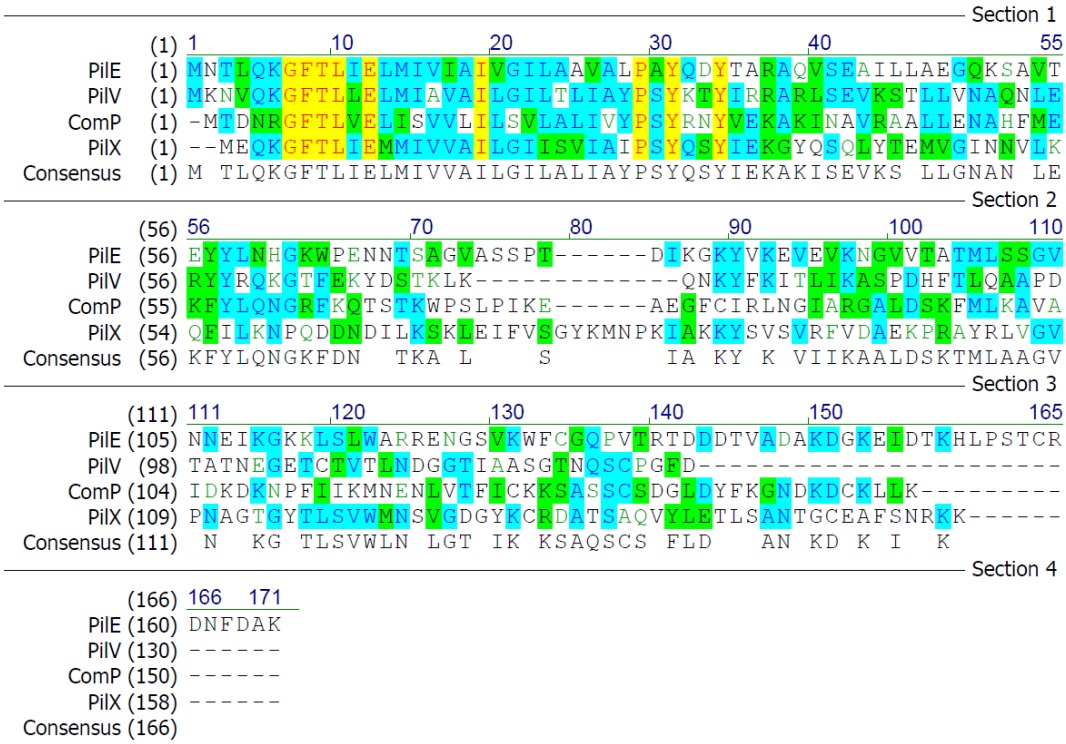


*i Protein sequence alignment for PilE, PilV, ComP and PilX in MS11*

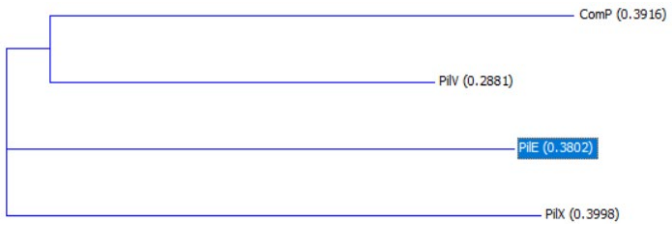


*ii Similarity closeness of protein sequences between major and minor pilin*

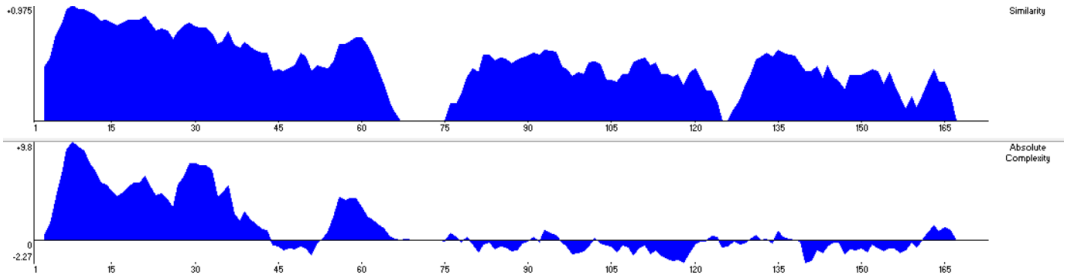


*iii N. gonorrhoeae major and minor pilin protein sequence alignment similarity*

PilE

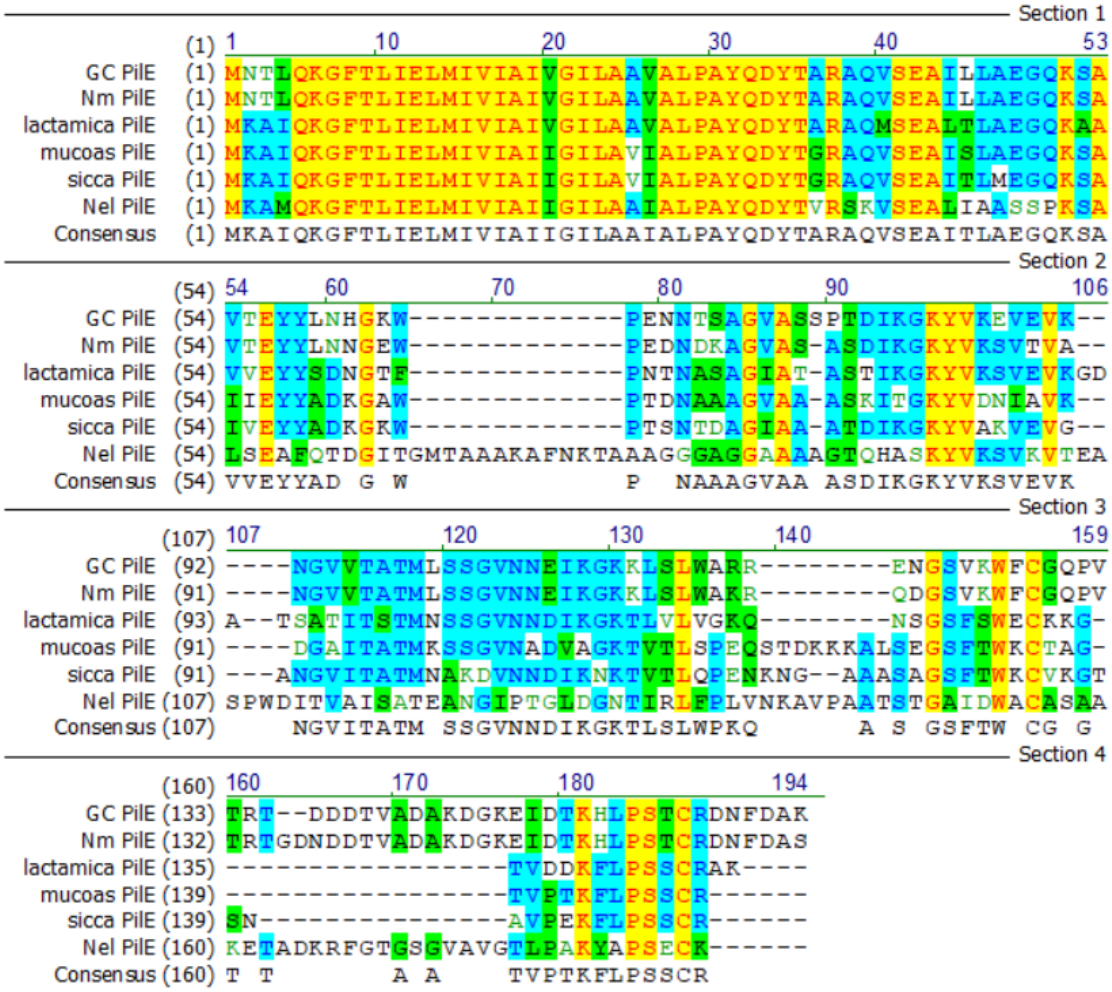


*iv PilE protein sequence alignment comparison between selected Neisseria species*

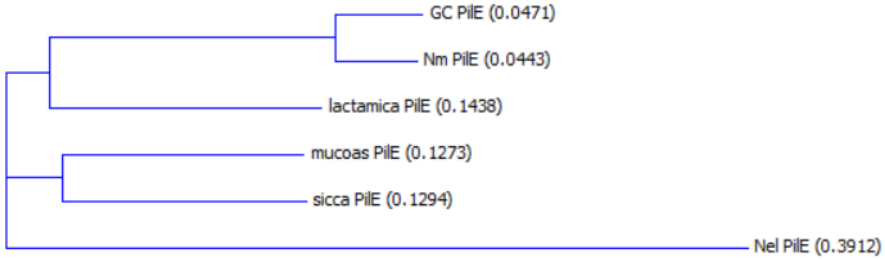


*v Phylogenetic tree based on Neisserial species PilE protein sequence similarity*

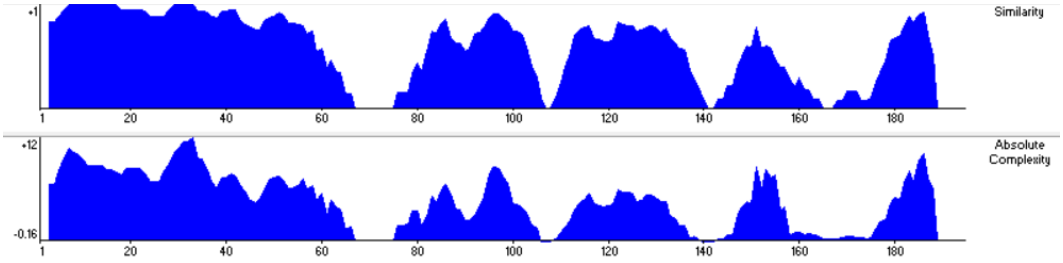


*vi Neisserial PilE protein sequence alignment similarity*

PilV

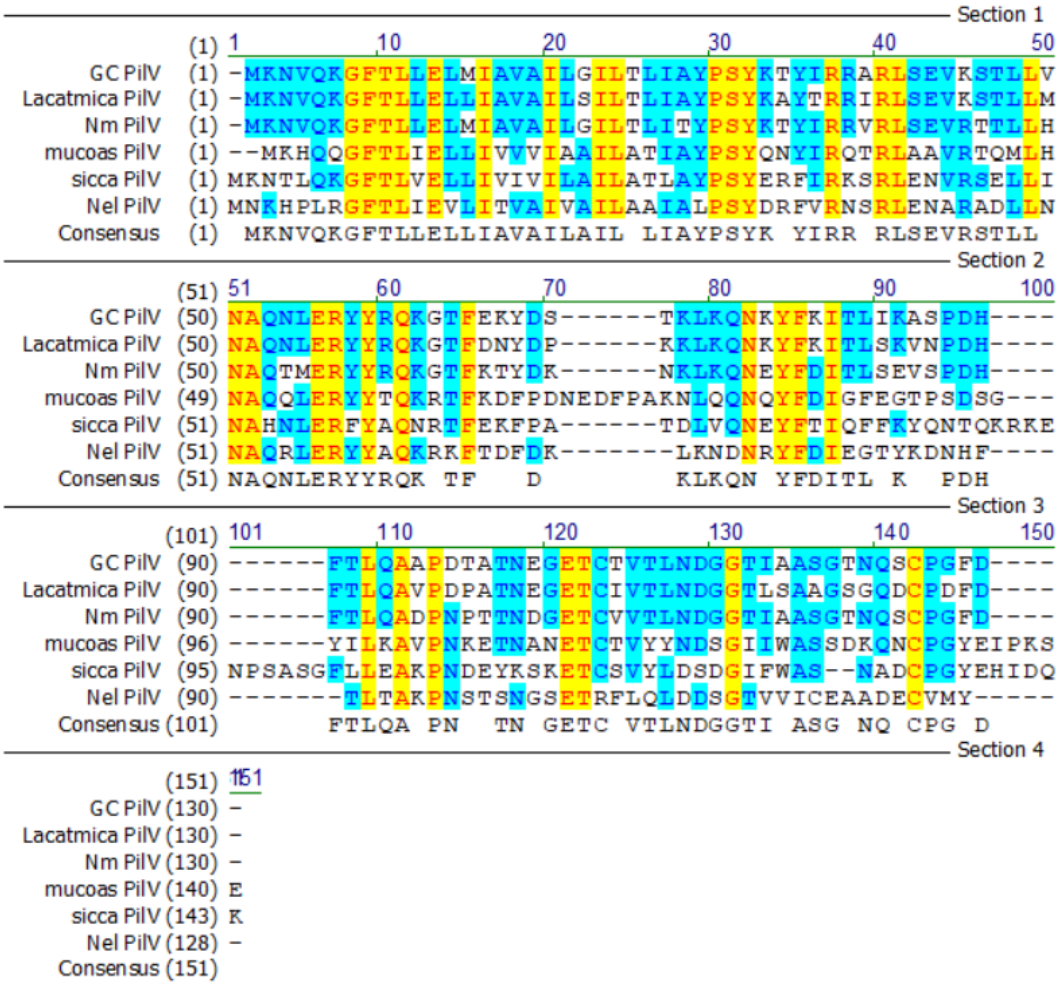


*vii PilV protein sequence alignment among Neisseria species*

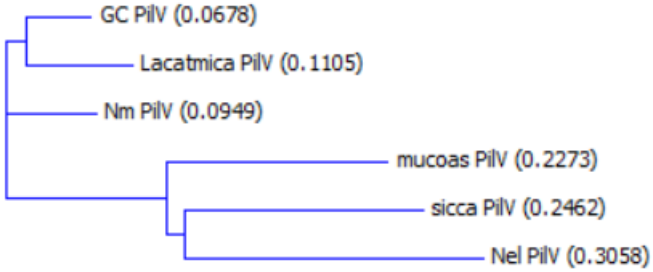


*viii Phylogenetic tree based on Neisseria species PilV protein sequence alignment*

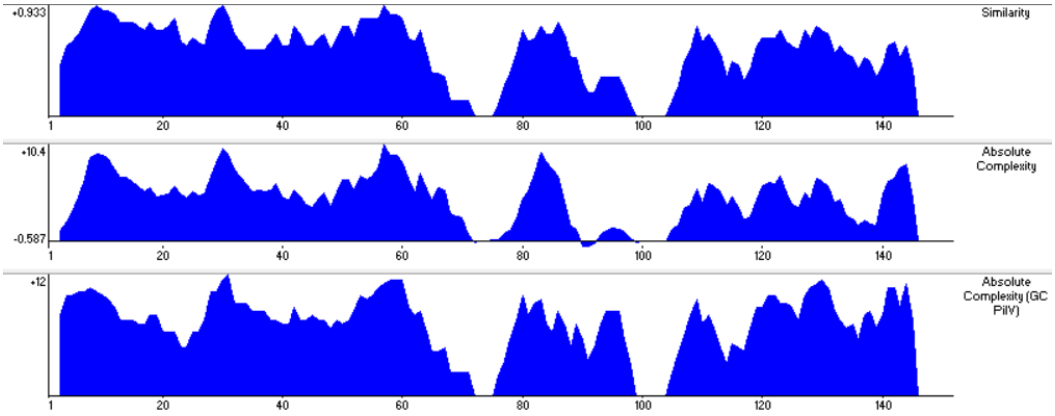


*ix Neisserial species PilV protein sequence alignment similarity*

ComP

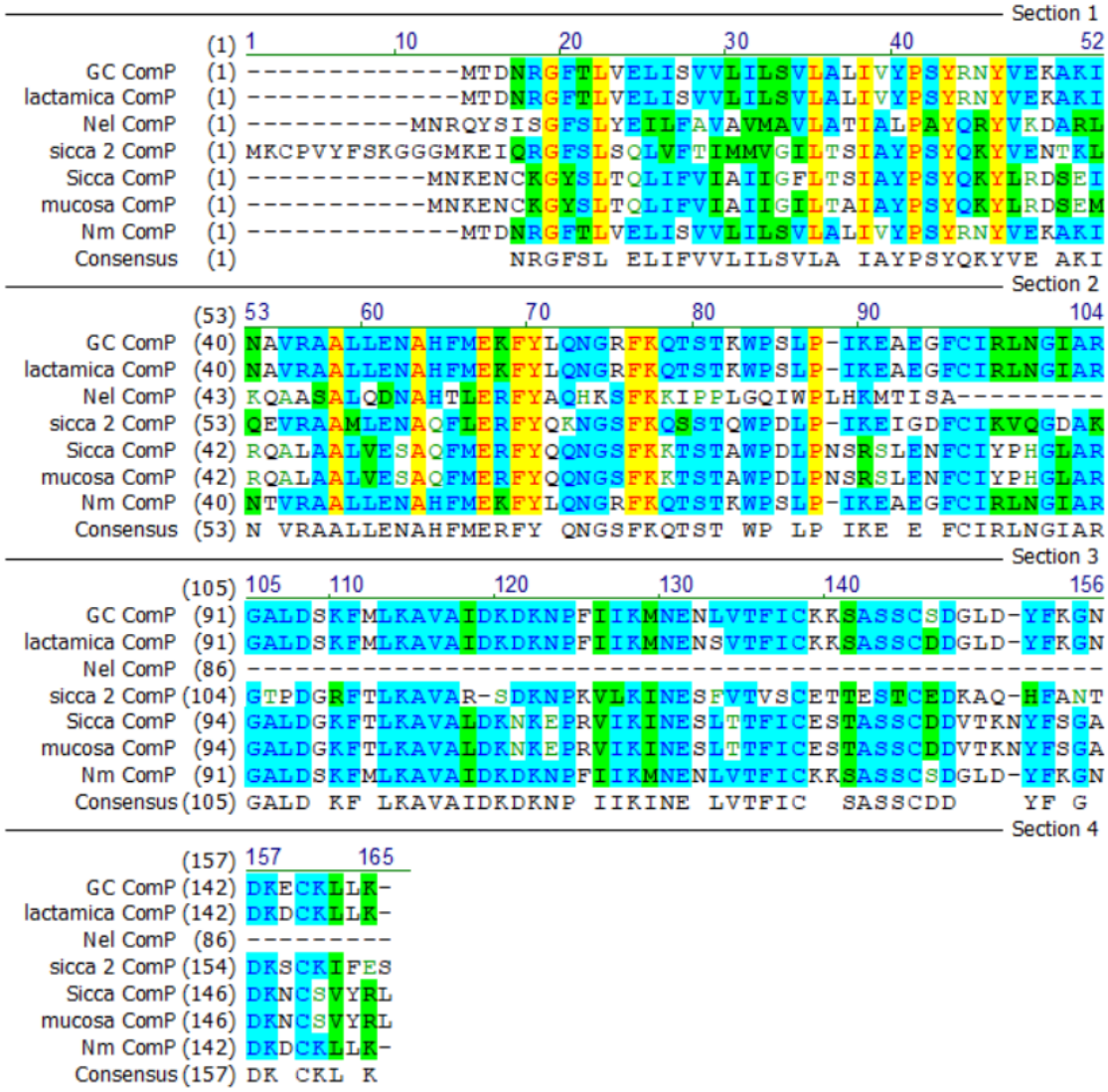


*x ComP protein sequence alignment comparison between selected Neisseria species*

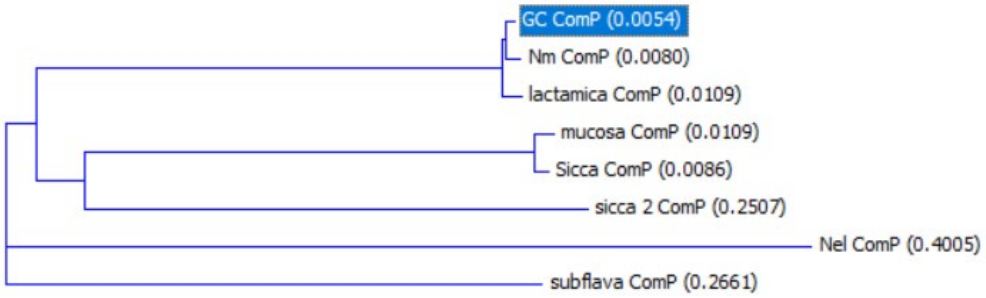


*xi Phylogenetic tree based on Neisserial species ComP protein sequence similarity*

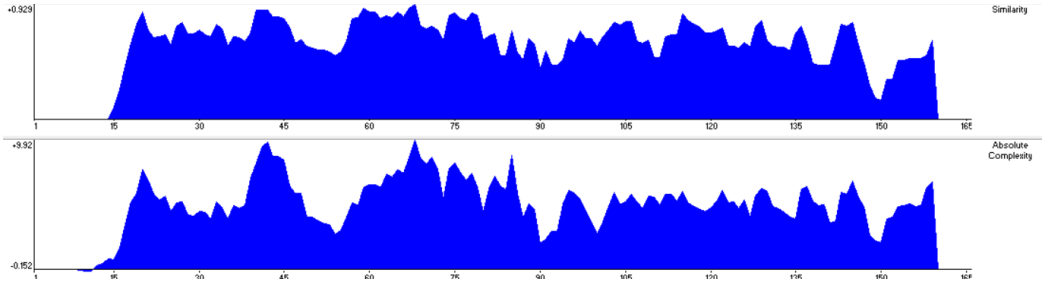


*xii Neisserial ComP protein sequence alignment similarity*

PilS and PilE

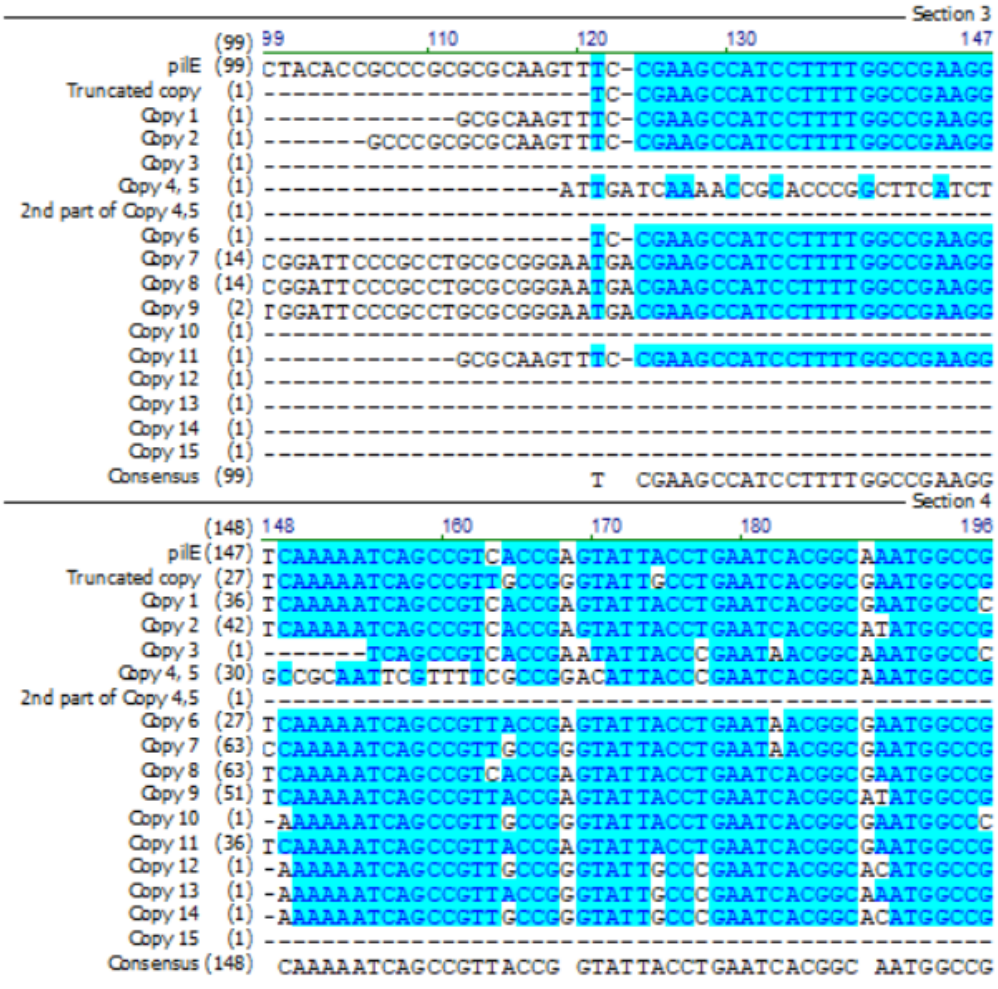

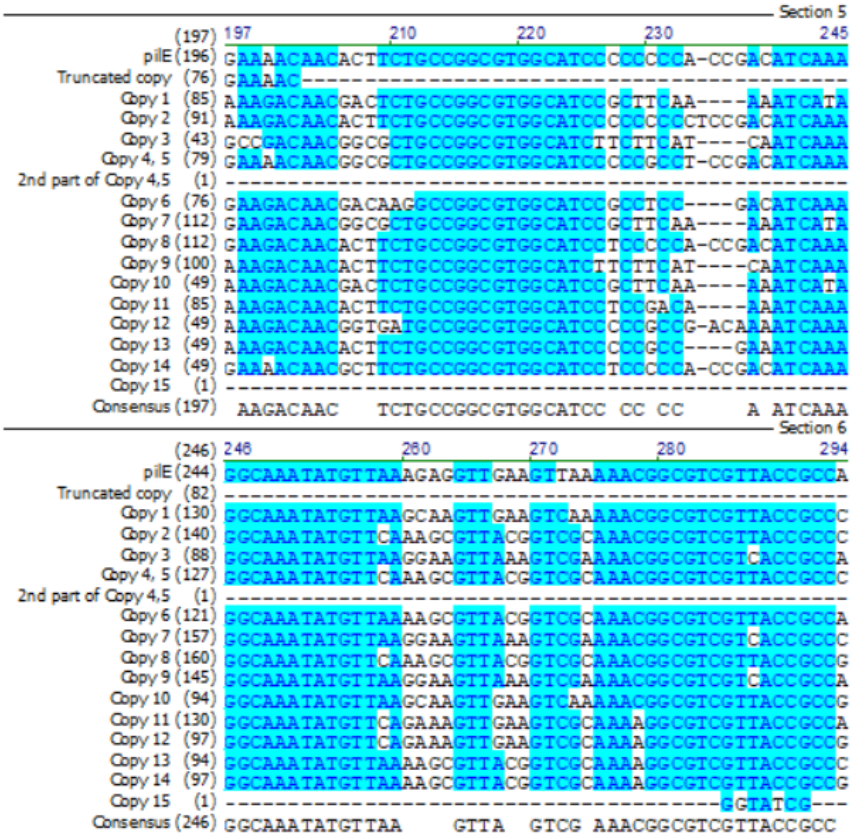
Section 5
Section 6
Section 7
Section 8

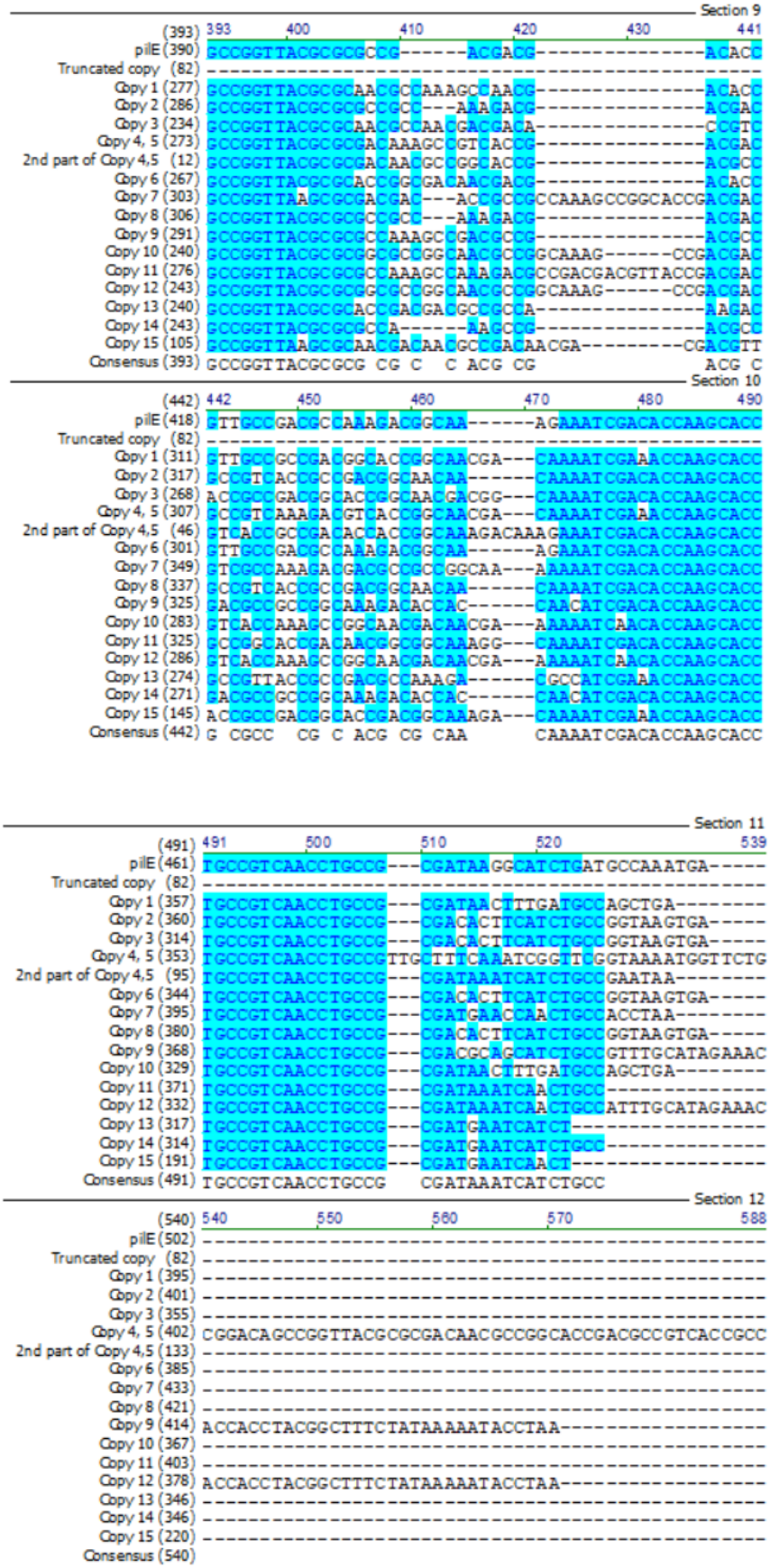


*xiii Sequence alignment between all PilS and PilE*

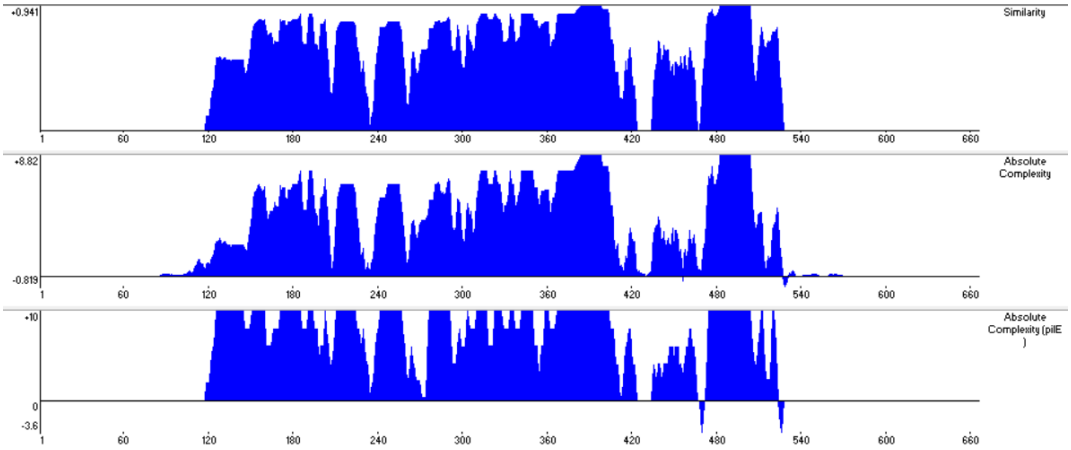


*xiv DNA sequence alignment of all pilS against pilE*

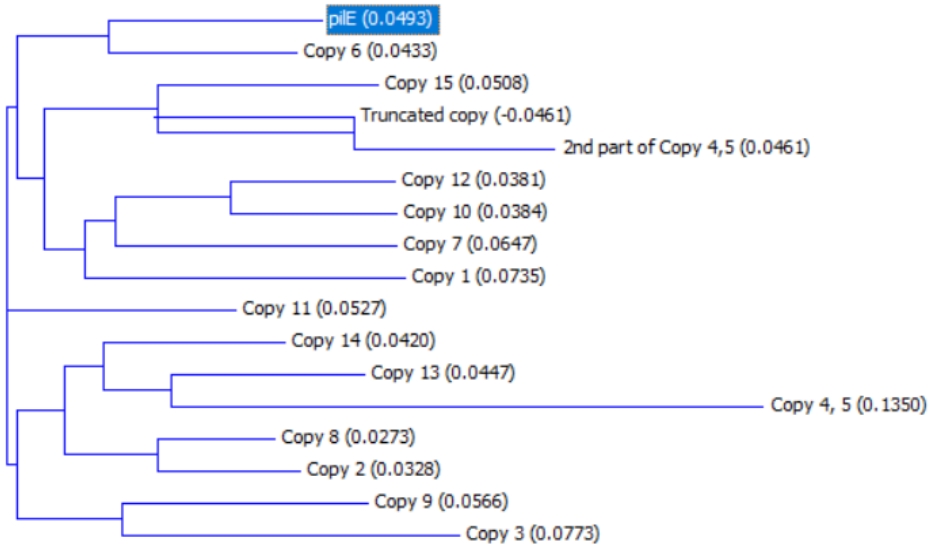


*xv Phylogenetic tree of PilS copies against pilE*

## Supplementary Figure and Tables

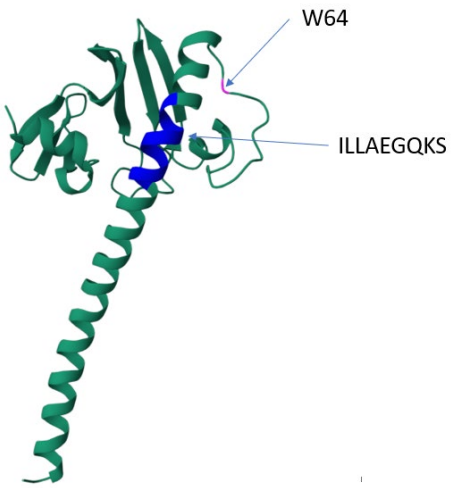


*xvi Position of residues on N. gonorrhoeae PilE*

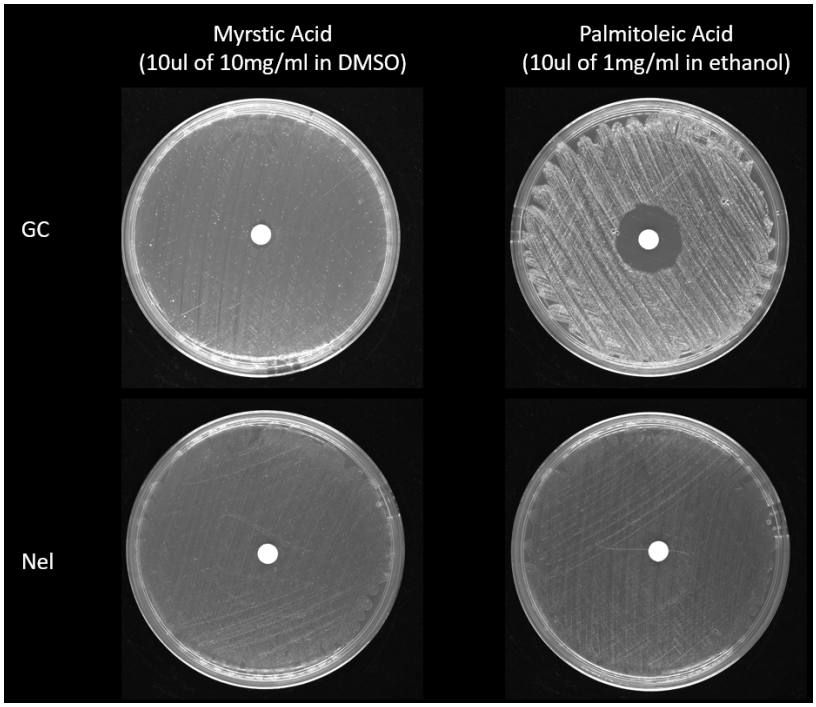


*xvii The effect of different fatty acids on inhibiting growth of N. gonorrhoeae (GC) and N. elongata (Nel)*

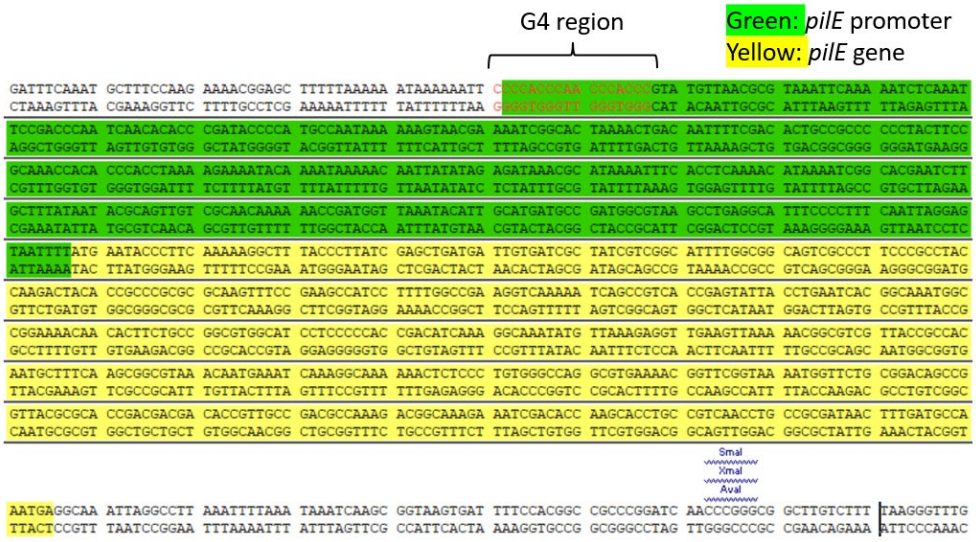


*xviii Location of G4 upstream of pilE gene that is replaced with Kan cassette in ΔG4 strain*

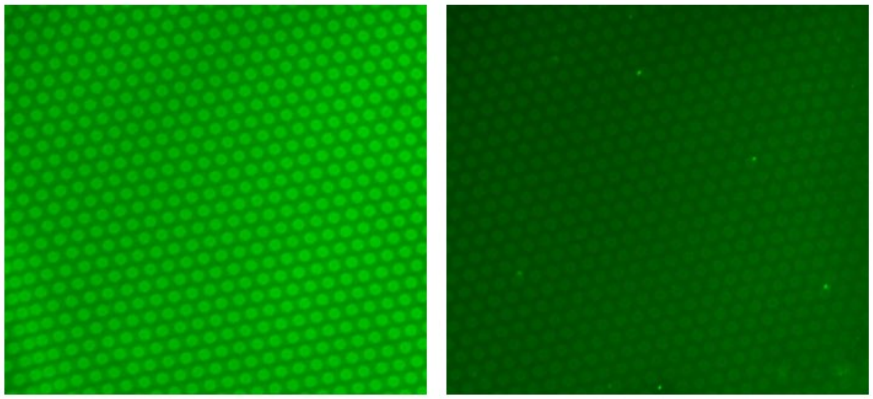

*xix Fluorescence channel image of micropillars when coated with fluorescent carboxylated beads (a) in water and (b) after washes with PBS*

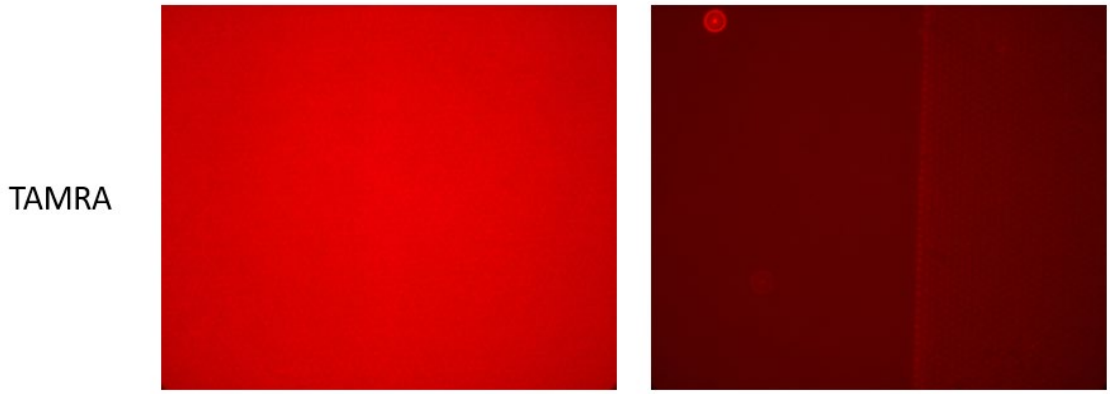


*xx Images showing the effect of washes with PBS on the TAMRA-DNA coating on micropillars*

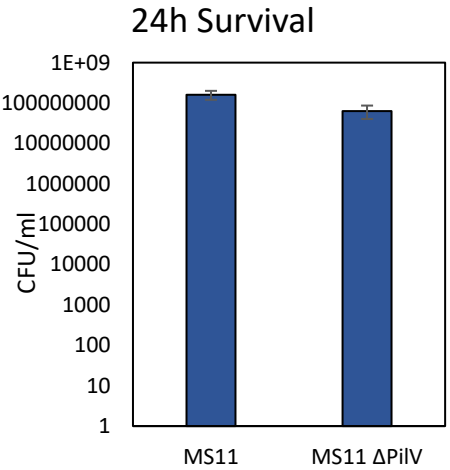


*xxi 24h survival of MS11 and MS11 ΔPilV*

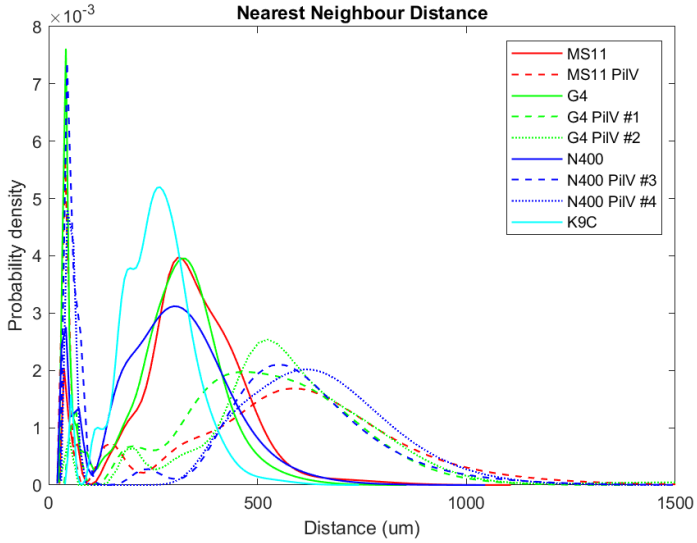


*xxii Near-neighbour-distance analysis of microcolonies between wild-type strains and their ΔPilV mutants*

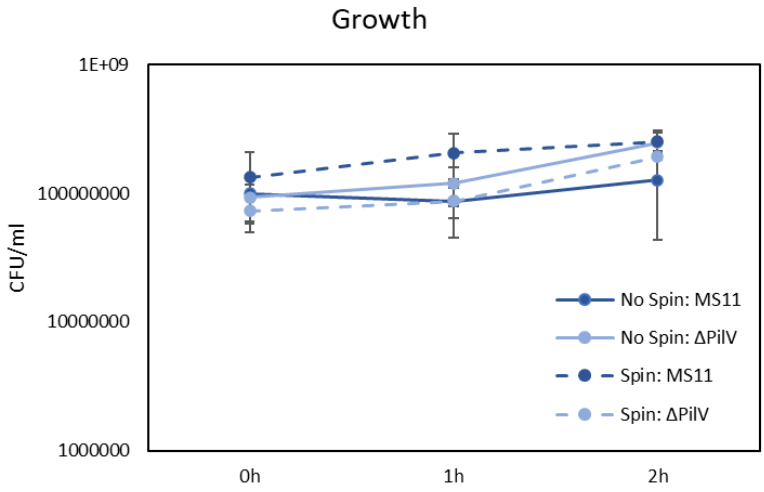


*xxiii Bacterial growth across first 2 hours in aggregation assay*

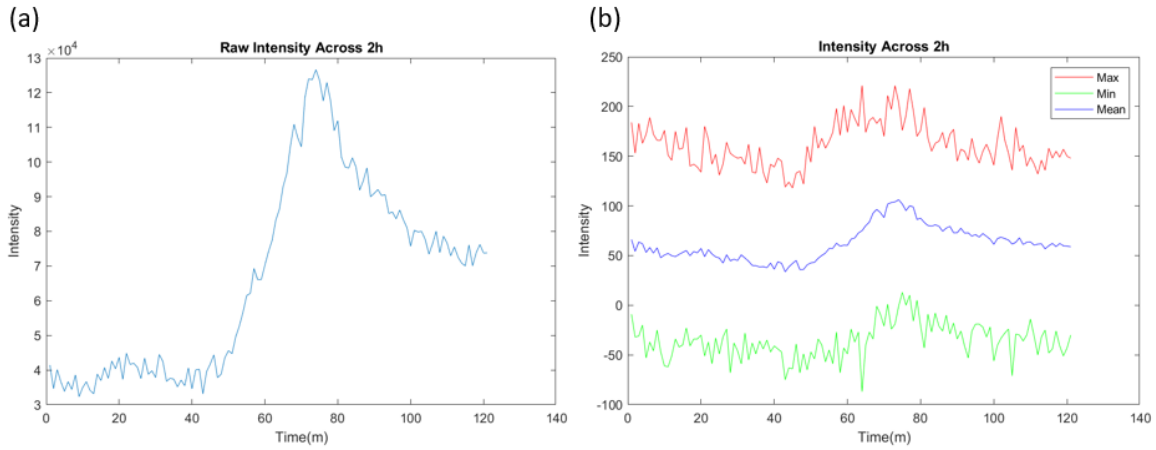


*xxiv Labelled DNA dynamics in MS11 across 2h: (a) Total fluorescence signal intensity in the cluster (b) Maximum, minimum and mean fluorescence signal intensity of the cluster*

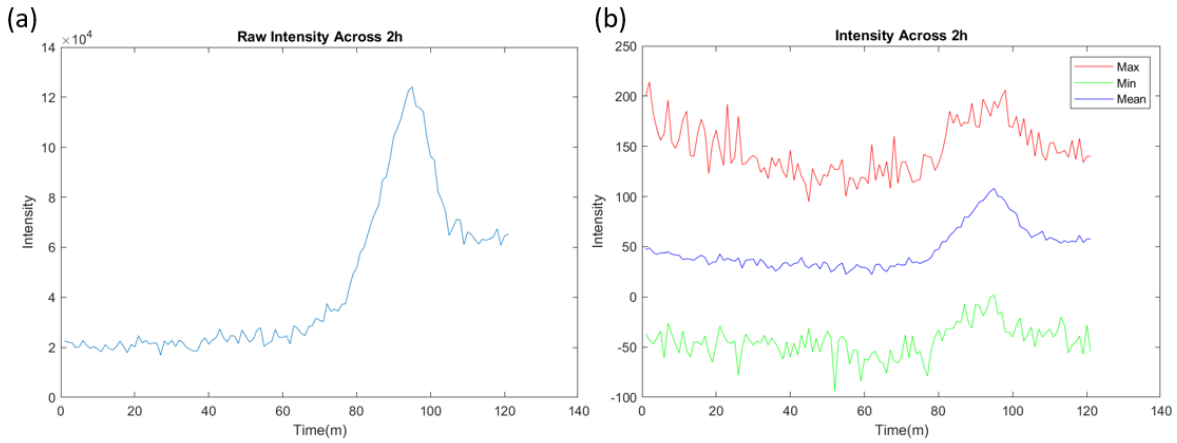


*xxv Labelled DNA dynamics in MS11 ΔPilV across 2h (b) Total fluorescence signal intensity in the cluster (c) Maximum, minimum and mean fluorescence signal intensity of the cluster*

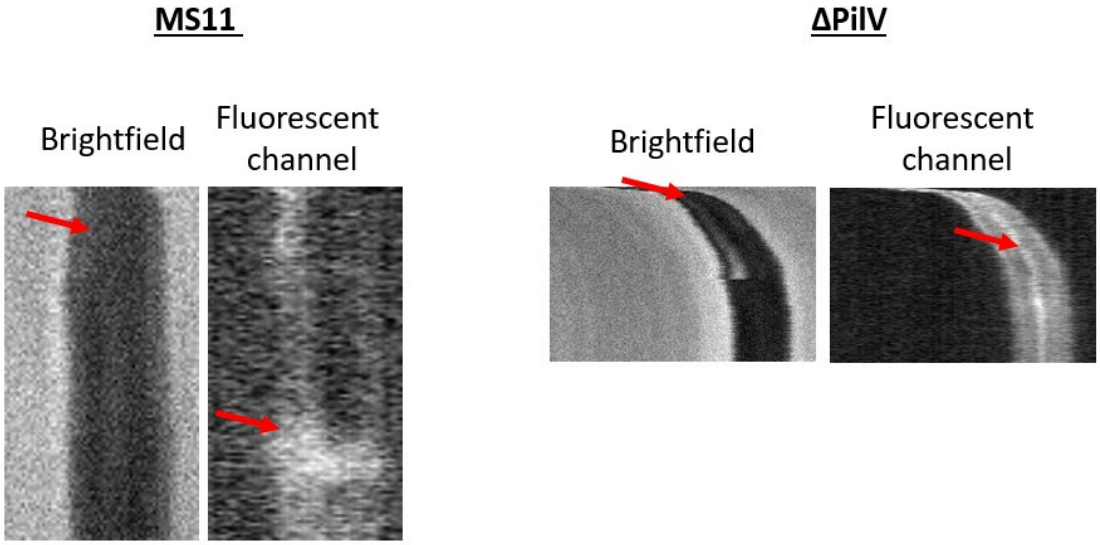


*xxvi Kymograph of DNA signal in MS11 and ΔPilV*

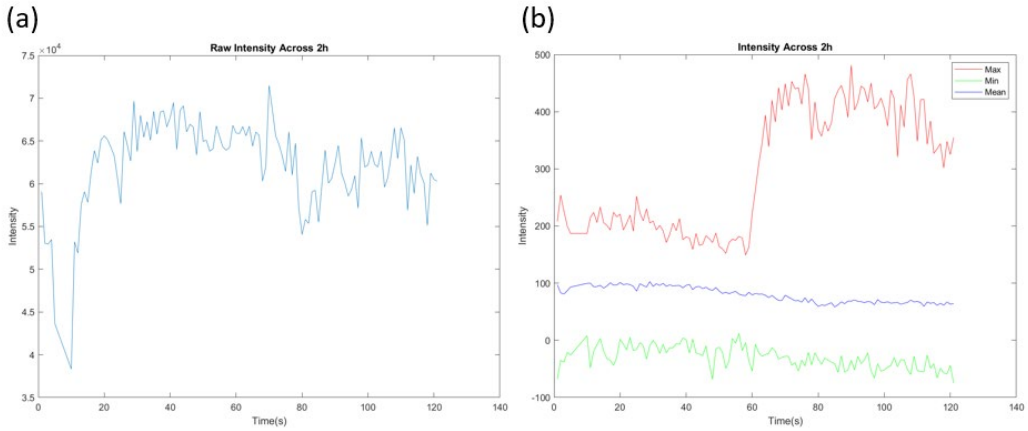


*xxvii Example of possible DNA secretion: (a) Total fluorescence signal intensity in the cluster and (b) Maximum, minimum and mean fluorescence signal intensity of the cluster*

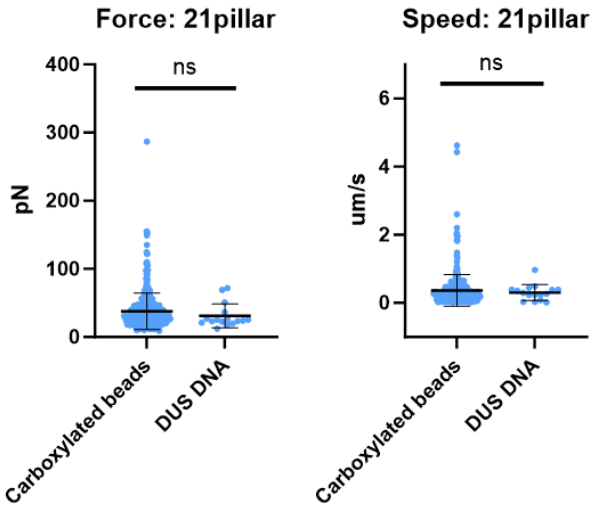


*xxviii Comparison of (a) force and (b) speed of MS11 pili retraction on '21pillar'*

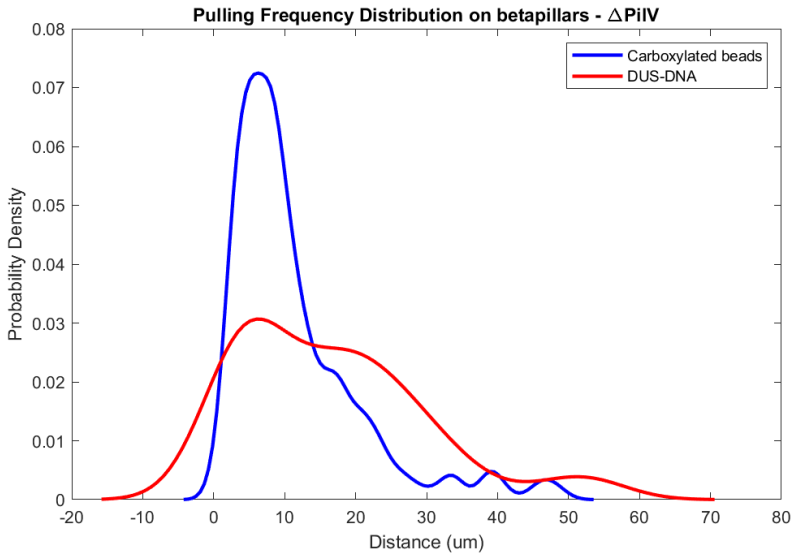


*xxix The probability density of MS11 ΔPilV pili retraction events according to distance away from the centre of the microcolony on 'betapillar' with different coating*

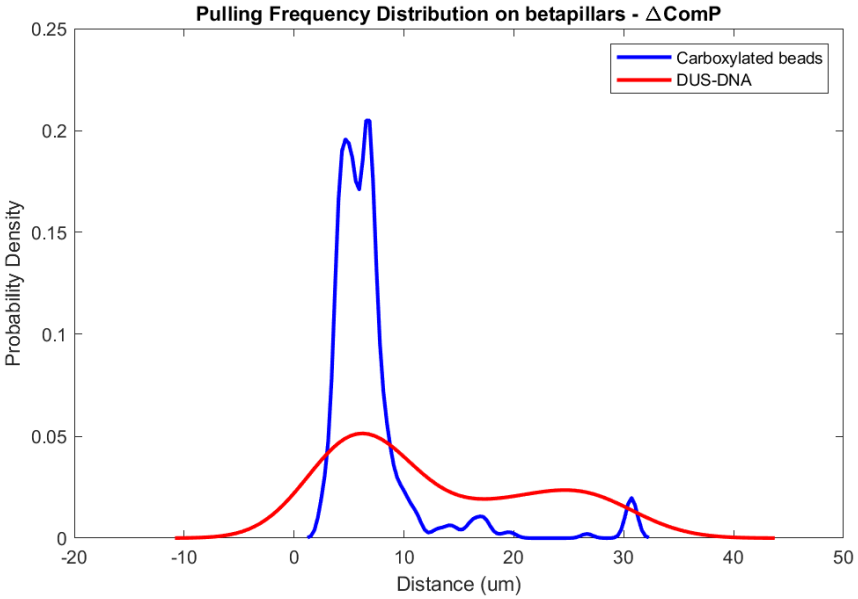


*xxx The probability density of MS11 ΔComP pili retraction events according to distance away from the centre of the microcolony on 'betapillar' with different coating*

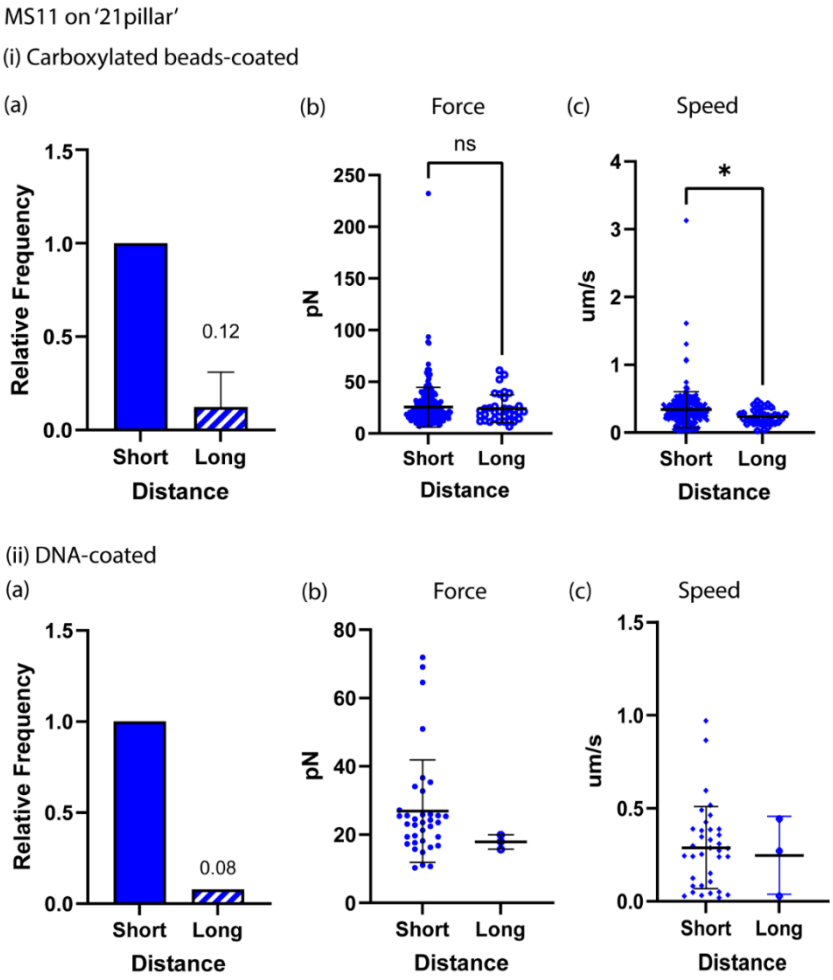


*xxxi Breakdown of pili retraction profile for MS11 on '21pillar' with (i) carboxylated beads-coating and (ii) DNA-coating, detailing the (a) relative frequency, (b) force, and (c) speed of Short and Long distance pili retraction events*

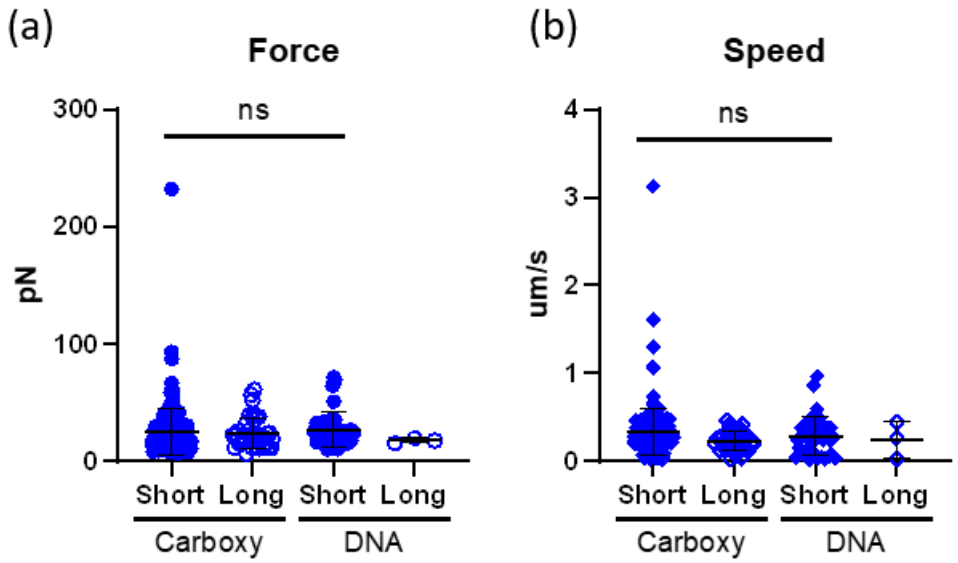


*xxxii Long-distance and short-distance pili events comparison for MS11 on '21pillar' different coating with their respective (a) force and (b) speed*

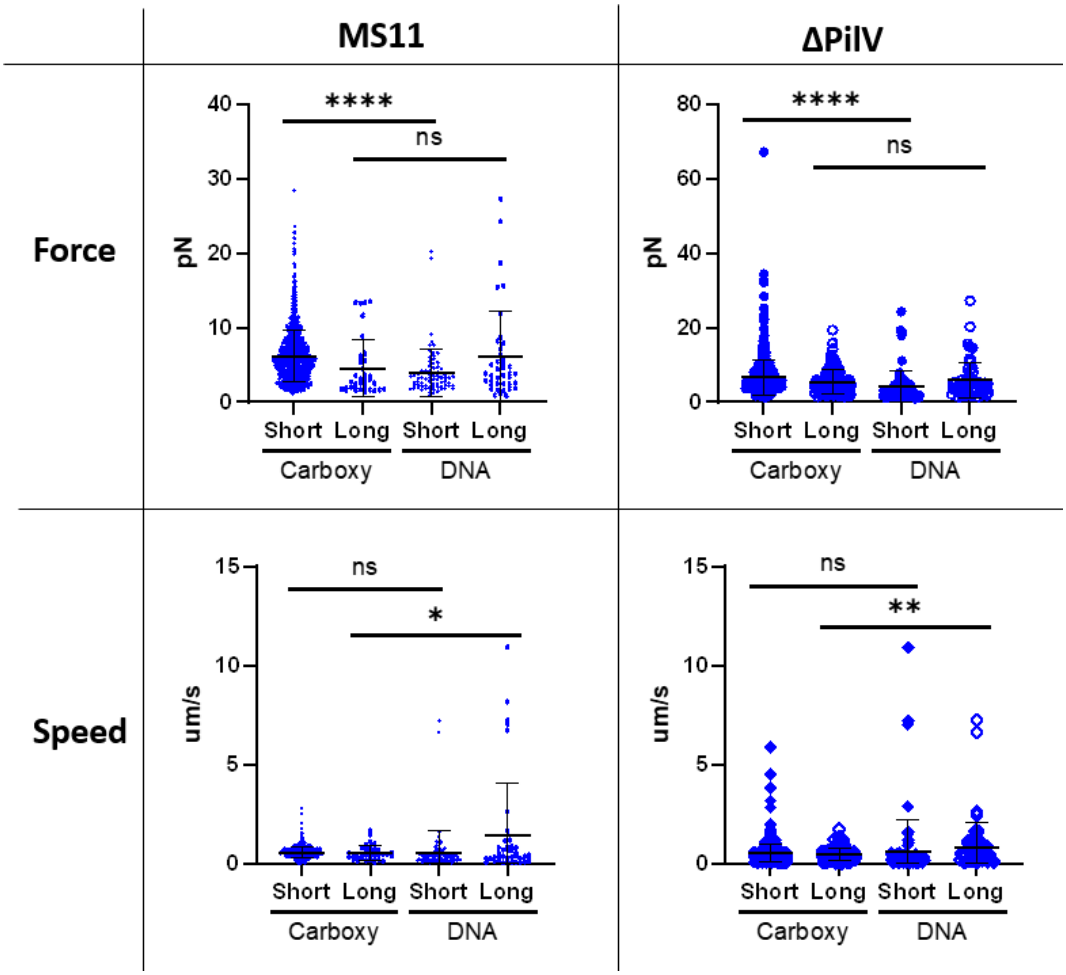


*xxxiii Comparison between pili retraction different coating on 'betapillar" for MS11 and ΔPilV*

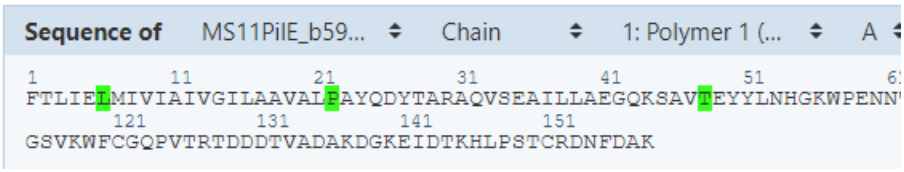


*xxxiv The three amino acids chosen as points to calculate the bending of the alpha helix arm*

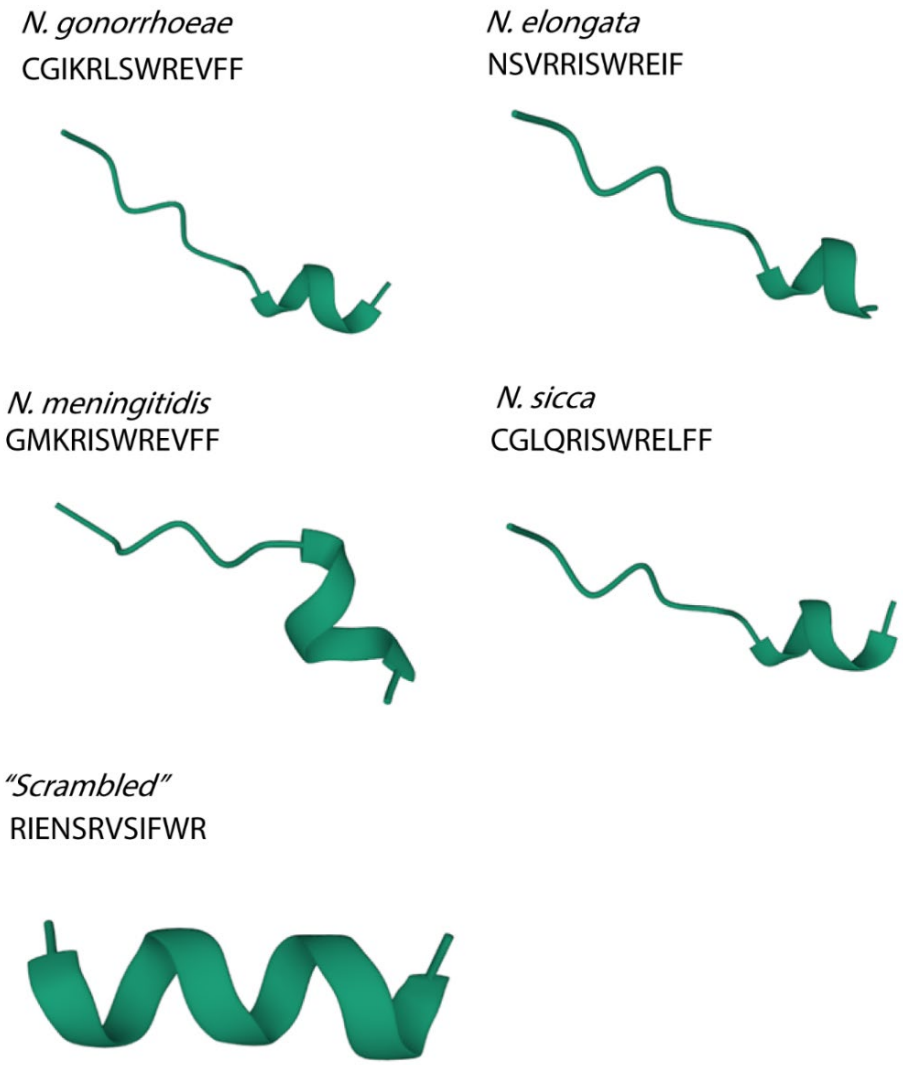


*xxxv The C-terminal peptide sequence of different species origins and their predicted structure using AlphaFold*

(a)

| | | 1 10 |
|---|---|---|
| N. gonorrhoeae | 1 | ---CGIKRLSWREVFF |
| N. elongata | 1 | ---NSVRRISWREIF- |
| N. meningitidis | 1 | ----GMKRISWREVFF |
| N. sicca | 1 | ---CGLQRISWRELFF |
| Scrambled | 1 | RIENSRVSIFWR---- |

(b)

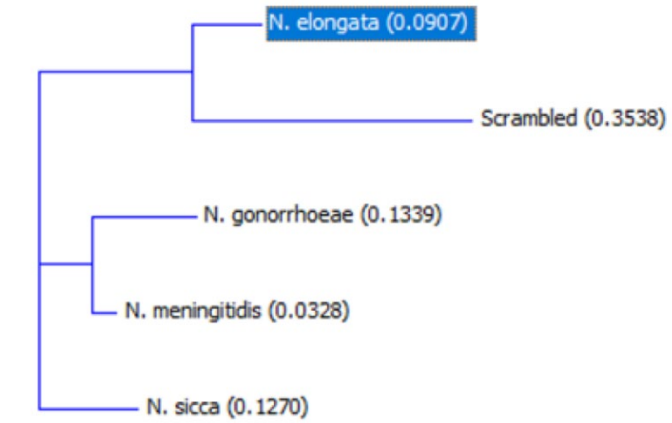


*xxxvi (a) Comparison of sequence similarity of the C-terminal peptides of different origins (b) Schematic representation of the similarities of the C-terminal peptides of different origins*

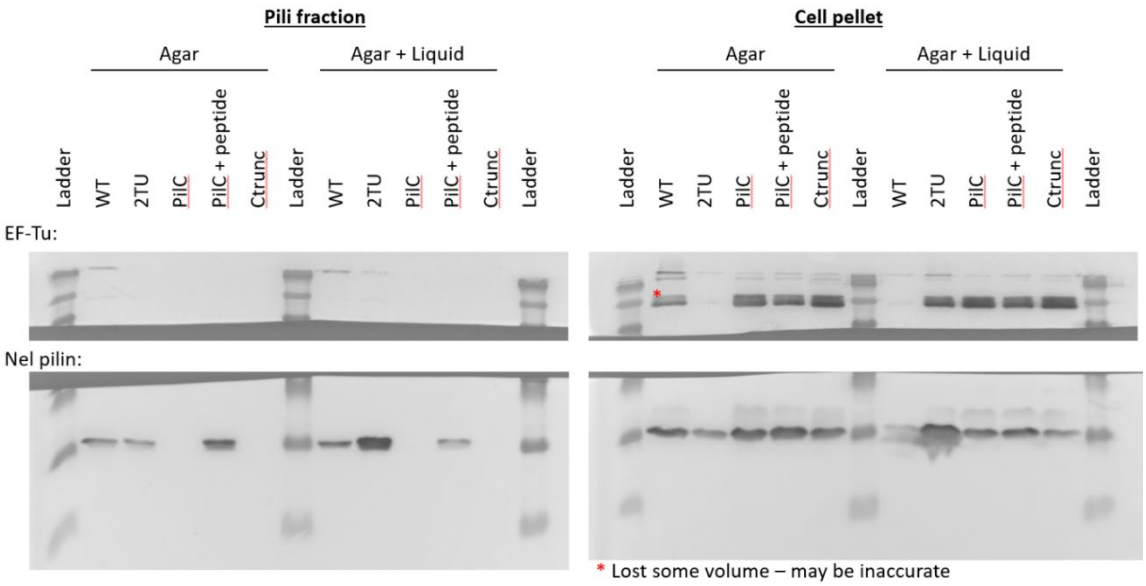


*xxxvii Western blot probing N. elongata pilin collected from overnight culture on solid medium*


*xxxviii The region 'SM1' in which the monoclonal antibody recognises*

First Run data

| | CHES MS11 | | | | AmmBiCarb MS11 | | | |
|---|---|---|---|---|---|---|---|---|
| | 1_10 HCCA | 1_3 H2O 1_1 HC | 1_10 SA | 1_3 H2O 1_1 SA | 1_10 HCCA | 1_3 H2O 1_1 HC | 1_10 SA | 1_3 H2O 1_1 SA |
| MH+ | | | | | not great signa | no signal | | |
| | | | | | | | 17698.624 | 17698.625 |
| | 17705.02 | 17711.026 | 17696.603 | 17701.634 | 17749.444 | | 17734.639 | 17739.023 |
| | | | | | 17876.257 | | 17817.214 | 17821.228 |
| | 17830.061 | 17834.878 | 17819.197 | 17823.594 | | | 17859.38 | 17862.198 |
| | | | Small: 18020.06 | Small: 18025.308 | | | | |

| | CHES G4 | | | | AmmBiCarb G4 | | | |
|---|---|---|---|---|---|---|---|---|
| | 1_10 HCCA | 1_3 H2O 1_1 HC | 1_10 SA | 1_3 H2O 1_1 SA | 1_10 HCCA | 1_3 H2O 1_1 HC | 1_10 SA | 1_3 H2O 1_1 SA |
| MH+ | 3 peaks around | 3 peaks around | 3 peaks around | 3 peaks around | refer to picture | refer to picture | | |
| | | some peaks around 7000 and 8000 | | | | | 17699.813 | 17697.621 |
| | | | | | 17749.056 | 17755.586 | 17739.745 | 17739.562 |
| | | | | | 17832.071 | 17836.082 | 17820.609 | 17822.031 |
| | | | | | 17873.833 | 17879.07 | 17863.338 | 17862.37 |
| | | | | | | | small bump arou | small bump around 18000 |

| | AmmBiCarb F MS11 | | | | AmmBiCarb F G4 | | | |
|---|---|---|---|---|---|---|---|---|
| | 1_10 HCCA | 1_3 H2O 1_1 HC | 1_10 SA | 1_3 H2O 1_1 SA | 1_10 HCCA | 1_3 H2O 1_1 HC | 1_10 SA | 1_3 H2O 1_1 SA |
| MH+ | | very low signal | very low signal | | low signal | no signal | | very small bump around 17700 |
| | | | | 17698.224 | 17716.629 | | | |
| | 17752.663 | | 17737.029 | 17741.222 | 17756.663 | | 17739.939 | 17742.21 |
| | very small signal round 17830 | | 17865.78 | 17825.245 | 17836.138 | | 17822.832 | 17826.809 |
| | 17875.044 | | | 17865.804 | 17873.045 | | 17863.805 | 17866.322 |

*xxxix The first run of samples on MALDI-TOF shows better resolution when using Ammonium bicarbonate as buffer and SA as the matrix*

*T- i Descriptive analysis of the Force of pili retraction in PilD mutants*

| | ΔG4 | C72S | C72SI134M | G93S | C72SG93S |
|---|---|---|---|---|---|
| Number of values | 2370 | 1291 | 5444 | 1471 | 3681 |
| Mean | 28.50 | 28.65 | 31.26 | 29.91 | 31.11 |
| Std. Deviation | 16.12 | 17.59 | 18.56 | 19.14 | 18.15 |
| Std. Error of Mean | 0.3311 | 0.4897 | 0.2515 | 0.4990 | 0.2992 |

*T- ii Statistical analysis of the 'Force' dataset distribution*

| | Unpaired t-test with ΔG4 |
|---|---|

| | C72S | C72SI134M | G93S | C72SG93S |
|---|---|---|---|---|
| P value | 0.7933 | <0.0001 | 0.0137 | <0.0001 |
| P value summary | ns | **** | * | **** |
| F test P-value | 0.0003 | <0.0001 | <0.0001 | <0.0001 |
| F test summary | *** | **** | **** | **** |

*T- iii Descriptive analysis of the Speed of pili retraction in PilD mutants*

| | ΔG4 | C72S | C72SI134M | G93S | C72SG93S |
|---|---|---|---|---|---|
| Number of values | 2370 | 1291 | 5444 | 1471 | 3681 |
| Mean | 0.3728 | 0.3459 | 0.3994 | 0.4057 | 0.4124 |
| Std. Deviation | 0.1863 | 0.1508 | 0.2107 | 0.2585 | 0.2378 |
| Std. Error of Mean | 0.003828 | 0.004198 | 0.002856 | 0.006740 | 0.003920 |

*T- iv Table 0.3 Statistical analysis of the 'Speed' dataset distribution*

| | Unpaired t-test with ΔG4 | | | |
|---|---|---|---|---|
| | C72S | C72SI134M | G93S | C72SG93S |
| P value | <0.0001 | <0.0001 | <0.0001 | <0.0001 |
| P value summary | **** | **** | **** | **** |
| F test P-value | <0.0001 | <0.0001 | <0.0001 | <0.0001 |
| F test summary | **** | **** | **** | **** |

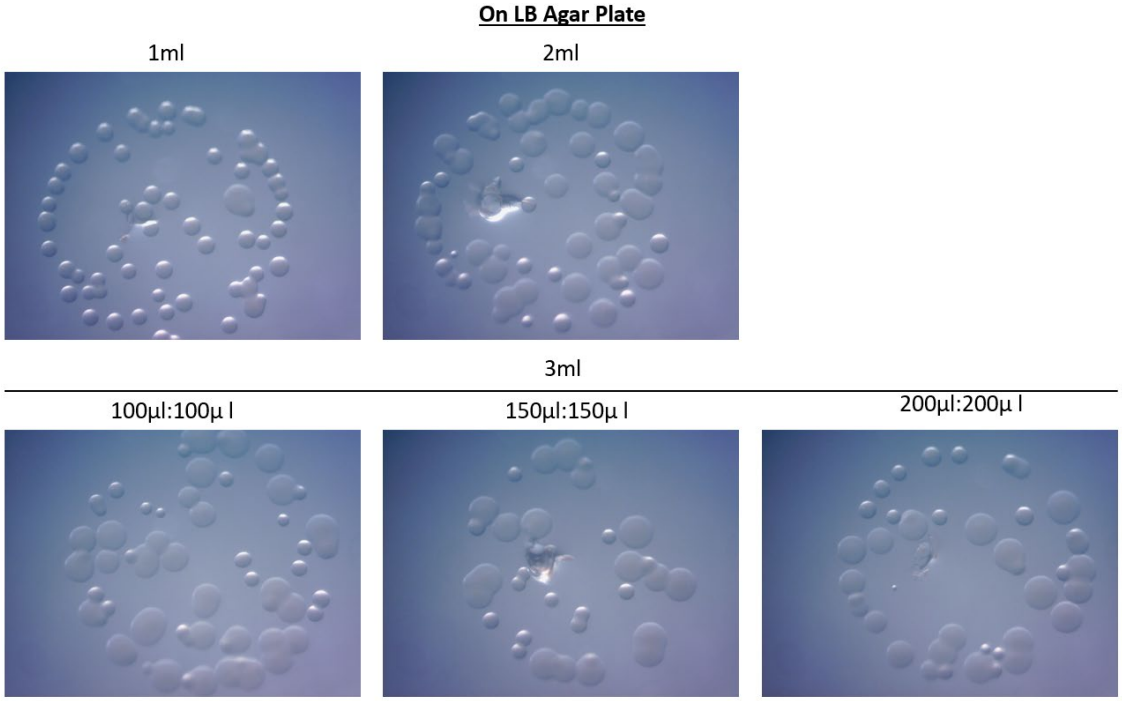


*xl Colony morphology in different conditions on LB agar plate*

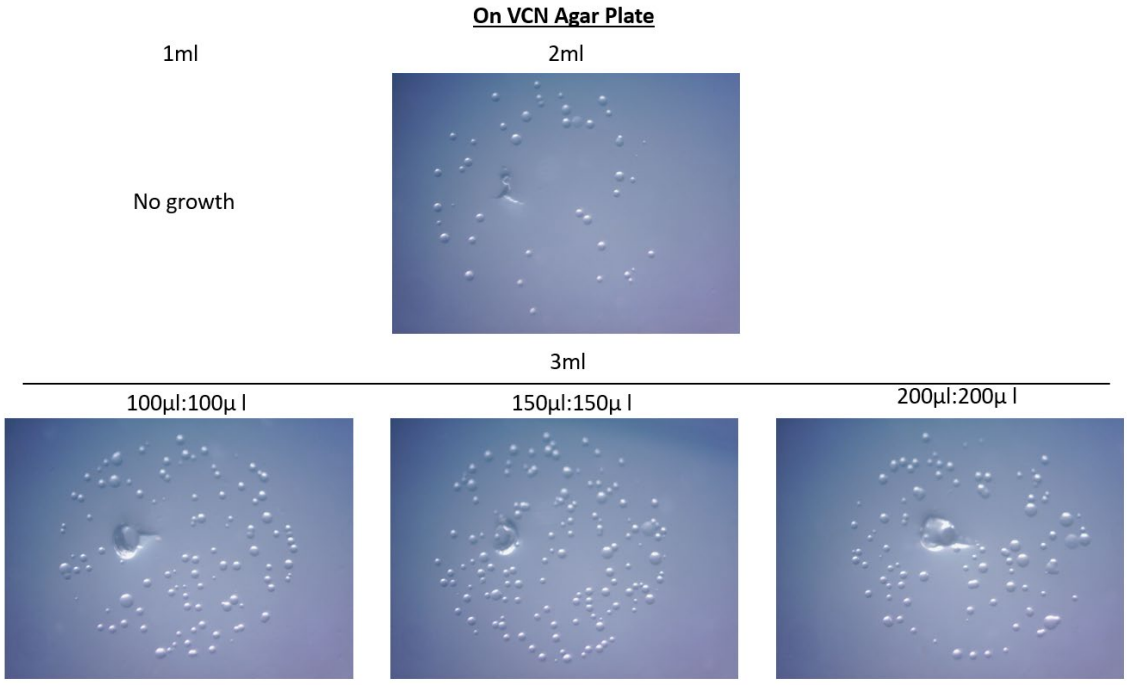


*xli Colony morphology in different conditions on VCN agar plate*

## Tn5 mutagenesis library screening mutants locus

glyK locus (514761-515875):

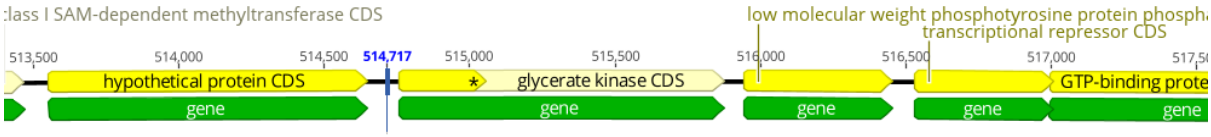


putP locus (1597688-1599214):

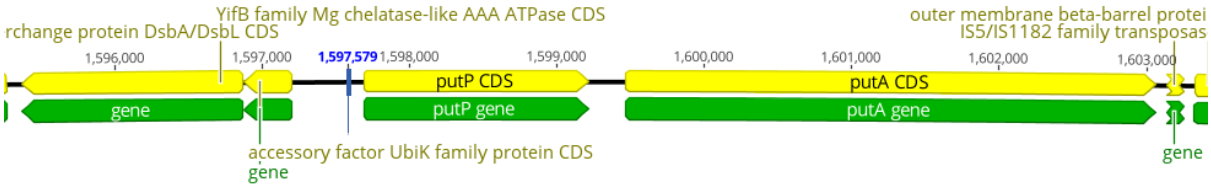


Na+H+ locus

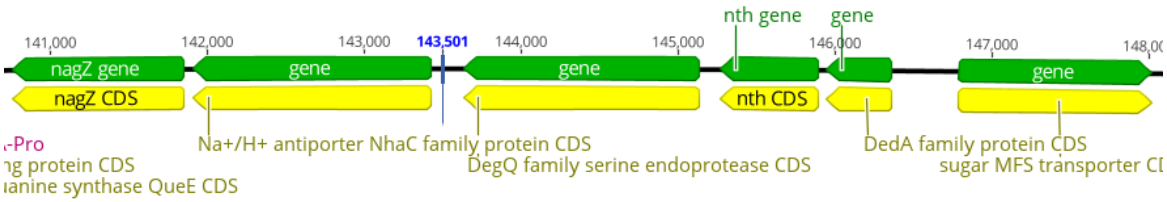


SIS-containing ->hexR locus

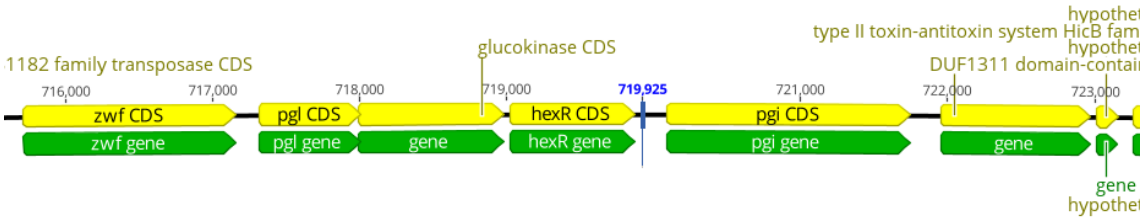


prmA locus:

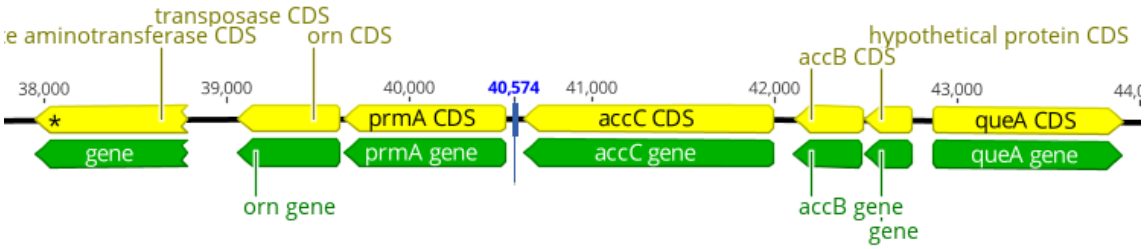

# Appendix II

## Study I: ROI Determination for Image Analysis

In the **circle method**, each cell body was identified first, and then a centre of mass coordinate was determined. From there, a circle with a set radius was drawn to include the cell body and the area around the cell. To determine the best radius to use for subsequent tests, we run a simple analysis with different radii around the same image. The larger the radius, the lower the mean intensity of the ROI. This is an expected outcome since the larger the radius, the more background signal was included. The hypothesis was that as we reduce the radius size, the intensity will saturate at a certain value and drop slightly if the signal gathers mainly at the cell's outer shell. Our results (xlii) showed no significant drop in mean intensity as the radius decreased. However, the mean intensity did increase as the radius decreased below r = 20. When we check the same method with puncta analysis (xlii), we also lose the resolution when the r drops lower than r = 20. Due to these findings, we decided to analyse with r = 20.

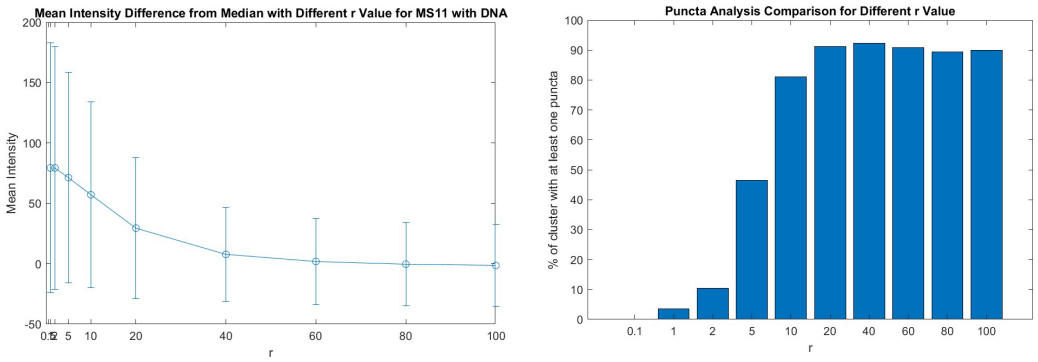


*xlii (Left) Determining ROI using circles with radii, r, with their corresponding mean intensity output (Right) Circle Method ROI circle with radii, r, and how that affects % of the cluster with at least one puncta*

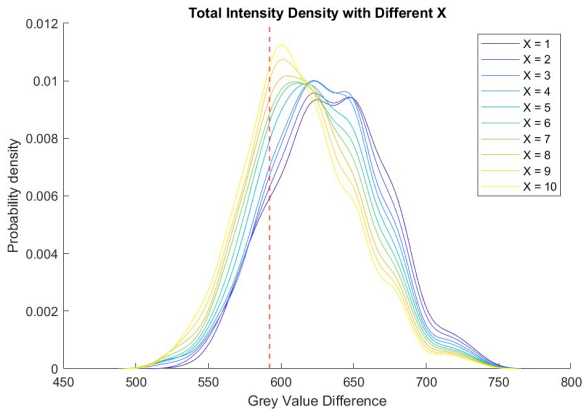


*xliii Figure 7.24 Probability density of intensity inside clusters when clusters are filtered with different spherical structural elements with the radius X*

We similarly identified each cell cluster as an object in the **cluster method**. However, instead of determining a given shape as ROI, we performed filters to increase the ROI region around the original ROI. To do that, we first used a Gaussian filter to blur the edge of cells, and then we used a spherical structural element with a radius X, in which the value of X is in pixels. Through this optimization, we intend to select the optimal X value for our subsequent analysis, which will include as much signal as possible and not lose any resolution. From our investigation using selected images, we can see the probability density of intensity is distributed more around 650 for X = 1 (xliii). When X increases, the probability peak shifts

towards a lesser grey value, nearer to the median value of the image, also set as the background in our image analysis. This observation is expected and fits our hypothesis that the bigger the ROI, the more signal we lose. In this case, we can see that X = 1 is already the best choice in selecting ROI in the Cluster Method.

After deciding on the details of ROI selection for both Circle and Cluster Methods, we tested the robustness of these two methods on images to see the difference in signal. Using the same data set, we looked at MS11 and ΔPilV under the conditions of no DNA and with DNA. Both analyses note that the Circle Method does not allow good resolution between 'no DNA' and 'DNA' (xliv). The tail on the right side of the peak in xlvi is very narrow, and when plotted as a violin plot, although the difference in distribution could be observed, the mean difference is not apparent. However, the Cluster Method analysis shows a distinct distribution for MS11 and ΔPilV with no DNA (xliv). For conditions with DNA, the distribution shifted significantly to the right, showing good resolution. This analysis can be confirmed by the violin plot as well.

The difference in outcome in the two methods only shows when analyzing the intensity. When we look at the analysis of puncta, both analyses for either the percentage of clusters with more than one puncta or the percentage of clusters with a different number of puncta, both Circle Method and Cluster Method, while having slight variations, do not differ (xlv). This shows that most of the puncta is well captured in the given ROI, hence the robustness of the analysis protocol. The distribution of pixel value density in ROIs between the two methods also shows that the Cluster Method has a higher sensitivity to capture the intricate nature of DNA fluorescence intensity within ROI . In the density we see from the Cluster Method, we observe more clusters with higher pixel value density in ΔPilV.

Cluster Method Details

Using the Cluster Method to determine ROIs, we investigated the nature of the signal intensity within these ROIs to get some preliminary information about the DNA molecules taken up into the cells. Our data on the pixel value against cell cluster area (Figure 1.46) shows that though

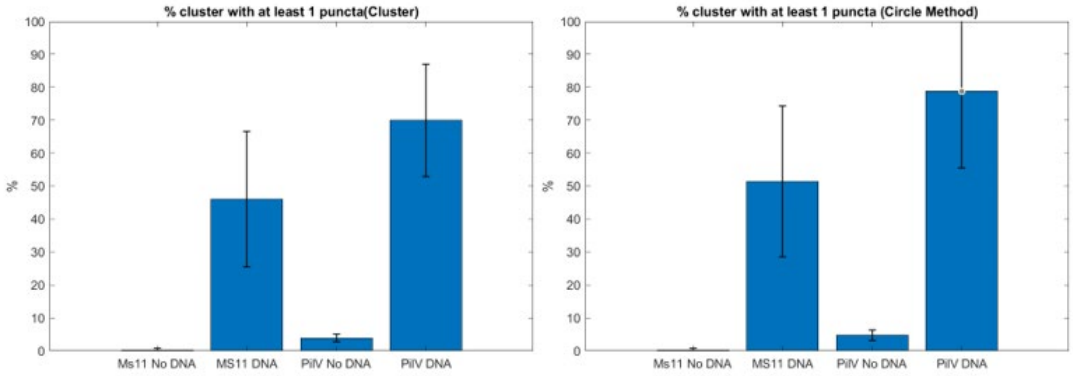


*xliv Comparison of the puncta analysis (at least one punctum) between (a) Cluster Method and (b) Circle Method*

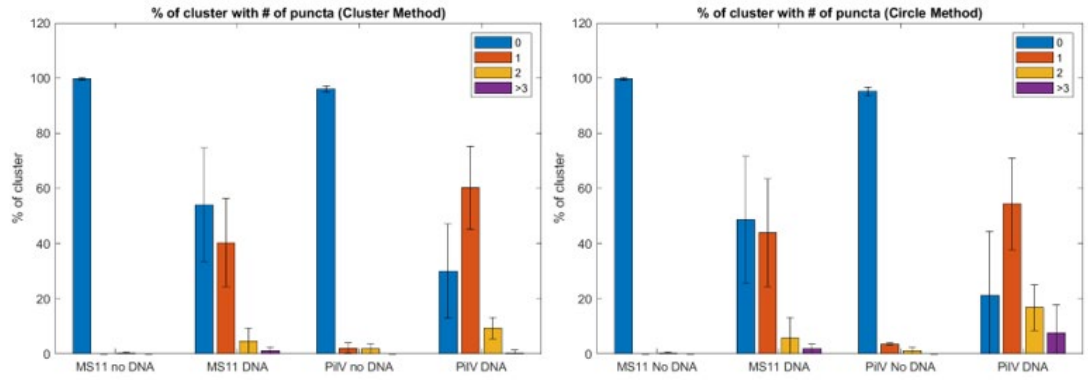


*xlv Comparison of the puncta analysis summary between (a) Cluster Method and (b) Circle Method*

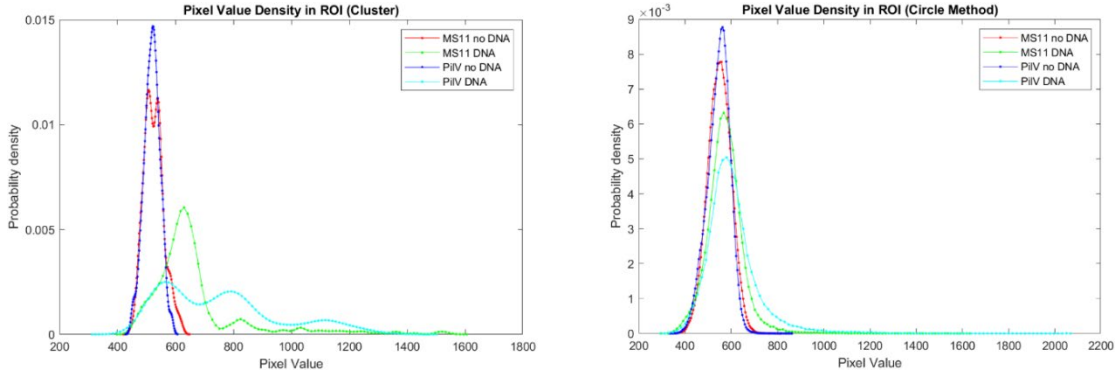


*xlvi Comparison of probability density of pixel value density in ROI between (a) Cluster Method and (b) Circle Method*

it is generally expected that a higher ROI area will lead to a higher total pixel value, it is not definite. We also observed some ROIs at the smaller area range presenting high signals. These could be cells that take up more DNA molecules. However, when we look at the mean intensity of these ROIs in relation to their area size, we observe the mean intensity of the ROIs stayed similar while higher on the ΔPilV side (xlviii). This shows that the mean intensity reading we took generally averaged out some potential signals that we captured. A quick look at the probability density of total intensity and mean intensity of ROIs in MS11 and ΔPilV shows that most ROI intensity profiles dabble around the same range, with ΔPilV's skewed towards the higher value. We then dissect this information according to each cell cluster by extracting their intensity profile like minimum, maximum and the difference between maximum and minimum. While most of the Cell Clusters have around the same minimum pixel intensity, we can identify some Cell Clusters with high maximums leading to high differences in pixel intensity in the cell cluster. This might point towards heterogeneity of fluorescence signal and probably means DNA molecules might present as puncta in the cell. The variation can also be confirmed when we map out their probability density. These higher maximum pixel intensity phenomena can be observed more often in ΔPilV and will be discussed in Chapter 4 on its implications.

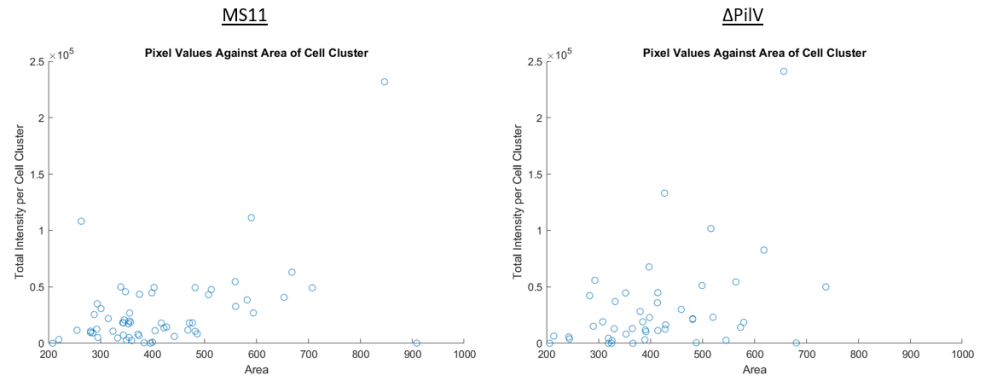


*xlvii Total intensity per Cell Cluster against area in (a) MS11 and (b) ΔPilV*

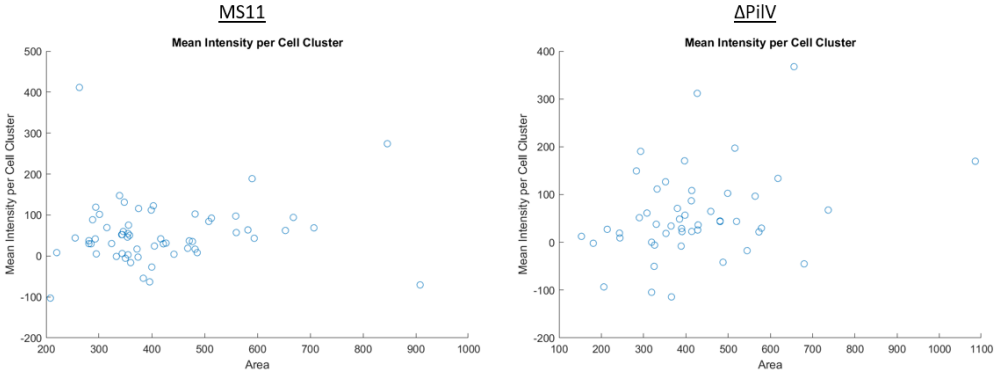


*xlviii Mean intensity per Cell Cluster against area in (a) MS11 and (b) ΔPilV*

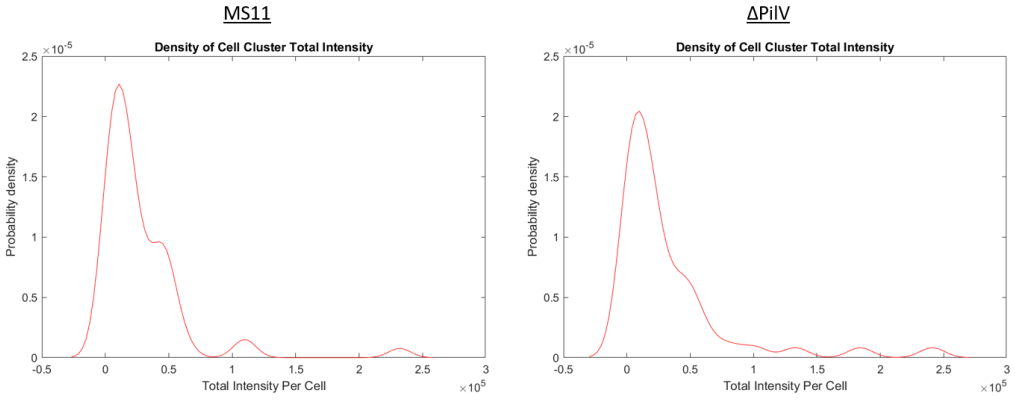


*xlix Probability density of Cell Cluster total intensity in (a) MS11 and (b) ΔPilV*

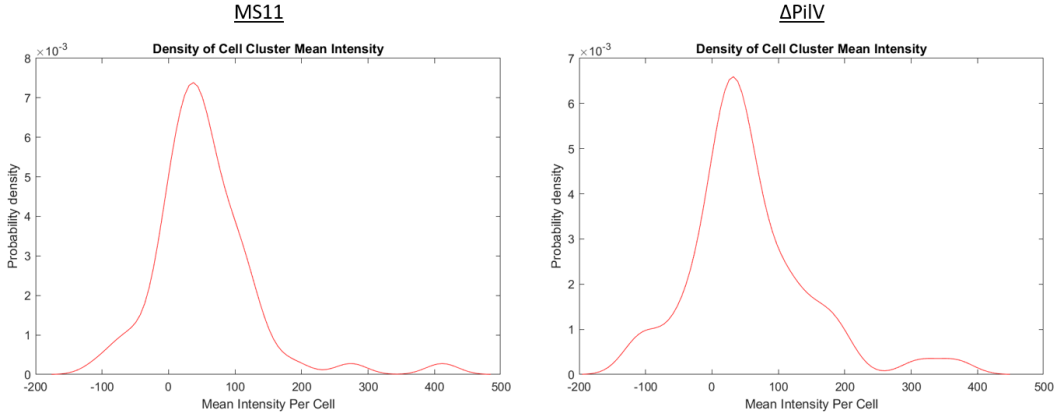


*l Probability density of Cell Cluster mean intensity in (a) MS11 and (b) ΔPilV*

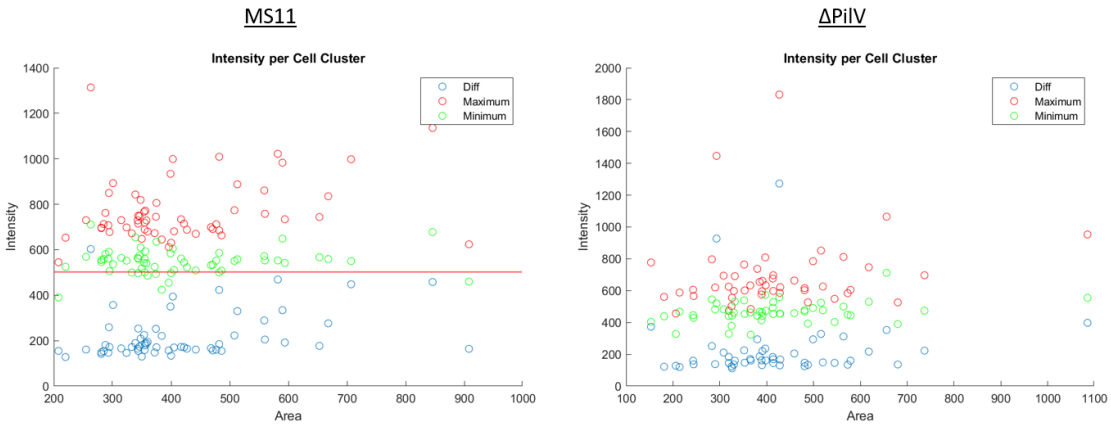


*li Pixel intensity profile of Cell Cluster in (a) MS11 and (b) ΔPilV*

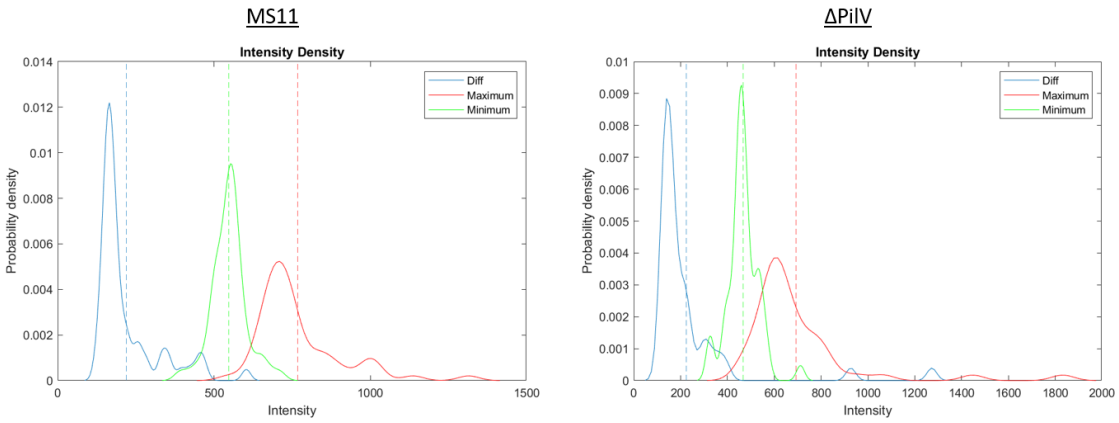


*lii Probability of Pixel intensity profile of Cell Cluster in (a) MS11 and (b) ΔPilV*

# Appendix III

## Study II: Effect of DNA Uptake Sequence (DUS) in DNA Uptake

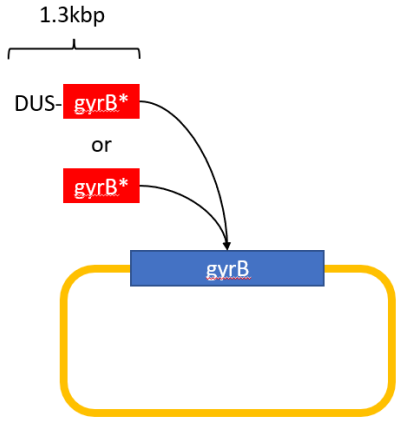


*liii Iluustration of the transformation of different tDNA with or without DUS in gyrB region*

Another important factor that can be studied about Type IV Pili and DNA uptake is DNA uptake sequence (DUS) due to its unique feature and close relation with Type IV Pili, as described in Chapter 1. It is canonically agreed that ComP, a minor pilin of T4P in *N. gonorrhoeae*, can interact with DUS sequences. Having one or more DUS sequences on a tDNA can greatly improve DNA transformation. Therefore, it's been commonly assumed that the lack of DUS will naturally lead to lesser transformation in *N. gonorrhoeae*. We replicated the same test in our hands using tDNA, introducing point mutation at *gyrB* region, either tagged with or without the DUS sequence at the 5' end (liii). Indeed, we observed a drastic drop in transformation efficiencies of MS11 when DUS is not present in tDNA (liv). However, we observed an opposite effect in ΔComP. Since DUS is reported to bind to ComP, we expected that the absence of ComP then would lead to not just a decrease in transformation efficiencies but the lack of preference to either DUS or noDUS tDNA will lead to no difference between both conditions. Yet, this is not observed in our results. This observation is interesting as it shows that DNA transformation is not as straightforward as we think. To investigate this further, we would like to check if this discrepancy between DUS and noDUS happens during the DNA uptake, transport or recombination level. To do that, we performed DNA uptake assay using these short tDNA labelled with fluorophores.

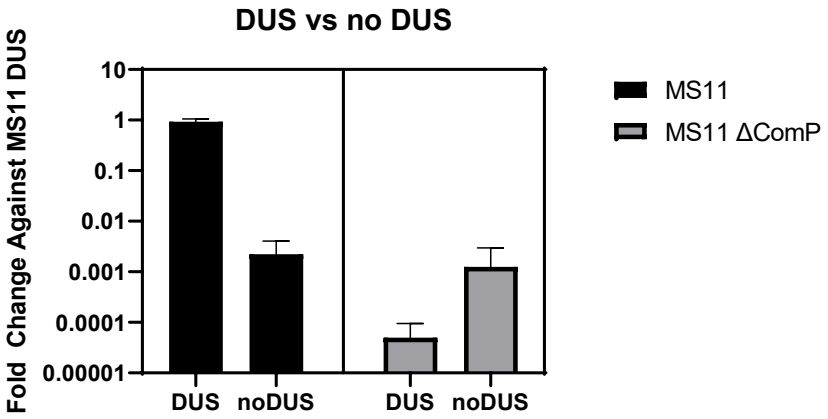


*liv The transformation efficiencies comparison between DUS and no DUS in MS11 and ΔComP*

In this experiment, we used a mix of 'DUS' and 'noDUS' labelled tDNA, labelled with different fluorophores (TM-Rhodamine, Red or MF488, Green). In our set-up, we tested RDgnd (Red DUS and green noDUS) and GDrnd (Green DUS and red noDUS). We tested these mixtures in MS11 to check if we can observe the DUS preference during DNA uptake. From the experiment, we observed that while it is evident that Green DUS seems to be preferred over red noDUS, it is not very obvious that Red DUS is preferred over green noDUS. What is observed instead is that each of the cells seems to be exclusive of one specific fluorophore, pointing towards a possible threshold of the amount of DNA uptake at a time within the experimental timeframe. We performed quantitative analysis on these images (lv). Statistically, our student t-test between experiment sets with MF488 (Green) DUS and noDUS is significantly different. As expected, the same difference is not statistically significant in the red channel, detecting TM-Rhodamine (Red). Overall, this result suggests that our experimental setup and microscope resolution may be insufficient in differentiating the signal.

To investigate further, we wondered if the difference in signal observed and the exclusivity of different fluorophore-labelled DNA in different cells could be an artefact from the fluorophore chemistry itself. Therefore, we checked the DUS tDNA mixture (MF488-DUS and TmRh-DUS) under the microscope. From our observation, the labelled tDNA of different fluorophores behave slightly differently, with TmRh-DUS aggregating more than MF488 (lvi). Nonetheless, we are not able to eliminate the possibility that this is due to variations between sample preparation. With this in mind, we could not further conclude the difference. However, we did a short DUS DNA uptake sequence with MF488-DUS and TmRh-DUS. In this case, with the understanding that both types of tDNA, therefore, we can rule out that the exclusivity we observed in the previous experiment is due to 'DUS' versus 'noDUS' preference. Interestingly, we still observe the same exclusivity among the cells with the different fluorophores (lvii). We conclude that it is possible that within this given time of DNA uptake assay, the cells took up mostly one tDNA, and it take some time for its turnover before they take up a second one. However, our experiment design is not robust enough to ascertain this theory.

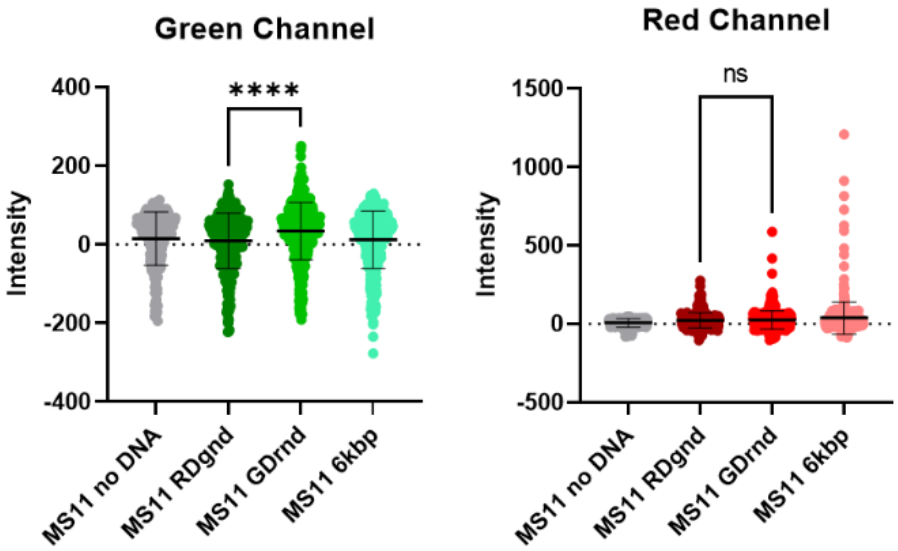


*lv Quantitative analysis of cell cluster intensity in DUS DNA uptake assay*

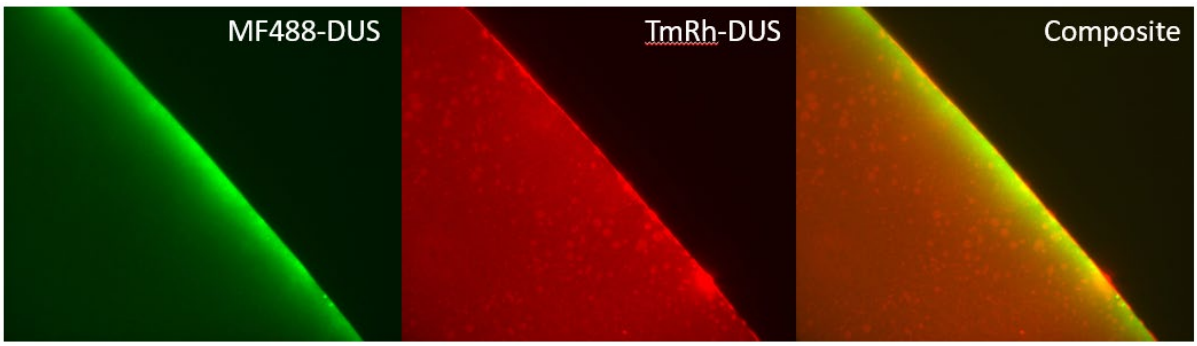


*lvi Microscope image of labelled DNA mixture with MF488-DUS and TmRh-DUS*

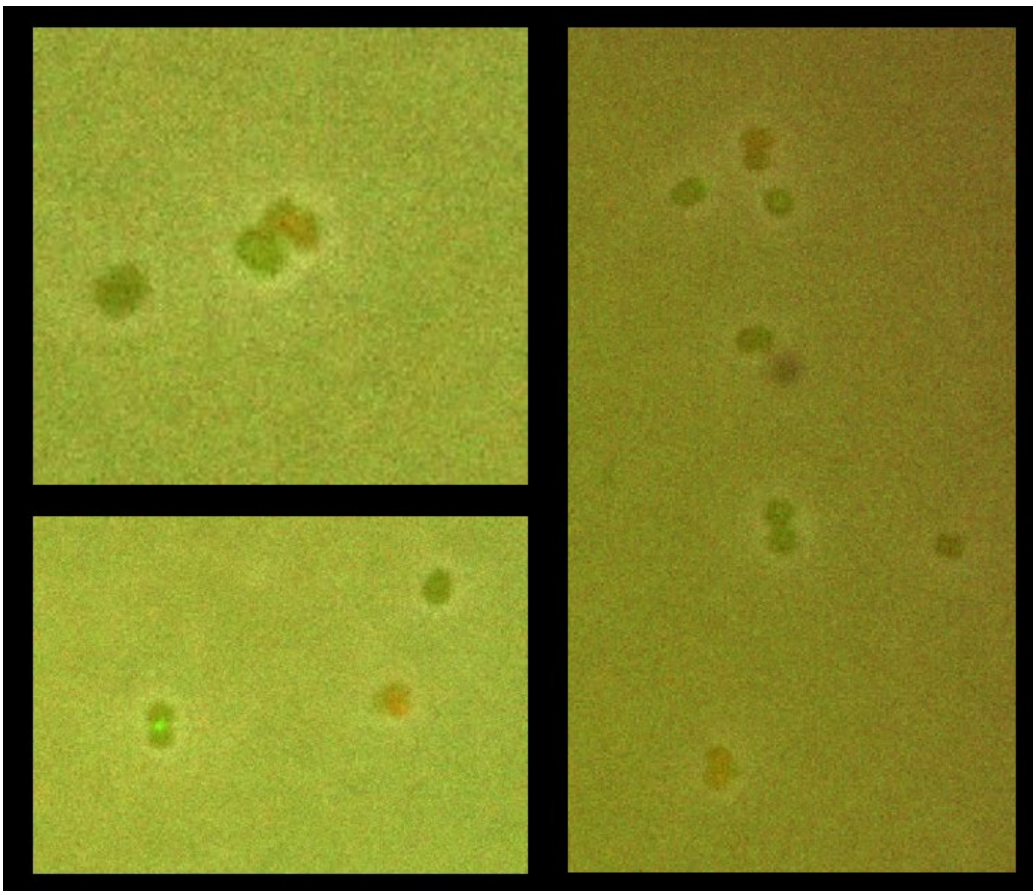

*lvii Example of exclusivity of fluorophore-labelled tDNA in different cells*

# Appendix IV

## Study III: A study on ΔComP, ΔPilV and ΔPilT combination strains

In this Section, we assessed these strains on four different aspects: (i) microcolony formation, (ii) 24-h survival, (iii) transformation efficiency, and (iv) DNA uptake.

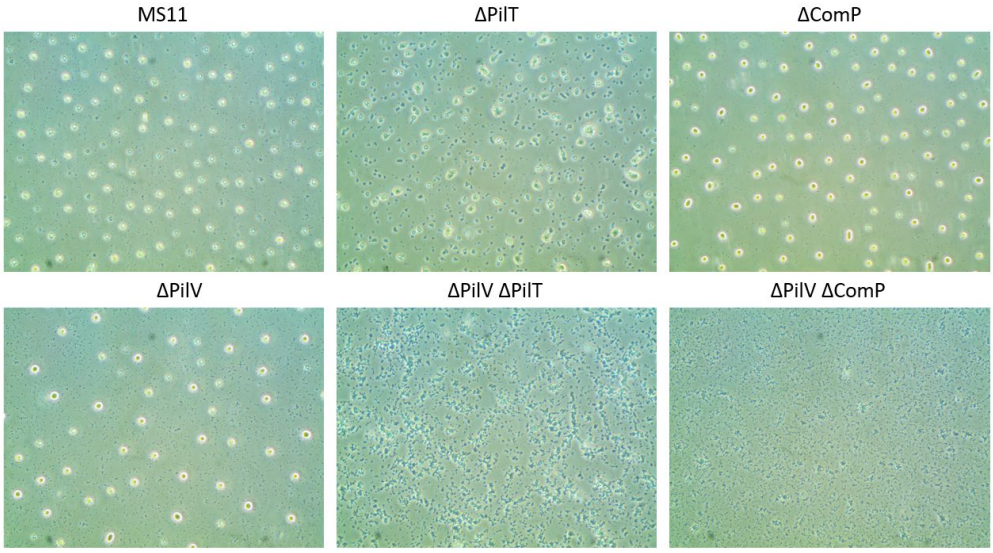


*lviii Microcolony formation assay for PilV combination mutants*

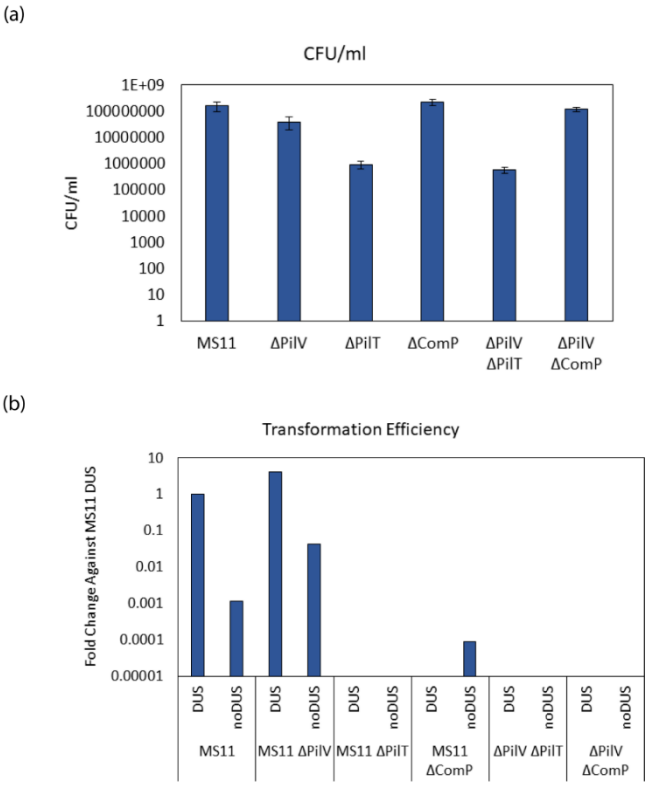


*lix 24-hour survival of PilV combination mutants (b) Transformation Assay for DUS and noDUS tDNA in PilV combination mutants*

In the microcolony formation assay (lviii), we saw that Wild Type and ΔPilV present similar small differences in microcolony spacing. This difference can also be observed in ΔComP, albeit very slightly. In ΔPilT, microcolony formation was affected since there was no pili retraction. Any aggregation resulting in ΔPilT is probably due to the interaction of bacteria due to Brownian motion or simply close proximity in the process of settling down to the bottom of the well since ΔPilT pili still retain adhesive phenotype. In ΔPilV ΔPilT, we see less aggregation compounded by the lack of pili retraction and adhesion. This observation fits with the reported observation that PilV contributes to adhesion, especially to epithelial cells [158,163]. For ΔPilV ΔComP, we observed that despite the absence of serious microcolony formation defects in either ΔPilV or ΔComP, the double

mutant does not form any microcolony. This is interesting because given that both ΔPilV and ΔComP are minor pilins and missing either one does not lead to serious implications on pili function in terms of aggregating with one another, missing both minor pilins seems to imply a serious defect in pili function.

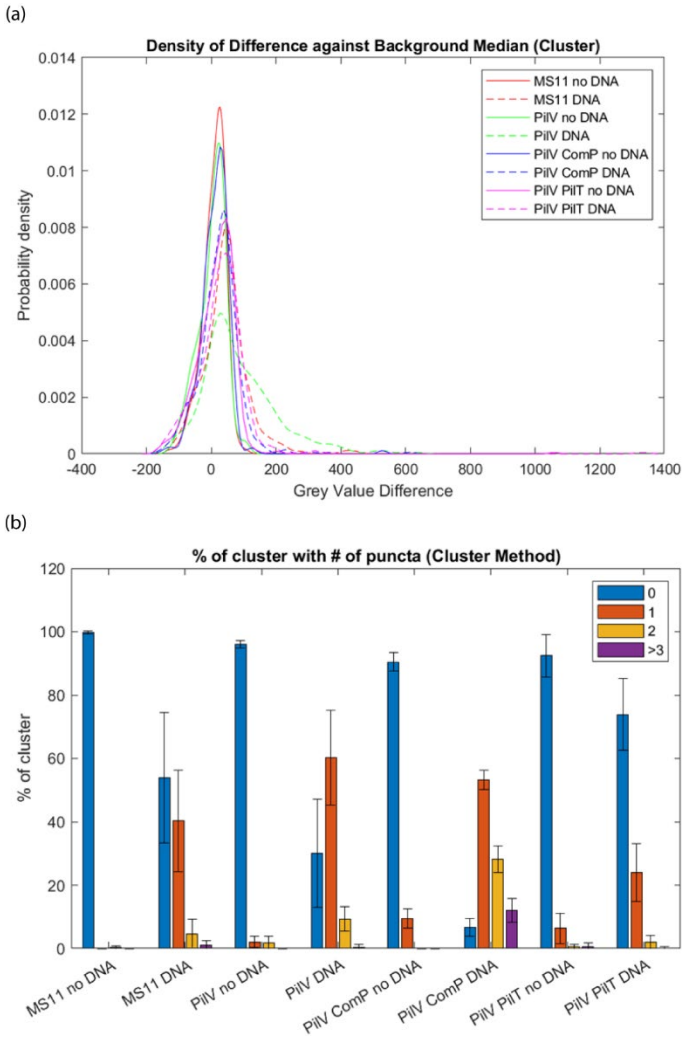


*lx (a) Transformation efficiency of ΔPilV combination strains (b) DNA uptake fluorescence signal of these strains (c) Puncta analysis of DNA uptake assay of these strains*

Next, we look at the 24-hour survival of these strains (lxiv). This assay is commonly used to assess the fitness or growth of *N. gonorrhoeae* strains. In our previous studies, we noticed that the 24-hour survival of *N. gonorrhoeae* strains that have a defect in Type IV Pili functions (e.g. ΔPilE and ΔPilT) tend to be poorer. We hypothesised that the ability to form microcolonies or Type IV Pili function may be coupled with the bacteria's metabolic states and, hence, shifting the bacteria growth curve and survival rate. Therefore, in this study, we initially expected a slight drop in 24-h survival for ΔPilV and ΔComP but a severe drop in survival for double mutants. We did not see much difference in the survival of either ΔPilV or ΔComP compared to the wild type, with ΔPilV surviving around half a log lower. Surprisingly, only survival of ΔPilV ΔPilT dropped to similar to that of ΔPilT for double mutants. ΔPilV ΔComP reverts to survival similar to that of wild type. Therefore, regarding their effect on gonococcal survival, PilT is more dominant than PilV and ComP, while ComP is most probably more dominant than PilV.

Our next assay is the transformation efficiency assay (lix). The rationale of this experiment stems from this information: (i) pili retraction facilitated by PilT is known to be crucial for DNA uptake, and (ii) ComP is one of the best-known minor pilin associated with DNA binding through its high binding affinity to DNA and DNA Uptake Sequence (DUS). Since ComP is known to have a higher binding preference to DUS sequences, we also performed a transformation efficiency test using transformed DNA with and without a DUS sequence. Our experiment result showed a straightforward conclusion. Between MS11 and MS11 ΔPilV, other than the expected improved transformation efficiencies, we observed a bigger increase in

efficiencies for MS11 ΔPilV when it is transformed with noDUS tDNA. We speculate from this result that we couldn't see a similar magnitude of increase in the DUS tDNA dataset, probably because it was near the maximum of the dynamic range of the experiment. On the other hand, our data from ΔPilV's enhanced transformation trait could not compensate for transformation defects resulting from ΔPilT or ΔComP. This concludes that PilT and ComP functions are more dominant than PilV. Available literature can support this conclusion [164].

Unfortunately, our DNA uptake assay could not provide any insightful information about these mutant strains (lx). As a control, we can detect significantly higher fluorescence intensity changes in ΔPilV. However, the increase in other mutants is very limited and difficult to conclude. The narrow dynamic range of this assay can contribute to this lack of distinction between negative control and samples.

After seeing some slight differences in the pili retraction profile between the strains, we deconstruct these data points into elements. Before doing that, we catalogued the pili retraction profile for reference. We first noticed ΔComP tend to have stronger and faster pili retraction events on DNA-coated pillars than carboxylated beads-coated pillars (lxi). When compared between MS11 and ΔPilV, ΔComP, ΔPilV ΔComP, and ΔPilV ΔPilT (lxii), we can start to notice the antagonistic nature of PilV and ComP (T- v and T- vi). However, it is worth noting that even though ΔPilT mutants are known to have little to no pili retractions, we do record some events in ΔPilV ΔPilT[334]. This mutant pili retraction speeds are not statistically different from others, but their forces are statistically different. By comparing MS11, ΔPilV, and ΔComP on DNA-coated pillar, we can see that ΔPilV tend to have weaker pulls, while ΔComP has stronger pulls compared to MS11 Regarding speed, ΔPilV tends to pull slightly faster than MS11, and ΔComP is the fastest among the three.

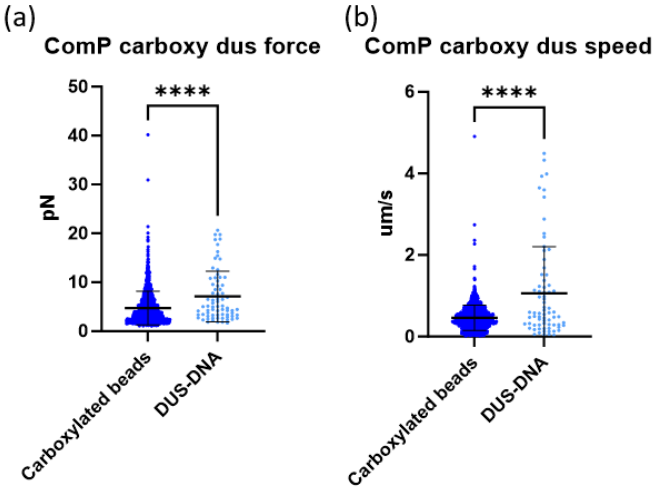


*lxi Pili retraction events profile for ΔComP for (a) force and (b) speed on differently coated pillars*

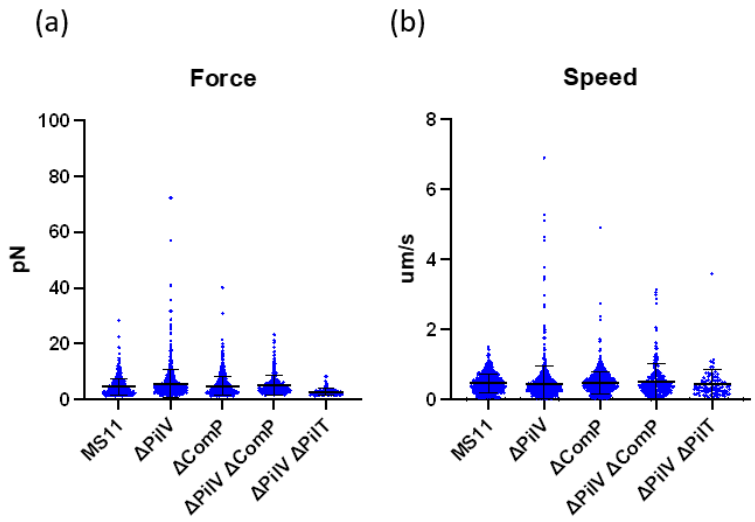


*lxii Pili retraction profile of different strains on 'betapillar' carboxylated beads-coated pillar: (a) force and (b) speed*

*T- v Student t-test significance value for pili retraction events force from different strains on carboxylated beads-coated 'betapillar'*

| | MS11 | ΔPilV | ΔComP | ΔPilV ΔComP | ΔPilV ΔPilT |
|---|---|---|---|---|---|
| MS11 | | **** | ns | * | **** |
| ΔPilV | | | **** | ns | **** |
| ΔComP | | | | ns | **** |
| ΔPilV ΔComP | | | | | **** |
| ΔPilV ΔPilT | | | | | |

*T- vi Table 4.4 Student t-test significance value for pili retraction events speed from different strains on carboxylated beads-coated 'betapillar'*

| | MS11 | ΔPilV | ΔComP | ΔPilV ΔComP | ΔPilV ΔPilT |
|---|---|---|---|---|---|
| MS11 | | ns | ns | * | ns |
| ΔPilV | | | ns | * | ns |
| ΔComP | | | | * | ns |
| ΔPilV ΔComP | | | | | ns |
| ΔPilV ΔPilT | | | | | |

# Appendix V

## Study IV: Studies using truncated PilC and ΔPilK

Other than studying the effect of external peptide supplementation in ΔPilC, we also explored its effect on strains that are likely to be related. We constructed a truncated PilC mutant, PilCtrunc, in which the region with the peptide sequence was removed. We wondered if truncating just 12 amino acids from PilC itself leads to loss of PilC function, and if yes, will supplementation of peptides have an effect? Other than that, we also looked at **ΔPilC, PilCtrunc in ΔPilT background**. In our experiment, the result shows that all of them are able to aggregate after being supplemented with peptides (lxiii). Even though ΔPilC ΔPilT should still be piliated according to the literature, the lack of pili retraction prevented the cells from pulling each other into microcolonies. However, the presence of pili and slight interaction can be observed because there is some pattern formation in the ΔPilC ΔPilT set even without peptide supplementation. Our PilCtrunc set showed that losing 12 amino acids at the C-terminal of PilC leads to the loss of PilC function since it behaved almost the same as ΔPilC. During the competence assay, we noted that PilCtrunc, in fact, has a higher basal competence compared to ΔPilC without any intervention of peptide supplementation (lxiv). However, with the supplementation of peptides, ΔPilC and PilCtrunc could restore competence to a similar level as the Wild Type.

Next, we tested the effect of peptide supplementation on **ΔPilK, ΔPilK ΔPilT, ΔPilC ΔPilK, and ΔPilC ΔPilK ΔPilT**. These strains were selected due to the prediction in which PilK can interact with PilC during pili biogenesis. In our aggregation assay, all of these strains could not aggregate, with and without peptide supplementation (lxv). Our competence assay (results not shown) also showed that they are not competent with and without peptide supplementation. This result suggests that PilK is upstream of the pili biogenesis pathway.

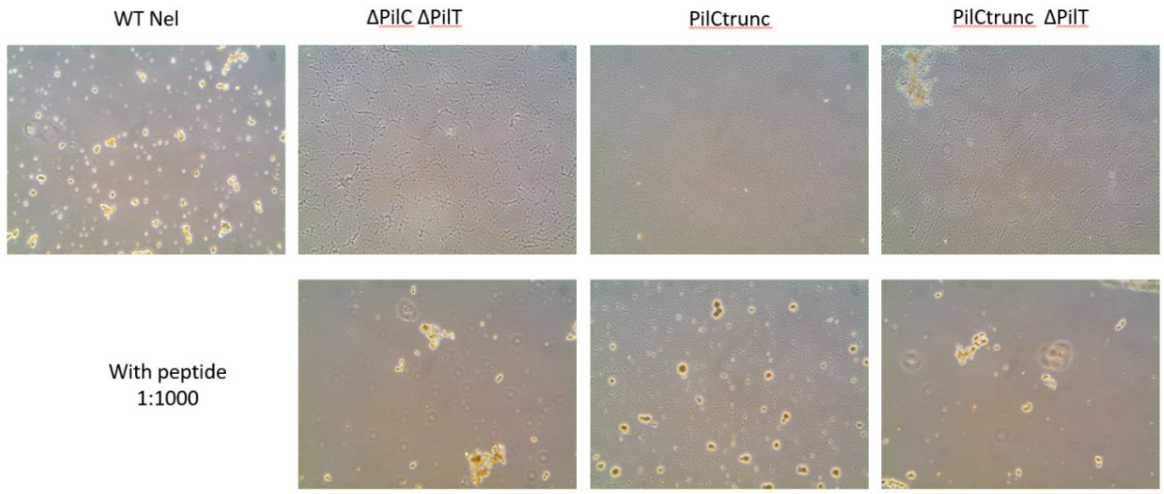


*lxiii Aggregation assay for ΔPilC ΔPilT, PilCtrunc and PilCtrunc ΔPilT with supplementation of peptides*

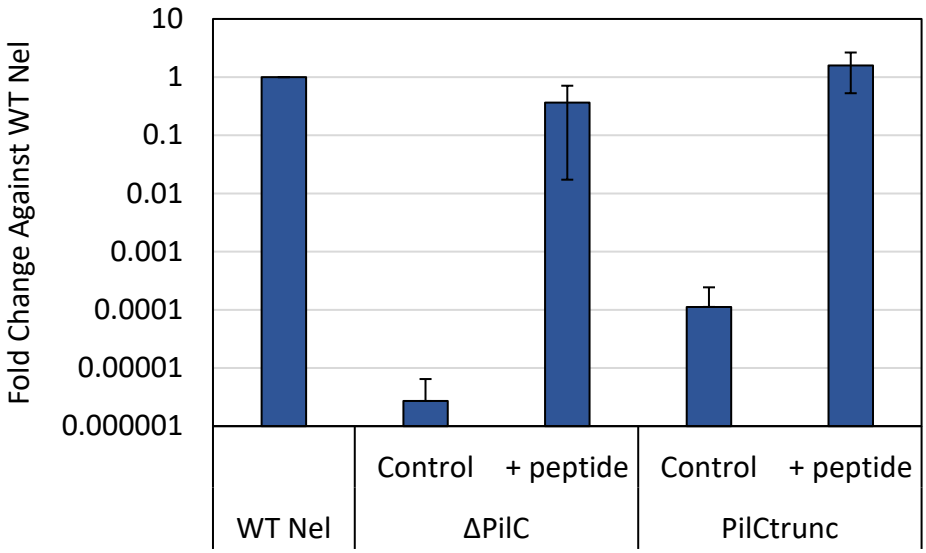


*lxiv Competence assay for PilC and PilCtrunc with the supplementation of peptide*

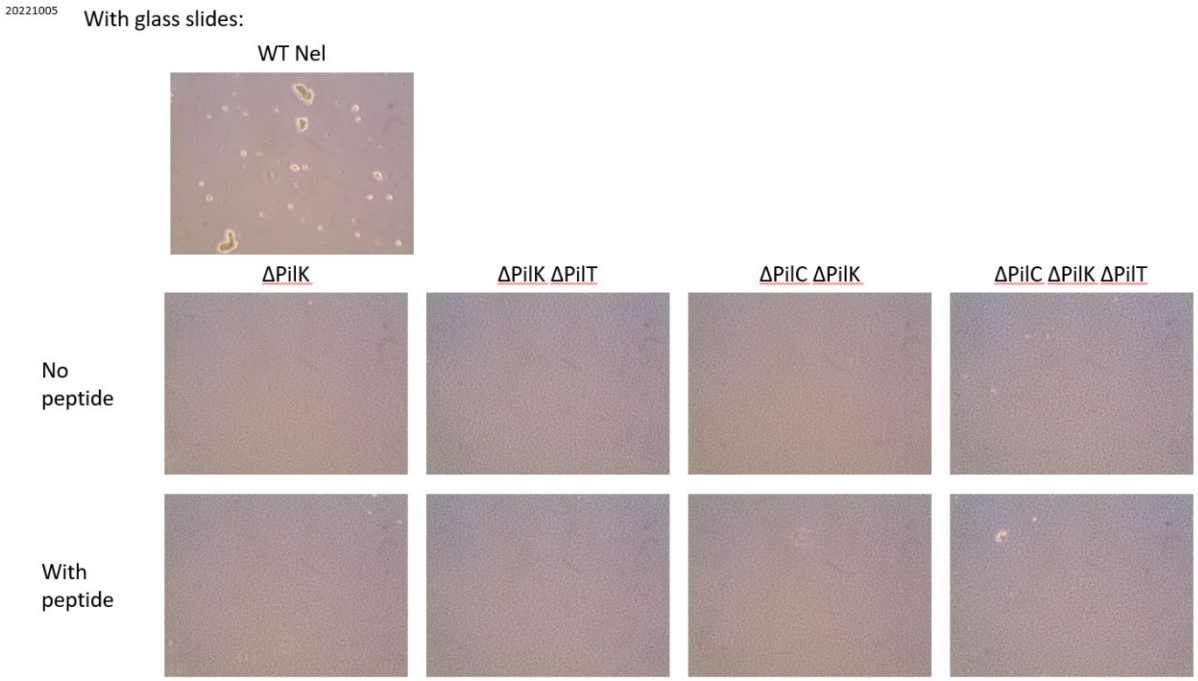


*lxv Aggregation assay for ΔPilC, ΔPilK, and ΔPilT combination strains*

# Appendix IV

## Study V: PilV in *Neisseria elongata*

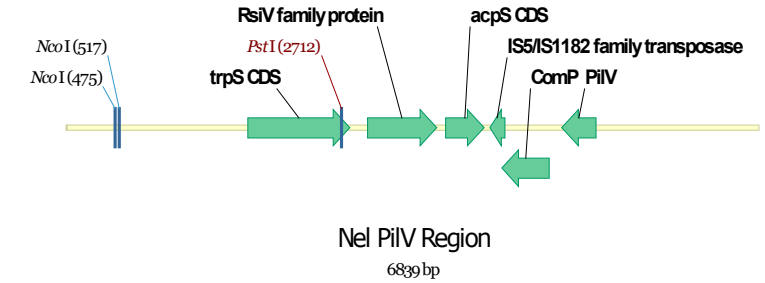


*lxvii Region around pilV ORF in N. elongata*

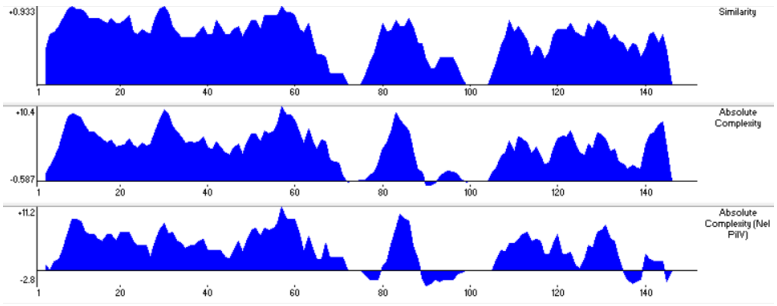


*lxvi Protein sequence alignment of N. elongata PilV with other Neisseria species*

The discovery of PilV's role in *N. gonorrhoeae* gives us a glimpse of the complexity of Type IV Pili regulation. Due to its homologous status to minor pilin, PilV has also been studied in *N. meningitidis*. In our hand, we can check if PilV also plays a similar role in a commensal *Neisseria, N. elongata*. However, a quick protein sequence of alignment shows that the genomic arrangement of PilV in *N. elongata* is slightly different from that of *N. gonorrhoeae.* In *N. elongata*, its PilV is phylogenetically further from *N. gonorrhoeae* compared to *N. meningitidis* and many other common *Neisseria* species. The ORF containing *pilV* in *N. elongata* is also interesting in the sense that after the *pilV* gene, it is followed by the *comP* gene. The fact that these two proteins are recognised for their antagonistic nature, being next to each other, brings about possible regulation or balancing within the *Neisseria* metabolism. Protein sequence alignment also shows conserved regions within PilV, especially the N-terminal region. This means that if there is indeed a required pilin-pilin interaction along the alpha-helix arm, it is highly conserved.

ΔComP in *N. elongata*

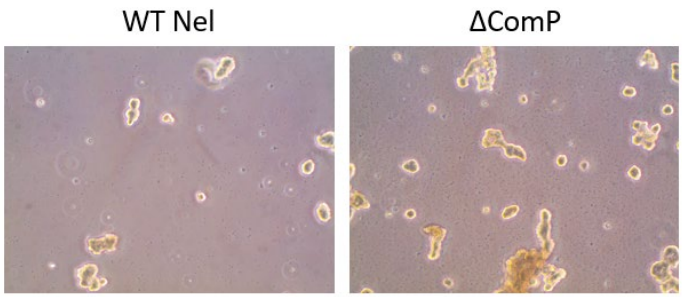


*lxviii ΔComP microcolonies formation*

In ΔComP, we note that the bacteria still aggregate roughly the same way as in wild-type *N. elongata* (lxviii). Without ComP, the bacteria seems to survive better at 24-h survival. This result aligns with what we noticed in *N. elongata*: those with pili defect seem to have much better survival at 24 hours (lxix). ΔComP in *N. elongata* also transforms less (lxix), similar to what we observed in *N. gonorrhoeae.*

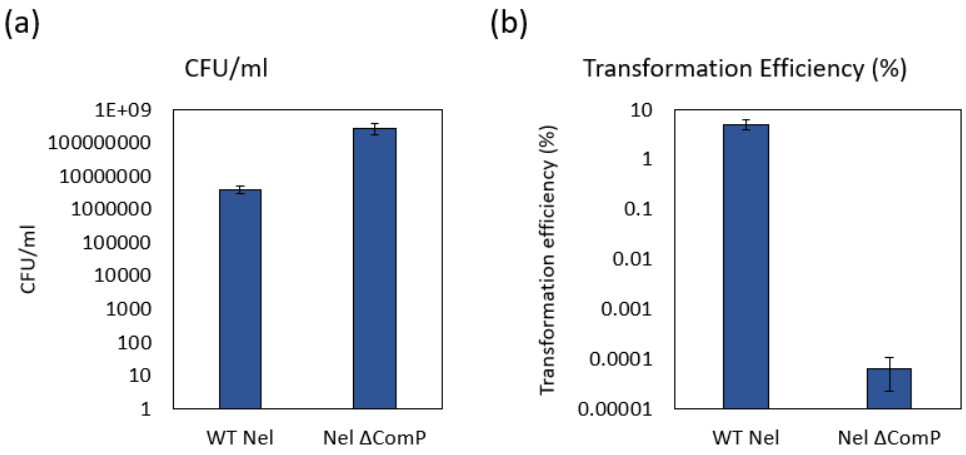


*lxix ΔComP information: (a) 24-hour survival and (b) transformation efficiencies*

ΔPilV in *N. elongata*

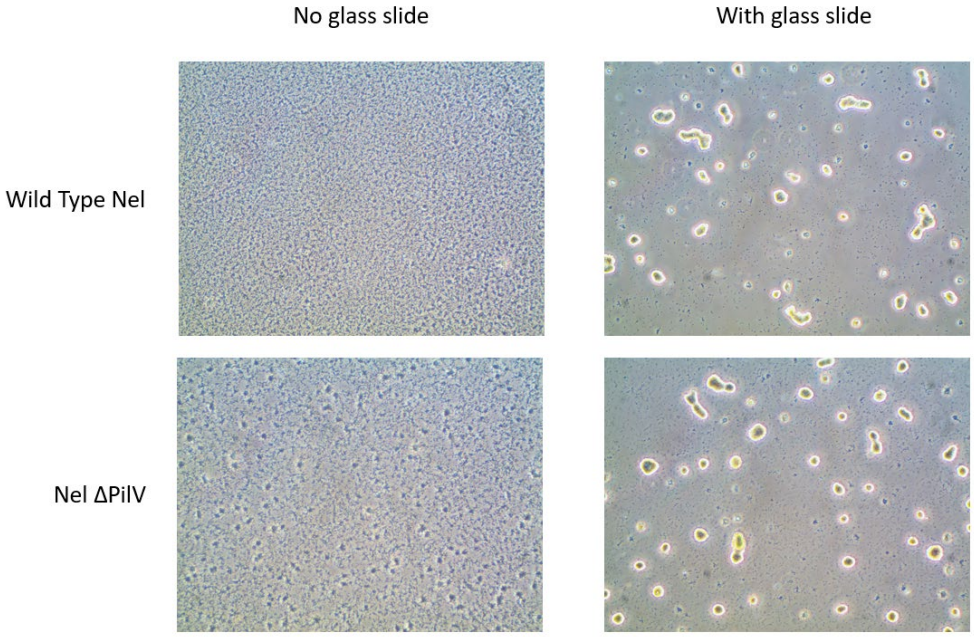


*lxx ΔPilV microcolonies formation*

With ΔPilV, we observe that although we observe a similar pattern in microcolony formation or cell aggregation with a glass slide (lxx). When we incubate them without a glass slide, which changes the surface substrate to polystyrene, we notice a slight difference in the cell aggregation. This is a sign that we altered the pili function slightly with ΔPilV. Similar to *N. gonorrhoeae*, ΔPilV does not differ from the Wild Type in terms of 24-hour survival but improved its competence (lxxi).

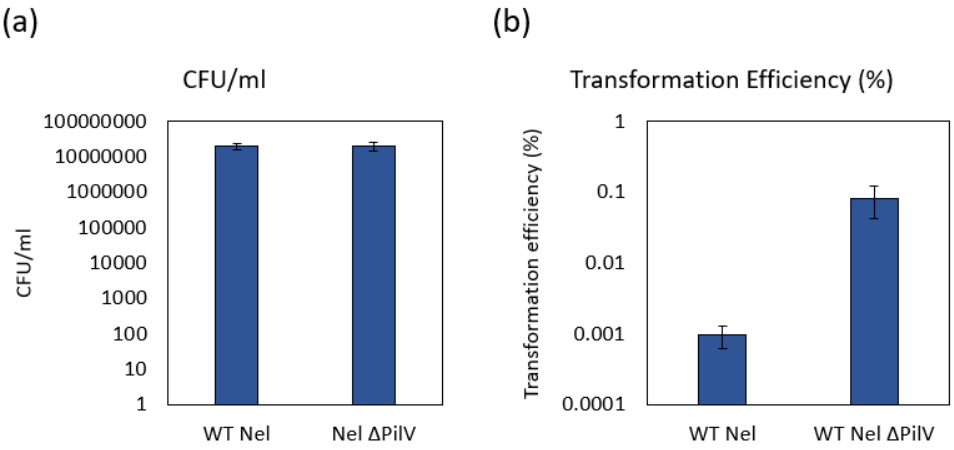


*lxxi ΔPilV information: (a) 24-hour survival and (b) transformation efficiencies*

Cysteine mutant and ΔPilV

We intended to expand our knowledge of *N. gonorrhoeae* into *N. elongata*. We screened through some potential amino acids in PilE1, one of the major pilins in *N. elongata*. In the end, we identified a few mutants that allowed us to visualise dynamical pili activities: T111C, T147C, and T117C (lxxii). Through our experiments, we consistently get good labelling with T11C. Therefore, we will study PilE and PilV interactions using T117C. We can see from here that in *N. elongata,* the microcolony formation ability was not severely affected with or without the PilE mutation or PilV (lxxiii). 24-hour survival of ΔPilV does not differ from their parent strain, and we only see slight differences between Wild Type and T117C (lxxiv). In both cases, competence was enhanced in ΔPilV. It is also interesting to see that the extent of enhancement is higher in T117C (lxxiv). When we observed labelled pili in T117C ΔPilV, we also noted a smaller population of cells with log active pili. Unfortunately, more studies need to be done before we can conclude.

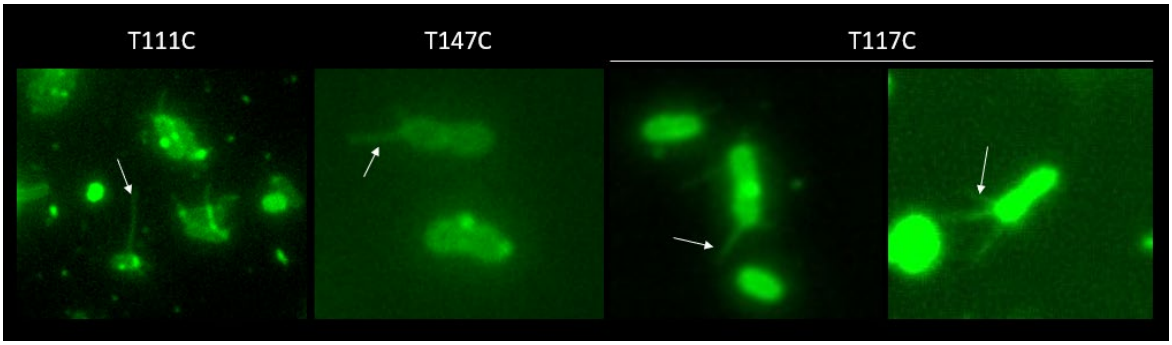


*lxxii Cysteine mutants pili labelling in N. elongata*

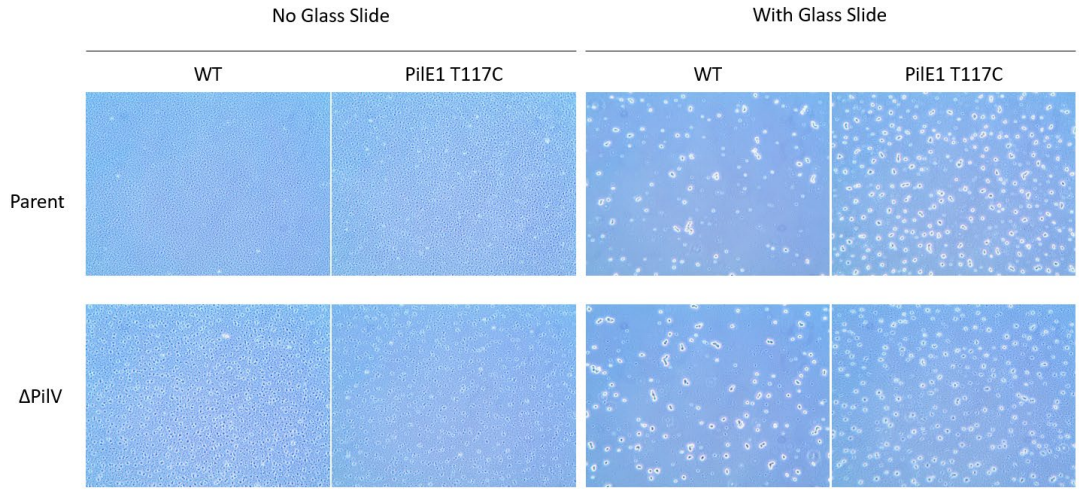


*lxxiii Microcolony formation assay for PilE1 T117C*

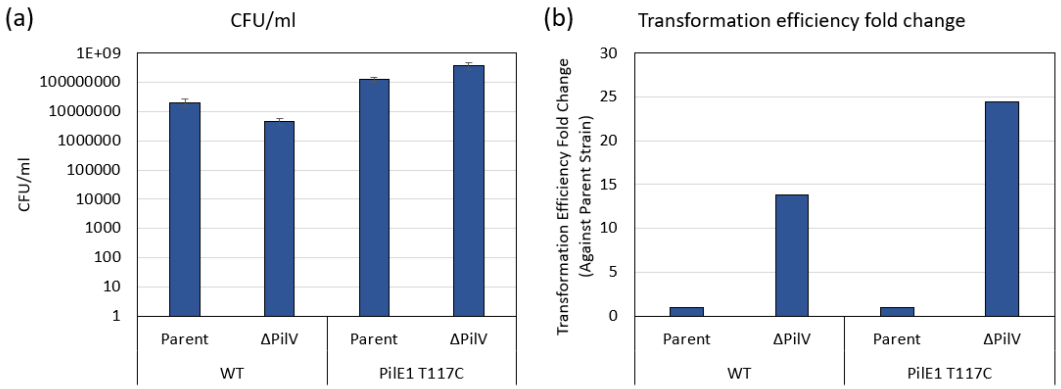


*lxxiv Wild Type and PilE1 T117C with their ΔPilVs: (a) 24-hour survival and (b) transformation efficiencies*

# Appendix VI

## Calculations for Chapter 3

The increment fold change is calculated as such:

$$Increment\ fold\ change\ at\ t_n = \frac{Average\ intensity\ at\ t_n - Average\ intensity\ at\ t_{n-1}}{Average\ intensity\ at\ t_{n-1}}$$

Where $t_n$ = time point n, and n = 0.25h, 1h, 2h, or 3h.

Transformation % was calculated as such:

$$Transformation\ \%\ at\ t_n = \frac{Amount\ of\ positive\ transformant\ at\ t_n}{Amount\ of\ total\ bacteria\ at\ t_n}$$

Transformation efficiency fold change was calculated as such:

$$Transformation\ efficiency\ fold\ change\ (TEfc)\ at\ t_n = \frac{Transformation\ \%\ at\ t_n}{Transformation\ \%\ at\ t_{0.25h}}$$

The rate of change was calculated as such:

$$Rate\ of\ change = \frac{TEfc\ at\ t_n - TEfc\ at\ t_{n-1}}{TEfc\ at\ t_{n-1}}$$

Where $t_n$ = time point n, and n = 0.25h, 1h, 2h, or 3h. For 0.25h, $TEfc\ at\ t_{n-1}$ is set at n = 0.25h.

# List of Figures

# List of Tables

# List of Appendix Figures

# List of Appendix Tables

# Abstract

Antibiotic resistance is a global health crisis, exemplified by the case of the etiological agent of gonorrhea, the bacterial species *Neisseria gonorrhoeae*. Understanding its mechanisms, particularly the role played by natural transformation, remains vital. Despite its discovery in 1928, natural transformation remains a phenomenon with many unanswered questions, in particular the role of a ubiquitous prokaryotic appendage named the type IV pilus. *N. gonorrhoeae*'s dependence on Type IV Pili makes it an ideal model for studying this exact problem. Central to this comprehensive study is the pivotal role attributed to Type IV Pilus, a multifunctional and essential player in orchestrating DNA transformation in *N. gonorrhoeae*.

This research meticulously lays the groundwork, introducing molecular biology techniques essential for genetic engineering within *N. gonorrhoeae*. We also explore microscopy tools development tailored to study DNA uptake and transformation. To understand Type IV pili dynamics during DNA uptake, we engineered tools and a streamlined workflow capable of visualizing and quantifying the dynamics of both pili and DNA molecules. Additionally, we utilized hydrogel micropillars, either specific or non-specific DNA interacting, to delve into the mechanical properties of pili retractions.

This in-depth investigation also involves scrutinizing the behaviour of mutants deprived of some of the proteins involved in the type IV pili machinery (PilV, PilC and PilD), unveiling some insights into the regulatory mechanisms of Type IV Pili and their consequential impact on the dynamics of DNA uptake. Particularly noteworthy is the revelation that PilV deletion induce alterations in translocation of the major pilin PilE, resulting in the emergence of shorter yet efficient pili. This discovery underscores the adaptive nature of *N. gonorrhoeae* in manipulating the diversity of Type IV Pili to optimize DNA uptake processes.

Furthermore, our studies highlight the influence of posttranslational modifications on PilE, thereby accentuating the heterogeneous composition of Type IV Pili and their robust functionality as a polymer. We also include a short study examining the interplay between commensal and pathogenic *Neisseria* species within the context of DNA uptake.

While this expedition leaves certain questions unanswered, its depth and breadth offer extensive insights into the intricate mechanisms of DNA transformation and the dynamic role played by Type IV Pili in the remarkable adaptability of *N. gonorrhoeae*. Not only does this thesis provide solutions to existing queries, but it also illuminates novel pathways for future research, sparking curiosity and fascination in unravelling the functional intricacies of pili structures and their profound implications in DNA transformation.

Keywords :[Microbiology ; Type IV Pili ; Horizontal gene transfer ; DNA transformation]

# Résumé

La résistance aux antibiotiques est une crise sanitaire mondiale, illustrée par le cas de l'agent étiologique de la gonorrhée, l'espèce bactérienne *Neisseria gonorrhoeae*. Comprendre ses mécanismes, en particulier le rôle joué par la transformation naturelle, reste vital. Malgré sa découverte en 1928, la transformation naturelle reste un phénomène avec de nombreuses questions sans réponse, en particulier le rôle d'une appendice procaryotique ubiquitaire, le pilus de type IV. La dépendance de *N. gonorrhoeae* à l'égard des Pili de type IV en fait un modèle idéal pour étudier ce problème précis. Le rôle central de cette étude détaillée est attribué au Pilus de type IV, un acteur multifonctionnel et essentiel dans l'orchestration de la transformation de l'ADN chez *N. gonorrhoeae*.

Cette recherche prépare méticuleusement le terrain, en introduisant des techniques de biologie moléculaire essentielles pour le génie génétique chez *N. gonorrhoeae*. Nous explorons également le développement d'outils de microscopie adaptés à l'étude de l'absorption et de la transformation de l'ADN. Pour comprendre la dynamique des pili de type IV pendant l'absorption de l'ADN, nous avons mis au point des outils et un flux de travail rationalisé capables de visualiser et de quantifier la dynamique des pili et des molécules d'ADN. En outre, nous avons utilisé des micropiliers d'hydrogel, interagissant avec l'ADN de manière spécifique ou non, pour étudier les propriétés mécaniques des rétractions des pili.

Cette étude approfondie implique également l'examen du comportement de mutants privés de certaines des protéines impliquées dans la machinerie des pili de type IV (PilV, PilC et PilD), ce qui permet de mieux comprendre les mécanismes de régulation des pili de type IV et leur impact sur la dynamique de l'absorption de l'ADN. Il est particulièrement intéressant de noter que la délétion de PilV induit des altérations dans la translocation de la piline majeure, PilE, ce qui entraîne l'émergence de pili plus courts mais efficaces. Cette découverte souligne la nature adaptative de *N. gonorrhoeae* dans la manipulation de la diversité des pili de type IV pour optimiser les processus d'absorption de l'ADN.

En outre, nos études mettent en évidence l'influence des modifications post-traductionnelles sur PilE, accentuant ainsi la composition hétérogène des pili de type IV et leur fonctionnalité robuste en tant que polymère. Nous incluons également une courte étude examinant l'interaction entre les espèces de Neisseria commensales et pathogènes dans le contexte de l'absorption de l'ADN.

Bien que cette expédition laisse certaines questions sans réponse, sa profondeur et son étendue offrent des aperçus conséquents sur les mécanismes complexes de la transformation de l'ADN et le rôle dynamique joué par les Pili de type IV dans l'adaptabilité remarquable de *N. gonorrhoeae.* Non seulement cette thèse apporte des solutions aux questions existantes, mais elle ouvre également de nouvelles voies pour la recherche future, suscitant la curiosité et la fascination pour l'élucidation des complexités fonctionnelles des structures pili et leurs implications profondes dans la transformation de l'ADN.
Mots-clés : [Microbiologie ; Pili de type IV ; Transfert horizontal de gènes ; Transformation de l'ADN]